EFFECTS OF HINDGUT BUFFERS ON INTESTINAL FERMENTATION AND MICROBIOTA IN DAIRY CATTLE

by

Shane Kevin Cronin

A dissertation submitted to the Faculty of the University of Delaware in partial fulfillment of the requirements for the degree of Doctor of Philosophy in Animal and Food Sciences

Summer 2024

EFFECTS OF HINDGUT BUFFERS ON INTESTINAL FERMENTATION AND MICROBIOTA IN DAIRY CATTLE

by

Shane Kevin Cronin

Approved: ____
Erin E. Connor, Ph.D.
Chair of the Department of Animal and Food Sciences

Approved: ____
Brian E. Farkas, Ph.D.
Dean of the College of Agriculture and Natural Resources

Approved: ____
Louis F. Rossi, Ph.D.
Vice Provost for Graduate and Professional Education and
Dean of the Graduate College

I certify that I have read this dissertation and that in my opinion it meets the academic and professional standard required by the University as a dissertation for the degree of Doctor of Philosophy.

Signed: ______________________________

Tanya F. Gressley, Ph.D.
Professor in charge of dissertation

I certify that I have read this dissertation and that in my opinion it meets the academic and professional standard required by the University as a dissertation for the degree of Doctor of Philosophy.

Signed: ______________________________

Amy S. Biddle, Ph.D.
Member of dissertation committee

I certify that I have read this dissertation and that in my opinion it meets the academic and professional standard required by the University as a dissertation for the degree of Doctor of Philosophy.

Signed: ______________________________

Ryan J. Arsenault, Ph.D.
Member of dissertation committee

I certify that I have read this dissertation and that in my opinion it meets the academic and professional standard required by the University as a dissertation for the degree of Doctor of Philosophy.

Signed: ______________________________

Catherine M. K. Bradley, Ph.D.
Member of dissertation committee

I certify that I have read this dissertation and that in my opinion it meets the academic and professional standard required by the University as a dissertation for the degree of Doctor of Philosophy.

Signed: ______________________________

Limin Kung, Jr., Ph.D.
Member of dissertation committee

ACKNOWLEDGMENTS

I'd like to begin by thanking my advisor, Dr. Tanya Gressley. You've been such a role model over the 8 years that I've been working in your lab. Thank you for supporting and nurturing my love of science and allowing me to diversify my experiences in the fields of nutrition, microbiology, and immunology. You have been such an incredible advisor and mentor in both life and science, and I'm forever grateful to have worked with you.

Thank you to my committee who have all shaped my life in their own ways, expanding my skillset and helping me achieve this degree. Thank you to the University of Delaware Dairy Farm Crew who have helped me gain confidence in working with dairy cattle. Thank you to my lab mates and collaborators, Merrick Smith, Dr. Alexa Johnson, Dr. Famatta Perry, Dr. Xiaojing Liu, and Kasey Hobert for always allowing me the chance to chat and bounce ideas off of you. Thank you to the army of undergraduate helpers who have allowed this research to happen, including but absolutely not limited to Lorik Tamazian, Brianna Krebs, Georgia Weiner, and Reiko Matrisciano. Thank you to Shania Twain for keeping me motivated.

Thank you to my friends both in and out of the ANFS department, and thank you to my parents and partner for supporting and loving me. From listening to me complain about issues with lab work, helping me puzzle out microbial or nutrient interactions, or just nodding along even though you didn't understand what I was talking about, I appreciate it all. Your endless positivity helped make this happen.

TABLE OF CONTENTS

Appendix

LIST OF TABLES

LIST OF FIGURES

ABSTRACT

Lactation in dairy cattle is an energetically costly process, leading cows to pull resources from bodily stores if energy and nutrients are not sufficiently provided in the diet. Producers regularly feed energetically dense diets to lactating cows, typically by feeding increased levels of rapidly fermentable carbohydrates like starch. However, increased dietary starch can induce acidosis along the gastrointestinal tract, both in the rumen and hindgut. Increased starch levels may lead to rapid declines in pH due to increased volatile fatty acid (VFA) and lactate production, which can degrade the rumen and intestinal epithelial barriers. Additionally, increased starch levels and the subsequent changes to digesta pH affect the gastrointestinal microbiota, encouraging microbial dysbiosis through the death of fiber-fermenting bacteria and the release of lipopolysaccharide (LPS). LPS is highly immunogenic and induces inflammation when entering systemic circulation through disrupted epithelial barriers, negatively impacting animal well-being and milk production. Thus, dietary tools to mitigate acidosis events may positively contribute to animal health and production.

Ruminal acidosis has been widely studied over the years, and the use of dietary buffers to counteract the effects of high starch diets on rumen pH is common. However, high levels of dietary starch may still increase the amount of undigested starch entering the intestines, potentially leading to hindgut acidosis regardless of apparent rumen health. The first objective of this dissertation was to assess the effects of hindgut acidosis from corn starch on the intestinal fermentation and microbiome, nutrient digestibility, and systemic inflammation. The second objective was to

evaluate whether two buffers (buffer A: blend of calcium carbonate, magnesium oxide and crushed oyster shell; buffer B: magnesium oxide) could alter these factors, ideally counteracting the negative effects of hindgut acidosis. Two experiments were conducted to achieve these objectives, one in vivo and one in vitro.

In vivo abomasal infusions of corn starch decreased fecal pH and dry matter and starch digestibilities, and increased lymphocyte immunometabolic signaling as compared to the control. Corn starch infusions did not increase milk production, fecal LPS and total VFA, or serum acute phase proteins, and minimally affected measures of fecal microbial diversity as compared to the control. Lack of effects on acute phase proteins and the intestinal fermentation profile and microbiome were surprising, but this was likely due to unintentional SARA induction due to the moderately high starch total mixed ration. Buffer addition increased fecal pH, increased fecal acetate and total VFA, and decreased fecal score as compared to infused starch alone. Responses of serum acute phase proteins, lymphocyte immunometabolic signaling, and the fecal microbiome depended on the type and dosage of buffer. Buffer A, particularly at a higher dosage, increased serum acute phase proteins, and exaggerated negative responses to acidosis in immunometabolic signaling and the fecal microbiome. Signals related to immune response were increased while microbial taxa associated with inflammation increased in abundance. Buffer B in turn seemed to alleviate negative responses due to acidosis, reducing immunometabolic signaling and increasing the relative abundance of beneficial microbial taxa.

In vitro corn starch inclusion increased cumulative gas production, lactate, butyrate, LPS, and total protein, and decreased culture pH, propionate, and ammonia nitrogen as compared to the control. Additionally, corn starch decreased the relative abundance of fibrolytic microbes and increased the relative abundance of amylolytic bacteria. Buffer inclusion in the presence of corn starch further increased gas production, acetate, propionate, butyrate, and culture pH, but did not affect culture microbiome. In the absence of corn starch both buffers A and B increased acetate and total VFA and changed microbial beta diversity as compared to the control, but buffer B additionally increased culture pH and microbial alpha diversity, seemingly improving maintenance of microbial functionality.

Overall, starch inclusion induced changes to fermentation profiles both in vivo and in vitro, but only meaningfully changed microbial profiles in vitro. Increased immunometabolic lymphocyte signaling, particularly pro-inflammatory signaling, suggests negative systemic effects due to starch infusions. In vitro decreases in pH and increases in LPS corroborate this induction of inflammation seen in the in vivo experiments, and changes in microbial beta diversity and taxa relative abundance due to starch suggest contribution to microbial dysbiosis. Buffer inclusion, both in vivo and in vitro, increased fecal pH and VFA concentration. In vivo, buffer A induced additional pro-inflammatory signaling, and at the higher dosage negatively impacted the fecal microbiome, while not affecting culture microbiome in vitro in the presence of starch. Buffer B decreased pro-inflammatory signaling in vivo and impacted the fecal microbiome, but again did not affect culture microbiome in the presence of starch when evaluated in vitro. In summary, starch inclusion induced acidotic conditions in both trials, suggesting a more pro-inflammatory and dysbiotic profile as compared to the control. Buffers increased fecal pH in the presence of starch but also increased VFA concentration. Buffer A and B differentially affected immunometabolic signaling and the fecal microbiome, with buffer B producing the

more diverse microbial profile. Despite the increased pH, buffer inclusion in the presence of high starch increased VFA, potentially further challenging cows. Although buffers consistently aided in raising intestinal pH, effects on hindgut health were variable between buffer types.

Chapter 1

INTRODUCTION

1.1 Ruminant Digestive System

1.1.1 Foregut

Dairy cattle are ruminants, which are characterized by a unique digestive system, vastly different from that of a monogastric animal. While monogastrics rely on their glandular stomachs to break down feed, ruminants are foregut fermenters, relying on microbial communities to break down their food. The ruminant stomach is separated into four compartments that are composed of the rumen, reticulum, omasum, and abomasum. The rumen can hold approximately 120 liters and is the primary site of foregut digestion. This massive chamber increases the mean retention time of feed particles, allowing for increased fermentation. The reticulum, composed of honeycomb-structured epithelium, aids in rumination, including the muscular contractions needed to force a food bolus from the rumen back to the esophagus and mouth. While ruminants depend on microbial breakdown of feed sources, physical mastication is necessary to increase surface area for microbial attachment. Once small enough, feed particles move past the reticulorumen into the omasum. The omasum is characterized by page-like folds of epithelium, reabsorbing water, electrolytes, and allowing small particles to make their way to the abomasum. The abomasum is the true stomach, similar to the monogastric stomach, and uses hydrochloric acid and digestive enzymes to continue breaking down feed particles and any attached rumen microbes.

As the main site of foregut fermentation, the rumen contains a multitude of microbes. This includes bacteria, archaea, fungi, and protozoa. This diverse community of microbes digest plant proteins and carbohydrates such as cellulose, hemicellulose, and starches. Through fermentation of these substrates, rumen microorganisms produce volatile fatty acids, or VFAs. Volatile fatty acids such as acetate, propionate, and butyrate provide 70% of the energy needed to maintain lactation (Bergman, 1990) and are primarily produced through breakdown of carbohydrates. Protein fermentation produces additional VFAs including valerate, isovalerate, and isobutyrate (Katzinger, 2020; Zarling and Ruchim, 1987). The rumen papillae facilitate VFA absorption, with the health and density of the tissue playing a major role in clearance rate (Van Soest, 1994). Rumen papillae are formed by keratinized, non-glandular epithelium with multiple layers, providing some protection from injury due to acidic conditions. Upon reaching the omasum, the majority of VFAs should be absorbed out of the reticulorumen and into the bloodstream, where they can be processed to provide energy to the body. Rumen microbes can use carbohydrates and protein provided in the diet to supply the energy and nitrogen needed to multiply, increasing their abundance. Microbes can use protein from plant or animal feed products as nitrogen sources, or non-protein nitrogen sources such as urea or ammonia. As feed particles flow out of the rumen and into the abomasum and intestines, rumen microbes will be digested along with them. Rumen microbes can comprise over 50% of the protein metabolized by the ruminant (Hackmann et al., 2013).

1.1.2 Small Intestine and Hindgut

After chemical and enzymatic degradation in the abomasum, feed enters the small intestine and ruminant hindgut. The ruminant hindgut is comprised of the cecum and large intestine. The small intestine is approximately 43 to 52 meters long and includes the duodenum, jejunum, and ileum (Espe and Cannon, 1940). As in monogastrics, the small intestine is the major site of nutrient absorption, using finger-like projections of epithelial cells, or villi, to increase surface area. The pancreas releases amylase and lipase into the small intestine to further break down starches and fats missed during ruminal fermentation, and bile from the liver increases the pH and emulsifies lipids for ease of digestion. Ingesta from the small intestine continues to the cecum and large intestine, which is approximately 14 meters long in dairy cattle (Espe and Cannon, 1940). The colon absorbs additional VFAs and water, and any ingesta remaining or material produced will be excreted as feces. The further into the hindgut ingesta travels, the higher the bacterial load, the pH value, and the lower the level of oxygen (Donaldson, 2016). Microbes within the colon continue to ferment available nutrients into VFAs and produce microbial protein. As in the rumen, protein can be fermented to VFA in the hindgut. However, protein cannot be absorbed by the colon, any microbial protein produced in the cecum or colon is excreted in the feces.

The small and large intestines are both made up of simple columnar epithelial cells, with the small intestine epithelium focused more on absorption than protection. Small intestinal epithelial cells include stem cells, goblet cells which produce mucus, and paneth cells which produce antimicrobial peptides, and are produced in crypts. A layer of mucus covers the small intestinal villi, allowing microbial attachment and keeping the cells at a relatively stable pH. Mucus also keeps microbes from attaching directly to the epithelium, which would detrimentally affect absorption and increase the risk of bacterial invasion beyond the epithelium. Paneth cells modulate the intestinal microbiome, mediating the inflammatory response through defensins, lysozyme, and other secreted peptides (Lueschow and McElroy, 2020). In the large intestine, the epithelium is arranged as shallow crypts and covered in a double layer of mucus, providing more protection against the more abundant microbial community (Steele et. al., 2016). Despite these protective features, certain diets, particularly those containing high levels of starch, can cause injury to the intestinal epithelium and lead to inflammation.

1.1.3 Intestinal Barriers

In order to protect against bacterial invasion, the intestines have multiple barriers that, when intact, keep the animal healthy. Within the intestines, goblet cells secrete mucus that prevents chemical and physical injury to the absorptive epithelial cells. Mucus is primarily made up of secreted mucins, which are glycosylated glycoproteins linked to diverse O-linked oligosaccharide side chains (Hollingsworth and Swanson, 2004). Although there are many different types of mucins, MUC2 is the most common mucin secreted by goblet cells. In the large intestine, the two layers of mucus add additional protection against microbial product injury and invasion. The inner layer is tightly adhered to the epithelial surface, while the outer layer allows for microbial attachment. Thick layers of mucus yield positive results for the host, as mice deficient in MUC2 exhibit increased intestinal permeability and spontaneous colitis (Van der Sluis et al., 2006; Van der Sluis, 2001).

Intestinal epithelial cells, or enterocytes, are held together by apical junctional complexes. These consist of tight and adherens junctions and desmosomes on the lateral apical membrane of cells. Tight junctions consist of four transmembrane proteins, known as junctional adhesion molecules, claudins, occludin, and tricellulin (Madara, 1987). A selectively permeable barrier is formed through interactions between neighboring cells. This barrier allows water, electrolytes, and dietary nutrients to transfer from the lumen into systemic circulation (Blikslager et al., 2007). This paracellular pathway permeability is defined by the pore size in tight junction proteins and is dependent on water movement in response to electrochemical or osmotic gradients in the epithelium. The transcellular pathway transports large molecules through endocytosis or exocytosis that is mediated by cell membrane receptors and can be performed by many epithelial cell types. Enterocytes can sample molecules such as food antigens through endocytosis, bringing the molecule to the underlying tissue (Tordesillas et al., 2013). While enterocytes selectively absorb nutrients from the intestinal lumen, they also function to form a strong barrier that keeps out antagonistic compounds and bacteria. “Sentinel” goblet cells found in mice can sample intestinal contents and produce additional MUC2 to expel bacteria (Birchenough et al., 2016). Additionally, microfold, or M cells, sample luminal antigens and present them to a lymphoid follicle while dendritic cells will migrate to and from the epithelial layer to sample bacterial antigens. The barrier formed by intestinal epithelial cells serves to protect the body from antigenic and pathogenic molecules, while certain intestinal cells sample and survey the luminal contents. When these molecules breach the barrier, localized or systemic inflammation occurs, accompanied by a swift immune response.

1.2 Carbohydrates

1.2.1 Composition and Structure

Lactating dairy cattle diets are high in carbohydrates, both fiber and starch. Plant fiber fed to dairy cattle is primarily made up of cellulose, hemicellulose, and lignin. Cellulose is the most abundant carbohydrate on earth and is composed of linear chains of glucose. These glucose monomers are connected by beta-1,4 glycosidic linkages, which cannot be degraded by animal enzymes (Berg et al., 2002). Ruminants rely on anaerobic microbial digestion within the rumen in order to begin breaking down plant fiber into available nutrients, as microbes can hydrolyze beta-1,4 glycosidic bonds. Hemicellulose is more complex than cellulose and is composed of branched chains of xylans and beta-glucans. Hemicellulose branches are hydrogen bonded to cellulose to improve plant structural integrity but are difficult to digest due to cross-linkages with lignin (Scheller and Ulvskov, 2010). Lignin is a phenylpropanoid structure that is extremely complex, providing the plant structure and resistance to environmental stressors. Lignin is not digestible anaerobically, so no rumen microbes or animal enzymes can break it down. This means that parts of every forage fed to cattle are indigestible. When describing animal diets, fiber is typically broken into two fractions: neutral detergent fiber (NDF) and acid detergent fiber (ADF). NDF total fiber is found in vegetative feedstuffs, containing cellulose, hemicellulose, and lignin. NDF is the structural components of the plant cell wall and is a predictor for dietary intake as it provides fill to the rumen. The digestibility of NDF in the diet is determined entirely by microbial fermentation in the animal. The ADF fraction contains cellulose and lignin, or the least digestible fractions of fiber.

Starch, which is soluble in the cell, is composed of two types of glucose polymers, amylose and amylopectin. Unlike cellulose or hemicellulose, the components of starch can be digested by animal enzymes. Amylose is made up of linear chains of alpha-1,4 linked glucose branching approximately every 200 glucose units (Buleon et al., 1998). Amylopectin is primarily branched, with alpha-1,4 glucose chains linked by alpha-1,6 bonds. Amylopectin is the most abundant component of starch. These two components make up starch granules found in feed ingredients, especially in cereal grains. Cereal grains are composed of three layers, the pericarp, germ, and endosperm. The pericarp is the outermost layer, serving to protect and aid in water regulation. The germ contains oils and genetic material for future plant growth. The endosperm, which is composed of four layers, contains high starch content and represents 60 to 90% of the grain volume (Eckhoff and Watson, 2009). The four layers are as follows: aleurone layer, peripheral endosperm, vitreous endosperm, and floury endosperm. The aleurone layer contains vitamins, minerals, and enzymes. The peripheral endosperm and vitreous endosperm contain starch granules that are encased in a protein matrix of prolamins and polysaccharides. This matrix is hydrophobic and resistant to enzymatic hydrolysis. The innermost layer, the floury endosperm, contains the majority of starch granules and does not contain a prolamin matrix (Giuberti et al., 2014). Due to its unprotected nature, the floury endosperm is most available to grain processing and enzymatic digestion.

Digestibility and availability of starch in the rumen or hindgut depends upon the grain species and subsequent processing (Silveira et al., 2007; Deckardt et al., 2013; Ferraretto et al., 2018). The starch and crude protein concentrations can vary greatly between different grain species (Fellner et al., 2008). When feeding other grain species, these factors will influence starch digestibility and resistance to digestion. For example, the presence of the corn prolamin matrix will lead to decreases in ruminal starch fermentation. Silage fermentation allows microbes prolonged exposure to the prolamin matrix, continually degrading it as ensiling time increases (Guiberti et al., 2014; Jurjanz and Monteils, 2005). Once in the rumen, broken prolamin linkages between starch granules can allow microbes to better degrade the feed (Hoffman et al., 2011). Additionally, the mean particle size of feed affects gastrointestinal starch digestibility. Gallo et al. (2016) found that increases in the average particle size of both corn and barley meal linearly decreased ruminal starch digestibility. The available surface area of the feed particle is directly related to bacterial attachment and enzymatic digestion (Guiberti et al., 2014), with larger particles providing a lower surface area to volume ratio, thus decreasing degradation. Finally, chemical processing of grain may increase starch resistance to ruminal starch degradation, potentially decreasing the risk of starch-induced health disorders (Deckardt et al., 2013).

Feeding both fiber and starch are vital to maintaining animal health and productivity. Starch proves the most important energetic component to lactating dairy cattle diets, providing glucose for microbial growth (Zebeli et al., 2010) and gluconeogenic substances for the host. Although fiber also provides energy, it is mainly fed because it is slow to break down and maintains rumen health. Physically effective fiber, or fiber that promotes rumination, allows for long rumen retention times and increases salivary buffering. Both components are important to the diet, as too much degradable starch will reduce rumen function, milk yield, and feed intake (Nocek and Tamminga, 1991; Mertens, 1997), but too much fiber will decrease feed intake, energy levels, and production (Mertens, 1997). Depending on the type of forage, NDF retained above 1.18 mm in length should make up 30% or more of the diet (Zebeli et al., 2010). This will maintain rumen health and prevent production losses.

1.2.2 Rumen and Hindgut Starch Digestion

When feed enters the rumen from the esophagus, carbohydrates are degraded by either fibrolytic or amylolytic bacteria and other microbes. Starch is degraded by protozoa, fungi, and amylolytic bacteria within the rumen. Ruminal degradation accounts for approximately 75 to 80% of starch intake, making it the predominant location of starch digestion (Harmon, 2009). Protozoa ingest and digest starch granules independent of bacterial digestion, sequestering some of the starch that enters the rumen from bacterial fermentation. Fungal hyphae aid in starch digestion by disrupting plant cellular membranes, making it easier for amylolytic bacteria to attach to feed particles. Attachment prompts bacteria to begin secreting enzymes, making it an important first step in ruminal digestion of starch. Approximately 75% of protein and carbohydrate digestion occurs from bacteria that are attached (McAllister et al., 1994). After attachment, amylolytic bacteria can produce endo- and exo-alpha amylases to hydrolyze the alpha-1,4 and alpha-1,6 bonds found in starch granules. This releases oligosaccharides that can further be broken down into VFAs that provide energy for microbial growth or are absorbed by the cow.

Continued digestion of starch occurs when any starch that escapes ruminal degradation enters the small intestine. When in the lumen of the proximal small intestine, alpha-amylase released from the pancreas begins to hydrolyze the internal alpha-1,4 glycosidic bonds found in starch granules, producing maltose, maltotriose, and limit dextrins (Harmon et al., 2004; Harmon 1993). Alpha-amylase is an endoglycosidase produced by acinar cells in the pancreas and is packaged into zymogen granules until being released into the duodenum. Oligosaccharidases secreted by intestinal enterocytes break down the leftover oligosaccharides, completing starch digestion. Glucose is then absorbed across the intestinal wall, providing energy to the cow.

Final digestion of starch occurs in the large intestine and cecum. The hindgut accounts for approximately 5% of total-tract starch digestion in lactating cows (Gressley et al., 2011). Despite the hindgut having a lower capacity for fermentation than the rumen, any decreased starch digestion in the rumen will be associated with higher hindgut starch concentrations (Gressley et al., 2011). As in the rumen, microbes in the hindgut attach to any undigested starch granules and digest them to produce VFAs. One major difference in starch digestion between the rumen and the hindgut is the lack of protozoa in the hindgut, providing no sequestering of starch or slowing of VFA production (Hume, 1997; Jouany et al., 1988). As with ruminal digestion, the higher the concentrations of starch, the more volatile fatty acids produced, providing energy to the microbes and to the ruminant animal.

1.3 VFA Absorption and GI Buffering

As microbes within the rumen and intestinal tract ferment plant carbohydrates and proteins, they produce VFAs, lactic acid, CO2, and microbial protein. Carbon dioxide is typically lost through eructation, and microbial protein is either digested and absorbed in the small intestine or excreted in the feces. Volatile fatty acids and lactate, however, can manipulate the pH environment of the gastrointestinal tract. Volatile fatty acid absorption out of the gastrointestinal tract can occur through passive diffusion or active transport. Passive diffusion into the epithelial cells can only occur with undissociated acids. Acetate, propionate, and butyrate have pKas of 4.76, 4.82, and 4.87, respectively, and will immediately dissociate once in the cell due to its internal pH of approximately 7 (Dijkstra et al., 2012). The H^+ ion concentration inside the cell is then increased and exchanged with luminal Na^+ through sodium/hydrogen exchangers (Martens and Gäbel, 1988). This exchange maintains intracellular pH while continuing uptake and utilization of volatile fatty acids. Transport of a dissociated volatile fatty acid involves an exchange of a bicarbonate ion through carrier proteins. The dissociated VFA is brought into the cell and neutralized when the enzyme carbonic anhydrase catalyzes the reaction of water and carbon dioxide from the bloodstream into a hydrogen proton and bicarbonate anion (Aafjes, 1967). The bicarbonate is then released into the lumen of the gastrointestinal tract to buffer the environment, while the hydrogen proton returns to the lumen through the sodium/hydrogen exchangers. The hydrogen proton can then react with the bicarbonate anion to produce water and carbon dioxide, or to produce an undissociated VFA and restart the cycle of absorption.

Gastrointestinal tract buffering proves particularly important, especially in the rumen. According to Erdman (1988), rumen pH is a function of ruminal bacterial production of VFAs and their rate of absorption, as well as water influx and outflow, feed acidity, and the inflow of buffers and saliva. Saliva contains high levels of bicarbonate, buffering the rumen environment and providing approximately half of the bicarbonate that enters the rumen (Owens et al., 1998). Forage chop length represents an important contributor to dietary buffering, as longer feed particle size increases cow rumination. The reticulo-omasal orifice has a diameter of approximately 2 cm when dilated for feed passage (Herdt, 2020) and while particles of 5 cm may pass from the rumen, most particles leaving the rumen are smaller than 1 mm (Welch, 1986). To achieve the particle size necessary to leave the foregut, multiple rounds of rumination may be necessary, which increases the amount of saliva entering the rumen. Higher levels of forage with effective fiber as compared to grain will increase the rates of rumination, thereby increasing the saliva and bicarbonate entering the rumen (Maekawa et al., 2002). Buffering occurs when bicarbonate enters the rumen and is protonated to become carbonic acid. Carbonic acid reaches equilibrium with water and dissolved carbon dioxide, and when carbon dioxide is eructated from the rumen the buffering efficiency increases. In addition to endogenous bicarbonate buffering, exogenous buffers are commonly supplemented in the ration. These include sodium bicarbonate, calcium carbonate, magnesium oxide, and sodium carbonate, which work to increase the pH in the gastrointestinal tract. In dairy cattle, buffers contribute to a healthy rumen pH, increased milk fat percentage, and changing VFA production and feed digestibility levels (Erdman, 1988; Erdman et al., 1982).

1.4 Acute, Subacute Ruminal Acidosis, and Hindgut Acidosis

1.4.1 Acute Ruminal Acidosis

When fed high levels of forage, the slow microbial fermentation of fiber provides a steady production of VFAs which can be quickly absorbed by rumen epithelial cells into the bloodstream. Combined with continuous buffering from salivary bicarbonate due to frequent rumination, rumen pH can remain relatively stable at approximately 6.0 - 6.8, with a diverse and balanced microbial community. One of the significant challenges in adding higher starch content to cattle diets is the increased likelihood of ruminal acidosis. Acidosis is classified as either acute or subacute, depending on the magnitude of pH depression. Acute ruminal acidosis refers to highly acidic conditions in the rumen, with ruminal pH reaching 5.2 or lower. These low pH levels can lead to feed intake and milk depression, lameness, and even death (Owens et al., 1998). Acute ruminal acidosis is primarily a concern in beef cattle due to high starch concentrations in the ration.

Increasing levels of quickly fermented carbohydrates such as starch due to high concentrate diets begins the initial reduction of rumen pH (Steele et al., 2011; Plazier et al., 2008). Microbially, fiber fermenters are sensitive to pH changes. If the pH drops too low, fibrolytic bacteria will not be able to grow, and fiber fermentation lessens. Fiber fermenting bacteria in the rumen such as *Ruminococcus albus* and *Fibrobacter succinogenes* exhibit lowered abundance when exposed to acidosis-inducing diets (Ogunade et al., 2019). At pH 6.0-6.3, cellulose digestion begins to slow (Stewart, 1997; Erdman, 1988), and at pH <5.9 most fiber fermenting bacteria including ruminococci and *F. succinogenes* begin to die (Russell and Dombrowski, 1980; Nagaraja and Titgemeyer, 2007). Amylolytic bacteria, on the other hand, thrive in lower pH levels, with higher rates of growth and activity (Mackie et al., 1978). The drop in rumen pH will initially increase the absorption of VFAs out of the rumen due to increased permeability of rumen epithelial cells to their undissociated forms (pKa of approximately 4.8 for the most common VFAs) (Danielli et al., 1945). However, if the pH continues to decrease, fibrolytic bacteria will not be able to survive and production of VFAs will rest entirely on amylolytic bacteria. When fermenting starch or soluble sugars, amylolytic bacteria generally have two endpoints: propionate or lactate. Lactate, with a pKa of 3.86, is a much stronger acid than the main VFAs, and will continue to decrease the pH, further favoring lactate-producers (Dijkstra et al., 2012;

Tajima et al., 2000). High levels of grain and low pH lead to increased abundance of gram-negative bacteria such *Megasphaera elsdenii*, *Selenomonas ruminantium*, *Proteobacteria*, and lactate-producers such as *Lactobacillus* and *Streptococcus bovis* (Tajima et al., 2000). Eventually, even the lactate-producing and lactate-utilizing bacteria will die off, leaving an extremely acidic rumen with no bacteria that can utilize it. Acute acidosis can lead to gastrointestinal tract injury, coma, and possible animal death (Vestweber et al., 1974; Mohamed Nour et al., 1998).

1.4.2 Subacute Ruminal Acidosis

The downward spiral from a healthy rumen into acute acidosis does not occur every time the rumen pH declines, but continued feeding of high starch diets can still cause subacute ruminal acidosis (SARA). SARA is not as immediately threatening, but long-term or chronic SARA occurrences can lower performance and negatively affect cow health. Far more widespread and more difficult to diagnose, SARA commonly affects dairy cattle and refers to the rumen pH dropping below a threshold value. Common values are either when the rumen pH drops below 5.6 for at least 3 hours a day (Gozho et al., 2005), or below 5.8 with no threshold of time (Beauchemin et al., 2003). As there remains some variability in the definitions of the disease and an inability to directly measure rumen pH in non-cannulated cows, SARA diagnoses are difficult to achieve. Subacute ruminal acidosis is a metabolic disease that affects up to an estimated 26% of dairy cattle in the United States, costing the dairy industry roughly $400 per cow per lactation (Plaizier et al., 2008). Similarities between acute acidosis and SARA include decreased feed intake and diet digestibility, lameness, localized or systemic inflammation, and decreased production (Plaizier et al., 2008;

Krause and Oetzel, 2006; Khafipour et al., 2009a). Additionally, SARA typically results in altered milk composition and diarrhea (Noeck, 1997).

Although rumen pH does not drop as significantly during bouts of SARA as it would during acute acidosis, fiber fermenters are still affected. As mentioned previously, most fibrolytic bacteria are unable to survive below a pH of 5.8, which is a common threshold value marking SARA onset. Due to acidic conditions, fibrolytic bacterial functions are impaired, lowering fiber digestion (Krajcarski-Hunt et al., 2002; Shi and Weimer, 1992). Acidic conditions in the rumen are caused by starch fermentation, producing VFAs more rapidly than they are absorbed. At a rumen pH of 5.6 to 6.0, the growth rate and activity of *S. bovis*, a lactate producer, and *M. elsdenii*, a lactate utilizer, were found to be in equilibrium (Goad et al., 1998; Enemark et al., 2002). Unlike acute acidosis, this suggests that decreases in rumen pH during SARA are due to high VFA concentrations, not lactate. Chronic low pH conditions can cause microlesions and parakeratosis in rumen epithelium, slowly breaking down the rumen barrier (Kleen et al., 2003; Steele et al., 2009). Any reduction in absorption of VFAs out of the rumen caused by inflammation or parakeratosis in the rumen wall from low pH will both increase the risk of SARA and increase its dangers (Plaizier et al., 2008). As mentioned previously, high levels of concentrate and low pH will change the microbial community makeup, altering VFA production. Increased fiber digestion will increase acetate:propionate levels while starch digestion decreases this ratio (Erdman, 1988). Acetate concentrate is a primary driver of milk fat production, so the lower levels of acetate production seen in cows with SARA decreases milk fat (Bauman and Griinari, 2003).

While this reduction in fatty acid production can be somewhat attributed to a decline in acetate, reduction mainly occurs due to trans-10,cis-12-conjugated linoleic acid (CLA) production (Baumgard et al., 2000). When feeding diets high in concentrate, triglycerides are hydrolyzed into glycerol and free fatty acids. Glycerol is fermented to propionate, but free fatty acids are toxic to rumen microbes (Jenkins and Palmquist, 1984). Unsaturated fatty acids are then biohydrogenated to become saturated fatty acids, eventually leaving the rumen for digestion in the intestines. During the lowered pH associated with SARA, biohydrogenation is inhibited and remains incomplete, producing intermediate conjugated linoleic acids (CLA) such as trans-10,cis-12. Trans-10,cis-12 CLA inhibits milk fat synthesis (Baumgard et al., 2001), changing milk fatty acid profiles for up to 4 days after animal exposure (Harvatine and Bauman, 2011).

The transition cow represents a unique situation in which the dairy cow is predisposed towards metabolic disease and inflammation, specifically SARA. The transition period is generally referred to as between the 3 weeks before and 3 weeks after parturition. Changes during this time include giving birth, producing milk, energy deficit, and switching from a high fiber forage-based diet to a higher starch diet to support milk production. Due to these major metabolic, immune, and dietary changes, as well as reduced absorptive capacity of rumen papillae that occurs during the dry period, the transition cow experiences higher incidences of SARA (Dirksen et al., 1985).

1.4.3 Hindgut Acidosis

Increased starch flow to the hindgut can cause excessive fermentation, leading to hindgut acidosis. Not as heavily studied as acute ruminal acidosis or SARA, hindgut acidosis occurs concurrently, with many of its symptoms typically attributed to the two more studied types of acidosis. Hindgut acidosis involves starch fermentation resulting in increased VFA production, leading to a drop in fecal pH and possible injury to intestinal tissue (Gressley et al., 2011; Hall, 2002). While there is not yet a standardized threshold for fecal pH to characterize hindgut acidosis, the range typically considered is from 6.0 to 6.6 (Neubauer et al., 2020; Metzler-Zebeli et al., 2013). Due to low hindgut pH levels, the epithelium layers slough off, decreasing barrier function. Meanwhile, the body attempts to protect the injured tissue by producing additional fibrin and mucin, which make their way into the feces (Hall, 2002; Argenzio et al., 1988). As the hindgut does not have access to salivary bicarbonate for acid buffering and does not have a protective epithelial layer of keratinized cells, uncontrolled acid production will cause more damage than it would in the rumen. Excessive fermentation increases microbial activity, producing microbial protein and CO2 which give the feces a frothy appearance (Plaizier et al., 2008). This increase in microbial protein production drops apparent total tract protein digestibility.

1.4.4 Endotoxin

The presence of highly fermentable starch prompts rapid growth of gram-negative bacteria, as well as bacterial lysis and death due to low pH conditions. Gram negative bacteria naturally contain the glycolipid lipopolysaccharide (LPS), also known as endotoxin, within their outer cellular membrane (Nagaraja et al., 2007). The LPS molecule consists of two or three regions depending on bacterial strain: lipid A, inserted into the cell wall, the core oligosaccharide, and the variable outer O-antigenic side chain (Monteiro and Faciola, 2020). A common structural part of gram-negative bacteria, LPS is always found in the gastrointestinal tract. Cattle experiencing experimentally induced SARA demonstrate higher free ruminal LPS levels as opposed to their healthy peers. In a study conducted by Gozho et al. (2006), ruminal LPS concentrations were 6,310, 18,197, and 26,915 EU/ml in steers fed an all-forage diet, 61% concentrate diet, and when SARA was induced, respectively. Similarly, Li et al. (2012) demonstrated ruminal LPS concentrations of 10,405 EU/ml when fed a 70% forage diet as compared to 168,391 EU/ml when fed a diet in which 34% of dietary dry matter was replaced with ground wheat and barley. LPS concentrations in the gastrointestinal tract vary greatly due to diet. LPS can reach other areas of the GI tract, including the small intestine and hindgut. When gram negative bacteria or free LPS from the rumen enter the abomasum, acidic conditions can deactivate LPS (Ribeiro et al., 2010). Additionally, any LPS that escapes deactivation in the abomasum can also be degraded by bile salts in the duodenum (Bertok, 2004). However, up to 44% of starch can bypass the rumen and be digested in the lower GI tract (Allen, 2000), suggesting that any increased LPS presence in the intestines is mainly caused by postruminal starch fermentation. In a study from Li et al. (2012), dairy cows given a grain-based SARA inducing diet had higher levels of starch reach the cecum, and higher LPS levels in the cecum and feces as compared to the control, suggesting LPS production due to hindgut fermentation. Post-ruminal starch infusions have been shown to increase the concentration of gram-negative and coliform bacteria in the hindgut (Van Kessel et al., 2002), again suggesting that post-ruminal starch fermentation can lead to increases in endotoxin.

1.4.4.1 Endotoxin Inflammation

High levels of concentrate in the diet causes low pH and endotoxin production, which can lead to inflammation and damage to the gastrointestinal tract. When fed an acidosis-inducing diet, dairy cattle experienced reductions in ruminal epithelial layer width, exhibiting papillary lesions and a decrease in structural integrity (Steele et al., 2011). Sloughing of the outer layers of epithelium in the rumen can lead to barrier permeability, allowing LPS and other potentially toxic substances produced by SARA diets into systemic circulation (Saleem et al., 2012; Plaizier et al., 2008). The lipid A region of endotoxin is biologically active and is a potent antigen that stimulates a strong pro-inflammatory immune response once past the gastrointestinal epithelial barrier (Erridge et al., 2002). Depending on the type of bacteria, LPS induces differing levels of immune responses. For example, *Escherichia coli* LPS exhibits stronger virulence than *Bacteroidetes* due to subtle differences in lipid structure (Sonesson et al., 1994; Berezow et al., 2009). Lipopolysaccharide can diffuse across rumen and colon tissues independent of pH value through the transcellular and paracellular routes but decreases in pH will allow other toxic compounds to translocate (Emmanuel et al., 2007). While abscesses in the rumen epithelia may be a path of entry for microbial toxins, the intestines may also be a site of LPS entry. In an experiment using intestinal epithelial cell lines, Chin et al. (2006) observed increased cell apoptosis, increased permeability, and disrupted tight junction proteins due to increases in luminal LPS. Endotoxin can also inhibit enterocyte pH regulatory systems, such as the sodium-hydrogen pump (Cetin et al., 2004). Thus, when exposed to acidic conditions, enterocytes are unable to maintain cellular pH homeostasis. Lipopolysaccharides and other toxic compounds can reach systemic circulation through lymphatic vessels or the portal vein after entering a ruminal barrier breach or a “leaky” gut junction. When in circulation, chronic conditions such as pneumonia, arthritis, endocarditis, pyelonephritis, and even liver abscesses (Oetzel, 2007).

After passing through the epithelial barrier, free endotoxin and microbes can encounter immune cells that begin the inflammatory process. Once in circulation, LPS-binding protein (LBP) complexes with LPS and binds to CD14 found on the surface of macrophages, neutrophils, and dendritic cells. CD14 associates with TLR-4, a pattern recognition receptor, which complexes with the protein myeloid differentiation-2, or MD-2, leading to myeloid cell activation (Beutler et al., 2003). Once activated, these innate immune cells will produce pro-inflammatory cytokines, commonly interleukin-1 (IL-1), IL-6, and TNF-α. These cytokines will circulate and result in the production of acute phase proteins as part of the acute phase response. For responses to endotoxin, common acute phase proteins include serum amyloid A (SAA) and haptoglobin. In cattle, LBP, SAA, and haptoglobin are used to detect inflammation due to LPS. When observing the serum levels of LBP and haptoglobin in calves infected with gram negative bacteria, LBP levels rose significantly 6 hours after infection and reached their peak at 24 hours, while haptoglobin rose 12 hours after infection and peaked at 48 hours (Schroedl et al., 2001). Both plasma proteins prove useful diagnostic markers in detecting endotoxin invasion. In response to grain-induced SARA, plasma LPS, serum LBP and SAA were all increased (Khafipour et al., 2009a). Similarly, in a study where SARA diets increased both ruminal and hindgut starch fermentation, circulating LBP levels were increased due to LPS translocation (Li et al., 2012). Overall, the acute phase response commonly causes decreased feed intake, changes in metabolism, and fever (Steiger et al., 1998).

1.5 Fed Buffers to Alleviate Acidosis

1.5.1 Rumen Buffers

As mentioned previously, dietary buffers are commonly added into lactating dairy cattle rations to increase rumen pH and regulate rumen health. High starch diets will decrease gastrointestinal tract pH levels, making dietary buffers especially useful in keeping levels from dropping to dangerous levels. By definition, a buffer must be water soluble, a weak acid, base, or salt, and it must have a pKa near the physiological pH of the system it is buffering (Erdman, 1988). In the case of dairy cattle, a dietary buffer should be a weak base or salt in order to keep rumen pH just below neutral. According to Clark et al. (1989), mineral salts such as sodium bicarbonate, magnesium oxide, and calcium carbonate function by maintaining hydrogen ion concentrations in the gastrointestinal tract, by increasing liquid rate of passage out of the rumen, or by both.

The most commonly added dietary buffer into dairy cattle diets is sodium bicarbonate. When added to the diet, sodium bicarbonate typically increases milk fat yield, milk fat percentage, and rumen pH (Erdman et al., 1982; Rogers et al., 1985). In a meta-analysis looking at sodium bicarbonate additions to the diet, Hu and Murphy (2005) found no changes in milk production, milk protein proportion, or milk protein yield. They did discover increases in dry matter intake and milk fat due to increases in ruminal pH and changes in ruminal VFA proportions. Across experiments, ruminal propionate proportions were decreased by approximately 2.4 percentage units when fed buffer on a corn-based diet, increasing acetate:propionate ratios (Hu and Murphy, 2005). In another study, the addition of sodium bicarbonate and roughage increased rumen pH and decreased the flow of trans-CLAs out of the rumen, which increased milk fat (Troegeler-Meynadier et al., 2007). This demonstrates the positive effects that sodium bicarbonate buffers can have on ruminant animal production levels. Sodium bicarbonate supplementation has been shown to increase total tract nutrient digestibility of ADF (Erdman et al., 1982; Marden et al., 2008) and NDF (Erdman et al., 1982). When fed, sodium bicarbonate positively affects ruminal fermentation, increasing the pH and therefore increasing dry matter intake, ADF and NDF digestibility, and milk fat production.

A mineral salt commonly fed to dairy cattle, magnesium oxide, also acts to raise gastrointestinal pH. Despite low solubility in the rumen at normal pH, magnesium is a strong alkalinizing agent and can still raise rumen pH (Erdman, 1988; Schaefer et al., 1982, Le Ruyet and Tucker, 1982). As magnesium is absorbed in the rumen prior to the abomasum (Martens and Rayssiguier, 1980) and its solubility depends on rumen pH and particle size (Xin et al., 1989), the alkalizing ability of magnesium oxide within the rumen can be variable. Rumen pH can be increased (Erdman et al., 1982), increased depending on the source of magnesium oxide (Xin et al., 1989; Bach et al., 2018), or unaffected by dietary magnesium oxide (Stokes et al., 1986; Neiderfer et al., 2020). Ruminal VFA levels are also variably affected by magnesium oxide supplementation. Total rumen VFA concentrations do not change (Neiderfer et al., 2020; Xin et al., 1989; Erdman et al., 1982), but molar proportions of acetate, propionate, butyrate, and isobutyrate can (Neiderfer et al., 2020; Erdman et al., 1982; Stokes et al., 1986; Xin et al., 1989). When fed a diet with corn as the primary source of forage, low levels of magnesium oxide in the diet can increase intake, milk yield or milk fat (Erdman et al., 1982; Teh et al., 1985). Higher levels of magnesium oxide, up to 40 g/kg, can increase milk fat percentage but not affect milk yield or milk fat production (Xin et al., 1989). When included in diets not based on corn silage, magnesium oxide did not significantly increase intake or milk fat (Bach et. al, 2018; Holtenius et al., 2008; Stokes et al., 1986). Total tract nutrient digestibility changes due to magnesium oxide supplementation remain conflicting. In some studies, dry matter, fiber, or starch digestibilities were increased due to supplementation (Erdman et al., 1982; Stokes et al., 1986; Pierce et al., 1983), while others observed no effects (Neiderfer et al., 2020; Christiansen and Webb, 1990).

Calcium carbonate, or limestone, is another commonly fed dietary buffer. Similarly to magnesium oxide, calcium carbonate has high alkalizing ability, but low solubility in the rumen due to pH (Erdman, 1988). However, calcium carbonate has been shown to increase rumen pH and change VFA concentrations of butyrate and isovalerate in one study (Keyser et al., 1985), but not in others (Rogers et al., 1982, 1985; Clark et al., 1989; Neiderfer et al., 2020). When fed calcium carbonate, animals had reductions in dry matter intake, milk production, or milk protein, and no changes in milk fat production as compared to control diets (Rogers et al., 1982, 1985; Clark et al., 1989). As with magnesium oxide, total tract nutrient digestibility changes due to calcium carbonate supplementation remain inconsistent. In some studies, dry matter, organic matter, or starch digestibilities were increased due to supplementation (Rogers et al., 1982; Clark et al., 1989), while others observed no effects (Neiderfer et al., 2020; Rogers et al., 1985; Christiansen and Webb, 1990). Rogers et al. (1982) observed decreased protein digestibility, most likely due to increased microbial activity in the hindgut due to higher pH levels.

1.5.2 Hindgut Buffers

When feeding cows, the dairy industry typically includes 20-30% starch in the diet to support lactation (Chase, 2007; Dann et al., 2014). Dietary buffers are fed to increase rumen pH and productivity. However, these starch-rich diets increase fermentation in the hindgut, prompting interest in hindgut buffers that would alleviate the acidic conditions in the hindgut. Due to their limited rumen solubility, magnesium oxide and calcium carbonate are possible hindgut buffers (Neiderfer et al., 2020). Magnesium oxide consistently increases fecal pH and decreases fecal consistency and dry matter (Erdman et al., 1982; Schaefer et al., 1982; Teh et al., 1985). Decreases in fecal consistency and dry matter are likely due to the osmotic activity of unabsorbed magnesium salts in the intestines (Donowitz, 1991). Calcium carbonate has been observed to increase intestinal and fecal pH (Christiansen and Webb, 1990; Clark et al., 1989; Rogers et al., 1982), or to have no effect on fecal pH (Keyser et al., 1985). The increase in fecal pH is likely connected to decreases in fecal starch (Clark et al., 1989; Rogers et al., 1982), suggesting that calcium carbonate buffers the small intestine, increasing enzymatic starch digestion (Wheeler and Noller, 1977). The goal of hindgut buffers is to buffer the intestines, reducing incidences of increased fermentation and reduced digestibility. However, in one study, buffer inclusion increased total fecal VFA, acetate, and propionate levels, indicating increased fermentation in the hindgut despite increased fecal pH (Neiderfer et al., 2020).

1.6 Microbial Communities in the Gastrointestinal Tract

1.6.1 Microbial Colonization of the Gut

The mammalian gastrointestinal tract is colonized by microorganisms immediately following birth due to random sampling from the surrounding environment. Colonization can occur from microbes in the vagina during delivery, skin or rearing material surfaces during suckling, colostrum, and milk (Curtis and Sloan, 2004; Lindberg et al., 2004). Milk and colostrum will carry microbiota that can colonize the gut (Liu et al., 2020; Hunt et al., 2011). Many of these microbes are considered commensal, or beneficial. For example, certain *Bifidobacterium* species commonly found in mammalian colostrum and milk can prevent mortality in mice due to colonization of pathogenic *Eschericia coli* (Fukuda et al., 2011). Commensal or beneficial bacteria do not produce toxins and may ferment carbohydrates or aid in immune function (Keerthi et al., 2021). Signals produced by commensal organisms can increase gut barrier integrity, change gut vasculature, as well as communicate with other body organs such as the skin, lungs, brain, and heart (Stappenbeck et al., 2002; Kalliomäki et al., 2001; Arrieta et al., 2015; Tomlinson et al., 2002; Duewell et al., 2012). Therefore, colonization of the gut with beneficial microbes remains an important factor when assessing animal health.

As adolescent animals mature, many factors contribute to the gut microbial community. Changes in diet, feeding management, age, geographic location, season, stress, use of antibiotics, and general environment can affect the rumen microbiome (Puniya et al., 2015; Shanks et al., 2011), as well as the lower tract (Petri et al., 2019; Hagey et al., 2019). The impact of dietary changes is the most studied, and the composition of the rumen and intestinal microbiome can be changed by shifts in diet (Tajima et al., 2001; Plaizier et al., 2017a). Microbial community modifications will be reflective of available substrate and can therefore change dramatically based on diet. Typically, higher diversity within the gastrointestinal tract allows for better stability and resistance of dysbiosis (Lozupone et al., 2012).

1.6.2 Rumen and Hindgut Composition

As mentioned before, the rumen is the primary site of microbial fermentation, containing a diverse ecosystem of microorganisms. The most abundant of these, bacteria, are found in a concentration of approximately 10^{10} - 10^{11} cells/mL, with over 200 species (McSweeney and Mackie, 2012). The second most abundant, archaea, are approximately 10^{6} - 10^{8} cells/mL (Lin et al., 1997). Commonly known as methanogens, rumen archaea are anaerobic organisms that can produce methane by reducing carbon dioxide with hydrogen gas. Thus, methanogens compete for H_2 and carbon sources. Ciliate protozoa are found in an abundance of 10^{4} - 10^{6} cells/mL, and work to digest starch, fiber, and other bacteria (McSweeney and Mackie, 2012; Bach et al., 2005). Protozoa, larger in size than bacteria, can account for approximately 40% of rumen microbial biomass (Russell and Rychlik, 2001). Finally, ruminal fungi, found at approximately 10^{3} - 10^{6} zoospores/mL, assist in degrading dietary plant cell walls (Matthews et al., 2018). The diversity and abundance of microorganisms found in the rumen allows it to better weather extreme conditions such as acidosis, as well as digest complex carbohydrates such as cellulose and hemicellulose. In the hindgut, bacteria are the primary microorganisms that continue fermentation at a concentration of approximately 10^{10} - 10^{11} cells/mL (Callaway et al., 2010). The hindgut lacks protozoa, but archaea (between 10^{8} - 10^{10} cells/g DM in human colon) and fungi (10^{3} - 10^{5} zoospores/mL DM) present aid in continued digestion of nutrients (Hume, 1997; Davies et al., 1993; Miller and Wolin, 1986; Gordon and Phillips, 2007).

Among bacteria, the gram-negative Bacteroidetes and the gram-positive Firmicutes phyla are the most abundant in the foregut and hindgut of cattle and can represent up to 95% of bacteria (Khafipour et al., 2016; Plaizier et al., 2017b). Reductions in richness, evenness, and diversity in the rumen, hindgut, and fecal microbiome occur when exposed to high starch diets, as well as changes in lower abundance phyla (Plaizier et al., 2017a; Plaizier et al., 2017b). When fed high amounts of starch, the relative abundances of fiber fermenters such as Bacteroidetes and Fibrobacteres decline while Firmicutes increase in the rumen (Mao et al., 2013; Khafipour et al., 2009b; Plaizier et al., 2017a). However, these changes to primary phyla do not always prove true in the hindgut and feces. In a study looking at microbial changes in the rumen, cecum, and feces due to a grain-based SARA challenge, Plaizier et al. (2017b) only observed decreased Lentisphaerae and Verrucomicrobia in the cecum, and decreased Lentisphaerae and Cyanobacteria in the feces. Petri et al. (2019) observed decreases in fecal Fibrobacteres and Cyanobacteria with increasing dietary starch, and a trend for increasing Proteobacteria. In addition, Plaizier et al. (2017a) observed increased fecal Actinobacteria but decreases in Tenericutes, Proteobacteria, Cyanobacteria, Fibrobacteres, and Verrucomicrobia, with a trend for increased Spirochaetes when exposed to SARA conditions.

1.7 Species Specific Kinome Arrays

1.7.1 Phosphorylation Measuring Protein Activity

Bovine research has no shortage of work published using transcriptomic techniques to measure changes in diseased or stressed states, describing both animal (Liao et al., 2009; Rosa et al., 2021) and milk production responses (Wellnitz et al., 2011; Zhang et al., 2018; Fougère and Bernard, 2018). Transcriptomic techniques provide plentiful in-depth information describing mRNA expression changes, showing which genes are being expressed. However, transcriptional analysis does not always highly correlate with phenotypical changes due to post-transcriptional events. mRNA transcription of a gene does not ensure protein translation, and certainly does not ensure a functional protein. Post-transcriptional regulatory events like gene silencing, protein turnover, mRNA stability, and activation or deactivation of proteins, among others, are not accounted for when analyzing mRNA transcripts (Arsenault et al., 2011). When analyzing mRNA transcripts, the absence of correlation between mRNA quantity and protein quantity is in part due to mRNA translation regulation, further adding to the challenges in relating transcriptional analysis to phenotypical changes (Greenbaum et al, 2003). Additionally, frequent regulatory events that direct protein location and functionality exist, and these post-translational modifications include phosphorylation, ubiquitination, sumoylation, and glycosylation (Mann and Jensen, 2003). Therefore, studying the activity of these protein kinases which affect post-translational modifications proves valuable in providing a clearer view of cellular activities.

Phosphorylation is the most common of these post-translational modifications. Many proteins involved in immunological and metabolic signaling pathways are controlled by phosphorylation. This phosphorylation can activate or deactivate these proteins, regulating the pathway. Species-specific kinome arrays use genomic information available for different species, predicting phosphorylation sites based on conserved human and mouse phosphorylation target sites (Jalal et al., 2009). These arrays can be used to observe the phosphorylation of different proteins involved in innate and adaptive immune and metabolic signaling pathways (Arsenault et al., 2014; Aylward, 2020). As the level of phosphorylation on a specific protein site can change quickly, within 10-30 minutes after exposure to different stimuli (Consitt et al., 2008;

Olsen et al., 2006), these species-specific peptide arrays can be used to rapidly visualize the immunometabolic signaling response.

1.8 Significance of Research

Lactating dairy cows are often fed starch-rich diets in order to meet the demands of milk production. However, these diets can lead to excessive starch fermentation in the rumen and in the hindgut, damaging the gastrointestinal epithelium and contributing to local and systemic inflammation. Dietary buffers are commonly fed to alleviate these negative effects in the rumen, but little is known about their impact in the intestines. The goal of this work was to evaluate the potential for two prototype buffer mixes to alter intestinal fermentation under high starch conditions. By feeding a high starch diet while simultaneously abomasally infusing additional starch, we sought to induce excessive hindgut fermentation. We hypothesized that infusing starch would induce hindgut fermentation, decrease nutrient digestibility, and negatively affect cow health. We predicted that feeding the buffer mixes would attenuate the negative effects of the infused starch, and positively affect cow health. By investigating the fecal microbiome, we strove to identify shifts in the hindgut microbial community that could provide a clearer picture of VFA and endotoxin production, as well as diet digestibility. Additionally, through measuring changes in the white blood cell kinome due to infused starch and fed buffers, we sought to identify activated immunometabolic pathways and get a better understanding of cow gastrointestinal health under these conditions.

REFERENCES

Aafjes, J.H. 1967. Carbonic anhydrase in the wall of the forestomachs of cows.. Br. Vet. J. 123:252–256. doi:10.1016/S0007-1935(17)39956-6.

Allen, M.S. 2000. Effects of diet on short-term regulation of feed intake by lactating dairy cattle. J. Dairy Sci. 83:1598–1624. doi:10.3168/jds.S0022-0302(00)75030-2.

Argenzio, R.A., C.K. Henrikson, and J.A. Liacos. 1988. Restitution of barrier and transport function of porcine colon after acute mucosal injury. https://doi.org/10.1152/ajpgi.1988.255.1.G62 255. doi:10.1152/AJPGI.1988.255.1.G62.

Arrieta, M.C., L.T. Stiemsma, P.A. Dimitriu, L. Thorson, S. Russell, S. Yurist-Doutsch, B. Kuzeljevic, M.J. Gold, H.M. Britton, D.L. Lefebvre, P. Subbarao, P. Mandhane, A. Becker, K.M. McNagny, M.R. Sears, T. Kollmann, W.W. Mohn, S.E. Turvey, and B.B. Finlay. 2015. Early infancy microbial and metabolic alterations affect risk of childhood asthma. Sci. Transl. Med. 7. doi:10.1126/scitranslmed.aab2271.

Arsenault, R.J., B. Trost, and M.H. Kogut. 2014. A comparison of the chicken and turkey proteomes and phosphoproteomes in the development of poultry-specific immuno-metabolism kinome peptide arrays. Front. Vet. Sci. 1:1–11. doi:10.3389/fvets.2014.00022.

Arsenault, R., P. Griebel, and S. Napper. 2011. Peptide arrays for kinome analysis: New opportunities and remaining challenges. Proteomics 11:4595–4609. doi:10.1002/pmic.201100296.

Aylward, B.A. 2020. A COMPARATIVE EVALUATION OF THE GASTROINTESTINAL IMMUNE RESPONSE OF THE MODERN AND HERITAGE BROILER CHICKEN. University of Delaware,.

Bach, A., S. Calsamiglia, and M.D. Stern. 2005. Nitrogen metabolism in the rumen. J. Dairy Sci. 88:E9–E21. doi:10.3168/jds.S0022-0302(05)73133-7.

Bach, A., I. Guasch, G. Elcoso, J. Duclos, and H. Khelil-Arfa. 2018. Modulation of rumen pH by sodium bicarbonate and a blend of different sources of magnesium oxide in lactating dairy cows submitted to a concentrate challenge. J. Dairy Sci. 101:9777–9788. doi:10.3168/jds.2017-14353.

Bauman, D.E., and J.M. Griinari. 2003. Nutritional regulation of milk fat synthesis. Annu. Rev. Nutr. 23:203–227. doi:10.1146/annurev.nutr.23.011702.073408.

Baumgard, L.H., J.K. Sangster, and D.E. Bauman. 2001. Milk fat synthesis in dairy cows is progressively reduced by increasing supplemental amounts of trans-10, cis-12 conjugated linoleic acid (CLA). J. Nutr. 131:1764–1769. doi:10.1093/jn/131.6.1764.

Beauchemin, K.A., W.Z. Yang, and L.M. Rode. 2003. Effects of particle size of alfalfa-based dairy cow diets on chewing activity, ruminal fermentation, and milk production. J. Dairy Sci. 86:630–643. doi:10.3168/jds.S0022-0302(03)73641-8.

Berezow, A.B., R.K. Ernst, S.R. Coats, P.H. Braham, L.M. Karimi-Naser, and R.P. Darveau. 2009. The structurally similar, penta-acylated lipopolysaccharides of Porphyromonas gingivalis and Bacteroides elicit strikingly different innate immune responses. Microb. Pathog. 47:68–77. doi:10.1016/J.MICPATH.2009.04.015.

Berg, J.M., J.L. Tymoczko, and L. Stryer. 2002. Cellulose, the Major Structural Polymer of Plants, Consists of Linear Chains of Glucose Units. 3rd ed. Freeman, W H, New York, NY.

Bergman, E.N. 1990. Energy contributions of volatile fatty acids from the gastrointestinal tract in various species. Physiol. Rev. 70:567–590. doi:10.1152/physrev.1990.70.2.567.

Bertók, L. 2004. Bile acids in physico-chemical host defence. Pathophysiology 11:139–145. doi:10.1016/j.pathophys.2004.09.002.

Beutler, B., K. Hoebe, X. Du, and R.J. Ulevitch. 2003. How we detect microbes and respond to them: the Toll-like receptors and their transducers. J. Leukoc. Biol. 74:479–485. doi:10.1189/jlb.0203082.

Birchenough, G.M.H., E.E.L. Nystrom, M.E.V. Johansson, and G.C. Hansson. 2016. A sentinel goblet cell guards the colonic crypt by triggering Nlrp6-dependent Muc2 secretion. Science (80-.). 352:1535–1542. doi:10.1126/science.aaf7419.

Blikslager, A.T., A.J. Moeser, J.L. Gookin, S.L. Jones, and J. Odle. 2007. Restoration of Barrier Function in Injured Intestinal Mucosa. Physiol. Rev. 87:545–564.

Buléon, A., P. Colonna, V. Planchot, and S. Ball. 1998. Starch granules: Structure and biosynthesis. Int. J. Biol. Macromol. 23:85–112. doi:10.1016/S0141-8130(98)00040-3.

Callaway, T.R., S.E. Dowd, T.S. Edrington, R.C. Anderson, N. Krueger, N. Bauer, P.J. Kononoff, and D.J. Nisbet. 2010. Evaluation of bacterial diversity in the rumen and feces of cattle fed different levels of dried distillers grains plus solubles using bacterial tag-encoded FLX amplicon pyrosequencing. J. Anim. Sci. 88:3977–3983. doi:10.2527/jas.2010-2900.

Cetin, S., J. Dunklebarger, J. Li, P. Boyle, O. Ergun, F. Qureshi, H. Ford, J. Upperman, S. Watkins, and D.J. Hackam. 2004. Endotoxin differentially modulates the basolateral and apical sodium/proton exchangers (NHE) in enterocytes. Surgery 136:375–383. doi:10.1016/J.SURG.2004.05.013.

Chase, L.E. 2007. Can we feed less starch to our cows? Pages 213–220 in Proceedings of the Cornell Nutrition Conference for Feed Manufacturers. Cornell University, Ithaca, NY.

Chin, A.C., A.N. Flynn, J.P. Fedwick, and A.G. Buret. 2006. The role of caspase-3 in lipopolysaccharide-mediated disruption of intestinal epithelial tight junctions. Can. J. Physiol. Pharmacol. 84:1043–1050. doi:10.1139/Y06-056.

Christiansen, M.L., and K.E. Webb. 1990. Intestinal acid flow, dry matter, starch and protein digestibility and amino acid absorption in beef cattle fed a high-concentrate diet with defluorinated rock phosphate, limestone or magnesium oxide.. J. Anim. Sci. 68:2105–2118. doi:10.2527/1990.6872105x.

Clark, J.H., A.W. Plegge, C.L. Davis, and G.C. McCoy. 1989. Effects of Calcium Carbonate on Ruminal Fermentation, Nutrient Digestibility, and Cow Performance. J. Dairy Sci. 72:493–500. doi:10.3168/jds.S0022-0302(89)79131-1.

Consitt, L.A., L. Wideman, M.S. Hickey, and R.F. Morrison. 2008. Phosphorylation of the JAK2-STAT5 pathway in response to acute aerobic exercise. Med. Sci. Sports Exerc. 40:1031–1038. doi:10.1249/MSS.0b013e3181690760.

Curtis, T.P., and W.T. Sloan. 2004. Prokaryotic diversity and its limits: Microbial community structure in nature and implications for microbial ecology. Curr. Opin. Microbiol. 7:221–226. doi:10.1016/j.mib.2004.04.010.

DANIELLI, J.F., and M.W. HITCHCOCK. 1945. The mechanism of absorption from the rumen as exemplified by the behaviour of acetic, propionic and butyric acids.. J. Exp. Biol. 22:75–84. doi:10.1242/jeb.22.1-2.75.

Dann, H.M., H.A. Tucker, K.W. Cotanch, P.D. Krawczel, C.S. Mooney, R.J. Grant, and T. Eguchi. 2014. Evaluation of lower-starch diets for lactating Holstein dairy cows. J. Dairy Sci. 97:7151–7161. doi:10.3168/JDS.2014-8341.

Davies, D.R., M.K. Theodorou, M.I.G. Lawrence, and A.P.J. Trinci. 1993. Distribution of anaerobic fungi in the digestive tract of cattle and their survival in faeces. J. Gen. Microbiol. 139:1395–1400. doi:10.1099/00221287-139-6-1395.

Deckardt, K., A. Khol-Parisini, and Q. Zebeli. 2013. Peculiarities of enhancing resistant starch in ruminants using chemical methods: Opportunities and challenges. Nutrients 5:1970–1988. doi:10.3390/nu5061970.

Dijkstra, J., J.L. Ellis, E. Kebreab, A.B. Strathe, S. López, J. France, and A. Bannink. 2012. Ruminal pH regulation and nutritional consequences of low pH. Anim. Feed Sci. Technol. 172:22–33. doi:10.1016/j.anifeedsci.2011.12.005.

Dirksen, G.U., H.G. Liebich, and E. Mayer. 1985. Adaptive changes of the ruminal mucosa and their functional and clinical significance. Bov. Pract. 20:116–120.

Donaldson, G.P., S.M. Lee, and S.K. Mazmanian. 2015. Gut biogeography of the bacterial microbiota. Nat. Rev. Microbiol. 14:20–32. doi:10.1038/nrmicro3552.

Donowitz, M. 1991. Magnesium-induced Diarrhea and New Insights into the Pathobiology of Diarrhea. N. Engl. J. Med. 324:1059–1060.

Duewell, P., H. Kono, K.J. Rayner, C.M. Sirois, G. Vladimer, F.G. Bauernfeind, G.S. Abela, L. Franchi, G. Nũez, M. Schnurr, T. Espevik, E. Lien, K.A. Fitzgerald, K.L. Rock, K.J. Moore, S.D. Wright, V. Hornung, and E. Latz. 2010. NLRP3 inflammasomes are required for atherogenesis and activated by cholesterol crystals. Nature 464:1357–1361. doi:10.1038/nature08938.

Eckhoff, S.R., and S.A. Watson. 2009. Corn and Sorghum Starches: Production. Starch 373–439. doi:10.1016/B978-0-12-746275-2.00009-4.

Emmanuel, D.G.V., K.L. Madsen, T.A. Churchill, S.M. Dunn, and B.N. Ametaj. 2007. Acidosis and Lipopolysaccharide from Escherichia coli B:055 cause hyperpermeability of rumen and colon tissues. J. Dairy Sci. 90:5552–5557. doi:10.3168/jds.2007-0257.

Enemark, J., R. Jorgensen, and P. Enemark. 2002. Rumen acidosis with special emphasis on diagnostic aspects of subclinical rumen acidosis: a review. Vet. ir Zootech. 20:16–29.

Erdman, R.A., R.W. Hemken, and L.S. Bull. 1982. Dietary Sodium Bicarbonate and Magnesium Oxide for Early Postpartum Lactating Dairy Cows: Effects of Production, Acid-Based Metabolism, and Digestion. J. Dairy Sci. 65:712–731. doi:10.3168/jds.S0022-0302(82)82259-5.

Erdman, R.A. 1988. Dietary Buffering Requirements of the Lactating Dairy Cow: A Review. J. Dairy Sci. 71:3246–3266. doi:10.3168/jds.S0022-0302(88)79930-0.

Erridge, C., E. Bennett-Guerrero, and I.R. Poxton. 2002. Structure and function of lipopolysaccharides. Microbes Infect. 4:837–851. doi:10.1016/S1286-4579(02)01604-0.

Espe, D., and C.Y. Cannon. 1940. The Length of the Intestine of Calves and its Bearing on the Absorption of the Nutrients from the Chyme. J. Dairy Sci. 23:1211–1214. doi:10.3168/jds.S0022-0302(40)92833-8.

Fellner, V., J.C. Burns, and D.S. Marshall. 2008. Effect of feeding corn, hull-less or hulled barley on fermentation by mixed cultures of ruminal microorganisms. J. Dairy Sci. 91:1936–1941. doi:10.3168/jds.2007-0078.

Ferraretto, L.F., W.I. Silva Filho, T. Fernandes, D.H. Kim, and H. Sultana. 2018. Effect of ensiling time on fermentation profile and ruminal in vitro starch digestibility in rehydrated corn with or without varied concentrations of wet brewers grains. J. Dairy Sci. 101:4643–4649. doi:10.3168/jds.2017-14329.

Fougère, H., and L. Bernard. 2019. Effect of diets supplemented with starch and corn oil, marine algae, or hydrogenated palm oil on mammary lipogenic gene expression in cows and goats: A comparative study. J. Dairy Sci. 102:768–779. doi:10.3168/jds.2018-15288.

Fukuda, S., H. Toh, K. Hase, K. Oshima, Y. Nakanishi, K. Yoshimura, T. Tobe, J.M. Clarke, D.L. Topping, T. Suzuki, T.D. Taylor, K. Itoh, J. Kikuchi, H. Morita, M. Hattori, and H. Ohno. 2011. Bifidobacteria can protect from enteropathogenic infection through production of acetate. Nature 469:543–549. doi:10.1038/nature09646.

Giuberti, G., A. Gallo, F. Masoero, L.F. Ferraretto, P.C. Hoffman, and R.D. Shaver. 2014. Factors affecting starch utilization in large animal food production system: A review. Starch/Staerke 66:72–90. doi:10.1002/star.201300177.

Goad, D.W., C.L. Goad, and T.G. Nagaraja. 1998. Ruminal Microbial and Fermentative Changes Associated with Experimentally Induced Subacute Acidosis in Steers. J. Anim. Sci. 76:234–241. doi:10.2527/1998.761234x.

Gordon, G.L.R., and M.W. Phillips. 1998. The role of anaerobic gut fungi in ruminants. Nutr. Res. Rev. 11:133–168. doi:10.1079/nrr19980009.

Gozho, G.N., D.O. Krause, and J.C. Plaizier. 2006. Rumen lipopolysaccharide and inflammation during grain adaptation and subacute ruminal acidosis in steers. J. Dairy Sci. 89:4404–4413. doi:10.3168/jds.S0022-0302(06)72487-0.

Gozho, G.N., J.C. Plaizier, D.O. Krause, A.D. Kennedy, and K.M. Wittenberg. 2005. Subacute ruminal acidosis induces ruminal lipopolysaccharide endotoxin release and triggers an inflammatory response. J. Dairy Sci. 88:1399–1403. doi:10.3168/jds.S0022-0302(05)72807-1.

Greenbaum, D., C. Colangelo, K. Williams, and M. Gerstein. 2003. Comparing protein abundance and mRNA expression levels on a genomic scale. Genome Biol. 4. doi:10.1186/gb-2003-4-9-117.

Gressley, T.F., M.B. Hall, and L.E. Armentano. 2011. Ruminant nutrition symposium: Productivity, digestion, and health responses to hindgut acidosis in ruminants. J. Anim. Sci. 89:1120–1130. doi:10.2527/jas.2010-3460.

Hackmann, T.J., B.L. Keyser, and J.L. Firkins. 2013. Evaluation of methods to detect changes in reserve carbohydrate for mixed rumen microbes. J. Microbiol. Methods 93:284–291. doi:10.1016/J.MIMET.2013.03.025.

Hagey, J. V., S. Bhatnagar, J.M. Heguy, B.M. Karle, P.L. Price, D. Meyer, and E.A. Maga. 2019. Fecal microbial communities in a large representative cohort of California dairy cows. Front. Microbiol. 10:1–14. doi:10.3389/fmicb.2019.01093.

Hall, M.B. 2002. Rumen acidosis: Carbohydrate feeding considerations. Proc. 12th Int. Symp. Lameness in Ruminants

Harmon, D.L. 1993. Nutritional regulation of postruminal enzymes in ruminants. J. Dairy Sci. 76:2102–2111.

Harmon, D.L., R.M. Yamka, and N.A. Elam. 2004. Factors affecting intestinal starch digestion in ruminants: A review. Can. J. Anim. Sci. 84:309–318. doi:10.4141/A03-077.

Harmon, D.L. 2009. Understanding Starch Utilization in the Small Intestine of Cattle. Asian-Austrialasian J. Anim. Sci. 22:915–922.

Harvatine, K.J., and D.E. Bauman. 2011. Characterization of the acute lactational response to trans-10, cis-12 conjugated linoleic acid. J. Dairy Sci. 94:6047–6056. doi:10.3168/jds.2011-4657.

Herdt, T.H. 2015. Nutritional Requirements of Dairy Cattle. Accessed January 18, 2022. https://www.merckvetmanual.com/management-and-nutrition/nutrition-dairy-cattle/nutritional-requirements-of-dairy-cattle.

Hoffman, P.C., N.M. Esser, R.D. Shaver, W.K. Coblentz, M.P. Scott, A.L. Bodnar, R.J. Schmidt, and R.C. Charley. 2011. Influence of ensiling time and inoculation on alteration of the starch-protein matrix in high-moisture corn. J. Dairy Sci. 94:2465–2474. doi:10.3168/jds.2010-3562.

Hollingsworth, M.A., and B.J. Swanson. 2004. Mucins in cancer: Protection and control of the cell surface. Nat. Rev. Cancer 4:45–60. doi:10.1038/nrc1251.

Holtenius, K., C. Kronqvist, E. Briland, and R. Spörndly. 2008. Magnesium absorption by lactating dairy cows on a grass silage-based diet supplied with different potassium and magnesium levels. J. Dairy Sci. 91:743–748. doi:10.3168/jds.2007-0309.

Hu, W., and M.R. Murphy. 2005. Statistical evaluation of early- and mid-lactation dairy cow responses to dietary sodium bicarbonate addition. Anim. Feed Sci. Technol. 119:43–54. doi:10.1016/j.anifeedsci.2004.12.005.

Hume, I.D. 1997. Fermentation in the hindgut of mammals. R.I. Mackie and B.A. White, ed. Chapman & Hall, New York, NY.

Hunt, K.M., J.A. Foster, L.J. Forney, U.M.E. Schütte, D.L. Beck, Z. Abdo, L.K. Fox, J.E. Williams, M.K. McGuire, and M.A. McGuire. 2011. Characterization of the diversity and temporal stability of bacterial communities in human milk. PLoS One 6. doi:10.1371/journal.pone.0021313.

Jalal, S., R. Arsenault, A.A. Potter, L.A. Babiuk, P.J. Griebel, and S. Napper. 2009. Genome to kinome: Species-specific peptide arrays for kinome analysis. Sci. Signal. 2.

Jenkins, T.C., and D.L. Palmquist. 1984. Effect of Fatty Acids or Calcium Soaps on Rumen and Total Nutrient Digestibility of Dairy Rations. J. Dairy Sci. 67:978–986. doi:10.3168/jds.S0022-0302(84)81396-X.

Jouany, J.P., D.I. Demeyer, and J. Grain. 1988. Effect of defaunating the rumen. Anim. Feed Sci. Technol. 21:229–265. doi:10.1016/0377-8401(88)90105-8.

Jurjanz, S., and V. Monteils. 2005. Ruminal degradability of corn forages depending on the processing method employed 54:3–15. doi:10.1051/animres.

Kalliomäki, M., P. Kirjavainen, E. Eerola, P. Kero, S. Salminen, and E. Isolauri. 2001. Distinct patterns of neonatal gut microflora in infants in whom atopy was and was not developing. J. Allergy Clin. Immunol. 107:129–134. doi:10.1067/mai.2001.111237.

Katzinger, J. 2020. Biomarkers for Stool Analysis. 5th ed.

Keerthi, T.R., R. Narayanan, K. Sreelekshmi, and C.H. Chandran. 2021. Immunity and Gut Microbiome: Role of Probiotics and Prebiotics.

Keyser, R.B., C.H. Noller, L.J. Wheeler, and D.M. Schaefer. 1985. Characterization of Limestones and Their Effects In Vitro and In Vivo in Dairy Cattle. J. Dairy Sci. 68:1376–1389. doi:10.3168/jds.S0022-0302(85)80974-7.

Khafipour, E., D.O. Krause, and J.C. Plaizier. 2009a. A grain-based subacute ruminal acidosis challenge causes translocation of lipopolysaccharide and triggers inflammation. J. Dairy Sci. 92:1060–1070. doi:10.3168/jds.2008-1389.

Khafipour, E., S. Li, J.C. Plaizier, and D.O. Krause. 2009b. Rumen microbiome composition determined using two nutritional models of subacute ruminal acidosis. Appl. Environ. Microbiol. 75:7115–7124. doi:10.1128/AEM.00739-09.

Khafipour, E., S. Li, H.M. Tun, H. Derakhshani, S. Moossavi, and K.J.C. Plaizier. 2016. Effects of grain feeding on microbiota in the digestive tract of cattle. Anim. Front. 6:13–19. doi:10.2527/af.2016-0018.

Kleen, J.L., G.A. Hooijer, J. Rehage, and J.P.T.M. Noordhuizen. 2003. Subacute ruminal acidosis (SARA): A review. J. Vet. Med. Ser. A Physiol. Pathol. Clin. Med. 50:406–414. doi:10.1046/j.1439-0442.2003.00569.x.

Krajcarski-Hunt, H., J.C. Plaizier, J.P. Walton, R. Spratt, and B.W. McBride. 2002. Short communication: Effect of subacute ruminal acidosis on in situ fiber digestion in lactating dairy cows. J. Dairy Sci. 85:570–573. doi:10.3168/jds.S0022-0302(02)74110-6.

Krause, K.M., and G.R. Oetzel. 2006. Understanding and preventing subacute ruminal acidosis in dairy herds: A review. Anim. Feed Sci. Technol. 126:215–236. doi:10.1016/j.anifeedsci.2005.08.004.

Le Ruyet, P., and W.B. Tucker. 1992. Ruminal Buffers: Temporal Effects on Buffering Capacity and pH of Ruminal Fluid from Cows Fed a High Concentrate Diet. J. Dairy Sci. 75:1069–1077. doi:10.3168/jds.S0022-0302(92)77851-5.

Li, S., E. Khafipour, D.O. Krause, A. Kroeker, J.C. Rodriguez-Lecompte, G.N. Gozho, and J.C. Plaizier. 2012. Effects of subacute ruminal acidosis challenges on fermentation and endotoxins in the rumen and hindgut of dairy cows. J. Dairy Sci. 95:294–303. doi:10.3168/jds.2011-4447.

Liao, S.F., E.S. Vanzant, D.L. Harmon, K.R. McLeod, J.A. Boling, and J.C. Matthews. 2009. Ruminal and abomasal starch hydrolysate infusions selectively decrease the expression of cationic amino acid transporter mRNA by small intestinal epithelia of forage-fed beef steers. J. Dairy Sci. 92:1124–1135. doi:10.3168/jds.2008-1521.

Lin, C., L. Raskin, and D.A. Stahl. 1997. Microbial community structure in gastrointestinal tracts of domestic animals: comparative analyses using rRNA-targeted oligonucleotide probes. FEMS Microbiol. Ecol. 22:281–294.

Lindberg, E., I. Adlerberth, B. Hesselmar, R. Saalman, I.L. Strannegård, N. Åberg, and A.E. Wold. 2004. High Rate of Transfer of Staphylococcus aureus from Parental Skin to Infant Gut Flora. J. Clin. Microbiol. 42:530–534. doi:10.1128/JCM.42.2.530-534.2004.

Liu, W., M. Chen, L. Duo, J. Wang, S. Guo, H. Sun, B. Menghe, and H. Zhang. 2020. Characterization of potentially probiotic lactic acid bacteria and bifidobacteria isolated from human colostrum. J. Dairy Sci. 103:4013–4025. doi:10.3168/jds.2019-17602.

Lozupone, C.A., J.I. Stombaugh, J.I. Gordon, J.K. Jansson, and R. Knight. 2012. Diversity, stability and resilience of the human gut microbiota. Nature 489:220–230. doi:10.1038/nature11550.

Lueschow, S.R., and S.J. McElroy. 2020. The Paneth Cell: The Curator and Defender of the Immature Small Intestine. Front. Immunol. 11:1–12. doi:10.3389/fimmu.2020.00587.

Mackie, R.I., F.M.C. Gilchrist, A.M. Robberts, P.E. Hannah, and H.M. Schwartz. 1978. Microbiological and chemical changes in the rumen during the stepwise adaptation of sheep to high concentrate diets. J. Agric. Sci. 90:241–254. doi:10.1017/S0021859600055313.

Madara, J.L. 1987. Intestinal absorptive cell tight junctions are linked to cytoskeleton. Am. J. Physiol. 253:C171-175.

Maekawa, M., K.A. Beauchemin, and D.A. Christensen. 2002. Effect of Concentrate Level and Feeding Management on Chewing Activities, Saliva Production, and Ruminal pH of Lactating Dairy Cows1. J. Dairy Sci. 85:1165–1175. doi:10.3168/jds.S0022-0302(02)74179-9.

Mann M, Jensen ON. Proteomic analysis of post-translational modifications. Nat Biotechnol. 2003 Mar;21(3):255-61. doi: 10.1038/nbt0303-255. PMID: 12610572.

Mao, S.Y., R.Y. Zhang, D.S. Wang, and W.Y. Zhu. 2013. Impact of subacute ruminal acidosis (SARA) adaptation on rumen microbiota in dairy cattle using pyrosequencing. Anaerobe 24:12–19. doi:10.1016/J.ANAEROBE.2013.08.003.

Marden, J.P., C. Julien, V. Monteils, E. Auclair, R. Moncoulon, and C. Bayourthe. 2008. How does live yeast differ from sodium bicarbonate to stabilize ruminal pH in high-yielding dairy cows?. J. Dairy Sci. 91:3528–3535. doi:10.3168/jds.2007-0889.

Martens, H., and Y. Rayssiguier. 1980. Magnesium metabolism and hypomagnesaemia. Dig. Physiol. Metab. Ruminants 447–466. doi:10.1007/978-94-011-8067-2_21.

Martens, H., and G. Gabel. 1988. Transport of Na and Cl across the epithelium of ruminant forestomachs: Rumen and omasum. A review. Comp. Biochem. Physiol. -- Part A Physiol. 90:569–575. doi:10.1016/0300-9629(88)90669-X.

Matthews, C., F. Crispie, E. Lewis, M. Reid, P.W. O’Toole, and P.D. Cotter. 2019. The rumen microbiome: a crucial consideration when optimising milk and meat production and nitrogen utilisation efficiency. Gut Microbes 10:115–132. doi:10.1080/19490976.2018.1505176.

McAllister, T.A., H.D. Bae, G.A. Jones, and K.J. Cheng. 1994. Microbial attachment and feed digestion in the rumen.. J. Anim. Sci. 72:3004–3018. doi:10.2527/1994.72113004x.

McSweeney, C., and R. Mackie. 2012. Micro-organisms and ruminant digestion: state of knowledge, trends and future prospects. Comm. Genet. Resour. Food Agric. 1–7.

Mertens, D.R. 1997. Creating a System for Meeting the Fiber Requirements of Dairy Cows. J. Dairy Sci. 80:1463–1481. doi:10.3168/jds.S0022-0302(97)76075-2.

Metzler-Zebeli, B.U., S. Schmitz-Esser, F. Klevenhusen, L. Podstatzky-Lichtenstein, M. Wagner, and Q. Zebeli. 2013. Grain-rich diets differently alter ruminal and colonic abundance of microbial populations and lipopolysaccharide in goats. Anaerobe 20:65–73. doi:10.1016/J.ANAEROBE.2013.02.005.

Miller, T.L., and M.J. Wolin. 1986. Methanogens in Human and Animal Intestinal Tracts. Syst. Appl. Microbiol. 7:223–229.

Mohamed Nour, M.S., M.T. Abusamra, and B.E.D. Hago. 1998. Experimentally induced lactic acidosis in Nubian goats: Clinical, biochemical and pathological investigations. Small Rumin. Res. 31:7–17. doi:10.1016/s0921-4488(98)00116-3.

Monteiro, H.F., and A.P. Faciola. 2020. Ruminal acidosis, bacterial changes, and lipopolysaccharides. J. Anim. Sci. 98:1–9. doi:10.1093/jas/skaa248.

Nagaraja, T.G., and E.C. Titgemeyer. 2007. Ruminal Acidosis in Beef Cattle: The Current Microbiological and Nutritional Outlook,. J. Dairy Sci. 90:E17–E38. doi:10.3168/JDS.2006-478.

Neiderfer, K.P., A.M. Barnard, K.Z. Moyer, A.M. Trench, A.E. Taylor, S.K. Cronin, and T.F. Gressley. 2020. Effects of calcium carbonate, magnesium oxide and encapsulated sodium bicarbonate on measures of post-ruminal fermentation. J. Anim. Physiol. Anim. Nutr. (Berl). 104:802–811. doi:10.1111/jpn.13331.

Neubauer, V., R.M. Petri, E. Humer, I. Kröger, N. Reisinger, W. Baumgartner, M. Wagner, and Q. Zebeli. 1727. Starch-Rich Diet Induced Rumen Acidosis and Hindgut Dysbiosis in Dairy Cows of Different Lactations 10. doi:10.3390/ani10101727.

Nocek, J.E. 1997. Bovine Acidosis: Implications on Laminitis. J. Dairy Sci. 80:1005–1028. doi:10.3168/jds.S0022-0302(97)76026-0.

Nocek, J.E., and S. Tamminga. 1991. Site of Digestion of Starch in the Gastrointestinal Tract of Dairy Cows and Its Effect on Milk Yield and Composition. J. Dairy Sci. 74:3598–3629. doi:10.3168/jds.S0022-0302(91)78552-4.

Oetzel, G.R. 2007. Subacute ruminal acidosis in dairy herds: Physiology, pathophysiology, milk fat responses and nutritional management. Pages 89–119 in AABP 40th Annual Conference, Vancouver, BC, Canada.

Ogunade, I., A. Pech-Cervantes, and H. Schweickart. 2019. Metatranscriptomic analysis of sub-acute ruminal acidosis in beef cattle. Animals 9. doi:10.3390/ani9050232.

Olsen, J. V., B. Blagoev, F. Gnad, B. Macek, C. Kumar, P. Mortensen, and M. Mann. 2006. Global, In Vivo, and Site-Specific Phosphorylation Dynamics in Signaling Networks. Cell 127:635–648. doi:10.1016/j.cell.2006.09.026.

Owens, F.N., D.S. Secrist, W.J. Hill, and D.R. Gill. 1998. Acidosis in Cattle: A Review. J. Anim. Sci. 76:275–286. doi:10.2527/1998.761275x.

Peirce, S.B., L.D. Muller, and H.W. Harpster. 1983. Influence of sodium bicarbonate and magnesium oxide on digestion and metabolism in yearling beef steers abruptly changed from high forage to high energy diets.. J. Anim. Sci. 57:1561–1567. doi:10.2527/jas1983.5761561x.

Petri, R.M., M. Münnich, Q. Zebeli, and F. Klevenhusen. 2019. Graded replacement of corn grain with molassed sugar beet pulp modulates the fecal microbial community and hindgut fermentation profile in lactating dairy cows. J. Dairy Sci. 102:5019–5030. doi:10.3168/jds.2018-15704.

Plaizier, J.C., D.O. Krause, G.N. Gozho, and B.W. McBride. 2008. Subacute ruminal acidosis in dairy cows: The physiological causes, incidence and consequences. Vet. J. 176:21–31. doi:10.1016/j.tvjl.2007.12.016.

Plaizier, J.C., S. Li, A.M. Danscher, H. Derakshani, P.H. Andersen, and E. Khafipour. 2017a. Changes in Microbiota in Rumen Digesta and Feces Due to a Grain-Based Subacute Ruminal Acidosis (SARA) Challenge. Microb. Ecol. 74:485–495. doi:10.1007/s00248-017-0940-z.

Plaizier, J.C., S. Li, H.M. Tun, and E. Khafipour. 2017b. Nutritional models of experimentally-induced subacute ruminal acidosis (SARA) differ in their impact on rumen and hindgut bacterial communities in dairy cows. Front. Microbiol. 7. doi:10.3389/fmicb.2016.02128.

Puniya, A.K., R. Singh, and D.N. Kamra. 2015. Rumen Microbiology: From Evolution to Revolution. Springer, New Delhi, India.

Ribeiro, M.M., X. Xu, D. Klein, N.S. Kenyon, C. Ricordi, M.S.S. Felipe, and R.L. Pastori. 2010. Endotoxin deactivation by transient acidification. Cell Transplant. 19:1047–1054. doi:10.3727/096368910X500643.

Rogers, J.A., C.L. Davis, and J.H. Clark. 1982. Alteration of Rumen Fermentation, Milk Fat Synthesis, and Nutrient Utilization with Mineral Salts in Dairy Cows. J. Dairy Sci. 65:577–586. doi:10.3168/jds.S0022-0302(82)82235-2.

Rogers, J.A., L.D. Muller, C.L. Davis, W. Chalupa, D.S. Kronfeld, L.F. Karcher, and K.R. Cummings. 1985. Response of Dairy Cows to Sodium Bicarbonate and Limestone in Early Lactation. J. Dairy Sci. 68:646–660. doi:10.3168/jds.S0022-0302(85)80871-7.

Rosa, F., S. Busato, F.C. Avaroma, R. Mohan, N. Carpinelli, M. Bionaz, and J.S. Osorio. 2021. Short communication: Molecular markers for epithelial cells across gastrointestinal tissues and fecal RNA in preweaning dairy calves. J. Dairy Sci. 104:1175–1182. doi:10.3168/jds.2020-18955.

Russell, J.B., and D.B. Dombrowski. 1980. Effect of pH on the efficiency of growth by pure cultures of rumen bacteria in continuous culture. Appl. Environ. Microbiol. 39:604–610. doi:10.1128/aem.39.3.604-610.1980.

Russell, J.B., and J.L. Rychlik. 2001. Factors that alter rumen microbial ecology. Science (80-.). 292:1119–1122. doi:10.1126/science.1058830.

Saleem, F., B.N. Ametaj, S. Bouatra, R. Mandal, Q. Zebeli, S.M. Dunn, and D.S. Wishart. 2012. A metabolomics approach to uncover the effects of grain diets on rumen health in dairy cows. J. Dairy Sci. 95:6606–6623. doi:10.3168/jds.2012-5403.

Schaefer, D.M., L.J. Wheeler, C.H. Noller, R.B. Keyser, and J.L. White. 1982. Neutralization of Acid in the Rumen by Magnesium Oxide and Magnesium Carbonate. J. Dairy Sci. 65:732–739. doi:10.3168/jds.S0022-0302(82)82260-1.

Scheller HV, Ulvskov P. Hemicelluloses. Annu Rev Plant Biol. 2010;61:263-89. doi: 10.1146/annurev-arplant-042809-112315. PMID: 20192742.

Schroedl, W., B. Fuerll, P. Reinhold, M. Krueger, and C. Schuett. 2001. A novel acute phase marker in cattle: Lipopolysaccharide binding protein (LBP). J. Endotoxin Res. 7:49–52. doi:10.1177/09680519010070010801.

Shanks, O.C., C.A. Kelty, S. Archibeque, M. Jenkins, R.J. Newton, S.L. McLellan, S.M. Huse, and M.L. Sogin. 2011. Community structures of fecal bacteria in cattle from different animal feeding operations. Appl. Environ. Microbiol. 77:2992–3001. doi:10.1128/AEM.02988-10.

Shi, Y., and P.J. Weimer. 1992. Response surface analysis of the effects of pH and dilution rate on Ruminococcus flavefaciens FD-1 in cellulose-fed continuous culture. Appl. Environ. Microbiol. 58:2583–2591. doi:10.1128/aem.58.8.2583-2591.1992.

Silveira, C., M. Oba, W.Z. Yang, and K.A. Beauchemin. 2007. Selection of barley grain affects ruminai fermentation, starch digestibility, and productivity of lactating dairy cows. J. Dairy Sci. 90:2860–2869. doi:10.3168/jds.2006-771.

Sonesson, H.R.., U. Zahringer, H.D. Grimmecke, O. Westphal, and R.T. Rietschel. 1994. Bacterial endotoxin: Chemical structure biological activity. K.L. Brigham, ed. Marcel Dekker Inc., New York, NY.

Stappenbeck, T.S., L. V. Hooper, and J.I. Gordon. 2002. Developmental regulation of intestinal angiogenesis by indigenous microbes via Paneth cells. Proc. Natl. Acad. Sci. U. S. A. 99:15451–15455. doi:10.1073/pnas.202604299.

Steele, M.A., J. Croom, M. Kahler, O. Alzahal, S.E. Hook, K. Plaizier, and B.W. Mcbride. 2011. Bovine rumen epithelium undergoes rapid structural adaptations during grain-induced subacute ruminal acidosis. Am. J. Physiol. - Regul. Integr. Comp. Physiol. 300:1515–1523. doi:10.1152/ajpregu.00120.2010.

Steele, M.A., G.B. Penner, F. Chaucheyras-Durand, and L.L. Guan. 2016. Development and physiology of the rumen and the lower gut: Targets for improving gut health. J. Dairy Sci. 99:4955–4966. doi:10.3168/jds.2015-10351.

Steele, M.A., O. Alzahal, S.E. Hook, J. Croom, and B.W. Mcbride. 2009. Acta Veterinaria Scandinavica Ruminal acidosis and the rapid onset of ruminal parakeratosis in a mature dairy cow: a case report. doi:10.1186/1751-0147-51-39.

Steiger, M., M. Senn, G. Altreuther, D. Werling, F. Sutter, M. Kreuzer, and W. Langhans. 1999. Effect of a prolonged low-dose lipopolysaccharide infusion on feed intake and metabolism in heifers. J. Anim. Sci. 77:2523–2532. doi:10.2527/1999.7792523x.

Stewart, C.S. 1977. Factors affecting the feed. Biol. Conserv. 33:497–502.

Stokes, M.R., L.L. Vandemark, and L.S. Bull. 1986. Effects of Sodium Bicarbonate, Magnesium Oxide, and a Commercial Buffer Mixture in Early Lactation Cows Fed Hay Crop Silage. J. Dairy Sci. 69:1595–1603. doi:10.3168/jds.S0022-0302(86)80576-8.

Tajima, K., R.I. Aminov, T. Nagamine, H. Matsui, M. Nakamura, and Y. Benno. 2001. Diet-Dependent Shifts in the Bacterial Population of the Rumen Revealed with Real-Time PCR. Appl. Environ. Microbiol. 67:2766–2774. doi:10.1128/AEM.67.6.2766-2774.2001.

Tajima, K., S. Arai, K. Ogata, T. Nagamine, H. Matsui, M. Nakamura, R.I. Aminov, and Y. Benno. 2000. Rumen Bacterial Community Transition During Adaptation to High-grain Diet. Anaerobe 6:273–284. doi:10.1006/ANAE.2000.0353.

Teh, T.H., R.W. Hemken, and R.J. Harmon. 1985. Dietary Magnesium Oxide Interactions with Sodium Bicarbonate on Cows in Early Lactation. J. Dairy Sci. 68:881–890. doi:10.3168/jds.S0022-0302(85)80905-X.

Tomlinson, E., L. Fu, L. John, B. Hultgren, X. Huang, M. Renz, J.P. Stephan, S.P. Tsai, L.Y.N. Powell-braxton, D. French, and T.A. Stewart. 2002. Decreased Adiposity. Cardiovasc. Res. 143:1741–1747.

Tordesillas, L., C. Gómez-Casado, M. Garrido-Arandia, A. Murua-García, A. Palacín, J. Varela, P. Konieczna, J. Cuesta-Herranz, C.A. Akdis, L. O'Mahony, and A. Díaz-Perales. 2013. Transport of Pru p 3 across gastrointestinal epithelium - an essential step towards the induction of food allergy?. Clin. Exp. Allergy 43:1374–1383. doi:10.1111/cea.12202.

Troegeler-Meynadier, A., M.C. Nicot, and F. Enjalbert. 2007. Effects of fat source and dietary sodium bicarbonate plus straw on the conjugated linoleic acid content of milk of dairy cows. Arch. Anim. Nutr. 61:406–415. doi:10.1080/17450390701563474.

Van der Sluis. 2001. MUC2 Mucin Facilitates Epithelial Repair in a Mouse Model of IBD. Am. J. Gastroenterol. 96:606–7.

Van der Sluis, M., B.A.E. De Koning, A.C.J.M. De Bruijn, A. Velcich, J.P.P. Meijerink, J.B. Van Goudoever, H.A. Büller, J. Dekker, I. Van Seuningen, I.B. Renes, and A.W.C. Einerhand. 2006. Muc2-Deficient Mice Spontaneously Develop Colitis, Indicating That MUC2 Is Critical for Colonic Protection. Gastroenterology 131:117–129. doi:10.1053/j.gastro.2006.04.020.

Van Kessel, J.S., P.C. Nedoluha, A. Williams-Campbell, R.L. Baldwin VI, and K.R. McLeod. 2002. Effects of ruminal and postruminal infusion of starch hydrolysate or glucose on the microbial ecology of the gastrointestinal tract in growing steers. J. Anim. Sci. 80:3027–3034. doi:10.2527/2002.80113027x.

Van Soest, P.J. 1994. Nutritional Ecology of the Ruminant. 2nd ed. Cornel University Press, Ithica, NY.

Vestweber JG, Leipold HW, Smith JE. Ovine ruminal acidosis: clinical studies. Am J Vet Res. 1974 Dec;35(12):1587-90. PMID: 4473947.

Welch, J.G. 1986. Physical Parameters of Fiber Affecting Passage from the Rumen. J. Dairy Sci. 69:2750–2754. doi:10.3168/jds.S0022-0302(86)80723-8.

Wellnitz, O., E.T. Arnold, and R.M. Bruckmaier. 2011. Lipopolysaccharide and lipoteichoic acid induce different immune responses in the bovine mammary gland. J. Dairy Sci. 94:5405–5412. doi:10.3168/jds.2010-3931.

Wheeler, W.E., and C.H. Noller. 1977. Gastrointestinal tract pH and starch in feces of ruminants.. J. Anim. Sci. 44:131–135. doi:10.2527/jas1977.441131x.

Xin, Z., W.B. Tucker, and R.W. Hemken. 1989. Effect of Reactivity Rate and Particle Size of Magnesium Oxide on Magnesium Availability, Acid-Base Balance, Mineral Metabolism, and Milking Performance of Dairy Cows. J. Dairy Sci. 72:462–470. doi:10.3168/jds.S0022-0302(89)79128-1.

Zarling, E.J., and M.A. Ruchim. 1987. Protein origin of the volatile fatty acids isobutyrate and isovalerate in human stool. J. Lab. Clin. Med. 109:566–570.

Zebeli, Q., D. Mansmann, H. Steingass, and B.N. Ametaj. 2010. Balancing diets for physically effective fibre and ruminally degradable starch: A key to lower the risk of sub-acute rumen acidosis and improve productivity of dairy cattle. Livest. Sci. 127:1–10. doi:10.1016/j.livsci.2009.09.003.

Zhang, H., C. Ao, Khas-Erdene, and N. Dan. 2019. Effects of isonitrogenous and isocaloric total mixed ration composed of forages with different quality on milk fatty acid composition and gene expression of mammary lipogenic enzymes in mid-lactating dairy cows. Anim. Sci. J. 90:214–221. doi:10.1111/asj.13154.

Chapter 2

EVALUATION OF HINDGUT BUFFERS UNDER HIGH-STARCH DIET CONDITIONS IN LACTATING HOLSTEIN COWS

2.1 Abstract

Buffering of the rumen environment can alleviate some of the negative effects of acidosis, and the same may hold true in the hindgut. The objective of this study was to evaluate the potential for two dietary buffers at different dosages to alter fecal measures of intestinal fermentation and systemic inflammation due to hindgut acidosis. Ten ruminally cannulated lactating cows were assigned to a replicated 5×5 Latin squares with a 7-d adaptation period, 14-d experimental periods, and 7-d washout periods between each experimental period. Cows were fed a 30.9% starch TMR (on a DM basis). Treatments were abomasal infusion of water without fed supplemental buffer (CON), abomasal infusion of corn starch without fed supplemental buffer (IS), or abomasal infusion of starch with 150 g/d of buffer A (calcium carbonate, magnesium oxide, and crushed oyster shell blend; T1), 300 g/d of buffer A (T2), or 150 g/d of buffer B (100% magnesium oxide; T3). Abomasal starch infusions were 2 g/kg BW (BW) in period 1 and 4 g/kg BW in periods 2-5 and split into 2 bolus infusions, provided every 12 h. Data were analyzed in SAS, with serum acute phase proteins, apparent total tract digestibility, and fecal purine data evaluated using a model including the fixed effects of treatment, period, and block, and the random effect of cow within block. Repeated measures of rumen pH and VFA, and fecal score, pH, VFA, lactate, and lipopolysaccharide (LPS) were analyzed using a model that included the fixed effects of treatment, period, time, block, and the interaction of treatment by time and the random effect of cow within block. The moderately high starch TMR seemed to induce subacute ruminal acidosis (SARA), while abomasal corn starch addition decreased fecal pH, and dry matter and starch digestibilities as compared to CON. Unexpectantly, starch infusion did not increase serum acute phase proteins, fecal LPS, or total fecal VFA, but was instead only partially undigested. Buffer addition increased fecal pH, fecal acetate and total VFA, and decreased fecal score compared to IS. The T2 treatment differed from CON, increasing LPS binding protein and serum amyloid A. Despite increased fecal pH, the inclusion of different buffer formulations and levels in high starch TMRs (~31% on a DM basis) seemed to increase hindgut fermentation and did little to alleviate the negative effects of abomasal starch infusions.

2.2 Introduction

To meet the heightened energy demands during early and peak lactation, producers often elevate the starch content in dairy cattle diets. However, these energetically rich diets increase the risk of SARA and hindgut acidosis. Characterized by increased VFA and lipopolysaccharide (LPS) and decreased pH, SARA can damage not only rumen but also large intestine epithelium (Steele et al., 2011; Li et al., 2012; Tao et al., 2014). High levels of starch in the diet increase the amount of undigested starch flowing into the intestines (Sanz-Fernandez et al., 2020). This can increase intestinal production of VFA, consequently dropping intestinal and cecal pH (Li et al., 2012) and loosening fecal consistency (Bissell and Hall, 2010). Low intestinal pH degrades the gut barrier integrity through sloughing of intestinal epithelial layers (Plaizier et al., 2008) and also causes the death of gram-negative bacteria, increasing concentrations of toxic LPS (Van Kessel et al., 2002; Li et al., 2012). LPS entry into systemic circulation through the leaky gut barrier leads to an acute phase response, partitioning energy away from milk production and instead to the immune system (Kvidera et al., 2017). Experimentally inducing SARA through high starch diets can impact both the rumen and intestines, but this approach lacks the ability to distinguish between ruminal and intestinal drivers of downstream inflammation. Inconsistent results in the literature regarding hindgut acidosis and inflammation suggest that additional study is necessary to elucidate these responses (Bissell and Hall, 2010; Abeyta et al., 2022; Abeyta et al., 2023).

Dietary buffers are commonly fed to support rumen health in lactating cows receiving relatively high levels of dietary starch. As high starch diets increase fermentation in the rumen and in the intestines, there could be potential benefits to using buffers or alkalinizing agents to modify intestinal fermentation. Both calcium carbonate ($CaCO_3$) and magnesium oxide (MgO) have limited solubility in the rumen (Erdman, 1988; Le Ruyet and Tucker, 1992), and presumably are promising buffers for the intestine. Increases in fecal pH in response to feeding $CaCO_3$- and MgO-based buffers (Schaefer et al., 1982; Rogers et al., 1985; Neiderfer et al., 2020) suggests a potential for those to be used to modify intestinal fermentation and alleviate negative local and systemic effects of intestinal acidosis. However, solubilities are highly variable and depend on the exact source of the buffering ingredients. (Khiaosa-ard et al., 2023; Abegaze & Chopra 2013).

The objective of this experiment was to evaluate the potential for two buffers fed at different dosages to alter fecal measures of intestinal fermentation, nutrient digestibility, and systemic inflammation in mid- to late-lactating cows fed a high starch diet and abomasally infused with corn starch to increase intestinal starch fermentation. We hypothesized that the fed buffers would increase fecal pH, reduce fecal LPS and VFA, and reduce circulating acute phase proteins.

2.3 Materials and Methods

2.3.1 Animals and Treatments

All work was approved by the University of Delaware's Institutional Animal Care and Use Committee, protocol number 115R, and was completed in fall of 2020. Ten ruminally cannulated multiparous lactating Holstein cows were used in this study. Cows were selected for the study based on the presence of preexisting rumen cannulas and stage of lactation. The experiment was originally scheduled to begin in March of 2020 with cows in mid-lactation. However, research at the University of Delaware was halted due to the SARS-CoV-2 global pandemic, and the start of the experiment was delayed until July 2020. At the start of the study, mean (± SD) DIM was 199 ± 61, milk yield was 36.1 ± 8.3 kg/d, and BW was 771 ± 43 kg.

The study was conducted as a replicated 5×5 Latin square design with a 7-d adaptation period, 14-d experimental periods, and a 7-d washout between each experimental period. The goal of the study was to induce hindgut acidosis through a combination of a moderately high starch diet and abomasal starch infusions. As described in more detail below, results of Period 1 suggested that the ruminal challenge from the moderately high starch diet was too great while the abomasal starch did not sufficiently challenge the intestines. Thus, changes were made to both the diet and abomasal starch infusions between Period 1 and subsequent periods. A more ideal solution would have been to re-start the study or add an additional period.

However, this was not an option because the initial pandemic-induced delay resulted in cows being advanced in lactation, and we did not have rumen cannulated replacements for several cows due to be dried off at the end of the study.

Cows were ad libitum fed for approximately 5% refusals. Feed offered and refused was recorded daily. During the adaptation and Period 1, cows were fed a TMR that contained 34.4% corn silage, 17.4% triticale silage, 44.8% grain mix, and 3.5% corn grain top dress (Table 2.1). The diet was balanced to contain 30.2% starch and 30.0% aNDF, but calculated values were slightly different at 30.9% starch and 30.2% NDF (Table 2.1). During the washout between Periods 1 and 2, one of the cows had loose, bloody feces, was diagnosed with duodenal hemorrhaging, and was removed from the study. As a precaution, we made a slight shift in the diet for subsequent periods by increasing corn silage to 38.0% of DM and decreasing the grain mix to 41.0% of DM (Table 2.1). This resulted in a minimal change in the predicted starch (30.0%), but a small increase in formulated aNDF to 31.0%. Calculated starch and NDF were similar to formulated at 30.9% starch and 31.2% NDF (Table 2.1).

At the end of the adaptation period, cows were split into 2 groups by milk production and then assigned to 1 of 2 5×5 Latin squares. Treatments were abomasal infusion of water without fed supplemental buffer (**CON**), abomasal infusion of starch without fed supplemental buffer (**IS**), or abomasal infusion of starch and 1 of 3 different buffer treatments (**T1**, **T2**, **T3**). As described in more detail below, cows on the IS, T1, T2, and T3 treatments received 2 and 4 g/kg BW per day of corn starch during Period 1 and Periods 2-5, respectively. Fed buffer treatments were either 150 g/d of buffer A (50% $CaCO_3$, 25% MgO, and 25% crushed oyster shell; T1), 300 g/d of buffer A (T2), or 150 g/d of buffer B (100% MgO; T3). All cows received 1 kg/d of ground corn grain topdress (Table 2.1) that was mixed by hand into individual feed bins during experimental periods or mixed into the feeding wagon during TMR preparation for adaptation and washout periods. For cows on the T1, T2, and T3 treatments, the buffers were mixed into the ground corn grain topdress prior to adding to the feed to maximize buffer intake. Abomasal infusions and supplemental buffer feeding did not occur during the washout periods.

Prior to the start of the experiment, abomasal infusions lines were inserted through the rumen cannula as described by Gressley et al. (2006). The infusion lines were left in the abomasum during the duration of the experiment and checked twice weekly to ensure proper placement. During Period 1, cows were abomasally infused with 4 L/d of tap water containing 0 (CON) or 2 (IS, T1, T2, and T3) g/kg BW per day of food grade corn starch product (Feed Binder GE modified corn starch; Ingredion, Westchester, IL). Period 1 data (not shown) indicated that abomasal infusions of 2 g/kg BW per day of corn starch reduced fecal pH less than 0.2 units (from 6.52 in CON to 6.35 in IS) and did not change fecal consistency. This suggested that the starch infusion was insufficiently challenging the intestines. Abomasal corn starch infusions were increased to 4 g/kg BW per day in 6 L/d tap water during periods 2-5. To gradually adapt cows to the higher level of infusion, 2, 3, and 4 g/kg BW corn starch per day were infused on d 1-2, 3-4, and 5-14 of each period, respectively. Abomasal infusions were administered twice daily in pulse doses at 12 h intervals (0800 h and 2000 h). At each infusion time, half of the daily dose of corn starch was suspended in tap water and infused into the abomasal infusion line using a veterinary stomach pump (Nasco, For Atkinson, WI). Infusions took approximately 3 min per cow, and 100% of the infusate was always delivered.

Due to the pandemic that resulted in experimental scheduling conflicts, cows were moved at the start of the washout period between Periods 4 and 5. For periods 1 through 4, cows were housed in a freestall barn containing deep sand bedded freestalls. Cows were individually fed using a Calan Broadbent Feeding System (American Calan Inc., Northwood, NH). During Period 5, cows were housed in a tiestall barn. Tiestalls contained rubber mattresses bedded with wood shavings twice daily. When fed with the Calan gates, 100% of the daily feed was provided at 0800 h. When housed in the tiestalls, 70% of the daily feed was provided at 0800 h and 30% of the daily feed provided at 1600 h. The T1, T2, and T3 buffer treatments mixed into the corn grain topdress was similarly split to provide 70% with the morning feed and 30% with the afternoon feed.

2.3.2 Milk and Feed Sampling and Analysis

Cows were milked twice daily at approximately 0430 h and 1530 h and milk yield at each milking was recorded throughout the study. Milk samples were collected from both the morning and afternoon milkings on d 6 and 7 of the adaptation period and d 13 and 14 of each experimental period. Milk samples were submitted to Dairy One Cooperative Inc. (Ithaca, NY) for analysis of lactose, protein, fat, SCC, and MUN using a MilkoScan FT+ (Foss, Hillerød, Denmark).

Samples of grain mix and corn grain topdress were collected once weekly, and samples of corn silage, triticale silage, and TMR were collected three times a week. On each sampling day, a portion of each sample was used for measurement of DM (60°C for 48 h in a forced air oven) to calculate DMI and to correct for TMR DM fluctuations. The remainder of the samples were frozen until composited by period. Period composites of forages, TMR, grain mix, and corn grain topdress, along with a single experimental composite corn starch infusate sample were mailed to Cumberland Valley Analytical Services (Waynesboro, PA) for wet chemistry analysis of DM (105°C for 3 h for forages; method 930.15, AOAC International, 2000, for grain), NDF (determined with amylase but not corrected for ash; Van Soest et al., 1991), ADF (method 973.18, AOAC International, 2000), N (method 990.03, AOAC International, 2000), starch (Hall, 2009), minerals (method 985.01, AOAC International, 2000), and ash (method 942.05, AOAC International, 2000). Ground corn grain topdress was additionally analyzed for micron particle size (Heinrichs and Kononoff, 2002), with the average particle size being 440 μm. The composite sample of the corn starch infusate contained 89.3% DM, 80.6% starch, 0.8% CP, 4.6% NDF, 0.0% uNDF, 3.0% ADF and 0.4% ash. Corn starch infusions were delivered on an as fed basis (not corrected for DM), and amount of chemical starch provided by the infusions equated to 1.42 g/kg BW in period 1 and 2.84 g/kg BW in periods 2-5 for the IS, T1, T2, and T3 treatments. Composite samples of buffers A and B were analyzed at the end of the study for minerals as described above, as well as chloride (Metrohm USA Inc, Riverview, FL, USA) and sulfur (Leco Organic Application Note, Leco Corporation, St. Joseph, MI, USA) to determine DCAD (Table 2.2).

2.3.3 Rumen and Fecal Sampling

Rumen and fecal samples were collected on d 12 (0800 h, 1400 h, 2000 h, 0200 h) and d 13 (1100 h, 1700 h, 2300 h, 0500 h) of each experimental period to collectively represent every 3 h over a 24 h period. Rumen fluid was collected from four areas in the ventral rumen sac, mixed, and strained through 2 layers of cheesecloth. Following pH measurement (Anaheim Scientific P771 pH meter, Yorba Linda, CA), 10 mL of the filtered rumen fluid was acidified with 0.2 mL of 50%

H_2SO_4 and stored at -20°C until VFA and lactic acid analysis. Fecal samples of approximately 200 g/cow per time point were collected by rectal palpation. Fecal scores were recorded at the time of fecal sampling and determined by the same individual throughout the study. Using a 5-point scale, fecal samples were scored from extremely loose consistency (score of 1) to extremely firm (score of 5) (Hulsen, 2006). Fecal pH, fecal VFA and lactic acid, and fecal LPS measurement sample preparation was performed from a subsample of feces as described in Cronin et al. (2023). Remaining feces was stored at -20°C for later determination of DM of individual samples and nutrient composition and fecal purines of samples pooled for each animal and each experimental period.

Rumen and fecal content of lactic acid and VFA were evaluated by HPLC as described by Mainardi et al. (2011) following the procedures of Muck and Dickerson (1988). DM content of fecal samples was determined following 72 h at 55°C in a forced air oven. The endotoxin concentration of fecal samples was determined using a commercial chromogenic endpoint amebocyte lysate kit according to manufacturer instructions (Pierce LAL Chromogenic Endotoxin Quantification Kit, Thermo Fisher Scientific, Rockford, IL) as described by Cronin et al. (2023). The intra-assay coefficient of variation was 3.1% and the inter-assay coefficient of variation was 13.3%. Fecal purine quantification of dried fecal samples ground to 1.5 µm was evaluated following the procedures of Zinn and Owens (1986) as modified by Makkar and Becker (1999) for the hydrolyzation step and by Ushida et al. (1985) for the filtering and centrifugation steps.

Apparent total tract nutrient digestibility was determined for each cow and each period. TMR samples were collected prior to the addition of the buffer treatments and corn grain topdress on d 13 and 14 of each period. Dried fecal samples were composited by cow and period and mailed with TMR samples to Cumberland Valley Analytical Services for analysis of DM, NDF, ADF, N, starch, minerals and metals, and ash as described above, as well as 240 h uNDF (Goering and Van Soest, 1970). Fecal output was calculated using 240 h uNDF as an internal marker. Nutrient intake was determined as the sum of intake from the TMR (nutrient composition as determined by the mean of the d 13 and 14 samples from that period), corn grain topdress (nutrient composition determined by the period composites), starch infusion (nutrient composition determined from a single experimental composite sample), and treatment buffers (nutrient composition determined from a single experimental composite sample for each buffer). Apparent total tract nutrient digestibility was then determined as the intake minus fecal excretion divided by intake.

2.3.4 Blood Sampling and Analysis

Blood samples were collected from the coccygeal vein at 6 h relative to feeding on d 14 of each experimental period. Blood from each cow was collected into two 10 mL serum separator tubes without anticoagulant (BD Vacutainer; Becton, Dickinson and Co., Franklin Lakes, NJ). Blood was allowed to coagulate at room temperature for 30 min before centrifugation at 1,500 × g for 30 min at 25°C and serum was collected. Serum was stored -80°C until analyzed for haptoglobin (Tridelta Development Ltd., Ireland), serum amyloid A (Tridelta Development Ltd., Ireland), and LPS binding protein (Hycult Biotech various species ELISA kit) using commercial kits. Intra- and inter-assay coefficients of variation were 6.5% and 24.6% for haptoglobin, and 5.1% and 16.0% for serum amyloid A, respectively.

Lipopolysaccharide binding protein samples were run on a single plate, and intra-assay coefficient of variation was 4.4%.

2.4 Statistical Analyses

All analyses were conducted using the GLIMMIX procedure of SAS (version 9.4; SAS Institute, Cary, NC, USA). Mean DMI, total DMI input, milk yield, and weighted milk composition were determined for the last 3 d of the adaptation period and each experimental period. Those effects were evaluated in a model including the fixed effects of treatment, period, and block, and the random effect of cow within block. Data collected during the adaptation period were included as covariates. Serum acute phase proteins, apparent total tract digestibility, and fecal purine data were evaluated using the same model except that no covariates were included. Repeated measures of rumen pH and VFA and fecal score, pH, VFA, lactate, and LPS were analyzed using a model that included the fixed effects of treatment, period, time, block, and the interaction of treatment by time and the random effect of cow within block. The RANDOM _RESIDUAL_ statement was used to specify time as a repeated measure and the subject was period × cow. Times were included as Time 1 = d 12 0800 h; Time 2 = d 12 1400 h; Time 3 = d 12 2000 h; Time 4 = d 12 0200 h; Time 5 = d 13 1100 h; Time 6 = d 13 1700 h; Time 7 = d 13 2300 h; Time 8 = d 13 0500 h. Because the times spanned across two days, an unstructured covariance structure was used. For all models, significance was declared at $P \leq 0.05$ and trends at $0.05 < P \leq 0.10$. When a main effect was observed ($P \leq 0.10$), the PDIFF function of SAS was used to differentiate among treatment means. Contrast statements were additionally used to differentiate among treatments. Contrasts were: 1) CON vs. (IS + T1 + T2 + T3); 2) IS vs. (T1 + T2 + T3). None of the data from the cow removed from the study due to duodenal hemorrhaging was included in any statistical analysis. One of the cows regularly threw her food out of the bin, so her DMI data were not included in analysis of intake or apparent total tract digestibility.

2.5 Results

2.5.1 DMI and Production

After the loss of the 1 cow between periods 1 and 2, all remaining animals completed the study without any additional adverse events. Treatment effects were observed for DMI and milk yield, and treatment tended to affect some milk components (Table 2.3). For DMI (sum of diet, corn grain topdress, and buffer only), T2 depressed intake in comparison to CON, IS, and T1 (P = 0.02). When total DMI input was calculated including abomasal corn starch, total DMI input of T2 and CON were lower than IS and T1, and T3 was intermediate (P = 0.02). In addition, the IS treatment tended to result in both greater DMI and total DMI input compared to T1, T2, and T3 combined (P = 0.09 for Contrast 2 for both variables). For milk yield, T2 yield (26.1 kg/d) was lower than CON, IS, and T1 (29.8 – 31.4 kg/d; P = 0.04), while T3 (28.3 kg/d) did not differ from any treatment. All treatments infused with abomasal corn starch tended to decrease milk yield (P = 0.08 for Contrast 1), and the buffer treatments tended to decrease milk yield compared to IS (P = 0.07 for Contrast 2). There was a tendency for treatment to affect milk fat percentage and milk protein yield. For milk fat percentage, the tendency (P = 0.07) was due to lower milk fat for the CON and IS treatments (3.80 and 3.76%, respectively) than the T2 treatment (4.13%; P = 0.02 and P = 0.01, respectively). The effect on milk protein yield (P = 0.09) was due to lower milk protein for the T2 treatment (0.82 kg/d) compared to the

CON and IS treatments (0.99 and 0.97 kg/d; *P* = 0.01 and *P* = 0.02, respectively). The differential effects of treatment on DMI, milk yield, and milk composition resulted in a lack of treatment effects on energy corrected milk yield. Treatment effects were not observed for milk fat yield, milk protein percentage, milk lactose percentage, somatic cell score, milk urea nitrogen concentration.

2.5.2 Serum Acute Phase Proteins

There were no significant treatment effects observed for serum haptoglobin, but both LPS binding protein and serum amyloid A were affected by treatment (Table 2.3). For LPS binding protein, T2 (2.08 µg/mL) was greater than CON, IS, and T1 (1.02 – 1.12 µg/mL), while T3 (1.43 µg/mL) did not differ from any treatment. For serum amyloid A, T2 was greater than all other treatments.

2.5.3 VFA Concentrations and LPS

There were no significant treatment effects or interactions of treatment by time for rumen pH, VFA, or lactate (Table 2.4). However, rumen pH was increased by buffer inclusion as compared to IS (contrast 2: *P* = 0.05). Rumen isobutyrate concentration tended to be affected by treatment (*P* = 0.08). This tendency was driven by the decrease in IS isobutyrate concentrations (0.94 mM) as compared to buffer treatments (ranged 1.13 to 1.28) (contrast 2: *P* = 0.03). Similarly, isobutyrate percentages were increased by buffer treatments in comparison to IS (contrast 2: *P* = 0.05).

Treatment by time interactions were observed for fecal pH, butyrate concentration, and valerate molar percentage and tended to affect concentrations fecal acetate, propionate, valerate, and total VFA (Table 2.5). For fecal pH, IS depressed pH in comparison to CON, T1, T2, and T3 (*P* = 0.004), but the interaction of treatment by time was due to this not being consistent across time points (Figure 2.1). The IS treatment was different from all other treatments on d 12 0800h and d 13 1700h, different from at least one other treatment on d 12 1400h, d 12 2000h, and d 13 0500h, but not different at the other times. Fecal score was affected by treatment (*P* = 0.001), with CON (score 3.20) being greater than T1, T2, and T3 (ranged 2.45 to 2.64). Additionally, IS (score of 2.97) differed from buffer treatments (2.54 average) (contrast 2: *P* = 0.004). For acetate concentration, T1, T2, and T3 (74.5 mM average) increased in comparison to CON and IS (61.2 mM average) (*P* = 0.002). This increase in acetate concentrations was reflected in total VFA concentrations, where T1, T2, and T3 (100.1 mM average) had higher VFA concentrations in comparison to CON and IS (84.8 mM average) (*P* = 0.003). For the significant interaction of treatment by time of butyrate (*P* = 0.04) and tendency for an interaction of treatment by time for acetate (*P* = 0.07) and total VFA (*P* = 0.06), all followed similar trends. For butyrate, acetate, and total VFA, the interaction was primarily driven by CON having lower VFA concentrations on d13 at 1700 h in comparison to IS, T1, T2, and T3 (data not shown). The tendency for a treatment effect on valerate concentrations (*P* = 0.09) was due to lower valerate concentrations for the T2 and T3 treatments in comparison to the CON treatment (*P* = 0.02 and *P* = 0.02, respectively). The tendency for treatment by time interaction of valerate concentration (*P* = 0.06) was primarily driven by the CON treatment exhibiting higher values in comparison to the T2 treatment on d 12 at 2000h and d 13 at 1100 h, 1700 h, and 0500 h (data not shown). Finally, the tendency for treatment by time interaction of propionate concentration (*P* = 0.06) was due to CON exhibiting higher concentrations than IS and T3 on d 13 at 1100 h (*P* = 0.02 and *P* =

0.02, respectively), as well as T2 displaying higher concentrations on d 12 at 2000 h than CON and IS (P = 0.01 and P = 0.03, respectively) (data not shown).

Fecal LPS tended to be affected by treatment (P = 0.06) (Table 2.5). This tendency was driven by the increase in LPS concentrations in the treatments receiving abomasally infused starch as compared to CON (contrast 1: P = 0.02).

2.5.4 Apparent Total Tract Digestibility

Treatment affected input, fecal output, and apparent total tract digestibility of most evaluated nutrients (Table 2.6). The effects on nutrient input (consumed in the TMR plus infused) were driven by treatment differences in TMR DMI and the starch infusion. When comparing treatments that included the starch infusion, input of DM, OM, NDF, ADF, and CP were lower or tended to be lower for T2 than for IS or T1 due to reduced TMR DMI for the T2 treatment. Input of those nutrients for T3 did not differ from any treatment for all variables except ADF due to the numerically intermediate TMR DMI. The numeric or significant decrease in DMI for the T2 and T3 treatments was similar to the DM provided in the starch infusion, resulting in no difference in total DM input among CON, T2, and T3. By design, total input of starch (TMR plus infusion) was greater for all treatments compared to CON (contrast 1: P = 0.001). For all treatments infused with starch, the average starch intake from the TMR was 6.67 kg/d and the average starch infused was 2.02 kg/d. Thus, the starch infusion accounted for approximately 23% of total starch input.

Predicted fecal output of DM significantly increased with the IS and T1 treatments compared to CON, and numerically increased for T2 and T3 (Table 2.6). Consequently, apparent total tract digestibility of DM was reduced for all treatments compared to CON. Similar effects were observed for OM digestibility. Fecal starch concentration increased dramatically from 4.2% on the CON treatment to an average of 15.3% for the other treatments, resulting in fecal starch output of 0.3 kg/d for CON and approximately 1.3 kg/d for the other treatments and apparent total tract starch digestibility of 95.6% for CON and a mean of 84.3% for the other treatments. Fecal NDF concentration was decreased by IS, T1, T2, and T3 in comparison to CON (contrast 1: $P = 0.001$. However, the fecal output as a proportion of input increased with these treatments. As such, apparent total tract digestibility of NDF tended to change based on treatment ($P = 0.08$), due to IS, T1, T2, and T3 treatments exhibiting lower digestibility than CON (contrast 1: $P = 0.007$). Fecal ADF percentage was affected by treatment ($P = 0.001$), with CON (36.0%) being greater than T1, T2, and T3 (28.3% average). Additionally, contrasts revealed that IS (30.9%) differed from T1, T2, and T3 ($P = 0.01$). Fecal output of ADF was greater for IS (2.9 kg/d) than T2 and T3 (2.3 and 2.4 kg/d, respectively), and output of ADF for CON and T1 (2.7 kg/d for both) was greater than T2. Despite the presence of these effects on fecal ADF percentage and fecal ADF output, treatment did not affect overall apparent total tract ADF digestibility. Crude protein exhibited similar responses, with fecal CP percentage decreased in IS, T1, T2, and T3 in relation to CON (contrast 1: $P = 0.001$). Fecal output of CP was greater for T1 than CON, T2, and T3, and IS was greater than T2. As with NDF, apparent total tract digestibility of CP numerically decreased in all treatments in comparison to CON, but only T1 significantly differed from CON.

Input of Mg and Ca from the basal TMR plus the starch infusion differed among diets due to the lower DMI for T2 compared to CON, IS, and T1 (Table 2.6). Total input of Mg (TMR plus starch infusion plus buffer treatment) was greatest for T2 and T3 (156 and 150 g/d, respectively), intermediate for T1 (132 g/d), and lowest for CON and IS (92 and 93 g/d, respectively). Fecal concentration of Mg differed among all treatments except for T2 and T3 (1.29 and 1.24%, respectively), which were greater than all other treatments (0.74%, 0.90%, and 1.08% for IS, CON, and T1, respectively). Fecal output of Mg was greater for T1, T2, and T3 (ranged 101 to 107 g/d) than CON and IS (66 and 71 g/d, respectively). Interestingly, there was no effect of treatment on apparent Mg digestibility which ranged from 21.8 to 29.4%. Total input of Ca was greater for T1 and T2 (165 and 177 g/d, respectively) than for CON, IS, and T3 (ranged 130 to 134 g/d). Fecal Ca content was greater for CON, T1, and T2 (1.48, 1.46, and 1.51%, respectively) than for IS and T3 (1.14 and 1.23%, respectively). Fecal Ca output was greater for T1 (137 g/d) than for CON, IS, and T3 (ranged 104 to 110 g/d), and T2 did not differ from any treatments (123 g/d). As with Mg, apparent total tract digestibility of Ca did not differ among treatments.

Treatment affected fecal purine concentration (Table 2.7). Purine concentrations were greater in CON than IS, with T1, T2, and T3 not differing from any treatment ($P = 0.03$). There were no differences among treatments in total daily purine excretion or purines as a fraction of CP. However, IS decreased purines as a fraction of CP (45.4 g/d in feces divided by kg/d fecal CP) as compared to buffer treatments (average 56.0 g/d in feces divided by kg/d fecal CP) (contrast 2: $P = 0.03$).

2.6 Discussion

This study abomasally infused 0 or 2 g/kg BW corn starch in period 1 and 0 or 4 g/kg BW corn starch in periods 2-5 split into 2 bolus infusions every 12 h. During period 1 this corresponded to an average of 0 or 1.1 kg/d starch. During periods 2-5 this corresponded to 0 or 2.2 kg/d starch. Dietary nutrient levels for this study were 15.8% CP, 30.2% NDF, 19.8% ADF, and 30.9% starch in period 1, with 15.1% CP, 31.2% NDF, 19.5% ADF, and 30.9% starch in periods 2-5. Mean consumed DMI (TMR, corn grain topdress, and buffer) was 25.6 kg/d in Period 1 and 23.7 kg/d in Periods 2-5. Using those numbers, cows had a mean consumed starch intake from TMR of 7.9 and 7.3 kg/d in periods 1 and 2-5, respectively. According to Sanz-Fernandez et al. (2020), ruminal starch degradation averages 72% when cows are fed less than 10 g/d/kg BW of starch. However, increased starch intakes are associated with decreased ruminal starch degradation, averaging 55% when fed above 10 g/d/kg BW of starch (Sanz-Fernandez et al., 2020), which will proportionately increase postruminal starch flow. For this study, the basal diet provided approximately 10.3 g/d/kg BW starch in period 1 and 9.5 g/d/kg BW starch in periods 2-5, just around the predicted threshold for decreasing ruminal starch degradation. Assuming 72% of starch degradation in the rumen, the resulting dietary duodenal starch flow was approximately 2.2 kg/d in period 1 and 2.1 kg/d in periods 2-5. On average, abomasal starch infusions added 1.1 kg/d of starch in period 1 and 2.2 kg/d of starch in periods 2-5. Based on these projections of starch flow to the duodenum from the diet, infusions should have increased total duodenal starch flow by approximately 50% in period 1 to 3.3 kg/d and 108% in periods 2-5 to 4.3 kg/d. Small intestinal starch digestion is limited compared to the rumen, with averages between 53% (Owens et al., 1986) and 66% (Offner and Sauvant, 2004) of duodenal starch flow. Based on this range of 53-66% duodenal starch digestion, large intestinal starch flow would be approximately 1.1 to 1.6 kg/d in period 1 with abomasal starch infusion, and between 1.5 and 2.0 kg/d in periods 2-5 with abomasal starch infusion.

DMI and milk yield were decreased by the T2 treatment as compared to CON, IS, and T1 (Table 2.3, $P < 0.05$). Calcium-based buffers fed at 1-2% of dietary DM have been shown to decrease DMI and milk production (Rogers et al., 1985; Clark et al., 1989). Based on the mean consumed DMI (TMR, corn grain topdress, and buffer) of 25.6 kg/d in Period 1 and 23.7 kg/d in Periods 2-5, the T2 treatment ($CaCO_3$, MgO, and crushed oyster shell) dose was fed at approximately 1.2% and 1.3% of the dietary DM, respectively. With the higher dose of buffer inclusion into the diet, T2 decreased both DMI and milk production, in agreement with the literature. While the additional of abomasal starch in IS did not affect milk yield as compared to CON, total DMI input was increased by IS and T1 compared to CON ($P = 0.02$). This increase was due to the abomasally infused starch present in IS and T1, while the addition of buffers in T2 and T3 decreased intake enough to be at the same level as CON, despite abomasal starch addition. Starch infusion did not affect milk yield, in agreement with reported results from studies that continuously abomasally infuse up to 3 kg/d of wheat starch or corn starch (Reynolds et al., 2001; van Gastelen et al., 2021). However, these cows were in mid- to late-lactation and likely did not shift the excess energy into milk production. Milk fat percentage and protein yield tended to change with treatment, increasing and decreasing for T2 as compared to IS, respectively ($P < 0.10$). The milk fat percentage increase can likely be attributed to the milk production decrease, as fat yield did not differ among treatments. Milk protein decreases exhibited in this study match those presented by others when feeding limestone at 1.4% and 2.4% of dietary DM (Rogers et al., 1982, 1985). While buffering the intestines could potentially alter abomasal pH and decrease small intestinal protein degradation, ultimately tending to lower milk protein (Rogers et al., 1982), the decrease in milk protein yield was likely a result of decreased milk production.

Our main interests in assessing rumen variables were to determine the impact of the moderately high starch diet on the rumen, to indirectly assess whether there was any backflow of the infused starch into the rumen, and to determine whether fed buffers affected the rumen environment. While rumen variables were not affected by treatment, rumen pH averages were lower than expected. For the CON treatment, the average rumen pH was 5.95, with the average nadir being 5.39. Despite the limitations of the small number of time points, the CON rumen pH observed in this experiment were similar to those in the literature observed when inducing SARA. When inducing SARA with a grain-based, 33.4% starch diet, Khafipour et al. (2009) reported an average rumen pH of 5.97. Similarly, a grain-based SARA challenge diet containing 33.7% starch resulted in an average rumen pHs of 5.98 (Li et al., 2012). While our intention was not to induce SARA, we did seem to be successful in lowering ruminal pH to that of SARA levels (Jaramillo-López et al., 2017). Abomasal starch infusion did not affect rumen total VFA (contrast 1: $P = 0.56$), suggesting significant backflow of starch out of the abomasum did not occur. When comparing IS to T1, T2, and T3, the buffer treatments increased rumen pH (contrast 2: $P = 0.05$), suggesting that there was some ruminal buffering that occurred by these treatments. However, the reduced voluntary DMI in T2 ($P = 0.02$) and numerical decrease in T3 as compared to CON, IS, and T1 may also account for some of the pH increase.

Based on our previous work, we hypothesized that abomasal starch infusions would decrease fecal pH (Cronin et al., 2023) and that fed buffers would raise fecal pH relative to the IS treatment (Neiderfer et al., 2020). As hypothesized, IS decreased fecal pH, and pH of the three buffer treatments did not differ from CON. The drop in fecal pH due to abomasal corn starch infusion (0.43 pH unit difference between CON and IS) was smaller than expected based on the literature. When abomasally infusing 4 kg/d of corn starch in pulse doses, Abeyta et al. (2023) observed a fecal pH drop of 0.91 units, from 6.76 in the control to 5.84 in the starch treatment. Van Gastelen et al. (2021) found that continuous abomasal infusions of 0, 1.5, and 3.0 kg of corn starch/d decreased fecal pH from 6.49 to 6.00 to 5.15. Based on the relationship between fecal pH and abomasal corn starch described by van Gastelen et al. (2021) (fecal pH = 6.74 – 0.59 × kg of corn starch abomasally infused), the IS treatment should have provided enough starch to reduce fecal pH to 6.09 in period 1 and to 5.44 in periods 2-5. Results from the literature did not accurately predict the relatively mild drop in fecal pH observed in the current study. The delivery method of abomasal starch likely contributes to these differences in the resultant fecal pH. The delivery of 2.2 kg/d of abomasal corn starch in our periods 2-5 was well above van Gastelen et al.'s (2021) suggested 1.25 kg/d. In our previous work, 0, 0.5, and 1.6 kg/d of abomasal starch split into twice daily pulse doses resulted in dropped fecal pH from 6.96 to 6.73 to 6.69 (Cronin et al., 2023), respectively, and that pH drop was similarly lower than expected based on findings in the literature (Reynolds et al., 2001; van Gastelen et al., 2021; Piantoni et al., 2022). While we used a twice daily pulse-dose method of delivery in previous experiments (Cronin et al., 2023) and the current study, others infused starch either 4 times a day (Abeyta et al., 2023) or continuously (Reynolds et al., 2001; van Gastelen et al., 2021; Piantoni et al., 2022). This suggests that the twice daily pulse-dose method does not induce the same level of challenge as more frequent administration. Based on the fecal starch present in the CON and IS treatments, only approximately 52% of the postruminally infused starch was digested (approximately 72% digested in P1 and 37% in P2-5; data not shown). The twice daily pulse-dose method seems to overwhelm the capacity for postruminal starch digestibility as evidenced by the dramatic increase in fecal starch as compared to the CON treatment.

Calcium- and magnesium-based buffers have been shown to consistently increase fecal pH in a range of dietary starch levels and with or without a postruminal starch challenge (Rogers et al., 1982; Teh et al., 1985; Christiansen and Webb, 1989; Neiderfer et al., 2020). In our previous work, a mixture of $CaCO_3$ and MgO fed at approximately 0.8% of DMI with a 26.5% starch diet increased fecal pH by 0.17 units (Neiderfer et al., 2020). At dietary starch levels higher than 50%, limestone fed at 2.4% DMI increased fecal pH by 2.54 units compared to the control (Rogers et al., 1982), and limestone and MgO fed at approximately 1.3% and 0.5% increased the fecal pH by 0.32 and 0.64 units, respectively, when compared to the control (Christiansen and Webb, 1989). Similarly, Erdman et al. (1982) observed a fecal pH increase of 0.64 units in comparison to the control when feeding 0.8% MgO to a 35.5% starch diet. We fed our buffers at approximately 0.5% (T1), 1.3% (T2), and 0.6% (T3) of total DMI, respectively, and we observed increases in fecal pH relative to IS of 0.3 to 0.5 units, which is in agreement the literature.

Decreases in fecal score in T1, T2, and T3 were not unexpected due to dietary magnesium levels. High levels of magnesium in the diet can increase the potential for diarrhea (NRC, 2001). The NRC (2001) recommends magnesium levels to not exceed 0.4% of the diet. With the basal TMR providing 0.32% Mg, the T1, T2, and T3 treatments provided a total of approximately 0.46, 0.65, and 0.59% Mg in each diet, respectively. Based on these calculations, each treatment dose provided more magnesium than suggested by the NRC. Therefore, any changes to the intestinal osmotic gradient that would cause a lower fecal score can likely be attributed to the magnesium levels in the T1, T2, and T3 treatments. When feeding levels of approximately 0%, 0.7%, or 1.4% MgO in the diet, Schaefer et al. (1982) found that increasing MgO decreased fecal consistency.

Fecal VFA concentrations did not change as expected, with no differences between CON and IS treatments. The addition of abomasal corn starch was intended to enhance intestinal fermentation, increasing VFA concentrations. Abomasal corn can increase total VFA (Robbers et al., 2018; Westreicher-Kristen et al., 2018; van Gastelen et al., 2021), acetate (Robbers et al., 2018; Westricher-Kristen et al., 2018) and butyrate (Robbers et al., 2018; Westreicher-Kristen et al., 2018; van Gastelen et al., 2021a, 2021b; Cronin et al., 2023), and decrease propionate (van Gastelen et al., 2021b). It's likely that the moderately high starch diet and unintentional SARA induction in this study blunted the effects of the infused starch, as the previously cited studies described dietary starch values ranging between 0 and 20.6%. The lack of effect on fecal VFA was likely additionally due to the poor starch digestibility in this study, in combination with the twice daily pulse dosing not allowing enough time for digestion of abomasal starch. However, buffer inclusion considerably changed fecal VFA concentrations. On average, fecal acetate increased by 16.2 mM due to buffer treatments as compared to CON, which resulted in increased total VFA concentrations. Rumen acetate molar percentage may increase, and propionate molar percentage may decrease with the supplementation of MgO (Erdman et al., 1982; Stokes et al., 1986) but reported data on fecal VFAs is limited when supplemented with fed buffers. $CaCO_3$ or limestone supplementation to the diet between 1.4 and 2.4% failed to change rumen acetate or propionate molar percentage as compared to the control (Rogers et al., 1982, 1985; Clark et al., 1989). However, when infused with

1 g/kg BW abomasal corn starch and fed 200 g/d $CaCO_3$ or a blend of 125 g/d $CaCO_3$ and 75 g/d MgO, fecal acetate increased on average by 6.75 mM as compared to the control (Neiderfer et al., 2020). In the same experiment, fecal propionate increased by 1.7 mM relative to the control (Neiderfer et al., 2020). In this experiment, there were no differences due to treatment in the primary VFA when expressed as molar percentages.

The decrease in NDF, ADF, and CP input (TMR, infusion, and buffer) in T2 as compared to CON are primarily driven by the reduced DMI exhibited when cows were subjected to T2. Similarly, the starch intake (TMR alone) was decreased in T2 as compared to CON, but starch input (TMR, infusion, and buffer) still decreased T2 as compared to IS. In the current study, IS reduced DM, OM, and starch digestibility, and tended to reduce NDF digestibility as compared to CON. Postruminal infusion of starch may reduce (van Gastelen et al., 2021b), increase (Reynolds et al., 2001), or have no effect on starch digestibility (Knowlton et al., 1998; Cronin et al., 2023). With moderately high dietary starch concentrations around 30%, it’s likely that the additional abomasal corn starch in this study overwhelmed the limited capacity of postruminal starch digestion, leading to reductions in total tract digestibility. The lower retention time in the colon coupled with the massive influx of infused starch likely contributed to these reductions in digestibility. The inclusion of mineral buffers did not rescue reduced nutrient digestibilities, although this was expected. Though buffers may have increased intestinal pH to improve the ability of microbes to ferment digesta, the relative contribution of the large intestine to nutrient digestion is small in cattle. The effects of adding MgO, limestone, or $CaCO_3$ to the diet remains varied in the literature, sometimes increasing digestibility of DM, fiber, or starch (Rogers et al., 1982; Erdman et al., 1982; Pierce et al., 1983; Clark et al., 1989), while others reported no differences (Rogers et al., 1985; Christiansen and Webb, 1990; Neiderfer et al., 2020). CP digestibility decreased due to starch infusion as compared to CON (contrast 1: $P = 0.01$). Infused starch decreasing apparent total tract digestibility of CP is commonly observed and thought to be the result of increased microbial fermentation leading to microbial protein synthesis (Gressley and Armentano, 2007; Gressley et al., 2011; van Gastelen et al., 2021). Similar to our results, Christiansen and Webb (1990) and Neiderfer et al. (2020) found that CP digestibility was not affected by the addition of limestone, though Rogers et al. (1982) found that it decreased CP digestibility.

We hypothesized that fecal purine concentrations would increase with abomasal starch infusions. Fecal purines typically increase when postruminal carbohydrate fermentation increases, due to higher microbial biomass (Gressley and Armentano, 2005; Westreicher-Kristen et al., 2018). However, no differences were observed between treatments for fecal purine excretion expressed as g/d or as a fraction of fecal CP. Although we calculated that approximately 52% of the infused starch disappeared postruminally, this did not manifest as an increase in fecal purines. However, this does agree with the modest effect observed on fecal pH and the lack of effect on fecal VFA. Instead, fecal purine concentration (mg/d DM) was lower in the treatments with abomasal starch infusions (contrast 1: $P = 0.009$). This was likely a result of the reduced nutrient digestibility, with the starch infusions diluting the microbial protein. In the infused starch treatments, fecal purine concentration expressed both as mg/g DM and g/kg fecal CP was increased with the inclusion of buffers (Contrast 2: $P = 0.03$ for both variables). Similar to the effects of buffers on fecal VFA, this suggests that the buffers increased microbial activity in the large intestine.

Induction of SARA through grain challenges prompts systemic inflammation as evidenced by increased acute phase proteins (Plaizier et al., 2008). This response is believed to be the result of SARA conditions increasing microbial antigens such as LPS that can cause localized effects or be translocated through damaged epithelium (Khafipour et al., 2009). Increased LPS and epithelial damage also occur in the hindgut following SARA induction, suggesting that hindgut effects may contribute to the systemic inflammatory response (Khafipour et al., 2009; Li et al., 2012; Tao et al., 2014).

We hypothesized that infused corn starch would increase bacterial growth and fermentation, as evidenced by decreased pH, increased VFA, and increased LPS, and this would result in a systemic inflammatory response as evidenced by an increase in acute phase proteins. We hypothesized that the buffer treatments would improve the conditions in the intestines to mitigate these effects. However, our results do not support these hypotheses. The abomasal corn starch only mildly impacted intestinal fermentation, likely because fermentation was already impacted by the unintentional SARA induction. The buffer treatments increased fecal pH, but they did not decrease LPS or acute phase proteins, and they actually increased VFA.

Although our lack of an inflammatory response to the abomasal corn starch might be explained by the challenging basal diet (30.9% starch on a DM basis), abomasal infusions to induce hindgut acidosis without concurrent ruminal acidosis also did not produce the predicted acute phase response (van Gastelen et al., 2021a, 2021b; Abeyta et al., 2022). Abomasal infusion of acidotic rumen fluid from grain challenged donor cows failed to produce an acute phase response in recipient cows, further suggesting that concurrent ruminal acidosis is necessary to induce systemic inflammation (Abeyta et al., 2023). In our study, treatments with infused starch tended to increase LPS levels as compared to CON (contrast 1: $P = 0.02$), but effects were modest. The back transformed means of our data demonstrate that LPS increased from 9 to 33% between CON and IS, T1, T2, and T3 (33,389 EU/g to 36,308 – 44,300 EU/g), with buffer treatments not differing from IS. Increases in fecal LPS may be induced by grain-based SARA challenges and are likely due to the growth of LPS-producing bacteria fermenting the undegraded carbohydrates that have entered the intestines from the rumen (Li et al., 2012). In our previous work, we observed a 175% increase (13,803 to 38,019 EU/g) in fecal LPS when cows were infused with similar levels of corn starch (3 g/kg BW) but fed a 20.6% starch diet (Cronin et al., 2023) and 40,616 EU/g of fecal LPS when cows were infused with only about 1/3 of the level of corn starch and fed a 26.5% starch diet (Neiderfer et al., 2020). As summarized by Cronin et al. (2023), there seems to be high variability in fecal LPS response to increased intestinal starch. The relatively small difference in LPS between the CON and infused starch treatments suggests that the starch infusion produced only a slight challenge. As suggested previously, this minimal response may be due to high levels of dietary starch and the twice-daily pulse dose delivery method of the abomasal starch. Treatment did not affect haptoglobin, but LPS binding protein and serum amyloid A were both increased in T2. However, acute phase protein concentrations for all treatments including T2 were within the range expected for healthy cows (Bannerman et al., 2003; Zeng et al., 2009; Humer et al., 2018; Trela et al., 2022). Despite this, when combining the lowered DMI and higher circulating acute phase proteins observed in T2 as compared to CON, this suggests that buffer A at the 300 g/d dose imparted a negative effect on the cows in this study. Intentional buffering of the hindgut has not been heavily studied, and our results suggest that feeding high levels of these buffers may exacerbate the challenge of hindgut acidosis. High hindgut pH, though important, is not the only driving factor for hindgut health.

2.7 Conclusions

Although our goal was to induce hindgut acidosis with abomasal starch supply in mid- to late-lactating dairy cows fed a high starch TMR, the infused starch was only partially digested resulting in only small changes in fecal pH and LPS and no changes in fecal score or VFA. Acute phase proteins were not increased for IS compared to CON, suggesting that the hindgut challenge did not generate an inflammatory response. The moderately high starch diet fed in this study likely increased intestinal starch flow on its own, limiting the effectiveness of the challenge model. Buffer supplementation increased fecal pH as expected, but it increased fecal VFA and fecal purines, suggesting increased hindgut fermentation. In addition, one buffer treatment (T2) increased 2 acute phase proteins relative to all other treatments. While there may be benefits to higher fecal pH, the buffers employed in this experiment did not alleviate the negative effects of abomasal starch infusions and, in the case of T2, may have presented an additional challenge.

TABLES

Table 2.1: Ingredient and nutrient composition of the total mixed ration, percent of DM unless otherwise stated.

Ingredient	Period 1	Periods 2-5
Corn silage	34.40	38.00
Triticale silage	17.35	17.31
Corn grain top dress, 1 kg/d[1]	3.49	3.69
Grain mix		
Ground corn grain	22.90	20.95
Protected soybean meal[2]	4.28	3.92
Solvent extracted soybean meal	3.90	3.57
Solvent extracted canola meal	3.24	2.97
Soybean hulls ground	2.74	2.51
Rumen bypass fat[3]	1.46	1.34
Blood meal ring dried	0.92	0.84
Corn gluten meal	0.76	0.70
Sodium bicarbonate	0.67	0.61
Corn distiller’s grain	0.61	0.56
Sugar	0.41	0.38
Trace mineral and vitamin mix[4]	0.41	0.38
Potassium carbonate[5]	0.39	0.36
Sodium chloride	0.38	0.35
Urea	0.35	0.32
Calcium carbonate	0.32	0.29
Rumen protected lysine[6]	0.28	0.26
Monocalcium phosphate[7]	0.22	0.20
Mold inhibitor[8]	0.17	0.16
Potassium and magnesium sulfate[9]	0.15	0.14
Methionine precursor[10]	0.09	0.08
Magnesium oxide	0.06	0.05
Rumen protected methionine[11]	0.04	0.04
B vitamins[12]	0.01	0.01
Monensin[13]	0.01	0.01

Table 2.1 continued

Chelated zinc[14]	0.01	0.01
Nutrient		
Crude protein	15.8	15.1 ± 0.3
NDF	30.2	31.2 ± 1.0
ADF	19.8	19.5 ± 0.5
Starch	30.9	30.9 ± 0.6
Ash	8.3	7.2 ± 0.3
NE_L, Mcal/kg	1.68	1.68 ± 0.01

[1]Mixed in the ration during adaptation and washout periods. Applied by hand with the treatments during the treatment periods.
[2]Extruded and expelled soybean meal (J. L. Moyer & Sons, Inc., Turbotville, PA).
[3]EnerG-3 (Virtus Nutrition, Corcoran, CA).
[4]Contained 5.13% calcium, 34% magnesium, 7.13% sulfur, 4.53% potassium, 660 mg/kg Fe, 4,213 mg/kg Zn, 818 mg/kg Cu, 4,099 mg/kg Mn, 65 mg/kg Se, 141 mg/kg Co, 191 mg/kg I, 400 KIU/kg Vitamin A, 100 KIU/kg Vitamin D, and 2,400 IU/kg Vitamin E. (1965 Mill Mix 4 MTX, Renaissance Nutrition, Roaring Spring, PA).
[5]DCAD Plus (Church & Dwight Co., Inc, Princeton, NJ).
[6]AjiPro-L (Ajinomoto Co., Inc., Tokyo, Japan).
[7]Biofos (Mosaic Crop Nutrition, LLC., Lithia, FL).
[8]Myco CURB (Kemin Industries, Inc., Des Moines, IA).
[9]Dynamate (18% K, 11% Mg, 22% S; The Mosaic Company, Plymouth, MN).
[10]HMTBa (MHA, Novus International, Inc., St. Charles, MO).
[11]Smartamine M (Adisseo, Antony, France).
[12]Lactation BV (Jefo, Saint-Hyacinthe, Quebec).
[13]Custom premix produced by Renaissance Nutrition (Roaring Spring, PA) containing 0.485% Rumensin 90.7 (Elanco, Greenfield, IN).
[14]MINTREX Zn (Novus International, Inc., St. Charles, MO).

Table 2.2: Analyzed anion and cation mineral content of the TMR (means of Periods 1-5) and buffers (single sample). Percent of DM unless otherwise stated.

	TMR	Buffer A	Buffer B
Ca	0.59 ± 0.03	21.47	6.54
Cl	0.38 ± 0.02	0.11	1.24
K	1.42 ± (0.05	0.26	0.25
Mg	0.32 ± 0.01	25.96	44.49
Na	0.35 ± 0.04	0.82	0.86
P	0.36 ± 0.02	0.00	0.01
S	0.23 ± 0.01	0.05	0.05
DCAD[1] (mEq/kg DM)	262 ± 25		
DCAD[2] (mEq/kg DM)	299 ± 29		

[1]DCAD = dietary cation–anion difference calculated as (Na + K) – (Cl + S). When including the dietary buffers, DCAD calculated using this equation was 262, 262, 261, 259, and 261 for CON, IS, T1, T2, and T3, respectively.

[2]DCAD = dietary cation–anion difference calculated as (Na + K + 0.15 × Ca + 0.15 × Mg) – (Cl + 0.6 × S + 0.5 × P). Assumes a valence of 1.8 for P. When including the dietary buffers, DCAD calculated using this equation was 299, 299, 326, 362, and 337 for CON, IS, T1, T2, and T3, respectively.

Table 2.3: Effects of treatment on dry matter intake, milk yield, milk composition (n = 8) for DMI and energy corrected milk; n = 9 for all other variables).

	Treatment[1]						*P* Values		
								Contrasts[2]	
	CON	IS	T1	T2	T3	SEM	Treatment	1	2
DMI[3], kg/d	24.4[a]	24.8[a]	24.9[a]	21.4[b]	22.5[ab]	1.3	0.02	0.30	0.09
Total DMI input[4], kg/d	24.5[b]	27.3[a]	27.4[a]	23.9[b]	24.9[ab]	1.3	0.02	0.15	0.09
Milk, kg/d	31.4[a]	30.9[a]	29.8[a]	26.1[b]	28.3[ab]	2.0	0.04	0.08	0.07
Fat, %	3.80	3.76	3.92	4.13	3.99	0.17	0.07	0.16	0.03
Fat, kg/d	1.20	1.18	1.15	1.07	1.13	0.08	0.55	0.32	0.40
Protein, %	3.16	3.20	3.22	3.24	3.24	0.06	0.52	0.14	0.39
Protein, kg/d	0.99	0.97	0.94	0.82	0.90	0.07	0.09	0.14	0.13
Lactose %	4.70	4.67	4.67	4.72	4.69	0.03	0.43	0.55	0.34
Energy corrected milk, kg/d	33.5	32.9	32.0	28.7	31.0	2.1	0.18	0.17	0.19
Somatic cell score	1.69	1.84	2.16	2.09	2.18	0.31	0.56	0.19	0.30
Milk urea nitrogen, mg/dL	9.7	9.5	9.8	9.9	9.0	0.6	0.66	0.84	0.93
Serum acute phase proteins, µg/mL									
Haptoglobin	112	106	104	96	106	14	0.95	0.55	0.80
LPS binding protein	1.12[b]	1.02[b]	1.02[b]	2.08[a]	1.43[ab]	0.29	0.05	0.38	0.12
Serum amyloid A	22.8[b]	22.0[b]	26.2[b]	71.5[a]	18.5[b]	9.0	< 0.01	0.94	0.12

[1]Treatments were control ration alone (CON), control ration plus abomasal infusion of starch (IS), control ration plus abomasal infusion of starch and 150 g/day fed buffer A (T1), control ration plus abomasal infusion of starch and 300 g/day fed buffer A (T2), and control ration alone plus abomasal infusion of starch and 150 g/day fed buffer B (T3).
[2]Contrasts were 1) CON vs. (IS + T1 + T2 + T3); 2) IS vs. (T1 + T2 +T3).
[3]DMI = DMI from TMR, corn grain topdress, and buffer.
[4]Total DMI input = DMI from TMR, corn grain topdress, buffer, and starch infusion.

Table 2.4: Effects of treatment on ruminal pH and volatile fatty acid and lactate concentrations (n = 9).

	Treatment[1]						*P* values				
										Contrasts	
	CON	IS	T1	T2	T3	SEM	Treatment	Time	Treatment × time	1	2
Rumen pH	5.95	5.84	5.88	5.96	6.00	0.06	0.13	0.001	0.94	0.51	0.05
VFA, mM											
Acetate	76.8	76.4	77.9	78.4	76.8	1.9	0.88	0.001	0.99	0.76	0.48
Propionate	27.5	28.7	28.5	27.8	27.3	1.3	0.86	0.001	0.22	0.64	0.52
Butyrate	14.6	15.0	15.3	14.4	14.6	0.7	0.77	0.001	0.65	0.79	0.78
Isobutyrate	1.28	0.94	1.13	1.14	1.28	0.10	0.08	0.07	0.59	0.15	0.03
Valerate	1.73	1.95	1.88	1.79	1.81	0.13	0.80	0.001	0.51	0.41	0.44
Isovalerate	2.02	1.86	2.03	2.1	2.03	0.15	0.67	0.001	0.35	0.97	0.20
Total VFA	123.6	124.5	126.8	125.6	123.9	13.4	0.88	0.001	0.95	0.56	0.75
Lactate, mM[3]	0.08	0.09	0.28	0.19	0.16	--	0.62	0.02	0.65	0.38	0.30
VFA, mol%											
Acetate	62.6	61.8	62.0	62.9	62.5	0.8	0.85	0.001	0.41	0.74	0.46
Propionate	22.7	22.3	22.3	21.8	21.8	0.6	0.79	0.001	0.08	0.30	0.64
Butyrate	11.6	11.8	11.8	11.2	11.6	0.4	0.74	0.001	0.35	0.87	0.56
Isobutyrate	1.0	0.8	0.9	0.9	1.0	0.1	0.11	0.001	0.59	0.12	0.05
Valerate	1.4	1.5	1.4	1.4	1.4	0.1	0.58	0.001	0.60	0.50	0.16
Isovalerate	1.6	1.5	1.6	1.7	1.6	0.1	0.78	0.07	0.46	0.90	0.34

[1]Treatments were as described in footnote 1 of Table 2.3.
[2]Contrasts were 1) CON vs. (IS + T1 + T2 + T3); 2) IS vs. (T1 + T2 +T3).
[3]Lactate was log transformed prior to analysis. Back transformed LS means are presented.

Table 2.5: Effects of treatment on fecal pH, fecal score, and volatile fatty acid and lactate concentrations (n = 9).

	Treatment[1]						*P* values			Contrasts[2]	
	CON	IS	T1	T2	T3	SEM	Treatment	Time	Treatment × time	1	2
Fecal pH	6.80^{a}	6.37^{b}	6.69^{a}	6.86^{a}	6.73^{a}	0.09	0.004	0.001	0.02	0.18	0.001
Fecal Score	3.20^{a}	2.97^{ab}	2.64^{bc}	2.45^{c}	2.54^{c}	0.15	0.001	0.52	0.24	0.001	0.004
VFA, mM											
Acetate	58.3^{a}	64.0^{a}	73.6^{b}	75.1^{b}	74.7^{b}	3.2	0.002	0.001	0.07	0.001	0.008
Propionate	12.6	13.3	13.3	14.1	12.8	1.2	0.88	0.02	0.06	0.58	0.91
Butyrate	7.4	8.2	9.2	8.5	8.8	0.8	0.40	0.001	0.04	0.11	0.40
Isobutyrate	1.58	1.44	2.10	2.26	2.12	0.27	0.16	0.01	0.77	0.20	0.03
Valerate	0.46	0.37	0.31	0.26	0.27	0.06	0.09	0.001	0.06	0.01	0.14
Isovalerate	0.23	0.31	0.31	0.35	0.40	0.05	0.17	0.06	0.69	0.05	0.14
Total VFA	81.5^{a}	88.0^{a}	99.1^{b}	101.2^{b}	100.0^{b}	4.2	0.003	0.001	0.06	0.002	0.01
Lactate, mM[3]	0.77	1.11	1.93	1.88	1.71	--	0.20	0.01	0.30	0.06	0.13
VFA, mol %											
Acetate	71.7	73.0	74.2	74.4	74.9	1.0	0.09	0.001	0.27	0.02	0.13
Propionate	15.7	15.0	13.7	14.0	12.8	1.0	0.23	0.003	0.53	0.09	0.18
Butyrate	8.9	9.3	9.2	8.3	8.9	0.6	0.58	0.001	0.11	0.99	0.39
Isobutyrate	2.03	1.68	2.06	2.18	2.10	0.26	0.63	0.33	0.67	0.93	0.13
Valerate	0.57^{a}	0.44^{ab}	0.36^{b}	0.30^{b}	0.28^{b}	0.06	0.01	0.001	0.04	0.002	0.07
Isovalerate	0.30	0.35	0.31	0.35	0.40	0.05	0.58	0.001	0.51	0.31	0.90
LPS, log10	4.52	4.61	4.56	4.63	4.65	0.05	0.06	0.001	0.42	0.02	0.91

[1]Treatments were as described in footnote 1 of Table 2.3.

[2]Contrasts were 1) CON vs. (IS + T1 + T2 + T3); 2) IS vs. (T1 + T2 +T3).

[3]Lactate was log 10 transformed prior to analysis. Back transformed means are presented.

Table 2.6: Effects of treatment on apparent total tract nutrient digestibility and fecal starch (n = 8).

	Treatment[1]						*P* values		
								Contrasts[2]	
	CON	IS	T1	T2	T3	SEM	Treatment	1	2
Dry Matter									
Input (TMR+buffer+Infusion), kg/d	24.45^{b}	27.27^{a}	27.37^{a}	23.94^{b}	24.93^{ab}	1.28	0.02	0.15	0.09
Fecal output, kg/d	7.36^{b}	9.45^{a}	9.50^{a}	8.28^{ab}	8.51^{ab}	0.52	0.01	0.004	0.22
Apparent digestibility, %	69.7^{a}	65.7^{b}	65.2^{b}	65.6^{b}	65.8^{b}	1.3	0.02	0.001	0.87
Organic matter									
Input (TMR+buffer+Infusion), kg/d	22.51^{b}	25.28^{a}	25.24^{a}	21.95^{b}	23.01^{ab}	1.17	0.01	0.13	0.06
Fecal OM, %	86.2^{b}	87.8^{a}	87.2^{ab}	87.4^{a}	88.1^{a}	0.4	0.02	0.003	0.72
Fecal output, kg/d	6.34^{b}	8.29^{a}	8.31^{a}	7.24^{ab}	7.50^{ab}	0.46	0.01	0.003	0.23
Apparent digestibility, %	71.6^{a}	67.6^{b}	67.0^{b}	67.2^{b}	67.4^{b}	1.3	0.02	0.001	0.75
Starch									
Intake from TMR, kg/d	6.94^{a}	7.01^{a}	7.01^{a}	6.03^{b}	6.38^{ab}	0.34	0.02	0.20	0.07
Input from infusion, kg/d	0.06^{b}	2.02^{a}	1.99^{a}	2.05^{a}	2.00^{a}	0.09	0.001	0.001	0.94
Total input (TMR+buffer+Infusion), kg/d	7.00^{c}	9.03^{a}	9.00^{a}	8.08^{b}	8.37^{ab}	0.35	0.001	0.001	0.08
Fecal starch %	4.2^{b}	13.7^{a}	14.2^{a}	15.8^{a}	17.3^{a}	1.6	0.001	0.001	0.27
Fecal output, kg/d	0.29^{b}	1.25^{a}	1.34^{a}	1.30^{a}	1.49^{a}	0.16	0.001	0.001	0.52
Apparent digestibility, %	95.6^{a}	86.1^{b}	84.8^{b}	84.3^{b}	82.1^{b}	1.9	0.001	0.001	0.26
NDF									
Input (TMR+buffer+Infusion), kg/d	8.52^{a}	8.82^{a}	8.82^{a}	7.52^{b}	7.93^{ab}	0.45	0.02	0.48	0.06
Fecal NDF, %	57.9^{a}	53.3^{b}	50.6^{b}	50.4^{b}	52.2^{b}	1.5	0.001	0.001	0.11
Fecal output, kg/d	4.29	4.90	4.76	4.11	4.44	0.25	0.07	0.27	0.08

Table 2.6 continued

Apparent digestibility, %	49.7	44.1	45.6	45.0	44.0	2.2	0.08	0.007	0.69
ADF									
Input (TMR+buffer+Infusion), kg/d	5.24^{ab}	5.45^{a}	5.42^{a}	4.64^{c}	4.88^{bc}	0.28	0.02	0.49	0.05
Fecal ADF, %	36.0^{a}	30.9^{ab}	28.6^{bc}	28.2^{c}	28.2^{c}	0.9	0.001	0.001	0.01
Fecal output, kg/d	2.67^{ab}	2.87^{a}	2.70^{ab}	2.32^{c}	2.38^{bc}	0.15	0.02	0.43	0.01
Apparent digestibility, %	49.4	47.5	50.1	50.0	51.1	1.4	0.21	0.78	0.03
Crude protein									
Input (TMR+buffer+Infusion), kg/d	3.28^{a}	3.35^{a}	3.33^{a}	2.83^{b}	3.01^{ab}	0.18	0.02	0.27	0.05
Fecal CP, %	15.8^{a}	13.6^{bc}	14.1^{b}	13.1^{c}	13.6^{bc}	0.5	0.001	0.001	0.97
Fecal output, kg/d	1.16^{bc}	1.29^{ab}	1.33^{a}	1.08^{c}	1.16^{bc}	0.09	0.02	0.37	0.14
Apparent digestibility, %	64.1^{a}	61.9^{ab}	59.8^{b}	61.9^{ab}	61.7^{ab}	1.6	0.05	0.01	0.50
Magnesium									
Input (TMR+Infusion), g/d	91.8^{a}	93.0^{a}	93.0^{a}	78.0^{b}	83.3^{ab}	5.0	0.01	0.19	0.054
Intake (buffer), g/d	0	0	38.8	77.7	66.5	--	--	--	--
Input (TMR+Infusion+buffer), g/d	91.8^{c}	93.0^{c}	131.8^{b}	155.6^{a}	149.7^{a}	5.0	0.001	0.001	0.001
Fecal Mg, %	0.90^{c}	0.74^{d}	1.08^{b}	1.29^{a}	1.24^{a}	0.06	0.001	0.001	0.001
Fecal Mg output, g/d	65.9^{b}	71.4^{b}	101.2^{a}	105.7^{a}	107.0^{a}	8.1	0.001	0.001	0.001
Apparent digestibility, %	27.6	25.4	21.8	31.9	29.4	5.2	0.36	0.91	0.61
Calcium									
Input (TMR+Infusion), g/d	132.0^{a}	133.6^{a}	132.9^{a}	112.5^{b}	120.2^{ab}	7.2	0.02	0.19	0.06
Intake (buffer), g/d	0	0	32.1	64.2	9.8	--	--	--	--
Input (TMR+Infusion+buffer), g/d	132.0^{b}	133.6^{b}	165.0^{a}	176.8^{a}	130.0^{b}	7.2	0.001	0.002	0.001
Fecal Ca, %	1.48^{a}	1.14^{b}	1.46^{a}	1.51^{a}	1.23^{b}	0.09	0.001	0.02	0.001
Fecal Ca output, g/d	108.7^{b}	110.0^{b}	136.5^{a}	123.2^{ab}	104.2^{b}	11.1	0.03	0.23	0.20

Table 2.6 continued

Apparent digestibility, %	16.2	18.1	16.0	29.1	20.0	6.3	0.15	0.31	0.47

[1]Treatments were as described in footnote 1 of Table 2.3.

[2]Contrasts were 1) CON vs. (IS + T1 + T2 + T3); 2) IS vs. (T1 + T2 +T3).

Table 2.7: Effects of treatment on fecal purine concentrations (n = 9).

	Treatment[1]						*P* values		
								Contrasts[2]	
	CON	IS	T1	T2	T3	SEM	Treat-ment	1	2
Purines, mg/g DM	9.12[a]	6.37[b]	7.82[ab]	7.83[ab]	7.68[ab]	0.65	0.03	0.009	0.03
Purines, g/d in feces	72.2	64.8	73.4	66.9	70.1	8.86	0.87	0.64	0.49
Purines, g/d in feces divided by kg/d of fecal CP	57.4	45.4	55.9	59.0	53.1	4.2	0.14	0.37	0.03

[1]Treatments were as described in footnote 1 of Table 2.3.
[2]Contrasts were 1) CON vs. (IS + T1 + T2 + T3); 2) IS vs. (T1 + T2 +T3).

FIGURES

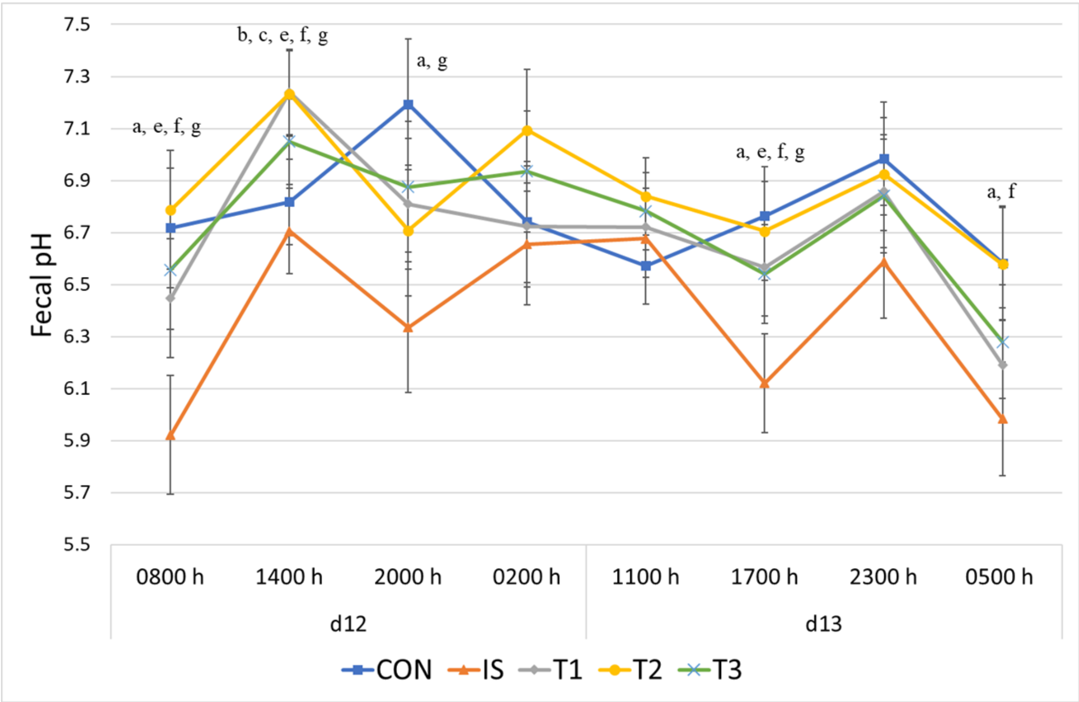

Figure 2.1: Least squares means for the interaction of treatment by time on fecal pH (consolidated into 24 hours; n = 9). [1]Treatments were as described in footnote 1 of Table 2.3. [a-j]Superscripts designate differences between treatments according to the PDIFF comparison among treatments in SAS ($P \leq 0.05$). a: CON different from IS, b: CON different from T1, c: CON different from T2, d: CON different from T3, e: IS different from T1, f: IS different from T2, g: IS different from T3, h: T1 different from T2, i: T1 different from T3, j: T2 different from T3.

REFERENCES

Abegaze, B., and R.C. Chopra. 2013. Ruminal Solubility and Effect of Calcite Powder Supplementation on Dairy Animal Performance Ruminal Solubility and Effect of Calcite Powder Supplementation on Dairy Animal Performance Ruminal Solubility and Effect of Calcite Powder Supplementation on Dairy Animal Performance 13.

Abeyta, M.A. 2022. Evaluating the metabolic, production, and inflammatory consequences of hindgut acidosis in dairy cows.

Abeyta, M.A., E.A. Horst, E.J. Mayorga, B.M. Goetz, M. Al-Qaisi, C.S. McCarthy, M.R. O'Neil, B.C. Dooley, P. Piantoni, G.F. Schroeder, and L.H. Baumgard. 2023. Effects of hindgut acidosis on metabolism, inflammation, and production in dairy cows consuming a standard lactation diet. J. Dairy Sci. 106:1429–1440. doi:10.3168/jds.2022-22303.

Bannerman, D.D., M.J. Paape, W.R. Hare, and E.J. Sohn. 2003. Increased Levels of LPS-Binding Protein in Bovine Blood and Milk Following Bacterial Lipopolysaccharide Challenge. J. Dairy Sci. 86:3128–3137.

Bissell, H.A., and M.B. Hall. 2010. Cattle differ in ability to adapt to small intestinal digestion of starch. J. Dairy Sci 93:845.

Christiansen, M.L., and K.E. Webb. 1990. Intestinal acid flow, dry matter, starch and protein digestibility and amino acid absorption in beef cattle fed a high-concentrate diet with defluorinated rock phosphate, limestone or magnesium oxide.. J. Anim. Sci. 68:2105–2118. doi:10.2527/1990.6872105x.

Clark, J.H., A.W. Plegge, C.L. Davis, and G.C. McCoy. 1989. Effects of Calcium Carbonate on Ruminal Fermentation, Nutrient Digestibility, and Cow Performance. J. Dairy Sci. 72:493–500. doi:10.3168/jds.S0022-0302(89)79131-1.

Council, N.R. 2001. Nutrient Requirements of Dairy Cattle. Seventh Re. National Academy Press.

Cronin, S.K., A.M. Barnard, S.J. Dietz, M. Lawrence, A.E. Kramer, and T.F. Gressley. 2023. Effect of short-term abomasal corn starch infusions on postruminal fermentation and blood measures. J. Dairy Sci. 106:8658–8669. doi:10.3168/jds.2022-23180.

Erdman, R.A., R.W. Hemken, and L.S. Bull. 1982. Dietary Sodium Bicarbonate and Magnesium Oxide for Early Postpartum Lactating Dairy Cows: Effects of Production, Acid-Based Metabolism, and Digestion. J. Dairy Sci. 65:712–731. doi:10.3168/jds.S0022-0302(82)82259-5.

Erdman, R.A. 1988. Dietary Buffering Requirements of the Lactating Dairy Cow: A Review. J. Dairy Sci. 71:3246–3266. doi:10.3168/jds.S0022-0302(88)79930-0.

Goering, H.K., and P.J. Van. 1970. Forage fiber analyses (Apparatus, Reagents, Procedures, and Some Applications). U.S. Dep. Agric. 387–598.

Gressley, T.F., and L.E. Armentano. 2005. Effect of abomasal pectin infusion on digestion and nitrogen balance in lactating dairy cows. J. Dairy Sci. 88:4028–4044. doi:10.3168/jds.S0022-0302(05)73089-7.

Gressley, T.F., M.B. Hall, and L.E. Armentano. 2011. Ruminant nutrition symposium: Productivity, digestion, and health responses to hindgut acidosis in ruminants. J. Anim. Sci. 89:1120–1130. doi:10.2527/jas.2010-3460.

Gressley, T.F., S.M. Reynal, J.J.O. Colmenero, G.A. Broderick, and L.E. Armentano. 2006. Technical note: Development of a tool to insert abomasal infusion lines into dairy cows. J. Dairy Sci. 89:3965–3967. doi:10.3168/jds.S0022-0302(06)72438-9.

Hall, M.B. 2009. Determination of starch, including maltooligosaccharides, in animal feeds: Comparison of methods and a method recommended for AOAC collaborative study. J. AOAC Int. 92:42–49. doi:10.1093/jaoac/92.1.42.

Heinrichs, J., and P. Kononoff. 2002. Evaluating particle size of forages and TMRs using the New Penn State Forage Particle Separator. Coll. Agric. Sci. DAS 02-42:1–14.

Hulsen, J. 2006. Cow Signals: A Practical Guide for Dairy Farm Management. Zutphen, Netherlands : Roodbont ; Bergen op Zoom, Netherlands : Vetvice, Zutphen, Netherlands.

Humer, E., R.M. Petri, J.R. Aschenbach, B.J. Bradford, G.B. Penner, M. Tafaj, K.H. Südekum, and Q. Zebeli. 2018. Invited review: Practical feeding management recommendations to mitigate the risk of subacute ruminal acidosis in dairy cattle. J. Dairy Sci. 101:872–888. doi:10.3168/jds.2017-13191.

Khafipour, E., D.O. Krause, and J.C. Plaizier. 2009. A grain-based subacute ruminal acidosis challenge causes translocation of lipopolysaccharide and triggers inflammation. J. Dairy Sci. 92:1060–1070. doi:10.3168/jds.2008-1389.

Khiaosa-ard, R., M. Ottoboni, S. Verstringe, T. Gruber, T. Hartinger, E. Humer, G. Bruggeman, and Q. Zebeli. 2023. Magnesium in dairy cattle nutrition: A meta-analysis on magnesium absorption in dairy cattle and assessment of simple solubility tests to predict magnesium availability from supplemental sources. J. Dairy Sci. 106:8758–8773. doi:10.3168/jds.2023-23560.

Knowlton, K.F., T.E. Dawson, B.P. Glenn, G.B. Huntington, and R.A. Erdman. 1998. Glucose Metabolism and Milk Yield of Cows Infused Abomasally or Ruminally with Starch. J. Dairy Sci. 81:3248–3258. doi:10.3168/jds.S0022-0302(98)75889-8.

Kvidera, S., E. Horst, M. Abuajamieh, E. Mayorga, M. Sanz Fernandez, and L. Baumgard. 2017. Glucose requirements of an activated immune system in lactating Holstein cows. doi:10.3168/jds.2016-12001.

Le Ruyet, P., and W.B. Tucker. 1992. Ruminal Buffers: Temporal Effects on Buffering Capacity and pH of Ruminal Fluid from Cows Fed a High Concentrate Diet. J. Dairy Sci. 75:1069–1077. doi:10.3168/jds.S0022-0302(92)77851-5.

Li, S., E. Khafipour, D.O. Krause, A. Kroeker, J.C. Rodriguez-Lecompte, G.N. Gozho, and J.C. Plaizier. 2012. Effects of subacute ruminal acidosis challenges on fermentation and endotoxins in the rumen and hindgut of dairy cows. J. Dairy Sci. 95:294–303. doi:10.3168/jds.2011-4447.

Mainardi, S.R., B.A. Hengst, S.J. Nebzydoski, L.M. Nemec, and T.F. Gressley. 2011. Effects of abomasal oligofructose on blood and feces of Holstein steers. J. Anim. Sci. 89:2510–2517. doi:10.2527/jas.2010-3348.

Makkar, H.P.S., and K. Becker. 1999. Purine quantification in digesta from ruminants by spectrophotometric and HPLC methods. Br. J. Nutr. 81:107–112. doi:10.1017/s0007114599000227.

Muck, R.E., and J.T. Dickerson. 1988. Storage Temperature Effects on Proteolysis in Alfalfa Silage.. Trans. Am. Soc. Agric. Eng. 31:1005–1009. doi:10.13031/2013.30813.

Owens, F.N., R.A. Zinn, and Y.K. Kim. 1986. Limits to starch digestion in the ruminant small intestine.. J. Anim. Sci. 63:1634–1648. doi:10.2527/jas1986.6351634x.

Peirce, S.B., L.D. Muller, and H.W. Harpster. 1983. Influence of sodium bicarbonate and magnesium oxide on digestion and metabolism in yearling beef steers abruptly changed from high forage to high energy diets.. J. Anim. Sci. 57:1561–1567. doi:10.2527/jas1983.5761561x.

Piantoni, P., M.A. Abeyta, G.F. Schroeder, H.A. Tucker, and L.H. Baumgard. 2022. Evaluation of feed restriction and abomasal infusion of resistant starch as models to induce intestinal barrier dysfunction in healthy lactating cows. J. Dairy Sci. 106:1453–1463. doi:10.3168/jds.2022-22376.

Plaizier, J.C., D.O. Krause, G.N. Gozho, and B.W. McBride. 2008. Subacute ruminal acidosis in dairy cows: The physiological causes, incidence and consequences. Vet. J. 176:21–31. doi:10.1016/j.tvjl.2007.12.016.

Reynolds, C.K., S.B. Cammell, D.J. Humphries, D.E. Beever, J.D. Sutton, and J.R. Newbold. 2001. Effects of postrumen starch infusion on milk production and energy metabolism in dairy cows. J. Dairy Sci. 84:2250–2259. doi:10.3168/jds.S0022-0302(01)74672-3.

Robbers, K., E. Westreicher-Kristen, A. Troescher, and A. Susenbeth. 2019. Effects of abomasally infused amylase and increasing amounts of corn starch on fecal excretion of starch, total and microbial nitrogen, and volatile fatty acids in heifers. J. Anim. Sci. 97:3984–3993. doi:10.1093/jas/skz243.

Rogers, J.A., C.L. Davis, and J.H. Clark. 1982. Alteration of Rumen Fermentation, Milk Fat Synthesis, and Nutrient Utilization with Mineral Salts in Dairy Cows. J. Dairy Sci. 65:577–586. doi:10.3168/jds.S0022-0302(82)82235-2.

Rogers, J.A., L.D. Muller, C.L. Davis, W. Chalupa, D.S. Kronfeld, L.F. Karcher, and K.R. Cummings. 1985. Response of Dairy Cows to Sodium Bicarbonate and Limestone in Early Lactation. J. Dairy Sci. 68:646–660. doi:10.3168/jds.S0022-0302(85)80871-7.

Sanz-Fernandez, M.V., J.B. Daniel, D.J. Seymour, S.K. Kvidera, Z. Bester, J. Doelman, and J. Martín-Tereso. 2020. Targeting the hindgut to improve health and performance in cattle. Animals 10:1–18. doi:10.3390/ani10101817.

Schaefer, D.M., L.J. Wheeler, C.H. Noller, R.B. Keyser, and J.L. White. 1982. Neutralization of Acid in the Rumen by Magnesium Oxide and Magnesium Carbonate. J. Dairy Sci. 65:732–739. doi:10.3168/jds.S0022-0302(82)82260-1.

Steele, M.A., J. Croom, M. Kahler, O. Alzahal, S.E. Hook, K. Plaizier, and B.W. Mcbride. 2011. Bovine rumen epithelium undergoes rapid structural adaptations during grain-induced subacute ruminal acidosis. Am. J. Physiol. - Regul. Integr. Comp. Physiol. 300:1515–1523. doi:10.1152/ajpregu.00120.2010.

Stokes, M.R., L.L. Vandemark, and L.S. Bull. 1986. Effects of Sodium Bicarbonate, Magnesium Oxide, and a Commercial Buffer Mixture in Early Lactation Cows Fed Hay Crop Silage. J. Dairy Sci. 69:1595–1603. doi:10.3168/jds.S0022-0302(86)80576-8.

Tao, S., Y. Duanmu, H. Dong, Y. Ni, J. Chen, X. Shen, and R. Zhao. 2014. High concentrate diet induced mucosal injuries by enhancing epithelial apoptosis and inflammatory response in the hindgut of goats. PLoS One 9. doi:10.1371/journal.pone.0111596.

Ushida, K., B. Lassalas, and J.P. Jouany. 1985. Determination of assay parameters for RNA analysis in bacterial and duodenal samples by spectrophotometry. Influence of sample treatment and preservation. Reprod. Nutr. Dev. 25:1037–1046. doi:10.1051/rnd:19850804.

van Gastelen, S., J. Dijkstra, S.J.J. Alferink, G. Binnendijk, K. Nichols, T. Zandstra, and A. Bannink. 2021. Abomasal infusion of corn starch and β-hydroxybutyrate in early-lactation Holstein-Friesian dairy cows to induce hindgut and metabolic acidosis. J. Dairy Sci. 104:12520–12539. doi:10.3168/jds.2021-20323.

van Gastelen, S., J. Dijkstra, K. Nichols, and A. Bannink. 2021. Abomasal infusion of ground corn and ammonium chloride in early-lactating Holstein-Friesian dairy cows to induce hindgut and metabolic acidosis. J. Dairy Sci. 104:4174–4191. doi:10.3168/jds.2020-19300.

Van Soest, P.J., J.B. Robertson, and B.A. Lewis. 1991. Methods for Dietary Fiber, Neutral Detergent Fiber, and Nonstarch Polysaccharides in Relation to Animal Nutrition. J. Dairy Sci. 74:3583–3597. doi:10.3168/jds.S0022-0302(91)78551-2.

Westreicher-Kristen, E., K. Robbers, R. Blank, A. Tröscher, U. Dickhoefer, S. Wolffram, and A. Susenbeth. 2018. Postruminal digestion of starch infused into the abomasum of heifers with or without exogenous amylase administration. J. Anim. Sci. 96:1939–1951. doi:10.1093/jas/sky082.

Zeng, R., B.J. Bequette, B.T. Vinyard, and D.D. Bannerman. 2009. Determination of milk and blood concentrations of lipopolysaccharide- binding protein in cows with naturally acquired subclinical and clinical mastitis. J. Dairy Sci. 92:980–989. doi:10.3168/jds.2008-1636.

ZINN, R.A., and F.N. OWENS. 1986. a Rapid Procedure for Purine Measurement and Its Use for Estimating Net Ruminal Protein Synthesis. Can. J. Anim. Sci. 66:157–166. doi:10.4141/cjas86-017.

Chapter 3

EFFECT OF ABOMASAL STARCH AND HINDGUT BUFFERS ON LACTATING COW FECAL MICROBIOME AND LYMPHOCYTE KINOME PROFILE

3.1 Abstract

Dietary buffers are often used to mitigate the negative effects of acidosis in the rumen and could prove useful in the hindgut. The objective of this study was to evaluate the potential for two dietary buffers at different dosages to alter the fecal microbiome and peripheral blood mononuclear cells (PBMC) immunometabolic phosphorylation signaling profile of cows that were challenged with abomasally infused starch. Nine ruminally cannulated cows were assigned to 5×5 Latin squares with a 7-d adaptation period, 14-d experimental periods, and 7-d washout periods between each experimental period. Treatments were abomasal infusion of water without fed supplemental buffer (CON), abomasal infusion of corn starch without fed supplemental buffer (IS), or abomasal infusion of starch with 150 g/d of buffer A (T1), 300 g/d of buffer A (T2), or 150 g/d of buffer B (T3). Abomasal starch infusions were 2 g/kg body weight in period 1 and 4 g/kg body weight in periods 2-5 and split into 2 bolus infusions, provided every 12 h. Fecal samples were collected on d 13 of each experimental period before DNA extraction and sequencing of the V4-V5 region of the 16S rRNA gene. Sequence analysis was performed in QIIME2 and RStudio. Blood samples were collected on d 14 of each experimental period and PBMC were isolated and applied to microarrays. Analysis of phosphorylation activity was performed using

PIIKA2, PhosphoSitePlus, and KEGG. Fecal 16S rRNA profiles (n = 45) revealed minimal differences between treatments, with no changes in alpha diversity measurements and only T2 changing beta diversity as compared to CON. Only minor differences in the relative abundance of microbial taxa were detected. T2 decreased *Alloprevotella* and increased *Romboutsia* as compared to IS and increased Firmicutes as compared to CON, while T3 increased *Ruminococcus 2* as compared to IS. The general lack of effect was attributed to the high starch TMR (~31% by DM). PBMC phosphorylation activity revealed decreased metabolic and pro-inflammatory activity in CON and T3 as compared to IS, and increased activity in T1 and T2. T2 further increased pro-inflammatory signaling compared to IS. Collectively, this suggests that buffer B alleviated some of the negative responses to the hindgut acidosis challenge while buffer A, particularly at the high inclusion level, exacerbated the negative response in the fecal microbiome and immunometabolic signaling. Additional research to determine a favorable dosage and type of buffer is needed before practical implementation.

3.2 Introduction

Energetically rich diets are fed to dairy cattle to support the demands of milk production but can lead to metabolic disorders. When fed high levels of starch, cows can experience increased risk of sub-acute ruminal acidosis (SARA) and hindgut acidosis. Nonstructural carbohydrates that escape the rumen during SARA are fermented in the intestines where they can lead to increased production of VFA, decreased intestinal pH, and increased concentrations of toxic compounds, specifically, lipopolysaccharide (LPS) (Li et al., 2012; Saleem et al., 2012; Cronin et al., 2023). The low pH can slough off intestinal epithelial layers, increasing the diffusion of LPS and other toxins into systemic circulation (Emmanuel et al., 2007), possibly leading to systemic inflammation (Li et al., 2012). Additionally, high carbohydrate levels and low luminal pH can lead to changes in the intestinal microbiota, increasing the relative abundance of starch degraders like *Firmicutes* and decreasing pH-sensitive fiber fermenters (Mao et al., 2013; Khafipour et al., 2009; Plaizier et al., 2018), and allow for the opportunistic growth of pathogenic bacteria (Jacob et al., 2008a,b). It therefore may be beneficial to stabilize the intestinal pH when the intestines are exposed to high levels of rapidly fermentable carbohydrates to inhibit microbial dysbiosis and systemic inflammation.

Dietary buffers can promote rumen health, especially when given to lactating cows fed high starch diets. Depending on the type of buffer, they may increase rumen pH (Wheeler and Noller, 1977; Mao et al., 2017; Bach et al., 2018), and can also increase rumen alpha diversity (Mao et al., 2017) or total microbe levels (Kang and Wanapat, 2013). Comparatively, the effects of high starch diets and buffering agents on the hindgut microbiome are unexplored. Calcium carbonate and magnesium oxide have potentially limited solubility in the rumen (Erdman, 1988; Le Ruyet and Tucker, 1992) and can increase fecal pH due to intestinal buffering (Neiderfer et al., 2020; Chapter 2). Previously, we found that buffers altered intestinal fermentation as evidenced by increased fecal pH and increased VFA (Chapter 2), and we suspected they may have altered the intestinal microbiome.

Although it is hypothesized that excessive intestinal starch fermentation may trigger systemic inflammation, postruminal starch infusions models to cause hindgut acidosis in the absence of SARA have generally failed to increase circulating acute phase proteins (Mainardi et al., 2010; Abeyta et al., 2023; Chapter 2). Peripheral blood mononuclear cells (PBMC) are involved in the modulation of immune function, particularly through activating inflammatory signaling pathways in response to molecules like LPS (Rodríguez-Lecompte et al., 2014). When studying their response to SARA conditions that decreased rumen pH increased free ruminal LPS, Stefanska et al. (2018) found increased abundance of LPS receptor complex associated genes in the circulating PBMC, suggesting this was a systemic immune response to the challenge. PBMC profiling can be a useful tool to further evaluate a systemic response to an acidosis challenge. Kinome arrays of white blood cell populations quantify phosphorylation of a range of proteins. Downstream prediction of phosphorylation impacts on immune and metabolic pathways allow for assessment of impact of different interventions on the functional activity of immune cells (Hunter, 2012; Arsenault et al., 2014; Ardito et al., 2017; Perry, 2023). Thus, studying phosphorylation events of PBMC through kinome peptide arrays can offer additional information about the immune response to hindgut acidosis induction and whether this response might be alleviated through buffer administration.

The objective of this experiment was to quantify the impact of hindgut acidosis on the fecal microbiome and PBMC kinome profile and to assess whether these effects could be mitigated by dietary buffers. We hypothesized that abomasal starch to induce hindgut acidosis would negatively affect the fecal microbiome and increase metabolic and pro-inflammatory signaling in PBMC. We additionally hypothesized that feeding buffers would alleviate the negative effects of the starch infusion by increasing microbial diversity and reducing pro-inflammatory signaling.

3.3 Materials and Methods

3.3.1 Animals and Treatments

All work was approved by the University of Delaware's Institutional Animal Care and Use Committee, protocol number 115R, and was completed in fall of 2020. Descriptions of the study design and treatments are described in Chapter 2. In brief, 9 ruminally cannulated Holstein cows completed the study (at the start of the study mean ± SD DIM was 199 ± 61, milk yield was 36.1 ± 8.3 kg/d, and body weight was 771 ± 43 kg). The study was conducted as a replicated 5×5 Latin square with a 7-d adaptation period, 14-d experimental periods, and a 7-d washout between each experimental period. Through a combination of abomasal starch infusions and a moderately high starch diet, this study sought to induce hindgut acidosis. Results of the first experimental period suggested that the ruminal challenge from the moderately high starch diet was too great while the abomasal starch did not sufficiently challenge the intestines. Thus, changes were made to both the diet and abomasal starch infusions between Period 1 and subsequent periods that are described in more detail in Chapter 2 and briefly summarized below. During the adaptation and Period 1, cows were fed a diet containing 34.4% corn silage, 17.4% triticale silage, 44.8% grain mix, and 3.5% corn grain top dress (Table B.1). In Periods 2-5, the diet contained 38.0% corn silage, 17.3% triticale silage, 41.0% grain mix, and 3.7% corn grain top dress.

At the end of the adaptation period, cows were split into 2 groups by milk production and then assigned to 1 of 2 5×5 Latin squares. Treatments were abomasal infusion of water without fed supplemental buffer (**CON**), abomasal infusion of starch without fed supplemental buffer (**IS**), or abomasal infusion of starch and 1 of 3 different fed supplemental buffer treatments (**T1**, **T2**, **T3**). Fed buffer treatments were either 150 g/d of buffer A (50% calcium carbonate, 25% magnesium oxide, and 25% crushed oyster shell) (T1), 300 g/d of buffer A (T2), or 150 g/d of buffer B (100% magnesium oxide) (T3). All cows received 1 kg/d of corn grain topdress (Table B.1) that was mixed by hand into the feed during experimental periods or mixed into the feeding wagon during TMR preparation for adaptation and washout periods. For cows on the T1, T2, and T3 treatments, the buffers were mixed into the corn grain topdress prior to adding to the feed. During Period 1, cows were abomasally infused tap water containing 0 (CON) or 2 (IS, T1, T2, and T3) g/kg body weight per day of food grade corn starch product (Feed Binder GE modified corn starch; Ingredion, Westchester, IL). For Periods 2-5, this was increased to 4 g/kg body weight per day. To allow acclimation to the higher starch infusion level, 2, 3, and 4 g/kg bodyweight corn starch per day were infused on d 1-2, 3-4, and 5-14 of each of period, respectively. Abomasal infusions were administered twice daily in pulse doses at 12 h intervals (0800 h and 2000 h). Abomasal infusions and supplemental buffer feeding did not occur during the washout periods.

3.3.2 Fecal Sampling, DNA Extraction, and Sequencing

Fecal samples were collected on d 13 (0800 h and 1400 h) of each experimental period. Fecal samples were collected through rectal palpation, with the sample obtained in a sterile beaker. Using a sterilized spatula, feces taken from the center of the fecal ball were aliquoted into 5 mL cryovials, and then stored at -80°C. Samples from both times were then pooled into 1 sample per cow per experimental period. Microbial DNA was extracted through use of QIAamp PowerFecal Pro DNA Kit (QIAGEN, Hilden, Germany) according to manufacturer's instructions. DNA was tested for quantity and quality using a Qubit 3.0 fluorometer (ThermoFisher Scientific, Waltham, MA, USA) and a Nanodrop spectrophotometer (ThermoFisher Scientific, Waltham, MA, USA). Frozen extracted samples were sent to RTLGenomics (Lubbock, TX, USA) for sequencing where the V4-V5 region of 16S rRNA genes was amplified using universal primers ((515yF 3′-GTGYCAGCMGCCGCGGTAA-5′/926pfR 3′-CCGYCAATTYMTTTRAGTTT-5′) and sequenced using normalized DNA pools and dual-barcoded Illumina MiSeq library preparation. Primer choices were based on established Earth Microbiome Protocols (Bolyen et al. 2019).

3.3.3 Bioinformatics and Statistical Analyses

Microbial data processing and statistics were performed using QIIME2 (Quantitative Insights into Microbial Ecology, v. 2020.8), following the workflow described in the "Moving Pictures" tutorial (https://docs.qiime2.org/2021.4/tutorials/moving- pictures/, accessed September 24, 2021). Sample sequences were denoised and filtered using DADA2 based on quality score (Callahan et al., 2016). Taxonomic assignments were made against the SILVA_132_99_16S database (Quast et al., 2012) and trained to the 515F/926R primer set.

ASV tables were exported to R (R Core Team, 2018) for further statistical analysis and visualizations using the "phyloseq" package (McMurdie et al., 2013). ASV tables were normalized to the median sequencing depth (8756.5 bp) per sample for beta diversity analysis. Alpha diversity measures (Observed species, Chao1, Shannon, and Simpson) were calculated using the normalized ASV table and tested with ANOVA and Tukey's multiple pairwise tests if normally distributed. If data was not normally distributed, Kruskal-Wallis test and Pairwise Wilcoxon Rank Sum test were used to determine significance.

To evaluate beta diversity, Bray-Curtis Dissimilarity and Weighted and Unweighted UniFrac principal coordinate analysis (PCoA) plots were calculated with normalized ASV tables. PERMANOVA (permutational multivariate analysis of variance) was used to determine whether community composition was different with respect to treatment using the Adonis function in the ‘vegan’ R package (Oksanen et al., 2019). Additional analysis of distance matrices was calculated using the ‘betadisper’ function, also in the ‘vegan’ R package. Pairwise PERMANOVA was calculated using the ‘pairwise.perm.manova’ function in the ‘RVAideMemoire’ R package (Herve, 2023).

Taxa bar plots were created using the ‘microbiome’ and ‘microbiomeutilities’ R packages and averaging by treatment (Lahti and Shetty, 2017). Bacterial abundances were statistically analyzed using Tukey’s HSD and Wilcoxon Rank Sum Tests, with significance determined at $P \leq 0.05$ and tendency for significance determined at $0.05 \leq P \leq 0.10$.

3.3.4 Blood Sampling and Peptide Array Analysis

Blood samples were collected for peptide array analysis from the jugular vein at 0 h relative to the morning feeding on d 14 of each experimental period. Blood was collected into five, 10 mL evacuated sodium heparin tubes, inverted, and placed on ice. Following centrifugation at 1,400 × g for 20 min at 20°C, white blood cells were isolated from the buffy coat, then layered onto a Histopaque gradient and centrifuged a second time. Once isolated, PBMC were allocated into 1.5 mL microcentrifuge tubes, flash frozen in liquid nitrogen, and stored at -80°C.

Kinomic analysis was completed as described by Arsenault et al. (2017). Briefly, frozen PBMC’s were thawed, lysed, and centrifuged before supernatant was activated with ATP and applied to customized PepStar Peptide Microarrays (JPT Peptide Technologies, Berlin, Germany) with lifted edge glass slips. Each microarray contained 1,278 unique kinase substrate target peptide sequences and each peptide was printed 9 times. Arrays were incubated at 37°C for 2 hours, then submerged in phosphate-buffered saline solution to remove the coverslip. Arrays were then washed, submerged in phosphostain, and covered and incubated for 1 hour on a reciprocating shaker. After incubation, slides were then washed in destaining solution and water. After drying, arrays were imaged with a Tecan PowerScanner microarray scanner (Tecan Systems, San Jose, CA) at 532 to 560 nm with a 580-nm filter to detect fluorescence signal from the phosphoprotein-specific dye. The kinome array images were gridded using the GenePix Pro software (version 7.2.29; Molecular Devices LLC., San Jose, CA), and the spot intensity signal was collected as the mean of pixel intensity using local feature background intensity calculation with the scanner saturation level set at 50%.

Files containing kinomic data were generated and analyzed using the online normalization and analysis tool PIIKA2 (Trost et al., 2013). When analyzed in PIIKA2, samples from each treatment were evaluated in relation to that of a “comparator” treatment, which in this case we defined as IS. Data from PIIKA2 was sorted by treatment, with *P*-value and fold changes generated by PIIKA2 used to sort peptides based on significance. Peptides with *P*-values greater than 0.05 were discarded. The sorted kinome peptide array data from PIIKA2 was analyzed using the online databases UniProt (Bateman et al., 2021), KEGG Mapper – Color tool (Kanehisa et al., 2022), and PhosphoSitePlus (Hornbeck et al., 2015). The sorted list of peptides was placed into Venny 2.1 (Oliveros, 2015). Venny provided a visual and numerical comparison of differences between peptides shared by and unique to each treatment.

3.4 Results

3.4.1 Microbiome Results

Total feature frequency across all sequenced DNA samples (n = 45) was 382,792 and an average feature frequency of 8,506 per sample (SD = 1,646; range = 4,066 – 12,634; median = 8792). Average read length was 400 (SD = 2.28; range = 358 – 407). Read counts following the denoising, quality filtering, and chimera checking steps as implemented in QIIME2 are reported in Table B.2.

Figure 3.1 displays the graphical comparison of treatments for observed species, Chao1, Shannon, and Simpson indices of alpha diversity. The observed species index estimates the true number of genera within samples while Chao1 estimates abundance, with more weight towards rare members. The Shannon index estimates sample richness and evenness, while Simpson assesses the number of species present and the relative abundance of each species. No significant differences were demonstrated between treatments for any alpha diversity metric ($P > 0.05$, Table 3.1). However, numerically the T3 treatment had the highest median values for all indices, while CON and IS exhibited the lowest.

Beta diversity principal coordinate analysis (PCoA) plots compared treatment types using Bray-Curtis Dissimilarity, Weighted UniFrac, and Unweighted UniFrac (Figure 3.2). Bray-Curtis Dissimilarity matrix measures community composition using an abundance-based approach to calculate dissimilarity between all samples. The Weighted UniFrac method uses phylogenetic relatedness in addition to abundance counts, while Unweighted UniFrac considers phylogenetic relatedness and presence/absence of taxa. Bray-Curtis plots showed a difference in treatment centroids (adonis, P = 0.04), while betadisper suggested that this was due to treatment assignments (betadisper, P = 0.02). However, the only difference observed using PERMANOVA was a tendency for a difference between CON and T2 (Table 3.2; P = 0.07). Unweighted UniFrac did not display significance in difference between treatment centroids (adonis, P = 0.17). Weighted UniFrac plots showed a difference in treatment centroids (adonis, P = 0.05), while betadisper suggested that this was due to treatment assignments (betadisper, P < 0.01). Similar to the Bray-Curtis results, this was driven by differences between CON and T2 (Table 3.2; P = 0.04).

Visualization of the top 10 taxa at the phylum, order, and family level (accounting for approximately 77, 30, and 4.7 % of populations, respectively) showed relatively few differences among treatments (Figure 3.3). To determine changes between treatments, differential abundance testing was performed on the phylum through genus taxa levels. One phylum, six families, and fourteen genera differed between treatment groups (Table 3.3).

3.4.2 Peptide Microarray Results

For kinome peptide array results, all treatments were compared to IS as a reference. Of the 1,278 peptides evaluated, a total of unique 553 peptides were changed for at least 1 treatment compared to IS. The 553 significantly affected peptides were explored using Venny 2.1 (Figure 3.4). Of those, 199 peptides (36% of total) were shared, meaning that all treatments differed from IS. Only 9 peptides (1.6%) were uniquely affected by CON in comparison to IS. A total of 212 peptides (38% of total) that differed from IS were not shared by CON and, thus, can be attributed to the effects of buffers. The largest of this group (76 peptides, 13.7%) were affected by all 3 buffers. 63 (11.4%), 8 (1.4%), and 16 (2.9%) peptides differed from IS for both T1 and T2, T1 and T3, and T2 and T3, respectively. 12 (2.2%), 28 (5.1%) and 9 (1.6%) peptides were uniquely affected by T1, T2, and T3, respectively. Together, these results demonstrate that the buffers had a greater impact on peptides than the starch infusion, and that the buffer effects were largely driven by T2.

The top 50 KEGG pathways containing peptides with altered phosphorylation were identified for each treatment, and the top 8 shared pathways between treatment comparisons are displayed in Table 3.4. For all shown pathways, T1 and T2 exhibited a greater number of peptides with changed phosphorylation levels relative to IS in comparison with CON and T3. Of the top 8 pathways, the insulin signaling pathway and *Salmonella* infection pathways were chosen for additional focus due to their immunometabolic relevance. The insulin signaling pathway contains information related to MAPK signaling and insulin resistance and describes aspects of metabolism including glucose and lipid homeostasis, protein synthesis, and proliferation and differentiation of cells. The *Salmonella* infection pathway describes the immunometabolic reactions that occur when cells are exposed to bacterial antigens such as LPS or bacterial infection, including membrane ruffling, macropinocytosis, production of inflammatory cytokines, macrophage proliferation, and apoptosis.

Figure 3.5 displays the KEGG insulin signaling pathway with peptides potentially affected by 1 or more treatments and the predicted phenotypic results to cellular metabolism. When examining the insulin signaling pathway differences between CON and IS, CON exhibited increased phosphorylation on the Y1189 activation site on insulin receptor (INSR) that begins signal transduction. However, insulin receptor substrate 1 (IRS1) demonstrated increased phosphorylation on its S312 degradation and S1101 inhibitory site. Additionally, phosphatidylinositol 4,5-bisphosphate 3-kinase catalytic subunit delta isoform (PI3K-CD) exhibited increased phosphorylation on its S1039 inhibitory site, while phosphatidylinositol 3-kinase regulatory subunit alpha (PI3K-R1) and phosphatidylinositol 3-kinase regulatory subunit beta (PI3K-R2) demonstrated reduced phosphorylation on their S608 activation and Y655 protein stabilization sites, respectively. Similarly, decreased phosphorylation on SHC-transforming protein 1 (SHC1) S36 and Y349 regulatory sites and increased phosphorylation on GTPase Hras (Hras) T144 protein degradation/transcription inhibition site suggests decreased mitogen-activated protein kinase (MAPK) pathway activity. Collectively, these data suggest reduced activity along the entire signaling pathway, lowering glycogen and starch metabolism, and decreasing proliferation and differentiation of cells for CON relative to IS (Table 3.5).

Figure 3.6 displays the KEGG *Salmonella* infection pathway with its potentially affected peptides and the aspects to an immune response. When examining the *Salmonella* infection pathway, PI3K-CD exhibited increased phosphorylation on its S1039 inhibition site and neural Wiskott-Aldrich syndrome protein (N-WASP) displayed reduced phosphorylation on its Y256 activation site suggesting decreased macropinocytosis, membrane ruffling, and bacteria containing vesicles for CON compared IS. Toll-like receptor 5 (TLR5) showed increased phosphorylation on its S805 site, possibly due to the presence of bacterial flagellin. In the nuclear factor kappa-light-chain-enhancer of activated B cells (NF-κB) signaling pathway, there was reduced phosphorylation on the NF-kappa-B inhibitor alpha (IkBa) S283 degradation site, suggesting decreased degradation of NF-kappa-B p105 subunit to p50 and p65, and consequently decreased inflammatory cytokine production. Along the MAPK signaling pathway, reduced phosphorylation on the regulatory dual specificity mitogen-activated protein kinase kinase 3 (MKK3) S218 activation site suggests reduced transmission of inflammatory signals initiated by cell surface toll-like receptor binding. Caspase-8 (CASP8) demonstrated increased phosphorylation on its S347 inhibitory site, suggesting reduced cellular apoptosis. These results demonstrate overall reduced vesicle formation, membrane ruffling and macropinocytosis, cellular apoptosis, and inflammatory cytokine production (through both MAPK and NF-κB pathways) for CON compared to IS (Table 3.5).

When examining differences between T1 and IS in the insulin signaling pathway, T1 decreased phosphorylation on the E3 ubiquitin-protein ligase CBL (Cbl) Y700 activation site suggesting a possible increase in glucose uptake relative to IS. Increased lipogenesis is likely due to the reduced phosphorylation on 5'-AMP-activated protein kinase subunit beta-1 (AMPK-B1) S108 activation site and acetyl-CoA carboxylase 1 (ACC1) reduced phosphorylation on its S1263 inhibition site. While INSR exhibited increased phosphorylation on its Y1189 activation site, IRS1 demonstrated increased phosphorylation on its S312 degradation site and PI3K-CD exhibited increased phosphorylation on its S1039 inhibitory site. This likely reduces the resultant glycogenesis, antilipolysis (inhibition of fat breakdown), and antiapoptosis (prevention of apoptosis) for T1 compared to IS. Activity along the MAPK signaling pathway, specifically decreased phosphorylation on the RAF proto-oncogene serine/threonine-protein kinase (Raf) S43 inhibition site, increased phosphorylation on the mitogen-activated protein kinase 1 (ERK2) activation site, and increased phosphorylation on the MAP kinase-interacting serine/threonine-protein kinase 1 (MNK) T255 activation site suggest increased protein synthesis and cell proliferation and differentiation. Overall, results demonstrate possible increased glucose uptake, lipogenesis, protein synthesis, and cell proliferation and differentiation for T1 relative to IS, along with reduction in glycogenesis, antilipolysis, and antiapoptosis (Table 3.5).

For the *Salmonella* infection pathway, T1 increased phosphorylation on the protein tyrosine phosphatase receptor type C (CD45) Y1216 activation site suggesting increased T-cell immunogenic activity compared to IS. With phosphatidylinositol 4,5-bisphosphate 3-kinase catalytic subunit gamma isoform (PI3K-CG) S582 and N-WASP Y256 activation sites both showing increased phosphorylation, it is likely that there was more membrane ruffling and macropinocytosis in T1 as compared to IS. Along the activation pathway for inflammatory cytokines, toll-like receptor 6 (TLR6) and toll/interleukin-1 receptor domain-containing adapter protein (TIRAP) displayed activity (the TIRAP Y86 activation site showed increased phosphorylation), suggesting a greater amount of signal initiation. On the NF-κB signaling pathway, inhibitor of nuclear factor kappa-B kinase subunit alpha (IKKa) T23 activation site showed increased phosphorylation, and NFκB-p105 showed increased phosphorylation on its S297 protein degradation site. IKKa phosphorylates inhibitors of the NF-κB, tagging them for destruction, while NFκB-p105 splits into p50 and p65, which can act as transcriptional activators of inflammatory cytokines. These results suggest increased NF-κB signaling pathway activity for T1 compared to IS. On the MAPK signaling pathway, ERK2 and mitogen-activated protein kinase 14 (p38A) both displayed increased phosphorylation on their activation sites, suggesting activation of the activator protein 1 (AP-1) transcription factor, leading to pro-inflammatory cytokine production. RAC-alpha serine/threonine-protein kinase (Akt1) exhibited increased phosphorylation on its T308 activation site while Ras-related C3 botulinum toxin substrate 1 (Rac1) exhibited increased phosphorylation on its S71 and T108 inhibition sites. These signals likely lead to lowered caspase activity, decreasing apoptosis and pyroptosis. Overall, these results suggest reduced apoptosis and pyroptosis, but increased membrane ruffling, macropinocytosis, and pro-inflammatory cytokine production through the NF-κB and MAPK pathways for T1 compared to IS (Table 3.5).

For the insulin signaling pathway comparing T2 to IS, Cbl, the negative regulator of the glucose uptake pathway, showed increased phosphorylation on its Y371 degradation site and decreased phosphorylation on its Y700 activation site. The Crk-like protein (CRKL) Y207 inhibition site showed decreased phosphorylation, likely increasing glucose uptake. For fatty acid biosynthesis, AMPK subunit beta-1 (AMPKB1) demonstrated decreased phosphorylation on its S108 activation site while ACC1 saw decreased phosphorylation on its S80 and S1263 inhibition sites. Coupled together, this suggests possible increased lipogenesis in T2 as compared to IS. cAMP-dependent protein kinase catalytic subunit alpha (PKACA) saw increased phosphorylation on its T198 and S339 activation sites, suggesting increased antilipolysis. Serine/threonine-protein kinase mTOR (mTOR) exhibited increased phosphorylation on its S2481 activation site, while regulatory-associated protein of mTOR (Raptor), its regulator, demonstrated decreased phosphorylation on its T706 activation site. Ribosomal protein S6 kinase beta-1 (p70S6K) displaying increased phosphorylation on its T252 and T412 activation sites, linked with MNK T255 activation site also showing increased phosphorylation suggests increased protein synthesis. Increased phosphorylation on the growth factor receptor-bound protein 2 (GRB2) Y160 cell growth site, reduced phosphorylation on the RAF proto-oncogene serine/threonine-protein kinase (Raf1) S43 inhibition site, and increased phosphorylation on the serine/threonine-protein kinase B-raf (BRAF) T599 activation site suggest possible increased cellular proliferation and differentiation. As compared to IS, overall T2 results demonstrate possible increased glucose uptake, lipogenesis, antilipolysis, protein synthesis, and cellular proliferation and differentiation.

When examining the *Salmonella* infection pathway, increased phosphorylation on the CD45 Y1216 activation site suggests increased T-cell immunogenic activity. Transforming protein RhoA (RhoA) exhibited reduced phosphorylation on its S188 inhibitory site while Rho-associated protein kinase 2 (ROCKII) showed increased phosphorylation on its Y722 inhibitory site, suggesting reduced membrane ruffling and macropinocytosis. Additionally, Rac1 displayed increased phosphorylation on its S71 and T108 inhibitory sites, likely resulting in lowered activation of serine/threonine-protein kinase PAK 1 (PAK). This reduction in signal transduction confirms the lowered membrane ruffling and macropinocytosis, as well as reducing the likelihood of formation and scission of nascent bacteria containing vesicles. TLR5 and TLR6 both displayed increased activation, likely due to bacterial flagellin and bacterial cell wall components, beginning signal transduction to potentially produce pro-inflammatory cytokines. Along the NF-κB signaling pathway, IkBa exhibited decreased phosphorylation along its S283 and S718 protein degradation sites. NFκB-p105 showed increased phosphorylation on its S927 protein degradation site. IkBa will act as an inhibitor for NFκB-p105, suggesting subsequent reduced degradation to p50 and p65, which should decrease pro-inflammatory cytokine production. Along the

MAPK signaling pathway, transcription factor AP-1 (Jun), exhibited increased phosphorylation on its S63 activation site and decreased phosphorylation on its S243 inhibitory site, suggesting increased activation of inflammatory cytokines along the MAPK pathway. Finally, Akt1 exhibited increased phosphorylation on its S129 inhibitory site and T308 (an activation site, but both T308 and S473 need to be activated for enzymatic activity changes). This suggests a decrease in the inhibition of inflammasome activation, increasing apoptosis and pyroptosis. As compared to IS, T2 results suggest increases in T-cell immunogenic activity, activation of signals due to bacterial flagellin and bacterial cell wall components, production of inflammatory cytokines through the MAPK pathway, apoptosis, and pyroptosis. Decreased membrane ruffling, macropinocytosis, and formation and scission of bacterial vesicles is likely, along with decreased activation and production of inflammatory cytokines due to the NF-κB signaling pathway. Overall, T2 increased metabolic activity and increased most immune-related activity as compared to IS (Table 3.5).

For the insulin signaling pathway comparing T3 to IS, INSR exhibited increased phosphorylation on its Y1011 inhibitory site, IRS exhibited increased phosphorylation on its S312 and S1102 protein degradation and inhibitory sites, and PIK3-CD demonstrated increased phosphorylation on its S1039 inhibition site. These results suggest reductions to the entire signaling pathway (Table 3.5). Similarly, glucose uptake was likely decreased in T3 as compared to IS due to adapter molecule crk (CrkII) S41 transcriptional inhibition site exhibiting increased phosphorylation.

When examining the *Salmonella* infection pathway, increased phosphorylation on the CD45 Y1216 activation site suggests increased T-cell immunogenic activity. Due to increased phosphorylation on the Rac1 S71 and T108 inhibition sites along with increased phosphorylation on the PIK3-CD S1039 inhibition site, there was likely reduced membrane ruffling, macropinocytosis, and formation/scission of nascent vesicles. Along the NF-κB signaling pathway, IKKa exhibited increased phosphorylation on its S473 protein stabilization site, and IKBa showed decreased phosphorylation on its S283 protein degradation site. This suggests that there was possible reduced dissociation/degradation of IKBa, reducing the activation of this pathway. P38A exhibited increased phosphorylation on its T123 and T182 inhibitory sites, while mitogen-activated protein kinase 8 (JNK) exhibited reduced phosphorylation on its Y185 activation site. This likely reduces JNK phosphorylation of Jun and proto-oncogene c-Fos (Fos), which are AP-1 transcription factors. Finally, increased phosphorylation of Akt1 T308 (an activation site, but both T308 and S473 need to be activated for enzymatic activity changes) and T450 (another activation site) suggest a possible increase in the inhibition of inflammasome activation, decreasing apoptosis and pyroptosis. As compared to IS, overall T3 results suggested possible increased T-cell immunogenic activity but decreased activity for other immune functions. Specifically, Decreased membrane ruffling, macropinocytosis, formation and scission of nascent bacteria containing vesicles, production of inflammatory cytokines (through NF-κB and MAPK pathways), apoptosis, and pyroptosis was likely for T3 relative to IS (Table 3.5).

3.5 Discussion

This study's ration contained 30.9% starch, providing approximately 7.9 kg/d (10.3 g/d/kg body weight) starch in period 1 and 7.3 kg/d (9.6 g/d/kg body weight starch in periods 2-5; Chapter 2). According to Sanz-Fernandez et al. (2020), ruminal starch levels greater than 10 g/d/kg body will decrease ruminal starch digestion, resulting in higher postruminal starch levels. Additionally, the basal diet produced lower ruminal pH than expected (mean 5.95 with average nadir of 5.39) (Chapter 2). Taken together, this suggests that the basal diet induced a SARA challenge and potentially reduced ruminal starch digestion. Assuming 72% ruminal starch degradation (Sanz-Fernandez et al., 2020), approximately 2.2 kg/d and 2.1 kg/d of dietary starch entered the small intestine from the rumen in period 1 and periods 2-5, respectively. The abomasal infusions provided 0 or 1.1 kg/d starch and 0 or 2.2 kg/d starch during periods 1 and 2-5, respectively, split into 2 bolus infusions every 12 hours. This corresponded to an increase in total duodenal starch flow of approximately 50% in period 1 (up to 3.3 kg/d from 2.2 kg/d) and approximately 108% in periods 2-5 (up to 4.3 kg/d from 2.1 kg/d) for the treatments with the infused starch relative to CON. Based on an estimated 53% (Owens et al., 1986) to 66% (Offner and Sauvant, 2004) of duodenal starch digestion, we expected approximately 1.1 to 1.6 kg/d of starch in period 1 and 1.5 to 2.0 kg/d of starch in periods 2-5 to flow into the large intestine (Chapter 2). Though we expected the infused corn starch to dramatically increase hindgut fermentation, intestinal disappearance was much less than expected, with approximately 48% of the infused starch recovered in the feces (Chapter 2).

In our previous work, we observed fecal changes in response to abomasal starch infusions and dietary buffers in short periods of 7 d (Neiderfer et al., 2020). However, others have observed continued fecal metabolite and microbial responses up to 28 d after induction of a SARA challenge, suggesting that longer experimental periods may help to capture changes in variables that are slower to stabilize (Neubauer et al., 2020; Wang et al., 2017). In this experiment we used a period length of 14 d and included a 7 d washout between periods to hopefully capture some of the longer term treatment responses while being mindful of our concerns that an extended hindgut challenge may negatively impact animal health.

Diet is a primary driver of gut microbial composition, with individual hosts providing additional variability in microbial consortia (Henderson et al., 2015; Mizrahi and Jami, 2018). Changes in the microbiome profile can be identified through alpha diversity and beta diversity, which did not differ when comparing CON and IS in this study ($P > 0.05$). Similarly, identified taxa abundance differences between CON and IS were minimal, only tending to change in 1 family and 3 genera. Although there has been little study on the effects of an independent hindgut acidosis challenge on the fecal microbiome, these results are surprising given the evidence that a SARA challenge will modify the fecal microbiome. SARA conditions can lead to decreased alpha diversity and changes in beta diversity and taxa abundance in both the rumen (Plaizier et al., 2017; Mu et al., 2022; Chen et al., 2021) and the feces (Plaizier et al., 2017; Neubauer et al., 2020). Changes in Firmicutes:Bacteroidetes are commonly seen in the rumen due to a switch from mixed forage and grain diets to a SARA-inducing diet (Plaizier et al., 2017). Members of the Bacteroidetes phylum are more efficient at degrading complex plant cell wall polysaccharides (El Kaoutari et al., 2013), suggesting that an increase in Firmicutes:Bacteroidetes would shift the microbial community away from fiber digestion and towards the digestion of simple carbohydrates (Plaizier et al., 2017). While not significant, CON displayed a numerically lower Firmicutes:Bacteroidetes as compared to treatments that received abomasal starch (2.3727 as compared to an average of 3.407), in agreement with general trends of expected fiber and starch availability for bacterial degradation. This change in Firmicutes relative abundance was not observed in IS compared to CON as expected, but instead with the addition of a higher dosage of buffer A. Of the minor differences observed between CON and IS in this study, IS tended to reduce uncultured *Parabacteroides* sp., uncultured Veillonellaceae, and uncultured rumen *Mollicutes RF39 bacterium* genera as compared to CON (Table 3.3). *Parabacteroides* species may aid in complex carbohydrate degradation and mitigate inflammation in humans (Cui et al., 2022), members of Veillonellaceae may utilize lactate (Rogosa and Bishop, 1964), and *RF39* taxa may produce acetate from simple sugars (Wang et al., 2020). These responses in bacterial abundance are fitting with other measured variables, as starch infusion reduced NDF digestibility, and did not increase lactate or acetate production (Chapter 2). In this study, fecal pH decreased with starch infusion but at lower levels than expected (0.43 pH unit decrease as compared to expected 0.65 and 1.30 pH decrease in periods 1 and 2-5, respectively) (van Gastelen et al. 2021; Chapter 2). This coupled with the dramatic increase in fecal starch for IS compared to CON (Chapter 2) suggests that the hindgut's capacity for starch degradation was overwhelmed. Thus, the lack of differences between CON and IS in alpha and beta diversity and taxa abundances could have been driven by our failure to sufficiently modify hindgut fermentation with the infused starch.

To confirm that the lack of a strong microbiome response to IS was not due to procedural errors, fecal samples taken from each cow before adaptation to the experimental diet were evaluated in the same manner as described in the methods section. At that time, the cows were fed the herd ration that contained 43% corn silage, 19% triticale silage, and 38% grain mix, and was formulated to provide 34.0% NDF, 23.5% starch, and 16.3% CP. When fed the herd ration as compared to CON, alpha diversity numerically decreased and beta diversity differed. Pairwise comparisons revealed that the lower-starch herd ration changed beta diversity as compared to CON (Bray-Curtis, $P = 0.02$; unweighted UniFrac, $P = 0.03$; weighted UniFrac, $P = 0.07$). Additionally, 2 phyla, 2 classes, 1 order, 5 families, and 18 genera were found to be differentially abundant between the herd ration and CON. These results suggest that our methodology to detect changes in the microbiome was appropriate, but the microbiota in CON did not alter drastically with the abomasal starch infusion, blunting potential changes to beta diversity and differential taxa abundances.

Alpha diversity was not affected by inclusion of buffers as compared to IS or CON ($P > 0.05$), and beta diversity was not affected by buffer supplementation when compared to IS ($P > 0.05$), although there was a difference in beta diversity between T2 and CON ($P = 0.04$). As with evaluating the effects of a hindgut acidosis challenge alone on the fecal microbiome, the effects of dietary buffers containing $CaCO_3$ or MgO on the fecal microbiome are lacking. However, there has been study on the effect of buffers on the rumen microbiome. The effect of buffers on the alpha diversity of the rumen microbiome is variable, with sodium bicarbonate increasing (Mao et al., 2017), and blends containing calcium and magnesium not affecting diversity (Arce-Cordero et al., 2022; Ramos et al., 2022). Similarly, buffer effects on beta diversity indices are variable, with sodium bicarbonate inclusion changing beta diversity (Mao et al., 2017) but calcium- and magnesium-based buffers failing to change diversity indices (Arce-Cordero et al., 2022) compared to their relative controls. In this study, fecal pH decreased with starch infusion and increased with buffer inclusion, but the impact of the starch challenge was not as dramatic as expected (Chapter 2). Despite the changes to fecal pH, IS and the three buffer treatments did not significantly alter alpha or beta diversity when compared to CON.

The challenge of high levels of starch present in the ration affected the microbiome by changing beta diversity and numerically affecting alpha diversity as compared to a more typical lactating cow diet. After adaptation to high starch levels, the microbiota in CON did not change remarkably when further challenged by abomasally infused starch and the fed buffers.

Despite the lack of effect of buffers on alpha or beta diversity, the buffer treatment did affect abundance of some taxa. Of the three buffer treatments, T2 most significantly affected microbial relative abundances when compared to IS. Specifically, T2 decreased the relative abundance of *Alloprevotella* ($P = 0.01$) and increased *Romboutsia* ($P = 0.048$), while their families, Prevotellaceae and Peptostreptococcaceae, respectively, both tended to follow the same patterns ($P = 0.06$ and 0.08, respectively). The *Alloprevotella* genus contains beneficial, commensal bacteria that may promote an anti-inflammatory environment (Pietrucci et al., 2022; Cheng et al., 2021). In humans, decreases in the relative abundance of *Alloprevotella* are associated with colitis (Zakerska-Banaszak et al., 2021; Miyanaga et al., 2022) and gastrointestinal dysbiosis (Tian et al., 2021; Pietrucci et al., 2022). In humans and mice, increased abundance of the *Romboutsia* genus has been linked to inflammatory bowel diseases (Dahal et al., 2023) and colitis (Jangid et al., 2020), while the Peptostreptococcaceae family has been associated with colitis (Lavelle et al., 2015). These results suggest that T2 may have contributed to dysbiosis with lowered abundance of beneficial microbes, and higher abundance of bacteria associated with inflammatory states. Although the T1 and T2 treatments both contained the same buffer (150 g/d of buffer A for T1 and 300 g/d of buffer A for T2), these negative effects were only observed for the higher level of supplementation with T2. Further experimentation is necessary to elucidate why T2 seemed to produce a more undesirable microbial profile as compared to IS.

Further support for a dysbiosis caused by T2 is provided by the differences in beta diversity and taxa abundances when compared to CON. CON and T2 exhibited differences in weighted UniFrac (P = 0.04) and tended to differ based on Bray-Curtis distance (P = 0.07), suggesting differences in abundance of microbes present. At the phylum level, only Firmicutes were differentially abundant, increasing in T2 as compared to CON (P = 0.05). The increase in relative abundance of Firmicutes observed in T2 subsequently increased the Firmicutes to Bacteroidetes ratio as compared to CON (P = 0.05). Buffer A contained calcium carbonate, and calcium phosphate supplementation has been shown to induce the proliferation of the Firmicutes phylum and *Romboutsia* genus when fed to rats (Fuhren et al., 2021). The higher levels of calcium intake in T2 may have driven some of the changes observed in T2 as compared to IS and CON.

The PBMC population consists of the peripheral lymphocytes and monocytes circulating through the body to react to antigens (Haudek-Prinz et al., 2012). PBMC act as sentinel cells to monitor and implement responses to systemic immune disturbances (Acosta Davila and Hernandez De Los Rios, 2019). Evaluating the post-translational modifications of PBMC is a minimally invasive tool to provide insight into the systemic inflammatory state. Changes in gut have been shown to drive changes in circulating PBMC, specifically in the case of Crohn’s disease and ulcerative colitis (Hatsugai et al., 2010) and in response to changes in gut microbiome profile or metabolite production (Shimizu et al., 2018).

For both the insulin signaling and *Salmonella* infection pathways, CON suggested decreased immunometabolic activity of PBMC as compared to IS. CON PBMC experienced decreased cellular proliferation and differentiation through reductions in the MAPK signaling pathway. The MAPK pathway transmits extracellular signals to drive intracellular responses, controlling cellular growth, gene expression, and inflammation (Cargnello and Roux, 2011). Production of pro-inflammatory cytokines like tumor necrosis factor alpha (TNF-α), interleukin-6 (IL-6), and interleukin-1β (IL-1β) from the MAPK and NF-κB pathways can be stimulated by LPS or other harmful compounds produced during SARA (Elmhadi et al., 2022). Zhao et al. (2018) found that cows exposed to SARA conditions responded with increased phosphorylation of IκBα, NF-κB, JNK, and ERK1/2 in ruminal epithelium cells resulting in increased mRNA and serum protein expression levels of TNF-α, IL-6, and IL-1β. Acidosis induction can produce toxic compounds (Saleem et al., 2012) and impair the gut barrier, allowing these compounds to drive local and systemic inflammatory responses (Emmanuel et al., 2007). Despite the absence of increasing to acute phase proteins in IS compared to CON, the heightened pro-inflammatory state due to MAPK signaling in IS suggests that abomasally infused starch induced the immune response hypothesized to occur due to hindgut acidosis (Li et al., 2012). This fits with our expectations, as abomasal starch in the IS treatment was expected to cause hindgut acidosis and potentially drive an inflammatory response.

Although the difference in PBMC kinome profile between CON and IS was as expected, surprisingly only 9 peptides (1.6% of total) were uniquely changed by CON compared to IS. We expected far more peptides to fall into that category that reflects unique responses to the dramatic increase in postruminal starch flow. While there is no established fecal pH threshold for hindgut acidosis (van Gastelen et al., 2021), these animals experienced a drop in fecal pH of 0.43 units between the CON and IS treatments (Chapter 2), suggesting induction of acidosis. Interestingly, IS did not increase total fecal VFA, serum acute phase proteins, or fecal LPS as compared to CON, and we hypothesized that the responses to infused starch were likely blunted by the moderately high starch diet (approximately 30%) and subsequent unintentional SARA induction (Chapter 2). Despite the lack of changes to fecal metabolites and serum acute phase proteins and the small number of peptides uniquely different between CON and IS, there were stark differences when comparing the PBMC kinomic profiles of CON and IS. Those differences were largely driven by shared responses of CON with buffer treatments when compared to IS. As discussed below, this suggests that the buffers, and particularly T3, may have mitigated some of the inflammatory response to the abomasal starch infusion.

Similar to CON, T3 decreased activity along the insulin signaling and *Salmonella* infection pathways as compared to IS. Both displayed similar levels of phosphorylation changes on the two pathways (41 and 29 for CON vs. 37 and 30 for T3, respectively; Table 3.4), and shared a total of 248 significantly affected peptides as compared to IS (44.9% of total changes; Figure 3.4). Of the 76 peptides shared by all buffer treatments, the activity due to T3 seemed to dampen the pro-inflammatory response, promoting a similar profile to CON, while T1 and T2 heightened the inflammatory response. As reported in Chapter 2, T3 increased fecal pH to the level of CON despite receiving abomasal starch infusions but did not significantly change fecal metabolite concentrations or apparent total tract nutrient digestibilities as compared to IS or the other buffer treatments (Chapter 2). Despite these minimal differences in animal responses, T3 did increase the relative abundance of *Ruminococcus 2* as compared to CON (6.934% vs. 2.005%, respectively; $P < 0.01$) and numerically increased abundance as compared to IS (6.934% vs 3.904%). Schluter et al. (2020) determined that increases in the total abundance of *Ruminococcus 2* were associated with increased white blood cell repletion after in humans after radiation depletion and a restoration of a balanced neutrophil to monocyte ratio. The relative increase in *Ruminococcus 2* may have positively impacted the immune system, resulting in the reduction in immunometabolic activity observed in T3.

When compared to IS, buffer A addition (T1 and T2) displayed similar levels of phosphorylation changes on the insulin signaling and *Salmonella* infection pathways (47 and 49 for T1 vs. 49 and 42 for T2, respectively; Table 3.4), and the two treatments shared 63 (11.4% of total changes) of the overall phosphorylation changes (Figure 3.4). Both treatments prompted similar predicted PBMC responses relative to IS, increasing glucose uptake, lipogenesis, protein synthesis, and cellular proliferation, and increasing the production of pro-inflammatory cytokines through the MAPK pathway. T2 additionally reduced membrane ruffling and macropinocytosis, increased T-cell immunogenic activity, saw activation of signals due to bacterial flagellin and bacterial cell wall components, increased apoptosis and pyroptosis, and decreased activation of the NF-κB signaling pathway. Overall, this suggests that T1 and T2 increased PBMC immunometabolic activity as compared to IS. Immune system activation requires large amounts of glucose, with a study from Kvidera et al. (2017) suggesting that approximately 1 kg of glucose is utilized every 12 hours by the active immune system in a lactating dairy cow. Increased signaling related to glucose uptake and cellular proliferation and differentiation in PBMC suggests immune activation due to inclusion of buffer A, followed by pro-inflammatory cytokine production.

Of the two buffer A treatments, T2 produced the most seemingly dysbiotic microbiota profile and greatest increase in PBMC immunometabolic activity. As compared to T1, T2 additionally exhibited increased cell death, T-cell activity, and affected pathways for the production of pro-inflammatory cytokines. As a percentage of DM, buffers A and B contained 21.47% and 6.54% calcium, respectively (Chapter 2). The calcium ion may act as a promoter of pro-inflammatory activity (Iamartino and Brandi, 2022). Indeed, high levels of extracellular calcium can exert a strong chemoattractant effect (Shi et al., 1996) and promote the release of pro-inflammatory cytokines from immune cells (Bornefalk et al.,1997). It is possible that the higher calcium dosage in buffer A compared to buffer B drove the pro-inflammatory signaling that was observed for T1 and T2, and that this was exacerbated for the higher dose in T2. Together, these results suggest that abomasal infusion of starch and addition of buffer A at the higher dose in treatment T2 induced minor microbial dysbiosis and pro-inflammatory signaling.

3.6 Conclusions

Acidotic conditions in the hindgut may contribute to intestinal microbial dysbiosis and systemic inflammation. Feeding mineral buffers can alleviate some of the negative effects of acidosis in the rumen, and we sought to determine whether they could improve the fecal microbiome and host immunometabolic response to a hindgut acidosis challenge. The abomasal starch infusion did not negatively affect the fecal microbiome as expected, failing to lower the alpha diversity or change the beta diversity as compared to the control. This lack of difference is likely due to the high starch level in the basal diet, effectively already providing a hindgut acidotic challenge in the CON treatment. Similarly, we expected buffer treatments to alleviate microbial dysbiosis when compared to IS, but this failed to occur. Instead, T2 exhibited changes in beta diversity as compared to CON, reflected by increased *Firmicutes* and *Romboutsia* and decreased *Alloprevotella*, suggesting a destabilized microbial profile. However, T3 did increase *Ruminococcus 2* when compared to IS, suggesting potential improvements to the microbiome-induced inflammatory state.

Kinomic analysis revealed decreased immunometabolic activity in circulating PBMC of CON as compared to IS, suggesting that the abomasal starch infusion did result in a systemic inflammatory response. T3 seemed to dampen this response, as it also resulted in decreased PBMC immunometablic activity as compared to IS. However, T1 and T2 increased immunometabolic activity as compared to IS, and this was most evident for the T2 treatment. Taken together, infused abomasal starch by itself did not dramatically affect the fecal microbiome but did heighten PBMC pro-inflammatory activity. The higher dosage of buffer A in T2 seemed to worsen the fecal microbiome as compared to CON and further exacerbate cow immunometabolic profile as compared to IS. Conversely, feeding buffer B in T3 seemed to reduce immunometabolic activity as compared to IS. Feeding buffers to alleviate hindgut acidosis may increase fecal pH and positively impact immunometabolic signaling, but this appears to depend on buffer composition and dosage.

TABLES

Table 3.1: Comparison of treatments under Observed, Shannon, Chao1, and Simpson alpha diversity measures with all samples.

Treatment		*P* Value			
Group 1	Group 2	Observed	Chao1	Shannon	Simpson
Control	Infused Starch	0.95	0.94	0.78	0.76
Control	T1	0.92	0.92	0.57	0.50
Control	T2	0.87	0.86	0.78	0.93
Control	T3	0.34	0.32	0.42	0.34
Infused Starch	T1	1.00	1.00	0.78	0.77
Infused Starch	T2	1.00	1.00	0.93	0.85
Infused Starch	T3	0.87	0.85	0.57	0.58
T1	T2	1.00	1.00	0.78	0.50
T1	T3	0.90	0.89	0.57	0.74
T2	T3	0.95	0.94	0.42	0.50

Table 3.2: Comparison of treatments under beta diversity measures through pairwise PERMANOVA.

Treatment		*P* Value		
Group 1	Group 2	Bray-Curtis	Unweighted UniFrac	Weighted UniFrac
Control	Infused Starch	0.68	0.93	0.62
Control	T1	0.16	0.76	0.23
Control	T2	0.07	0.35	0.04
Control	T3	0.16	0.23	0.22
Infused Starch	T1	0.73	0.94	0.72
Infused Starch	T2	0.60	0.57	0.48
Infused Starch	T3	0.83	0.93	0.60
T1	T2	0.68	0.93	0.62
T1	T3	0.83	0.94	0.72
T2	T3	0.72	0.88	0.61

Table 3.3: Mean relative abundances of taxa determined to be differentially abundant between different treatment groups. No differences were observed at the class and order levels.

	Treatment Abundance					*P*-value
	CON	IS	T1	T2	T3	Treatment
----------------Phyla---------------						
Firmicutes	62.542^{b}	64.648^{ab}	67.083^{ab}	73.637^{a}	67.247^{ab}	0.05
FB ratio[1]	2.3727^{y}	3.1537^{xy}	2.8037^{xy}	4.3382^{x}	3.3324^{xy}	0.04
---------------Family---------------						
Muribaculaceae[2]	1.273^{ab}	1.825^{bc}	2.798^{c}	1.762^{bc}	1.696^{bc}	0.09
Prevotellaceae[2]	7.601^{x}	8.233^{xy}	4.869^{xy}	3.683^{y}	5.090^{xy}	0.07
Defluviitaleaceae[3]	0	0	0	0	0.031	0.09
Peptostreptococcaceae[3]	4.728^{xy}	4.175^{y}	5.617^{xy}	8.954^{x}	6.164^{xy}	0.10
Unclassified Firmicutes family[3]	0^{y}	0^{y}	0^{y}	0.107^{x}	0.012^{x}	0.06
Uncultured Mollicutes RF39 Rumen bacterium[4]	0.103^{x}	0^{y}	0^{y}	0^{y}	0^{y}	0.01
---------------Genus---------------						
Uncultured Parabacteroides sp.[2]	0.163^{x}	0^{y}	0^{y}	0^{y}	0^{y}	0.01

Table 3.3 continued

Uncultured Muribaculaceae bacterium[2]	1.273	1.825	2.791	1.760	1.696	0.09
Alloprevotella[2]	0.386^{ab}	0.652^{a}	0.502^{ab}	0.011^{b}	0.603^{a}	0.01
Unclassified Clostridiales vadinBB60 group[3]	0	0	0	0	0.029	0.09
Defluviitaleaceae UCG 011[3]	0	0	0	0	0.032	0.09
Blautia[3]	0.457	0.731	1.471	1.339	1.417	0.09
Bacteroides Pectinophilus group[3]	0^{y}	0^{y}	0^{y}	0.225^{x}	0.182^{x}	0.01
Eubacterium Oxidoreductans group[3]	0.094^{y}	0.749^{xy}	0.612^{x}	0.331^{xy}	0.015^{xy}	0.05
Romboutsia[3]	2.325^{ab}	1.651^{a}	2.335^{ab}	3.599^{b}	2.211^{ab}	0.08
Uncultured Peptostreptococcaceae genus[3]	1.123	0.581	1.108	2.128	1.600	0.10
Ruminococcus 2[3]	2.005^{b}	3.904^{ab}	3.909^{ab}	4.954^{ab}	6.934^{a}	< 0.01
Uncultured Veillonellaceae[3]	0.054	0	0	0	0	0.09
Unclassified Firmicutes genus[3]	0	0	0	0.107	0.011	0.06
Uncultured rumen Mollicutes RF39 bacterium[4]	0.103^{x}	0^{y}	0^{y}	0^{y}	0^{y}	0.01

$^{a\text{-}c}$Superscripts within the row indicates $P \leq 0.05$ by pairwise Wilcoxon rank sum tests with post hoc testing using the Benjamini-Hochberg false discovery rate adjustment correction or Tukey's Honestly Significant Difference Test.
^{x,y}Superscripts within the row indicates $0.05 \leq P \leq 0.10$ by pairwise Wilcoxon rank sum tests with post hoc testing using the Benjamini-Hochberg false discovery rate adjustment correction or Tukey's Honestly Significant Difference Test.

[1]Firmicutes:Bacteroidetes ratio. [2]Belonging to the Bacteroidetes phylum. [3]Belonging to the Firmicutes phylum. [4]Belonging to the Tenericutes phylum.

Table 3.4: The number of changes (increased or decreased phosphorylation) in peptides related to the top 8 signaling pathways based on treatment comparisons to IS.

KEGG Pathways	**CON**	**T1**	**T2**	**T3**
Insulin signaling	41	47	49	37
Salmonella infection	29	36	42	30
MAPK signaling	49	66	71	52
T cell receptor signaling	33	33	39	29
Insulin resistance	29	31	36	25
B cell receptor signaling	23	25	30	25
FoxO signaling	29	34	37	28
Central carbon metabolism in cancer	23	32	35	29

Table 3.5: Summary table of indicated increased or decreased immunometabolic activity based on peptide phosphorylation activity in the insulin signaling and *Salmonella* infection pathways. Treatments listed are in comparison to IS. An up arrow indicates increased activity, while a down arrow indicates decreased activity. A dash indicates no significant difference in activity between the treatment and IS.

	CON	**T1**	**T2**	**T3**
Insulin signaling pathway				
Glucose uptake	↓	↑	↑	↓
Lipogenesis	↓	↑	↑	↓
Antilipolysis	↓	↓	↑	↓
Glycogen and starch metabolism	↓	↑	–	↓
Protein synthesis	↓	↑	↑	↓
Proliferation and Differentiation	↓	↑	↑	↓
***Salmonella* infection pathway**				
T-cell activity	–	–	↑	–
Membrane ruffling and macropinocytosis	↓	↑	↓	↓
Bacteria-containing vesicle formation and scission	↓	–	↓	↓
NF-κB pathway pro-inflammatory cytokines production	↓	↑	↓	↓
MAPK pathway pro-inflammatory cytokines production	↓	↑	↑	↓
Apoptosis	↓	↓	↑	↓
Pyroptosis	–	↓	↑	↓

FIGURES

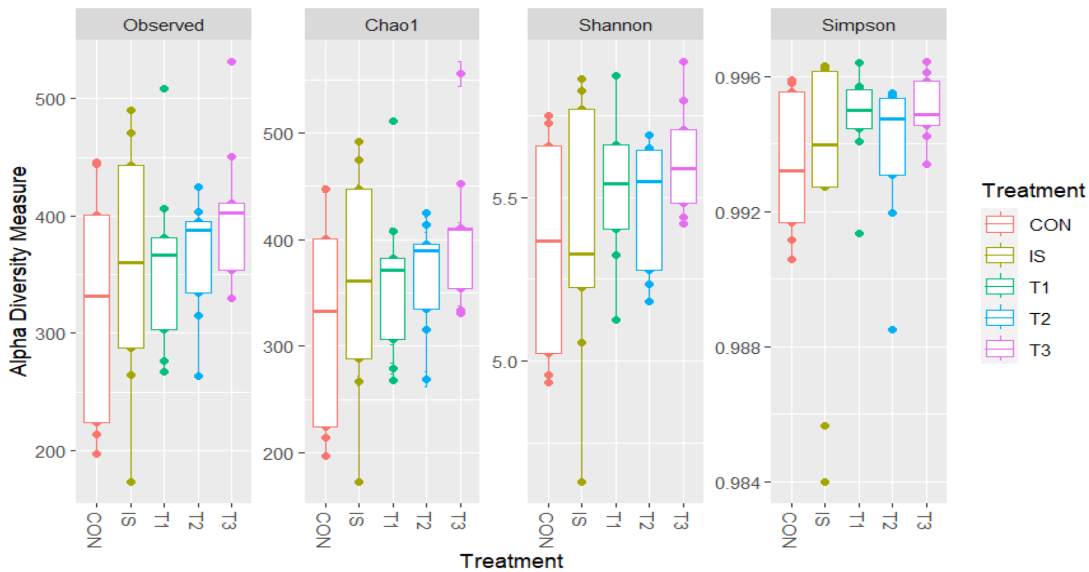

Figure 3.1 Alpha diversity box-and-whisker plots comparing treatments using observed species, Chao1, Shannon, and Simpson indices.

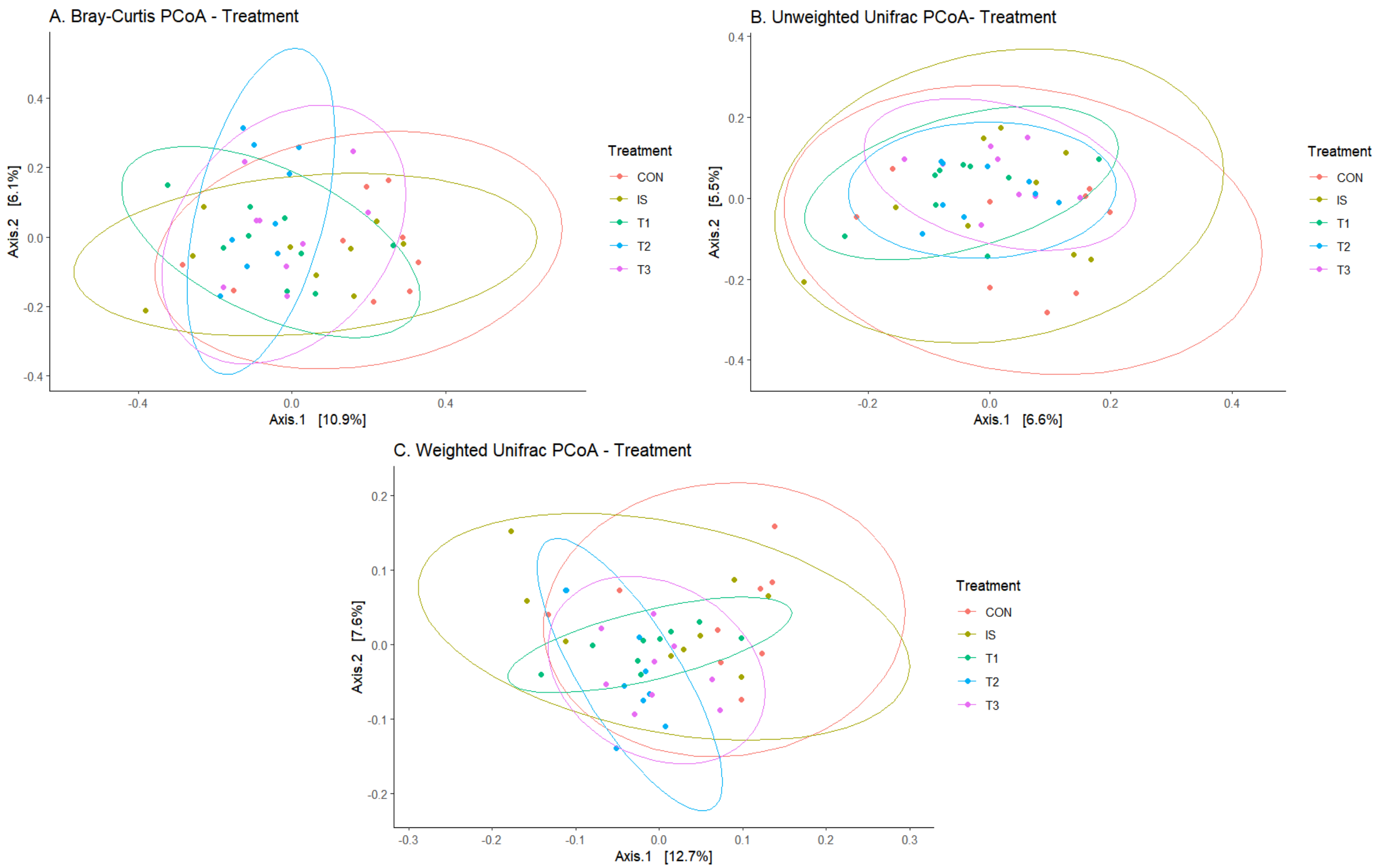

Figure 3.2: Beta diversity principal coordinate analysis (PCoA) plots comparing treatment types using Bray-Curtis Dissimilarity, Weighted UniFrac, and Unweighted UniFrac.

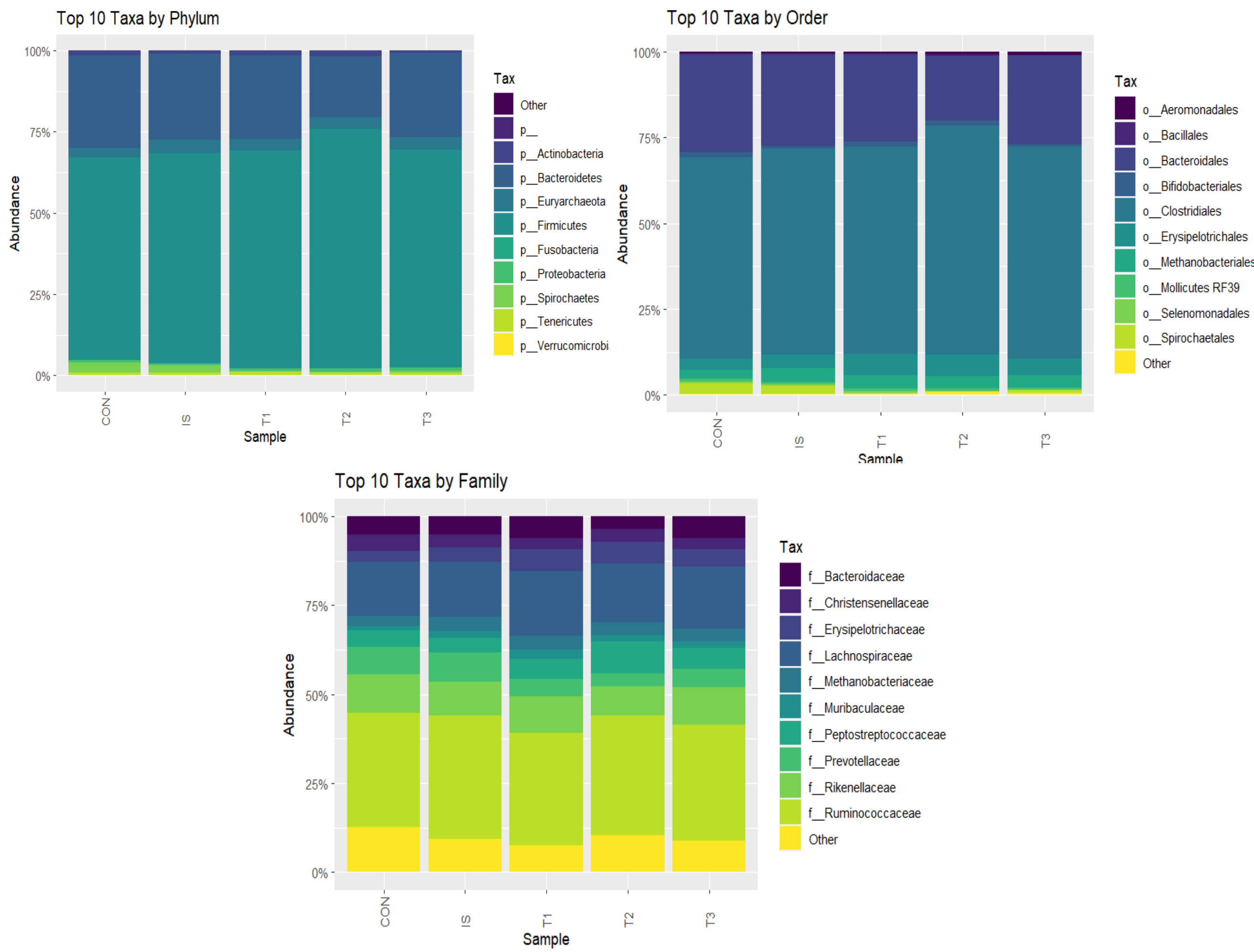

Figure 3.3: Relative abundance taxa bar plots of the top 10 bacteria at the phylum, order, and family levels.

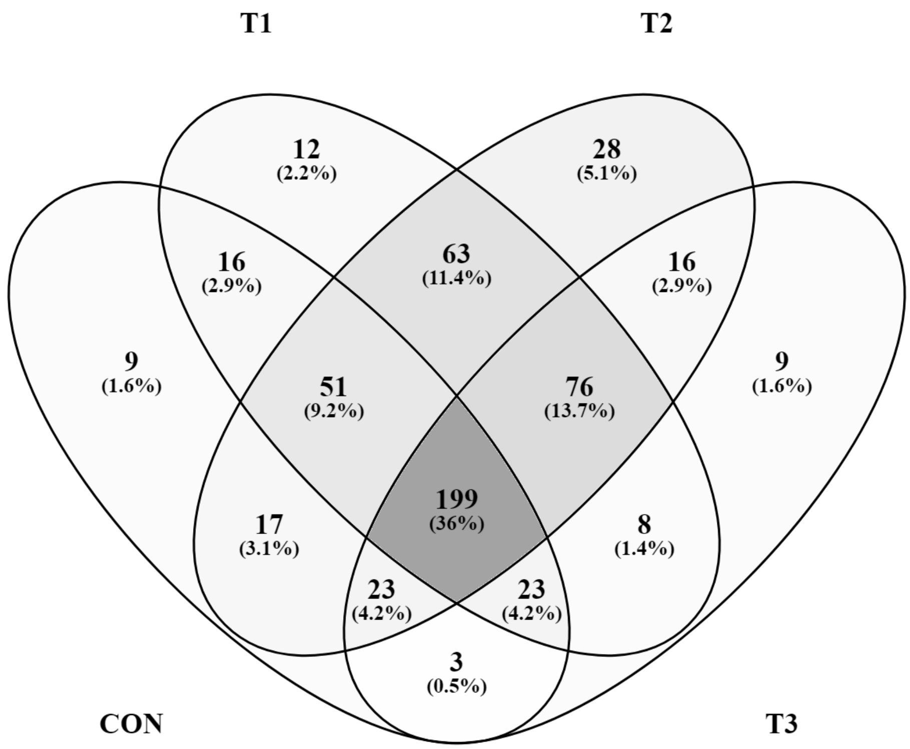

Figure 3.4: Comparison of the number of peptides shared and unique to each treatment type in comparison to IS with Venny 2.1.

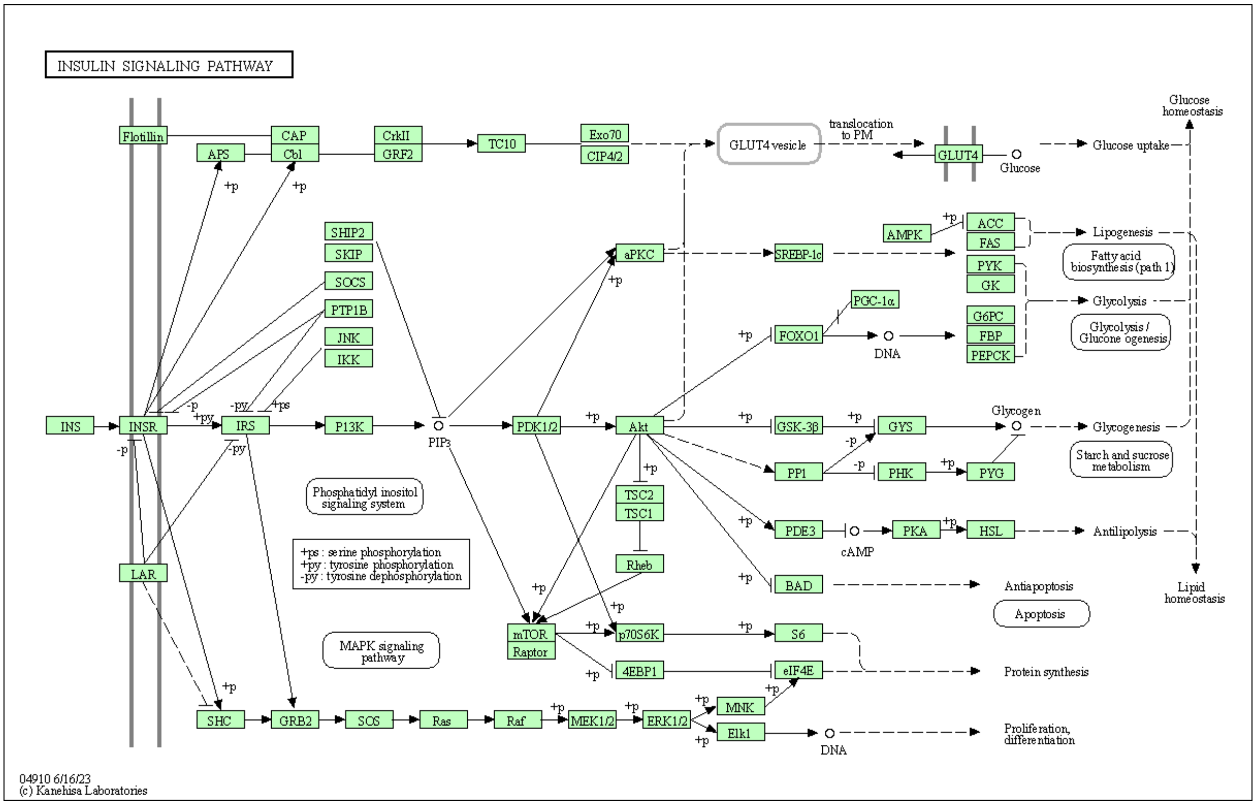

Figure 3.5: KEGG depiction of the insulin signaling pathway. Light green highlighted peptides are possible locations for increased or decreased phosphorylation signals of CON, T1, T2, and T3 as compared to IS.

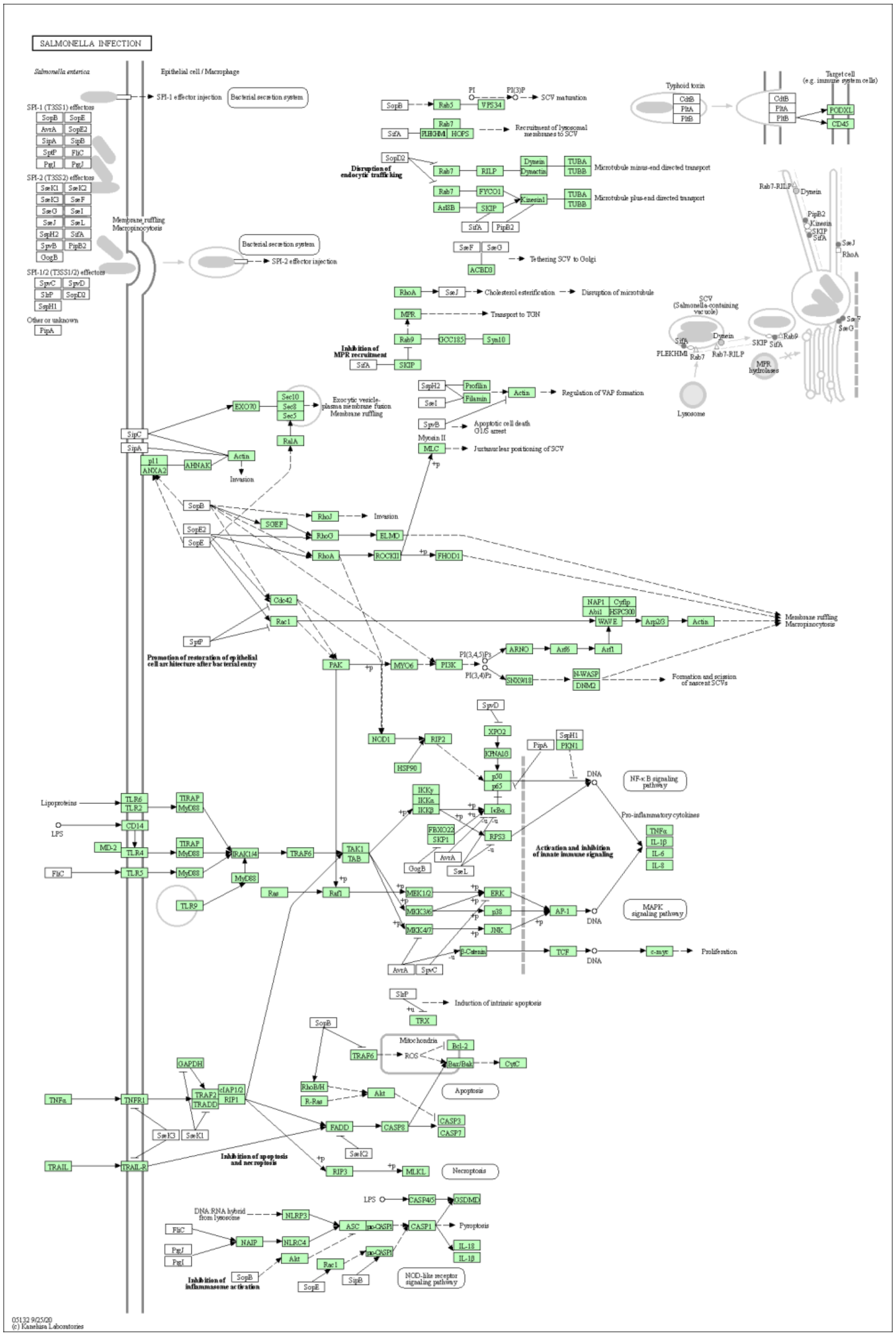

Figure 3.6: KEGG depiction of the *Salmonella* infection pathway. Light green highlighted peptides are possible locations for increased or decreased phosphorylation signals of CON, T1, T2, and T3 as compared to IS.

REFERENCES

Abeyta, M.A., E.A. Horst, B.M. Goetz, E.J. Mayorga, S. Rodriguez-Jimenez, M. Caratzu, and L.H. Baumgard. 2023. Effects of hindgut acidosis on production, metabolism, and inflammatory biomarkers in feed-restricted lactating dairy cows. J. Dairy Sci. 106:2890–2903. doi:10.3168/jds.2022-22689.

Abeyta, M.A., E.A. Horst, E.J. Mayorga, B.M. Goetz, M. Al-Qaisi, C.S. McCarthy, M.R. O'Neil, B.C. Dooley, P. Piantoni, G.F. Schroeder, and L.H. Baumgard. 2023. Effects of hindgut acidosis on metabolism, inflammation, and production in dairy cows consuming a standard lactation diet. J. Dairy Sci. 106:1429–1440. doi:10.3168/jds.2022-22303.

Acosta Davila, J.A., and A. Hernandez De Los Rios. 2019. An Overview of Peripheral Blood Mononuclear Cells as a Model for Immunological Research of Toxoplasma gondii and Other Apicomplexan Parasites. Front. Cell. Infect. Microbiol. 9:1–10. doi:10.3389/fcimb.2019.00024.

Arce-Cordero, J.A., T. Liu, A. Ravelo, R.R. Lobo, B.C. Agustinho, H.F. Monteiro, K.C. Jeong, and A.P. Faciola. 2022. Effects of calcium-magnesium carbonate and calcium-magnesium hydroxide as supplemental sources of magnesium on ruminal microbiome. Transl. Anim. Sci. 6:1–10. doi:10.1093/tas/txac092.

Ardito, F., M. Giuliani, D. Perrone, G. Troiano, and L. Lo Muzio. 2017. The crucial role of protein phosphorylation in cell signalingand its use as targeted therapy (Review). Int. J. Mol. Med. 40:271–280. doi:10.3892/ijmm.2017.3036.

Arsenault, R.J., J.T. Lee, R. Latham, B. Carter, and M.H. Kogut. 2017. Changes in immune and metabolic gut response in broilers fed β-mannanase in β-mannan-containing diets. Poult. Sci. 96:4307–4316. doi:10.3382/ps/pex246.

Bach, A., I. Guasch, G. Elcoso, J. Duclos, and H. Khelil-Arfa. 2018. Modulation of rumen pH by sodium bicarbonate and a blend of different sources of magnesium oxide in lactating dairy cows submitted to a concentrate challenge. J. Dairy Sci. 101:9777–9788. doi:10.3168/jds.2017-14353.

Bateman, A., M.J. Martin, S. Orchard, M. Magrane, R. Agivetova, S. Ahmad, E. Alpi, E.H. Bowler-Barnett, R. Britto, B. Bursteinas, H. Bye-A-Jee, R. Coetzee, A. Cukura, A. da Silva, P. Denny, T. Dogan, T.G. Ebenezer, J. Fan, L.G. Castro, P. Garmiri, G. Georghiou, L. Gonzales, E. Hatton-Ellis, A. Hussein, A. Ignatchenko, G. Insana, R. Ishtiaq, P. Jokinen, V. Joshi, D. Jyothi, A. Lock, R. Lopez, A. Luciani, J. Luo, Y. Lussi, A. MacDougall, F. Madeira, M. Mahmoudy, M. Menchi, A. Mishra, K. Moulang, A. Nightingale, C.S. Oliveira, S. Pundir, G. Qi, S. Raj, D. Rice, M.R. Lopez, R. Saidi, J. Sampson, T. Sawford, E. Speretta, E. Turner, N. Tyagi, P. Vasudev, V. Volynkin, K. Warner, X. Watkins, R. Zaru, H. Zellner, A. Bridge, S. Poux, N. Redaschi, L. Aimo, G. Argoud-Puy, A. Auchincloss, K. Axelsen, P. Bansal, D. Baratin, M.C. Blatter, J. Bolleman, E. Boutet, L. Breuza, C. Casals-Casas, E. de Castro, K.C. Echioukh, E. Coudert, B. Cuche, M. Doche, D. Dornevil, A. Estreicher, M.L. Famiglietti, M. Feuermann, E. Gasteiger, S. Gehant, V. Gerritsen, A. Gos, N. Gruaz-Gumowski, U. Hinz, C. Hulo, N. Hyka-Nouspikel, F. Jungo, G. Keller, A. Kerhornou, V. Lara, P. Le Mercier, D. Lieberherr, T. Lombardot, X. Martin, P. Masson, A. Morgat, T.B. Neto, S. Paesano, I. Pedruzzi, S. Pilbout, L. Pourcel, M. Pozzato, M. Pruess, C. Rivoire, C. Sigrist, K. Sonesson, A. Stutz, S. Sundaram, M. Tognolli, L. Verbregue, C.H. Wu, C.N. Arighi, L. Arminski, C. Chen, Y. Chen, J.S. Garavelli, H. Huang, K. Laiho, P. McGarvey, D.A. Natale, K. Ross, C.R. Vinayaka, Q. Wang, Y. Wang, L.S. Yeh, J. Zhang, P. Ruch, and D. Teodoro. 2021. UniProt: the universal protein knowledgebase in 2021. Nucleic Acids Res. 49:D480–D489. doi:10.1093/nar/gkaa1100.

Bolyen, E., J.R. Rideout, M.R. Dillon, N.A. Bokulich, C.C. Abnet, G.A. Al-Ghalith, H. Alexander, E.J. Alm, M. Arumugam, F. Asnicar, Y. Bai, J.E. Bisanz, K. Bittinger, A. Brejnrod, C.J. Brislawn, C.T. Brown, B.J. Callahan, A.M. Caraballo-Rodríguez, J. Chase, E.K. Cope, R. Da Silva, C. Diener, P.C. Dorrestein, G.M. Douglas, D.M. Durall, C. Duvallet, C.F. Edwardson, M. Ernst, M. Estaki, J. Fouquier, J.M. Gauglitz, S.M. Gibbons, D.L. Gibson, A. Gonzalez, K. Gorlick, J. Guo, B. Hillmann, S. Holmes, H. Holste, C. Huttenhower, G.A. Huttley, S. Janssen, A.K. Jarmusch, L. Jiang, B.D. Kaehler, K. Bin Kang, C.R. Keefe, P. Keim, S.T. Kelley, D. Knights, I. Koester, T. Kosciolek, J. Kreps, M.G.I. Langille, J. Lee, R. Ley, Y.X. Liu, E. Loftfield, C. Lozupone, M. Maher, C. Marotz, B.D. Martin, D. McDonald, L.J. McIver, A. V. Melnik, J.L. Metcalf, S.C. Morgan, J.T. Morton, A.T. Naimey, J.A. Navas-Molina, L.F. Nothias, S.B. Orchanian, T. Pearson, S.L. Peoples, D. Petras, M.L. Preuss, E. Pruesse, L.B. Rasmussen, A. Rivers, M.S. Robeson, P. Rosenthal, N. Segata, M. Shaffer, A. Shiffer, R. Sinha, S.J. Song, J.R. Spear, A.D. Swafford, L.R. Thompson, P.J. Torres, P. Trinh, A. Tripathi, P.J. Turnbaugh, S. Ul-Hasan, J.J.J. van der Hooft, F. Vargas, Y. Vázquez-Baeza, E. Vogtmann, M. von Hippel, W. Walters, Y. Wan, M. Wang, J. Warren, K.C. Weber, C.H.D. Williamson, A.D. Willis, Z.Z. Xu, J.R. Zaneveld, Y. Zhang, Q. Zhu, R. Knight, and J.G. Caporaso. 2019. Reproducible, interactive, scalable and extensible microbiome data science using QIIME 2. Nat. Biotechnol. 37:852–857. doi:10.1038/s41587-019-0209-9.

Bornefalk, E., S. Ljunghall, E. Lindh, O. Bengtson, A.G. Johansson, and Ö. Ljunggren. 1997. Regulation of interleukin-6 secretion from mononuclear blood cells by extracellular calcium. J. Bone Miner. Res. 12:228–233. doi:10.1359/jbmr.1997.12.2.228.

Callahan, B.J., P.J. McMurdie, M.J. Rosen, A.W. Han, A.J.A. Johnson, and S.P. Holmes. 2016. DADA2: High-resolution sample inference from Illumina amplicon data. Nat. Methods 13:581–583. doi:10.1038/nmeth.3869.

Cargnello, M., and P.P. Roux. 2011. Activation and Function of the MAPKs and Their Substrates, the MAPK-Activated Protein Kinases. Microbiol. Mol. Biol. Rev. 75:50–83. doi:10.1128/mmbr.00031-10.

Chen, X., X. Su, J. Li, Y. Yang, P. Wang, F. Yan, J. Yao, and S. Wu. 2021. Real-time monitoring of ruminal microbiota reveals their roles in dairy goats during subacute ruminal acidosis. npj Biofilms Microbiomes 7:1–14. doi:10.1038/s41522-021-00215-6.

Cheng, M., Y. Sun, L. Wang, L. Tan, H. Jin, S. Yan, S. Li, and X. Xiao. 2021. Integrative analysis of microbiome and metabolome in rats with gest-Aid plus oral liquid supplementation reveals mechanism of its healthcare function. Food Qual. Saf. 5:1–10. doi:10.1093/fqsafe/fyab010.

Cronin, S.K., A.M. Barnard, S.J. Dietz, M. Lawrence, A.E. Kramer, and T.F. Gressley. 2023. Effect of short-term abomasal corn starch infusions on postruminal fermentation and blood measures. J. Dairy Sci. 106:8658–8669. doi:10.3168/jds.2022-23180.

Cui, Y., L. Zhang, X. Wang, Y. Yi, Y. Shan, B. Liu, Y. Zhou, and X. Lü. 2022. Roles of intestinal Parabacteroides in human health and diseases. FEMS Microbiol. Lett. 369:1–11. doi:10.1093/femsle/fnac072.

Dahal, R.H., S. Kim, Y.K. Kim, E.S. Kim, and J. Kim. 2023. Insight into gut dysbiosis of patients with inflammatory bowel disease and ischemic colitis. Front. Microbiol. 14:1–14. doi:10.3389/fmicb.2023.1174832.

El Kaoutari, A., F. Armougom, J.I. Gordon, D. Raoult, and B. Henrissat. 2013. The abundance and variety of carbohydrate-active enzymes in the human gut microbiota. Nat. Rev. Microbiol. 11:497–504.

Elmhadi, M.E., D.K. Ali, M.K. Khogali, and H. Wang. 2022. Subacute ruminal acidosis in dairy herds: Microbiological and nutritional causes, consequences, and prevention strategies. Anim. Nutr. 10:148–155. doi:10.1016/j.aninu.2021.12.008.

Emmanuel, D.G.V., K.L. Madsen, T.A. Churchill, S.M. Dunn, and B.N. Ametaj. 2007. Acidosis and Lipopolysaccharide from Escherichia coli B:055 cause hyperpermeability of rumen and colon tissues. J. Dairy Sci. 90:5552–5557. doi:10.3168/jds.2007-0257.

Erdman, R.A. 1988. Dietary Buffering Requirements of the Lactating Dairy Cow: A Review. J. Dairy Sci. 71:3246–3266. doi:10.3168/jds.S0022-0302(88)79930-0.

Fuhren, J., M. Schwalbe, J. Boekhorst, C. Rösch, H.A. Schols, and M. Kleerebezem. 2021. Dietary calcium phosphate strongly impacts gut microbiome changes elicited by inulin and galacto-oligosaccharides consumption. Microbiome 9:1–17. doi:10.1186/s40168-021-01148-0.

Gressley, T.F., M.B. Hall, and L.E. Armentano. 2011. Ruminant nutrition symposium: Productivity, digestion, and health responses to hindgut acidosis in ruminants. J. Anim. Sci. 89:1120–1130. doi:10.2527/jas.2010-3460.

Hatsugai, M., M.S. Kurokawa, T. Kouro, K. Nagai, M. Arito, K. Masuko, N. Suematsu, K. Okamoto, F. Itoh, and T. Kato. 2010. Protein profiles of peripheral blood mononuclear cells are useful for differential diagnosis of ulcerative colitis and Crohn's disease. J. Gastroenterol. 45:488–500. doi:10.1007/s00535-009-0183-y.

Haudek-Prinz, V.J., P. Klepeisz, A. Slany, J. Griss, A. Meshcheryakova, V. Paulitschke, G. Mitulovic, J. Stöckl, and C. Gerner. 2012. Proteome signatures of inflammatory activated primary human peripheral blood mononuclear cells. J. Proteomics 76:150–162. doi:10.1016/j.jprot.2012.07.012.

Henderson, G., F. Cox, S. Ganesh, A. Jonker, W. Young, P.H. Janssen, L. Abecia, E. Angarita, P. Aravena, G.N. Arenas, C. Ariza, G.T. Attwood, J.M. Avila, J. Avila-Stagno, A. Bannink, R. Barahona, M. Batistotti, M.F. Bertelsen, A. Brown-Kav, A.M. Carvajal, L. Cersosimo, A.V. Chaves, J. Church, N. Clipson, M.A. Cobos-Peralta, A.L. Cookson, S. Cravero, O.C. Carballo, K. Crosley, G. Cruz, M.C. Cucchi, R. De La Barra, A.B. De Menezes, E. Detmann, K. Dieho, J. Dijkstra, W.L.S. Dos Reis, M.E.R. Dugan, S.H. Ebrahimi, E. Eythórsdóttir, F.N. Fon, M. Fraga, F. Franco, C. Friedeman, N. Fukuma, D. Gagić, I. Gangnat, D.J. Grilli, L.L. Guan, V.H. Miri, E. Hernandez-Sanabria, A.X.I. Gomez, O.A. Isah, S. Ishaq, E. Jami, J. Jelincic, J. Kantanen, W.J. Kelly, S.H. Kim, A. Klieve, Y. Kobayashi, S. Koike, J. Kopecny, T.N. Kristensen, S.J. Krizsan, H. LaChance, M. Lachman, W.R. Lamberson, S. Lambie, J. Lassen, S.C. Leahy, S.S. Lee, F. Leiber, E. Lewis, B. Lin, R. Lira, P. Lund, E. Macipe, L.L. Mamuad, H.C. Mantovani, G.A. Marcoppido, C. Márquez, C. Martin, G. Martinez, M.E. Martinez, O.L. Mayorga, T.A. McAllister, C. McSweeney, L. Mestre, E. Minnee, M. Mitsumori, I. Mizrahi, I. Molina, A. Muenger, C. Munoz, B. Murovec, J. Newbold, V. Nsereko, M. O'Donovan, S. Okunade, B. O'Neill, S. Ospina, D. Ouwerkerk, D. Parra, L.G.R. Pereira, C. Pinares-Patino, P.B. Pope, M. Poulsen, M. Rodehutscord, T. Rodriguez, K. Saito, F. Sales, C. Sauer, K. Shingfield, N. Shoji, J. Simunek, Z. Stojanović-Radić, B. Stres, X. Sun, J. Swartz, Z.L. Tan, I. Tapio, T.M. Taxis, N. Tomkins, E. Ungerfeld, R. Valizadeh, P. Van Adrichem, J. Van Hamme, W. Van Hoven, G. Waghorn, R.J. Wallace, M. Wang, S.M. Waters, K. Keogh, M. Witzig, A.D.G. Wright, H. Yamano, T. Yan, D.R. Yanez-Ruiz, C.J. Yeoman, R. Zambrano, J. Zeitz, M. Zhou, H.W. Zhou, C.X. Zou, and P. Zunino. 2015. Rumen microbial community composition varies with diet and host, but a core microbiome is found across a wide geographical range. Sci. Rep. 5. doi:10.1038/srep14567.

Herve, Maxime. 2023. Package "RVAideMemoire."

Hornbeck, P. V., B. Zhang, B. Murray, J.M. Kornhauser, V. Latham, and E. Skrzypek. 2015. PhosphoSitePlus, 2014: Mutations, PTMs and recalibrations. Nucleic Acids Res. 43:D512–D520. doi:10.1093/nar/gku1267.

Hunter, T., and T. Hunter. 2012. Why nature chose phosphate to modify proteins. Phil Trans. R. Soc. B 367:2513–2516. doi:10.1098/rstb.20.

Iamartino, L., and M.L. Brandi. 2022. The calcium-sensing receptor in inflammation: Recent updates. Front. Physiol. 13:1–17. doi:10.3389/fphys.2022.1059369.

Jacob, M.E., J.T. Fox, J.S. Drouillard, D.G. Renter, and T.G. Nagaraja. 2008. Effects of dried distillers' grain on fecal prevalence and growth of Escherichia coli O157 in batch culture fermentations from cattle. Appl. Environ. Microbiol. 74:38–43. doi:10.1128/AEM.01842-07.

Jacob, M.E., J.T. Fox, S.K. Narayanan, J.S. Drouillard, D.G. Renter, and T.G. Nagaraja. 2008. Effects of feeding wet corn distillers grains with solubles with or without monensin and tylosin on the prevalence and antimicrobial susceptibilities of fecal foodborne pathogenic and commensal bacteria in feedlot cattle. J. Anim. Sci. 86:1182–1190. doi:10.2527/JAS.2007-0091.

Jangid, A., S. Fukuda, M. Seki, T. Horiuchi, Y. Suzuki, T.D. Taylor, H. Ohno, and T. Prakash. 2020. Association of colitis with gut-microbiota dysbiosis in clathrin adapter AP-1B knockout mice. PLoS One 15:1–16. doi:10.1371/journal.pone.0228358.

Kanehisa, M., Y. Sato, and M. Kawashima. 2022. KEGG mapping tools for uncovering hidden features in biological data. Protein Sci. 31:47–53. doi:10.1002/pro.4172.

Kang, S., and M. Wanapat. 2013. Using plant source as a buffering agent to manipulating rumen fermentation in an In vitro gas production system. Asian-Australasian J. Anim. Sci. 26:1424–1436. doi:10.5713/ajas.2013.13153.

Khafipour, E., S. Li, J.C. Plaizier, and D.O. Krause. 2009. Rumen microbiome composition determined using two nutritional models of subacute ruminal acidosis. Appl. Environ. Microbiol. 75:7115–7124. doi:10.1128/AEM.00739-09.

Kvidera, S., E. Horst, M. Abuajamieh, E. Mayorga, M. Sanz Fernandez, and L. Baumgard. 2017. Glucose requirements of an activated immune system in lactating Holstein cows. doi:10.3168/jds.2016-12001.

Lahti, L., and S. Shetty. 2017. Tools for Microbiome Analysis in R. Accessed.

Lavelle, A., G. Lennon, O. O'Sullivan, N. Docherty, A. Balfe, A. Maguire, H.E. Mulcahy, G. Doherty, D. O'Donoghue, J. Hyland, R.P. Ross, J.C. Coffey, K. Sheahan, P.D. Cotter, F. Shanahan, D.C. Winter, and P.R. O'Connell. 2015. Spatial variation of the colonic microbiota in patients with ulcerative colitis and control volunteers. Gut 64:1553–1561. doi:10.1136/gutjnl-2014-307873.

Le Ruyet, P., and W.B. Tucker. 1992. Ruminal Buffers: Temporal Effects on Buffering Capacity and pH of Ruminal Fluid from Cows Fed a High Concentrate Diet. J. Dairy Sci. 75:1069–1077. doi:10.3168/jds.S0022-0302(92)77851-5.

Li, S., E. Khafipour, D.O. Krause, A. Kroeker, J.C. Rodriguez-Lecompte, G.N. Gozho, and J.C. Plaizier. 2012. Effects of subacute ruminal acidosis challenges on fermentation and endotoxins in the rumen and hindgut of dairy cows. J. Dairy Sci. 95:294–303. doi:10.3168/jds.2011-4447.

Mainardi, S.R., B.A. Hengst, S.J. Nebzydoski, L.M. Nemec, and T.F. Gressley. 2011. Effects of abomasal oligofructose on blood and feces of Holstein steers. J. Anim. Sci. 89:2510–2517. doi:10.2527/jas.2010-3348.

Mao, S.Y., R.Y. Zhang, D.S. Wang, and W.Y. Zhu. 2013. Impact of subacute ruminal acidosis (SARA) adaptation on rumen microbiota in dairy cattle using pyrosequencing. Anaerobe 24:12–19. doi:10.1016/J.ANAEROBE.2013.08.003.

McMurdie, P.J., and S. Holmes. 2013. Phyloseq: An R Package for Reproducible Interactive Analysis and Graphics of Microbiome Census Data. PLoS One 8. doi:10.1371/journal.pone.0061217.

Miyanaga, K., A. Asada, M. Komoto, Y. Ohshima, H. Morimoto, T. Yasukawa, R. Matsuura, K. Morito, K. Takayama, Y. Uozumi, and K. Nagasawa. 2022. Prophylactic Administration of Magnesium Oxide Prevents Dextran Sulfate Sodium-Induced Colonic Injury in Mice. Biol. Pharm. Bull 45:1312–1320.

Mizrahi, I., and E. Jami. 2018. Review: The compositional variation of the rumen microbiome and its effect on host performance and methane emission. Animal 12:S220–S232. doi:10.1017/S1751731118001957.

Mu, Y., W. Qi, T. Zhang, J. Zhang, and S. Mao. 2022. Multi-omics Analysis Revealed Coordinated Responses of Rumen Microbiome and Epithelium to High-Grain-Induced Subacute Rumen Acidosis in Lactating Dairy Cows. mSystems 7. doi:10.1128/msystems.01490-21.

Neiderfer, K.P., A.M. Barnard, K.Z. Moyer, A.M. Trench, A.E. Taylor, S.K. Cronin, and T.F. Gressley. 2020. Effects of calcium carbonate, magnesium oxide and encapsulated sodium bicarbonate on measures of post-ruminal fermentation. J. Anim. Physiol. Anim. Nutr. (Berl). 104:802–811. doi:10.1111/jpn.13331.

Neubauer, V., R.M. Petri, E. Humer, I. Kröger, N. Reisinger, W. Baumgartner, M. Wagner, and Q. Zebeli. 2020. Starch-Rich Diet Induced Rumen Acidosis and Hindgut Dysbiosis in Dairy Cows of Different Lactations 10. doi:10.3390/ani10101727.

Offner, A., and D. Sauvant. 2004. Prediction of in vivo starch digestion in cattle from in situ data. Anim. Feed Sci. Technol. 111:41–56. doi:10.1016/S0377-8401(03)00216-5.

Okba, A.M., M.M. Amin, A.S. Abdelmoaty, H.E. Ebada, A.H. Kamel, A.S. Allam, and O.M. Sobhy. 2019. Neutrophil/lymphocyte ratio and lymphocyte/monocyte ratio in ulcerative colitis as non.invasive biomarkers of disease activity and severity. Autoimmun. Highlights 10. doi:10.1186/s13317-019-0114-8.

Oksanen, J., G.L. Simpson, F.G. Blanchet, R. Kindt, P. Legendre, P.R. Minchin, R.B. O'Hara, and P. Solymos. 2022. Package "vegan."

Oliveros, J.C. 2007. Venny. An Interactive Tool for Comparing Lists with Venn's Diagrams. Accessed.

Owens, F.N., R.A. Zinn, and Y.K. Kim. 1986. Limits to starch digestion in the ruminant small intestine.. J. Anim. Sci. 63:1634–1648. doi:10.2527/jas1986.6351634x.

Perry, F. 2023. THE IMMUNOMETABOLIC AND MOLECULAR EFFECTS OF POTENTIAL ANTIBIOTIC ALTERNATIVES AS FEED SUPPLEMENTS IN BROILERS.

Pietrucci, D., A. Teofani, M. Milanesi, B. Fosso, L. Putignani, F. Messina, G. Pesole, A. Desideri, and G. Chillemi. 2022. Machine Learning Data Analysis Highlights the Role of Parasutterella and Alloprevotella in Autism Spectrum Disorders. Biomedicines 10:1–22. doi:10.3390/biomedicines10082028.

Plaizier, J.C., M.D. Mesgaran, H. Derakhshani, H. Golder, E. Khafipour, J.L. Kleen, I. Lean, J. Loor, G. Penner, and Q. Zebeli. 2018. Review: Enhancing gastrointestinal health in dairy cows. Animal 12:S399–S418. doi:10.1017/S1751731118001921.

Plaizier, J.C., S. Li, A.M. Danscher, H. Derakshani, P.H. Andersen, and E. Khafipour. 2017. Changes in Microbiota in Rumen Digesta and Feces Due to a Grain-Based Subacute Ruminal Acidosis (SARA) Challenge. Microb. Ecol. 74:485–495. doi:10.1007/s00248-017-0940-z.

Quast, C., E. Pruesse, P. Yilmaz, J. Gerken, T. Schweer, P. Yarza, J. Peplies, and F.O. Glöckner. 2013. The SILVA ribosomal RNA gene database project: improved data processing and web-based tools. Nucleic Acids Res. 41:D590–D596. doi:10.1093/NAR/GKS1219.

Rodríguez-Lecompte, J.C., A.D. Kroeker, A. Ceballos-Márquez, S. Li, J.C. Plaizier, and D.E. Gomez. 2014. Evaluation of the systemic innate immune response and metabolic alterations of nonlactating cows with diet-induced subacute ruminal acidosis. J. Dairy Sci. 97:7777–7787. doi:10.3168/jds.2014-8319.

ROGOSA, M., and F.S. BISHOP. 1964. the Genus Veillonella . Ii. Nutritional Studies.. J. Bacteriol. 87:574–580.

Sanz-Fernandez, M.V., J.B. Daniel, D.J. Seymour, S.K. Kvidera, Z. Bester, J. Doelman, and J. Martín-Tereso. 2020. Targeting the hindgut to improve health and performance in cattle. Animals 10:1–18. doi:10.3390/ani10101817.

Schluter, J., J.U. Peled, B.P. Taylor, K.A. Markey, M. Smith, Y. Taur, R. Niehus, A. Staffas, A. Dai, E. Fontana, L.A. Amoretti, R.J. Wright, S. Morjaria, M. Fenelus, M.S. Pessin, N.J. Chao, M. Lew, L. Bohannon, A. Bush, A.D. Sung, T.M. Hohl, M.-A. Perales, M.R.M. van den Brink, and J.B. Xavier. 2020. The gut microbiota is associated with immune cell dynamics in humans 588:303–307. doi:10.1038/s41586-020-2971-8.The.

Shi, H., N.J. Severs, and H. Robenek. 1996. Effects of calcium on the migration and recruitment of macrophages and macrophage-derived foam cells. FASEB J. 10:491–501. doi:10.1096/FASEBJ.10.4.8647348.

Shimizu, J., T. Kubota, E. Takada, K. Takai, N. Fujiwara, N. Arimitsu, M.A. Murayama, Y. Ueda, S. Wakisaka, T. Suzuki, and N. Suzuki. 2018. Propionate-producing bacteria in the intestine may associate with skewed responses of IL10-producing regulatory T cells in patients with relapsing polychondritis. PLoS One 13:1–17. doi:10.1371/journal.pone.0203657.

Stefanska, B., W. Człapa, E. Pruszynska-Oszmałek, D. Szczepankiewicz, V. Fievez, J. Komisarek, K. Stajek, and W. Nowak. 2018. Subacute ruminal acidosis affects fermentation and endotoxin concentration in the rumen and relative expression of the CD14/TLR4/MD2 genes involved in lipopolysaccharide systemic immune response in dairy cows. J. Dairy Sci. 101:1297–1310. doi:10.3168/jds.2017-12896.

Suchodolski, J.S. 2012. Gastrointestinal Microbiota. Elsevier Inc.

Tian, T., X. Zhang, T. Luo, D. Wang, Y. Sun, and J. Dai. 2021. Effects of short-term dietary fiber intervention on gut microbiota in young healthy people. Diabetes, Metab. Syndr. Obes. 14:3507–3516. doi:10.2147/DMSO.S313385.

Trost, B., J. Kindrachuk, P. Määttänen, S. Napper, and A. Kusalik. 2013. PIIKA 2: An expanded, web-based platform for analysis of kinome microarray data. PLoS One 8. doi:10.1371/journal.pone.0080837.

Wang, Y., J.M. Huang, Y.L. Zhou, A. Almeida, R.D. Finn, A. Danchin, and L.S. He. 2020. Phylogenomics of expanding uncultured environmental Tenericutes provides insights into their pathogenicity and evolutionary relationship with Bacilli. BMC Genomics 21:1–12. doi:10.1186/s12864-020-06807-4.

Wheeler, W.E., and C.H. Noller. 1977. GASTROINTESTINAL TRACT pH AND STARCH 1–5.

Zakerska-Banaszak, O., H. Tomczak, M. Gabryel, A. Baturo, L. Wolko, M. Michalak, N. Malinska, D. Mankowska-Wierzbicka, P. Eder, A. Dobrowolska, R. Slomski, and M. Skrzypczak-Zielinska. 2021. Dysbiosis of gut microbiota in Polish patients with ulcerative colitis: a pilot study. Sci. Rep. 11:1–13. doi:10.1038/s41598-021-81628-3.

Zhang, R., Z. Zhong, H. Ma, L. Lin, F. Xie, S. Mao, D.M. Irwin, Z. Wang, and S. Zhang. 2021. Mucosal Microbiota and Metabolome in the Ileum of Hu Sheep Offered a Low-Grain, Pelleted or Non-pelleted High-Grain Diet. Front. Microbiol. 12:1–12. doi:10.3389/fmicb.2021.718884.

Zhao, C., G. Liu, X. Li, Y. Guan, Y. Wang, X. Yuan, G. Sun, Z. Wang, and X. Li. 2018. Inflammatory mechanism of Rumenitis in dairy cows with subacute ruminal acidosis. BMC Vet. Res. 14:1–8. doi:10.1186/s12917-018-1463-7.

Chapter 4

IN VITRO EFFECTS OF STARCH WITH OR WITHOUT BUFFERS ON DAIRY CATTLE FECAL FERMENTATION AND MICROBIOME

4.1 Abstract

Dietary buffers can impact hindgut fermentation to increase fecal pH and may help to alleviate hindgut acidosis. The objective of this study was to evaluate how two buffers would alter in vitro fecal microbial fermentation and microbiota profile with and without a starch challenge. Four lactating Holstein cows were used as fecal donors for a series of batch cultivation trials with six treatments. Feces was anaerobically cultured at 1% weight to volume (w/v) in six different treatments: FECC (no additive), STAR (1% w/v food grade corn starch), SBA (1% w/v corn starch and 0.05% w/v of a calcium carbonate, magnesium oxide, and crushed oyster shell blend (buffer A)), SBB (1% w/v corn starch and 0.05% w/v magnesium oxide (buffer B)), BA (0.05% w/v buffer A), and BB (0.05% w/v buffer B). Samples were collected at 0, 3, 6, 12, 18, and 24 h to determine fermentation profile (gas production, pH, NH_3-N, VFA, lactate, total protein, total carbohydrate, and lipopolysaccharide (LPS)), and at 0, 6, and 24 h to determine microbial populations. Fermentation products were analyzed in JMP Pro using the Fit Model procedure with the main factors being treatment, time, cow, and the interaction of treatment by time. DNA was extracted from cell pellets and the V4-V5 region of the 16S rRNA gene was amplified and sequenced using Illumina MiSeq before additional analysis using QIIME2 and RStudio. Compared to FECC, STAR increased gas production, butyrate, lactate, LPS, and total protein, while decreasing

culture pH, propionate, and NH_3-N. STAR changed microbial beta diversity and tended to increase amylolytic bacteria like *Lactobacillus* and decrease fiber digesting bacteria like *Bacteroidetes*. Compared to FECC, BB increased culture pH, and both BA and BB increased acetate and total VFA. Both buffer treatments changed microbial beta diversity in the absence of starch, but BB additionally increased alpha diversity and positively correlated to microbial taxa involved in fiber and protein digestion, suggesting improved maintenance of microbial functionality through 24 h. Compared to STAR, SBA and SBB increased culture pH, gas production, acetate, propionate, and butyrate, but did not mitigate the negative effects of starch on the microbiome. While buffer treatments in the absence of starch aided in the preservation of culture microbiota, similar benefits were not observed in cultures with starch inclusion, even though buffers affected fermentation profile. Despite the higher pH, increased VFA production suggests that buffer inclusion during hindgut acidosis could further challenge cows.

4.2 Introduction

Lactating dairy cows are often fed diets rich in rapidly fermentable carbohydrates like starch to support the energetic demands of milk production. While important for maximizing production, too much dietary starch can lead to acidotic conditions in the rumen and hindgut. Rapidly fermentable carbohydrates like starch increase VFA and lactate production in the rumen and intestines (Nagaraja and Titgemeyer, 2007; Robbers et al., 2019), decreasing pH (Owens et al., 1998; Cronin et al., 2023). These decreases in gastrointestinal pH degrade the rumen and intestinal cell barriers (Steele et al., 2011; Wang et al., 2017) and cause the lysis of gram-negative bacteria, which increases the concentration of lipopolysaccharide (LPS) in the lumen

(Van Kessel et al., 2002; Li et al., 2012; Monteiro and Faciola, 2020). LPS proves highly immunogenic (Kent-Dennis et al., 2020), with entry into the systemic circulation due to acidosis-induced barrier disruption potentially causing systemic inflammation (Emmanuel et al., 2007; Li et al., 2012). Additionally, high levels of starch and acidotic conditions in the gut can cause shifts in the microbiota profile. High starch diets can reduce microbial alpha diversity and change beta diversity and taxa abundance in the rumen and feces (Plaizier et al., 2017a; Neubauer et al., 2020; Chen et al., 2021). Particularly, in both the rumen and feces, cellulolytic microbes exhibit decreased abundance and functional ability, while amylolytic microbes like those in the *Firmicutes* phylum display increased abundance (Mao et al., 2013; Plaizier et al., 2017a,b). Therefore, stabilizing the gastrointestinal pH to mitigate the effects of starch-rich diets may not only improve rumen health but may also contribute to intestinal health.

When fed to dairy cattle, dietary buffers can increase ruminal and fecal pH (Schaefer et al., 1982; Rogers et al., 1985; Erdman, 1988; Chapter 2), potentially supporting animal health. Dietary buffers can affect ruminal microbial diversity (Mao et al., 2017; Ramos et al., 2020), but there is a lack of research regarding their effects on the intestinal or fecal microbiome during acidosis. Determining the effects of dietary buffers on the hindgut during acidotic conditions could elucidate whether dietary buffers can help to maintain microbial diversity and functionality in challenged conditions.

In vitro fermentation experiments can be employed to generate information about microbial activity when exposed to differing environmental conditions without the influence of host interactions. Particularly when studying disorders like acidosis that may negatively affect animal health, in vitro experiments provide insight into microbial activity without risk to the animal (Biddle et al., 2013; Darwin et al., 2017; Ahmed et al., 2022). Our previous work suggested that calcium carbonate ($CaCO_3$) and magnesium oxide (MgO) buffers fed to lactating cows challenged with SARA induction and abomasal starch altered intestinal fermentation. Buffers increased fecal VFA despite higher fecal pH (Chapter 2) and changed the relative abundance of some microbial taxa (Chapter 3). Along with these changes to the intestinal environment, one buffer resulted in unexpected pro-inflammatory responses while the other resulted in anti-inflammatory responses. Thus, we sought to determine how the two buffers could alter fecal microbial fermentation when exposed to healthy or acidotic conditions in a more controlled in vitro environment. We hypothesized that starch inclusion would reduce in vitro culture pH through production of VFA and lactate, and display decreases in microbial diversity commonly observed in the presence of acidosis. We additionally hypothesized that both buffers would raise culture pH in the presence and absence of starch and but would differentially affect culture microbiota.

4.3 Materials and Methods

4.3.1 Fecal Samples

All work was approved by the University of Delaware's Institutional Animal Care and Use Committee, protocol number 79R, and was completed in summer of 2023. The in vitro study was replicated on 4 different dates (June 19th – July 12th, 2023), with a single cow used to provide the fecal inoculant on each date. The 4 fecal donors were Holstein cows in mid-lactation housed at the University of Delaware. None of the cows selected had any reported health issues for at least 3 months prior to sampling. Cows were maintained on herd milking group TMR (details below) and had ad libitum access to water and feed. Fecal samples were collected through rectal palpation and protected from oxygen exposure following collection by inverting the glove around the fecal material. The glove was immediately placed into a prewarmed container that was then evacuated of oxygen with a flame. Feces were transported back to the laboratory (< 10 min) in an insulated cooler with an internal temperature of 39°C.

4.3.2 In Vitro Experiment

Upon arrival in the laboratory, the fecal sample was transferred into an anaerobic chamber (Coy Laboratory Products, Grass Lake, MI) and a 3% w/v fecal slurry was prepared in pre-warmed (39°C) anaerobic dilution media (Bryant and Burkey, 1952). 25 mL of fecal slurry was added to pre-warmed (39°C) anaerobic culture serum bottles (125 mL, Wheaton, Millville, NJ) containing 50 mL of culture media with or without starch or buffer as described below. Culture media was as described by de Carvalho et al. (2011). The 6 treatments were as follows: control (**FECC**, no additive), starch (**STAR**, 750 mg corn starch), starch and buffer A (**SBA**, 750 mg corn starch and 37.5 mg buffer A), starch and buffer B (**SBB**, 750 mg corn starch and 37.5 mg buffer B), buffer A (**BA**, 37.5 mg buffer A), and buffer B (**BB**, 37.5 mg buffer B). The corn starch consisted of a food grade corn starch product (Feed Binder GE modified corn starch; Ingredion, Westchester, IL), buffer A was a blend of 50% $CaCO_3$, 25% MgO, and 25% crushed oyster shell, and buffer B was 100% MgO. Both buffers and the corn starch were from the same batch as described in Chapters 2 and 3. Experimental treatment bottles were prepared in triplicate on each of the 4 in vitro dates. After inoculation with feces, bottles were fitted with rubber stoppers, sealed with aluminum caps, removed from the anaerobic chamber, and transferred to a 39°C incubator. Corresponding feces-free controls (blanks), receiving the same treatments and media but no fecal inoculant, were prepared for each trial.

4.3.3 Sampling and Metabolite Analyses

Contents of each bottle were sampled at 0, 3, 6, 12, 18, and 24 h relative to the start of the incubation. At each time point, bottles were removed one at a time from the incubator, headspace gas volume was evacuated and measured with a 60 mL syringe, and 6 mL of culture contents were collected using a sterilized syringe. The bottles were then returned to the incubator for continued sampling through the end of the 24 h period.

From the 6 mL of culture contents, 2 drops were transferred to pH paper to measure pH (5.5 – 8.0 range pH paper (0.2-0.4 gradations) and 3.0 – 5.5 range pH paper (0.5 gradations); Hydrion, Micro Essential Laboratory, Brooklyn, NY). The remaining culture contents were then centrifuged at room temperature at 13,000 × g for 20 min. The supernatant and residual cell pellets were stored at -20°C and -80°C, respectively, until analysis.

Culture supernatant samples from all time points were analyzed for VFA, lactic acid, and NH_3-N. VFA and lactic acid concentrations were determined using high-performance liquid chromatography following the procedures of Muck and Dickerson (1998) as described by Mainardi et al. (2011). NH_3-N concentrations of culture supernatant were determined using the colorimetric method of Sievert and Shaver (1993). The endotoxin concentration was determined on 0, 6, and 24 h samples using a commercial chromogenic endpoint amebocyte lysate kit according to manufacturer instructions (Pierce LAL Chromogenic Endotoxin Quantification Kit, Thermo Fisher Scientific, Rockford, IL) as described by Cronin et al. (2023). The intra-assay coefficient of variation was 5.3% and the inter-assay coefficient of variation was 25.8%. Total protein was measured on 0 and 24 h samples, while a total carbohydrate assay was conducted on 0, 12, and 24 h samples. Total protein concentrations were determined following the manufacturer's instructions for the Pierce™ BCA Protein Assay Kit (Thermo Fisher Scientific, Waltham, MA), with samples diluted to 5%. Total carbohydrate concentrations of culture supernatant were determined using the anthrone method (Plummer, 1987).

The donor cows were fed a TMR that contained 41.0% corn silage, 13.3% alfalfa silage, and 45.7% grain mix on a DM basis. Samples of TMR were collected on each in vitro date. TMR samples and single experimental composites of corn starch and each buffer were mailed to Cumberland Valley Analytical Services (Waynesboro, PA) for wet chemistry analysis. Corn starch and TMR were evaluated for DM (method 930.15, AOAC International, 2000), NDF (determined with amylase but not corrected for ash; Van Soest et al., 1991), ADF (method 973.18, AOAC International, 2000), N (method 990.03, AOAC International, 2000), starch (Hall, 2009), minerals (method 985.01, AOAC International, 2000), and ash (method 942.05, AOAC International, 2000). Buffers A and B were analyzed for DM, ash, and minerals as described above, as well as chloride (Metrohm USA Inc, Riverview, FL, USA) and sulfur (Leco Organic Application Note, Leco Corporation, St. Joseph, MI, USA). The mean nutrient composition of the TMR samples was 16.2% CP, 33.7% NDF, 21.4% ADF, 24.1% starch, and 7.5% ash. The composite sample of the corn starch contained 89.3% DM, 80.6% starch, 0.8% CP, 4.6% NDF, 3.0% ADF and 0.4% ash. Buffer A contained 99.7% DM, 21.47% Ca, 0.11% Cl, 0.26% K, 25.96% Mg, 0.82% Na, 0% P, and 0.05% S. Buffer B contained 99.6% DM, 6.54% Ca, 1.24% Cl, 0.25% K, 44.49% Mg, 0.89% Na, 0.01% P, and 0.05% S.

4.3.4 Fermentation Profile Statistical Analyses

Gas production and supernatant profile data were statistically analyzed in JMP Pro 17.0.0 (SAS Institute Inc., Cary, NC, 1989-2023). The Univariate procedure was used to identify quantile range outliers that were removed prior to statistical testing. The Tail Quantile was set to 0.1 and Q was set to 2. Remaining data were analyzed using the Fit Model procedure for standard least squares, with the main factors being treatment, time point, cow, and the interaction of treatment and time point. If significance was detected for a specific effect or interaction ($P \leq 0.05$), means were differentiated using Tukey's Honestly Significant Difference.

4.3.5 Bioinformatic and Statistical Analyses

Culture cell pellets were pooled from triplicate bottles to provide a single pellet per cow per time per treatment. Microbial DNA was then extracted from culture cell pellets from 0, 6, and 24 h time points using the QIAamp PowerFecal Pro DNA Kit (QIAGEN, Hilden, Germany) according to manufacturer's instructions (n = 72). Microbial DNA from blank treatments at 0 and 24 h were extracted using the same methods (n = 11). DNA was tested for quantity and quality using a Qubit 3.0 fluorometer (ThermoFisher Scientific, Waltham, MA, USA) and a Nanodrop spectrophotometer (ThermoFisher Scientific, Waltham, MA, USA). Those DNA extracts were frozen (-80°C) and then sent to RTLGenomics (Lubbock, TX, USA) for sequencing. The V4-V5 region of 16S rRNA genes was amplified using universal primers (515F/926R) and sequenced using normalized DNA pools and dual-barcoded

Illumina MiSeq library preparation (RTL Genomics, Lubbock, TX, USA). Primer choices were based on established Earth Microbiome Protocols (Bolyen et al. 2019).

Microbial data processing and statistics were performed using QIIME2 (Quantitative Insights into Microbial Ecology, v. 2023.2), following the workflow described in the “Moving Pictures” tutorial (https://docs.qiime2.org/2021.4/tutorials/moving- pictures/, accessed November 3rd, 2023). Sample sequences were denoised and filtered using DADA2 based on quality score (Callahan et al., 2016). Taxonomic assignments were made against the SILVA_132_99_16S database (Quast et al., 2012) and trained to the 515F/926R primer set. QIIME2 plug-ins q2-composition (ANCOM differential abundance testing) were used for statistical analysis (Qiime2 v. 2023.2). The ANCOM F-statistic is a measure of the effect size difference for a particular species between study groups and the W-statistic is the strength of the ANCOM test for the tested number of species.

Amplicon sequencing variant (ASV) tables were exported to R (v. 2023.09.1; R Core Team, 2018) for further statistical analysis and visualizations using the “phyloseq” package (McMurdie et al., 2013). ASV tables were normalized to the median sequencing depth (16,335 bp) per sample for diversity analysis. Alpha diversity measures (Shannon index and observed species) were calculated using the normalized ASV table and tested with two-way repeated measures ANOVA to measure the effects of treatment, time, and their interaction. The Shannon index estimates sample richness and evenness, while the Observed index estimates the total number of species within samples.

The beta diversity measures of Bray-Curtis Dissimilarity and Weighted and Unweighted UniFrac principal coordinate analysis (PcoA) plots were calculated with normalized ASV tables. Bray-Curtis Dissimilarity matrix measures community composition using an abundance-based approach to calculate dissimilarity between all samples. The Weighted UniFrac method uses phylogenetic relatedness in addition to abundance counts, while Unweighted UniFrac considers phylogenetic relatedness and presence/absence of taxa. Statistical analysis of the distance matrices was calculated with PERMANOVA (permutational multivariate analysis of variance) to determine whether community composition was different with respect to treatment using the 'adonis' function in the 'vegan' R package (Oksanen et al., 2022). Additional analysis of distance matrices was calculated using the 'betadisper' function, also in the 'vegan' R package. Pairwise PERMANOVA was calculated using the 'pairwise.perm.manova' function in the 'RVAideMemoire' R package (Herve, 2023).

Taxa bar plots were created using the 'microbiome' and 'microbiomeutilities' R packages and averaging by treatment (Lahti and Shetty, 2017). Bacterial abundance residuals were analyzed for normality using the Shapiro-Wilk test. Bacterial abundance was then additionally analyzed using Kruskal-Wallis Test or ANOVA if data were determined to be non-parametric or parametric, respectively. Significance was determined at $P \leq 0.05$ and a tendency towards significance at $0.05 < P \leq 0.10$. If significantly different between treatment types, Wilcoxon Rank Sum test or Tukey's Honestly Significant Difference tests were performed depending on data normality. Pairwise Spearman rank correlations (ρ) were calculated with R statistical software and significance was determined at ($0.5 \leq \rho \leq -0.5$). The ρ is moderate with ($|0.5|$ to $|0.7|$), strong with ($|0.7|$ to $|0.9|$), and substantial with ($|0.9|$ to $|1.0|$).

4.4 Results

4.4.1 Fermentation Profiles

Treatment by time interactions were observed for gas production and all variables measured in the supernatant except isobutyrate and valerate concentrations (Table 4.1). Time effects were significant for all variables, and treatment effects were observed for all variables except valerate concentration. For most metabolites, the treatment by time interactions were largely driven by differences between treatments containing starch (STAR, SBA, and SBB) as compared to those that did not (FECC, BA, and BB).

pH declined over time for all treatments, but the treatment by time interaction for pH was driven by the sharper decline in culture pH of starch-containing treatments starting at 6 h as compared to treatments without starch ($P < 0.01$; Figure 4.1). Across all sampling times, starch inclusion reduced pH (FECC vs. STAR; $P < 0.01$) while SBA and SBB inclusion increased culture pH as compared to STAR, respectively ($P = 0.01$ and $P < 0.01$, respectively; Table 4.1). BB increased culture pH as compared to FECC ($P = 0.02$), while BA did not significantly increase pH when compared to FECC ($P = 0.36$). pH did not change in any treatment between 0 and 3 h. For treatments without starch, treatments did not differ from one another at any time point, but treatments containing starch displayed differences starting at 6 h. At 6 and 12 h, STAR decreased pH (average 4.94) as compared to SBB (average 5.31; $P < 0.05$), with SBA not differing from either treatment (average 5.19). Treatments containing starch did not differ from each other at 18 and 24 h. Overall, both buffer A and buffer B increased the pH when starch was present in the culture, but only buffer B significantly increased pH in the absence of starch (Table 4.1).

Cumulative gas production increased in all treatments beginning at 6 h as compared to 0 and 3 h ($P < 0.01$ for all comparisons within treatment of 6 through 24 h vs. 0 and 3 h; Figure 4.2). Across all time points, STAR, SBA, and SBB produced more gas (average 42.5 mL) as compared to FECC, BA, and BB (average 10.9 mL; $P < 0.01$; Table 4.1). From 12 to 24 h, SBB displayed increased cumulative gas production (average 75.7 mL) than STAR (average 57.0 mL; $P < 0.01$), while SBA tended to increase gas (average 73.4) as compared to STAR at 18 and 24 h (average 57.0 mL; $P = 0.08$).There were no effects of buffers on gas production in the absence of starch, with FECC, BA, and BB exhibiting similar gas production throughout the entire incubation time.

For the treatments not containing starch, NH_3-N did not change between 0 and 12 h (average 9.01 mg/dL) but increased at 18 and 24 h (average 13.6 mg/dL; $P < 0.05$; Figure 4.3). In addition, there were no differences at any time point among FECC, BA, and BB. For treatments containing starch, NH_3-N was not different at 0 and 3 h (average 8.64 mg/dL) but decreased from 6-24 h (average 4.66 mg/dL; $P < 0.05$). In addition, NH_3-N was lower for SBB than STAR at 12-24 h (average 3.81 mg/dL vs. average 5.82 mg/dL, respectively; $P < 0.05$) but SBA did not differ from STAR or SBB at any time. Total protein levels started at the same concentration for all treatments (average 11.9 mg/mL; Figure 4.4). Treatments without starch were decreased at 24 h (average of 7.5 mg/mL FECC, BA, and BB at 24 h; $P < 0.01$) but did not differ from each other. While starch-containing treatments did not differ in protein concentrations across time, SBA and SBB (average 11.4 mg/mL) did display lower concentrations than STAR at 24 h (12.6 mg/mL; $P < 0.05$).

Acetate concentrations did not change in any treatment between 0 and 3 h (average 4.96 mM; Figure 4.5). Between 3 and 24 h, all treatments without starch increased relatively linearly, but from 12-24 h, treatments with buffers (BA and BB) displayed greater concentrations than FECC (average of 14.0 vs. 10.6 mM; $P < 0.01$). BA and BB did not differ from each other at any time. For the treatments containing starch, acetate increased and then plateaued. Beginning at 6 h, acetate concentrations were higher for treatments containing buffer (SBA and SBB; average 14.0 mM) than for STAR (10.2 mM; $P < 0.01$). SBA and SBB did not differ from each other at any time. STAR and FECC did not differ in acetate concentration between 0 and 18 h, but FECC displayed increased acetate at 24 h as compared to STAR (16.0 vs. 13.00 mM; $P < 0.01$).

There were no differences among treatments for total VFA from 0 to 3 h (average 6.73 mM; Figure 4.6). Between 3 and 24 h, treatments without starch increased total VFA relatively linearly, but at 12 h, BB displayed greater concentrations than FECC (21.7 vs. 16.4 mM; $P < 0.01$), with BA not differing from either treatment (20.2 mM). At 18 h, both BA and BB exhibited increased VFA (average 28.6 mM) as compared to FECC (22.2 mM; $P < 0.01$) but did not differ from each other. At 24 h, BB again increased total VFA (35.0 mM) as compared to FECC (28.7 mM; $P < 0.01$), with neither treatment differing from BA (33.4 mM). STAR increased total VFA concentrations at 6 h as compared to 3 h (15.1 vs. 7.45 mM; $P < 0.01$), but plateaued starting at 6 h, with no change in total VFA from 6 to 24 h (average 17.9 mM). Total VFA concentrations for SBA and SBB increased to a greater extent than STAR before plateauing. SBB increased total VFA at 6 h as compared to STAR (20.7 vs. 15.1 mM; $P < 0.01$), with SBA not differing from either treatment (19.7 mM). From 12 to 24 h, SBA and SBB displayed higher total VFA (average 28.1 mM) as compared to STAR (18.8 mM; $P < 0.01$) but did not increase in concentration over time or differ from one another. From 0 to 18 h, FECC and STAR did not differ, but FECC displayed higher total VFA than STAR at 24 h (28.7 vs. 19.4 mM; $P < 0.01$).

Propionate concentrations did not change in any treatment between 0 and 6 h (average 1.49 mM; Figure 4.7). Between 6 h and 24 h, treatments without starch increased relatively linearly, with FECC, BA, and BB not differing from each other at any time point. At 12 h, BA and BB (average 4.89 mM) increased propionate concentrations as compared to 6 h (average 2.46 mM; $P < 0.01$), while FECC did not differ between 6 and 12 h. At 18 h, FECC, BA, and BB increased propionate as compared to 12 h ($P < 0.01$), while only FECC and BB further increased propionate at 24 h as compared to 18 h ($P < 0.01$). Comparatively, starch-containing treatments increased propionate to a lower extent than treatments without starch. STAR displayed increases in propionate concentration at 18 and 24 h (average 3.27 mM) as compared to 0 h (0.72 mM; $P < 0.05$). SBA, SBB, and STAR displayed similar concentrations of propionate at all times except at 24 h when SBB increased propionate relative to STAR (6.03 vs. 3.34 mM; $P = 0.01$). FECC displayed increased propionate starting at 18 h as compared to STAR ($P < 0.01$).

Butyrate concentrations did not change any in treatment between 0 and 3 h (average 0.55 mM; Figure 4.8). Between 3 and 24 h, treatments without starch numerically increased and did not differ from each other at any time. For treatments containing starch, butyrate increased and then plateaued. In the STAR treatment, butyrate concentrations increased at 6 h as compared to 3 h (2.45 vs. 0.70 mM; $P <$

0.01) but did not increase further between 6 to 24 h (average 2.83 mM). As with acetate concentrations, SBA and SBB increased butyrate to a greater extent than STAR before plateauing. SBB increased butyrate at 6 h as compared to STAR (3.60 vs. 2.45 mM; $P = 0.02$), with SBA not differing from either treatment (3.32 mM). At 12 h, SBA and SBB both increased butyrate (average 4.65 mM) as compared to 6 h (average 3.46 mM; $P < 0.01$). From 12 to 24 h, SBA and SBB displayed higher butyrate (average 4.70 mM) than STAR (average 2.96 mM; $P < 0.01$) but did not increase in concentration over time or differ from one another. From 6 to 18 h, STAR displayed higher butyrate than FECC (average of 2.79 vs. 1.44 mM; $P < 0.01$). At 24 h, FECC (1.93 mM) and STAR (2.95 mM) did not differ.

Isovalerate concentrations did not change in any treatment between 0 and 12 h (average 0.048 mM; data not shown). At 18 h, BB increased isovalerate (0.074 mM) as compared to FECC, STAR, SBA, and STAR (average 0.045 mM; $P < 0.05$), while BA increased isovalerate (0.060 mM) as compared to SBB and STAR (average 0.041 mM; $P < 0.05$). BA and BB did not differ from each other at 18 or 24 h. At 24 h, BA and BB increased isovalerate (average 0.076 mM) as compared to all other treatments (average 0.043 mM; $P < 0.05$), while FECC increased isovalerate as compared to STAR (0.052 vs. 0.036 mM; $P = 0.04$). Isobutyrate concentrations decreased with time, but BB displayed higher concentrations as compared to SBB (0.08 vs 0.07 mM; Table 4.1). Valerate exhibited increased concentrations at 6 h (0.08 mM) as compared to other time points (average 0.07 mM; $P < 0.04$). Overall, total VFA concentrations followed a similar pattern to acetate (Figure 4.4 and Figure 4.5). Differences in molar percentage of VFA by treatment are displayed in Table C.1.

Lactate concentrations did not change in any treatment between 0 and 3 h (0.55 mM; Figure 4.9). For treatments without starch, lactate increased and then decreased. Treatments without starch did not differ from each other from 6 to 24 h. At 6 and 12 h, treatments without starch displayed increased lactate (average 11.8 mM) as compared to 0 and 3 h (average 0.52 mM; $P < 0.01$). At 24 h, FECC displayed decreased lactate as compared to 12 h (7.71 vs. 14.2 mM; $P = 0.03$), while BA and BB displayed decreased lactate (average 4.23 mM) as compared to 6 h (average 11.2 mM; $P = 0.03$ and P < 0.01, respectively). For the treatments containing starch, lactate increased and then began to plateau. From 6 to 24 h, starch-containing treatments did not differ from each other. At 6 h, starch-containing treatments increased lactate (17.5 mM) as compared to 3 h (17.5 vs. 0.69 mM; $P < 0.01$), and at 12 h increased lactate (average 29.5 mM) as compared to 6 h ($P < 0.01$). Starch-containing treatments did not further increase lactate in 18 h (average 33.7 mM) as compared to 12 h and did not increase lactate at 24 h (average 37.2 mM) as compared to 18 h. From 12 to 24 h, FECC displayed decreased lactate (14.2 mM) as compared to STAR (average 35.7 mM; $P < 0.01$).

At 0 h, starch-containing treatments exhibited increased total carbohydrate as compared to treatments without starch (3,579 vs. 2,767 µg/mL; $P < 0.01$; Figure 4.10). All treatments decreased total carbohydrate from 0 h (average 3,173 µg/mL) to 12 h (291 µg/mL; $P < 0.01$). At 12 h, starch-containing treatments displayed increased total carbohydrate as compared to BB (mean of 475 vs. 95 µg/mL; $P < 0.05$), but no other treatments differed. At 24 h, treatments with starch displayed increased total carbohydrate (average 570 µg/mL) as compared to treatments without starch (average 51 µg/mL; $P < 0.01$). Treatments without starch did not differ from each other at 24 h, but STAR displayed increased total carbohydrate (756 µg/mL) than SBA and SBB (average 477 µg/mL; P = 0.03 and 0.04, respectively).

At 0 h, STAR increased LPS concentration (3.97 EU/mL, $\log_{10}$) as compared to BA and BB (average 3.70 EU/mL, $\log_{10}$; $P < 0.01$), while FECC, SBA, and SBB did not differ from any treatment (average 3.82 EU/mL, $\log_{10}$; Figure 4.11). All treatments increased LPS concentrations at 6 h as compared to 0 h (means of 4.55 vs. 3.81 EU/mL, $\log_{10}$; $P < 0.01$) and at 24 h as compared to 6 h (means of 5.08 vs. 4.55 EU/mL, $\log_{10}$; $P < 0.01$). At 6 h, starch-containing treatments increased LPS (average 4.68 EU/mL, $\log_{10}$) as compared to FECC (4.36 EU/mL supernatant, $\log_{10}$; $P < 0.01$), while BA and BB did not differ from any treatment (average 4.47 EU/mL, $\log_{10}$). Additionally, starch-containing treatments did not differ from each other and treatments without starch did not differ from each other. At 24 h, SBA and SBB increased LPS (average 5.34 EU/mL, $\log_{10}$) as compared to treatments without starch (4.90 EU/mL, $\log_{10}$; $P < 0.01$), and SBB increased LPS as compared to STAR (5.44 vs. 5.10 EU/mL, $\log_{10}$; $P < 0.01$). Additionally, STAR increased LPS concentration as compared to FECC (5.44 vs. 4.80 EU/mL, $\log_{10}$; $P < 0.01$), but no other treatments differed.

4.4.2 Fermentation Profile of Blanks

Table C.2 displays the gas production and other variables measured in the culture supernatant of blank treatments. There was a treatment by time interaction for cumulative gas production (Figure C.2), primarily driven by the increase in gas production at 24 h by the blanks without buffers (average 17.6 mL) as compared to the blanks with buffers at 24 h (average 3.69 mL; $P < 0.05$ for all comparisons), and their 0 h values (average 3.25 mL; $P < 0.01$). A difference in treatment was observed for total carbohydrate, with starch containing treatments having higher carbohydrate concentrations than treatments without starch ($P < 0.01$). Time differences were observed for NH_3-N ($P < 0.01$) and LPS ($P = 0.03$) concentrations and were driven by higher concentrations at 24 h (12.2 mg/dL and 3.54 EU/mL, $\log_{10}$, respectively) as compared to 0 h (10.7 mg/dL and 3.22 EU/mL, $\log_{10}$, respectively).

4.4.3 Microbiome Results

The total feature frequency across samples receiving fecal inoculum (n = 72) was 1,199,483 and an average feature frequency of 16,659 per sample (± s.d = 3,767; range = 5,332 – 26,222; median = 16,689). Average read length was 399 (± s.d = 3; range = 390 – 501). Read counts of all samples following the denoising, quality filtering, and chimera check steps as implemented in QIIME2 are reported in Table C.3. From the samples receiving fecal inoculum, we identified 187 classified genera belonging to 13 phyla.

Alpha diversity refers to the richness (number of species) and evenness (distribution of species) within each sample. Observed species estimates the true number of bacteria, while Shannon index measures richness and evenness. Observed species and Shannon index differences are visualized in Figure 4.12. Observed species differed between treatment groups and time points ($P = 0.01$ and $P < 0.01$, respectively), while their interaction did not display differences ($P > 0.05$). Observed species declined over time, with the 0 h time point displaying the highest values while the 6 and 24 h were lower and not different from one another. Across all times, BA exhibited higher observed species than STAR ($P < 0.01$) and BB displayed higher observed species than FECC ($P = 0.02$). At 6 h, BA had displayed higher observed species than FECC and STAR ($P = 0.01$), and at 24 h, BB exhibited higher observed species than FECC and SBA (*P* = 0.04, 0.05, respectively; Figure 4.12). Additionally, BA displayed a tendency for higher observed species compared to STAR at 24 h (*P* = 0.07). Shannon index differed between time points (*P* < 0.01) while effects of treatment and the interaction of treatment and time were not observed (*P* > 0.05). As with observed species, Shannon index displayed the highest values at the 0 h time point, with 6 and 24 h values lower but not differing from each other. Pairwise comparison tests between treatments found that BB exhibited higher Shannon diversity than FECC across all times (*P* = 0.02). At 6 h, BB displayed higher Shannon diversity than FECC (*P* = 0.04), and at 24 h, BA exhibited a higher Shannon score than STAR (*P* = 0.04; Figure 4.12).

For all beta-diversity measurements, time centroids were different from each other (adonis, *P* < 0.01; betadisper, *P* < 0.01; Figure 4.13). Bray-Curtis and Weighted UniFrac plots (Figure 4.13) did not show a difference in treatment centroids (adonis, *P* = 0.72 and *P* = 0.71, respectively). However, treatment showed a difference in Unweighted UniFrac group centroids (adonis, *P* = 0.02; betadisper, *P* < 0.01; Figure 4.13). Pairwise PERMANOVA between treatment groups and time assignments revealed differences between BA and STAR, SBA, and SBB, between BB and FECC, STAR, SBA, and SBB, and between FECC and STAR, SBA, and SBB at 24 h (Table 4.2, *P* = 0.04).

The greatest differences in alpha and beta diversity measurements between treatments were observed at the 24 h time point. As such, ANCOM differential abundance testing was performed at the phylum to genus level at the 24 h time point. ANCOM testing detected one phylum, one class, one order, two families, and one genus that differed among the treatment groups (Table 4.3). Specifically, Bacteroidetes, Deltaproteobacteria, Desulfovibrionales, Muribaculaceae, Lactobacillaceae, and *Lactobacillus* spp. differed in relative abundances between treatment types. These differences were primarily driven by comparisons between treatments with and without starch. For Spearman correlations at 24 h, the majority of negative correlations were to the STAR treatment, while the majority of positive correlations were to the BB treatment. While most correlated taxa were correlated with only a single treatment, *Bacteroides*, *Ruminobacter*, and *Rikenellaceae RC9 gut group* taxa were found to be negatively correlated with one treatment group and positively correlated with another (Table 4.4). ANCOM and Spearman correlations were also performed on cow assignments at the 24 h time point (Tables C.4 and C.5). ANCOM testing detected three phyla, three class, three order, one family, and two genera to be differentially abundant between cows, but each taxon detected was at lower than 1% relative abundance. The majority of Spearman correlations were with Cow 3.

Appendix tables and figures display sequencing statistics and alpha and beta diversity comparisons of blank treatment types (Table C.3, Figures C.2 and C.3). There were no differences between treatments or time points for measures of alpha or beta diversity (Figures C.2 and C.3).

4.5 Discussion

When investigating acidosis or excessive fermentation using in vitro conditions, equine and bovine models commonly include substrate at 1% w/v (Bailey et al., 2003; Biddle et al., 2013; Amanzougarene and Fondevila, 2020; Johnson, 2023). Thus, we set starch inclusion at 1% for the treatments containing starch. We sought to include buffers A and B at concentrations that most closely resembled our previous in vivo work. In Chapter 2, cows were fed 150 g/d of buffers A and B in treatments T1 and T3 and were predicted to have 1.5 to 2.0 kg of starch entering the large intestine due to passage of undigested dietary and infused starch. The 150 g of buffer contained 32.2 g and 38.9 g of Ca and Mg, respectively. When comparing the control treatment to the T1 treatment fed buffer A, the fecal output of Ca and Mg increased by 26.5 g and 29.8 g, respectively, suggesting that approximately 79% of these minerals or 119 g of fed buffer was excreted in the feces. Similar calculations using fecal Mg changes in response to buffer B suggest that 80 g of fed buffer B was excreted in the feces. Thus, the flow of buffer to the large intestine (80-119 g/d) was 4.0-7.9% of the predicted flow of starch to the large intestine (1.5 to 2.0 kg/d). With starch fixed at 1% w/v, we determined that inclusion of buffers A and B at 0.05% w/v most closely matched the intestinal environment provided in our previous in vivo experiment (Chapter 2).

We hypothesized that starch inclusion would decrease culture pH and that buffer inclusion would increase culture pH. As expected, pH decrease was greater for the treatments with starch. Excess starch entering the hindgut can decrease fecal pH (van Gastelen et al., 2021a; Piantoni et al., 2022; Abeyta et al., 2023), and the same is true in in vitro conditions (Biddle et al., 2013). Both buffers increased culture pH in starch-containing treatments but only BB increased pH in treatments without starch. In our previous work, abomasal infusion of starch decreased fecal pH, and including buffers A and B at approximately 5% of the level of starch entering the hindgut increased fecal pH (Chapter 2). Thus, we found similar results in this in vitro experiment as in vivo. Depending on the type of buffer, supplementation into the diet can increase fecal pH in conditions of both low and high dietary starch (Christiansen and Webb, 1989; Neiderfer et al., 2020; Chapter 2). The efficacy of calcium- and magnesium-based buffers depends on multiple factors, particularly particle size (Bach et al., 2018) and digesta pH (Xin et al., 1989; Clark et al., 1989). Buffer B (100% MgO) was more effective at raising culture pH in the absence of starch as compared to buffer A (50% $CaCO_3$, 25% MgO, 25% crushed oyster shell), but both buffers increased pH in the presence of starch.

Interestingly, treatments containing starch generally did not increase total VFA. Increases of rapidly fermentable carbohydrates into the intestines can increase fecal VFA concentrations (Robbers et al., 2019), but this was not observed in the current in vitro study or in our in vivo study (Chapter 2). Treatments without starch saw linear increases of total VFA concentrations over time, while treatment with starch displayed a plateau in VFA concentrations after 6 h, with VFA particularly depressed at the later time points for the STAR treatment. Decreases in pH in the closed in vitro system may have reduced the ability of starch-containing treatments to continue substrate fermentation to VFA, especially for the non-buffered STAR treatment. Treatments containing buffers increased total VFA both with and without starch, perhaps due to alleviation of the negative feedback of decreased pH. Similar findings were observed in Chapter 2, with buffers increasing total VFA in the presence of hindgut starch.

Both starch and buffers also altered the proportions of VFA. Starch inclusion decreased propionate concentrations but increased butyrate. Excess starch entering the hindgut has been shown to increase butyrate (van Gastelen et al., 2021a,b; Cronin et al., 2023) and decrease propionate (van Gastelen et al., 2021a), in agreement with our findings. Both buffers increased acetate concentration both with and without the inclusion of starch, and buffers increased butyrate concentration only in the presence of starch. In our previous work, $CaCO_3$- and MgO-based buffers increased fecal acetate and subsequently total VFA but did not affect butyrate concentrations (Neiderfer et al., 2020; Chapter 2). The difference in the in vitro and in vivo responses to butyrate may relate to the greater rates of butyrate absorption from the intestinal epithelium than the shorter chain VFA (Vogt and Wolever, 2003; Bedford and Gong, 2018). Butyrate has been shown to enhance intestinal barrier function and immune function (Liu et al., 2018), and higher levels of butyrate due to buffering in the presence of starch may provide health benefits. There were no effects of buffers on propionate concentration in the absence of starch, but SBB increased propionate concentration compared to STAR (P = 0.02). In our corresponding in vivo trial, we found no changes to fecal propionate concentrations in response to feeding buffers A and B (Chapter 2), but Neiderfer et al. (2020) observed an increase in fecal propionate in cows fed $CaCO_3$- and MgO-based buffers.

Lactate concentrations increased with starch inclusion, regardless of buffer supplementation, by an average of 13.5 mM ($P < 0.01$). High starch entering the hindgut may increase colonic or fecal lactate (Wang et al., 2017; Robbers et al., 2019) or cause no change (Westricher-Kristen et al., 2018; Cronin et al., 2023). However, in vitro concentrations of lactate in fecal cultures increases when exposed to starch substrate (Biddle et al., 2013; Klostermann et al., 2023; Johnson, 2023). In non-starch treatments, lactate was produced and then decreased, suggesting utilization of lactate to VFA, while starch treatments continued to increase lactate concentrations. In starch-containing treatments, any lactate utilizing microbes present did not seem to be able to significantly mitigate the increase in lactate through conversion to VFA. Overall, lactate concentration responses to starch seem to be variable in in vivo studies but more consistent in in vitro experiments. This is likely due to the closed nature of the system allowing for additional accumulation as compared to the in vivo environment.

Gas (composition contains CO_2 but also H_2, CH_4, and H_2S) is produced through the fermentation of available nutrients to VFA, primarily carbohydrates to acetate and butyrate (Getachew et al., 1998). Protein fermentation also produces gas, but in lower quantities as compared to carbohydrate sources (Wolin, 1960). Starch-containing treatments produced the most gas, with production being greatest between the 3 and 12 h time points. That time period also corresponds to the greatest increases in acetate, butyrate, and lactate concentrations in starch-containing treatments, as well as decreases in pH. In the starch-containing treatments, gas production was increased when buffers were included, likely due to the greater rates of acetate and butyrate production. Gas production and VFA concentrations were higher in SBA and SBB as compared to STAR, likely due to higher culture pH allowing for continued fermentation.

Concentrations of LPS increased in starch-containing treatments regardless of buffer inclusion ($P < 0.01$). The back transformed means of our data show that LPS was approximately 74% greater for treatments containing starch (average 39,811 EU/mL) compared to treatments without starch (average 22,909 EU/mL). As a strong acid with a pKa of 3.86 (as compared to acetate, propionate, and butyrate with pKas of 4.76, 4.82, and 4.87, respectively), lactate can quickly decrease the environmental pH (Dijkstra et al., 2012), further producing an environment that favors amylolytic bacteria as compared to cellulolytic bacteria (Mackie et al., 1978; Tajima et al., 2000). Simple carbohydrates like starch may be fermented into lactate in the gut (Mackie et al., 1978; Biddle et al., 2013; Klostermann et al., 2024), and can stimulate the growth and lysis of LPS-producing bacteria (Khafipour et al. 2009; Li et al., 2012). In fact, LPS presence may stimulate the growth of lactate-producing bacteria (Dai et al., 2020), further enhancing the positive correlation between the two metabolites. However, in both the present study and our in vivo experiment (Chapter 2), buffer inclusion did not decrease lactate or LPS concentrations following a starch challenge. In those models, prevention of LPS accretion by altering dietary buffering capacity did not occur.

The initial culture contained glucose provided by the culture media (final starting concentration: 2,667 μg/mL), providing rapidly fermentable carbohydrate at the start of incubation to each treatment type. At 0 h, the total carbohydrate concentration measured in the treatments without starch (mean of 2,767 μg/mL) was similar to this expected concentration (Figure 4.10). For STAR, SBA, and SBB, 6,667 μg/mL of carbohydrate from starch were present in addition to the 2,667 μg/mL from glucose. The total carbohydrate concentration measured at 0 h for the starch containing treatments (mean of 3,579 μg/mL). Assuming 2,667 μg/mL of total carbohydrates was provided by glucose, this suggests that approximately 812 μg/mL or 12% of the starch was solubilized in the supernatant. For the treatments without starch, total carbohydrate levels in the supernatant were heavily depleted by the 12 h time point and did not decrease concentrations further at 24 h. When cultured in a media with multiple substrate types, microbes will often utilize simpler nutrients before fermenting more complex sources of energy. Beginning at 12 h, FECC, BA, and BB displayed increased NH_3-N concentrations and decreased total protein as compared to starch-containing treatments (P < 0.01). By 18 h, BB increased isovalerate concentrations as compared to all other treatments except BA, and at 24 h, both BA and BB displayed increased isovalerate concentrations compared to all other treatments. Increases in NH_3-N and branched chain VFA concentrations are reflective of protein and amino acid degradation by microbes (Raab et al., 1983; Zarling and Ruchim, 1987; Firkins et al., 2007). Together, these results suggested that the cultures without starch shifted from glucose fermentation in the early time points to protein fermentation in the later time points. For the starch containing treatments, total carbohydrate concentration in the supernatant also decreased dramatically from 0 to 12 h but were approximately 343% and 1,009% greater than the non-starch containing treatments at 12 and 24 h, respectively. This suggests that supplemented starch continued to be solubilized to support fermentation. The lack of change in isovalerate and protein concentrations over time for the starch containing treatments suggests minimal protein fermentation. In fact, the decreased NH_3-N over time suggests possible accretion of microbial protein. These results support in vivo responses to increased intestinal starch fermentation of reduced fecal isovalerate concentrations (Cronin et al., 2023) and increased fecal microbial protein (Westreicher-Kristen et al., 2018).

Increased starch inclusion into the diet can lower the gut pH and decrease alpha diversity in the rumen and the feces (Plaizier et al., 2017a,b; Neubauer et al., 2020). Though only numeric differences, treatments with starch supplementation displayed the lowest observed species and Shannon index values at 24 h (average 396 and 2.84, respectively) as compared to treatments without starch (average 677 and 3.63, respectively; Figure 4.12). Buffer supplementation has been shown to increase alpha diversity in the rumen (Mao et al., 2017), though others have failed to find effects on alpha diversity metrics in the rumen or feces (Ramos et al., 2022; Arce-

Cordero et al., 2022; Chapter 3). In this study, BA exhibited increased alpha diversity compared to STAR (observed species) and BB exhibited increased alpha diversity as compared to FECC (observed species and Shannon index). Buffer inclusion seemed to sustain alpha diversity in BA and BB as compared to other treatments, particularly at the 24 h time point.

Unweighted UniFrac differences based on treatment (P = 0.02) again generally grouped treatments into those with and without starch, suggesting differences in the presence or absence of microbes. Acidosis through high starch inclusion can change beta diversity and affect microbial taxa abundances in the rumen (Plaizier et al., 2017a; Chen et al., 2021; Mu et al., 2022) and in the feces (Plaizier et al., 2017a; Neubauer et al., 2020). At 24 h, the unweighted UniFrac of FECC differed from STAR, in agreement with the literature (P = 0.04; Table 4.2). In fact, FECC, BA, and BB all differed at 24 h from starch containing treatments (P = 0.04 for all comparisons). Buffer inclusion can modify beta diversity and taxa abundances in rumen cultures (Mao et al., 2017; Ramos et al., 2022). At 24 h, FECC and BB were different based on unweighted UniFrac (P = 0.04), but FECC and BA did not differ. Interestingly, STAR did not differ from SBA and SBB at any time for any metric, suggesting that buffer inclusion was not enough to change beta diversity. Coupled with changes to metabolites and alpha diversity, BA and BB seemed to restore some of the functionality to the community as compared to starch-containing treatments and increase the microbiome’s capacity to utilize energy sources present in the culture media.

Differential abundance testing and Spearman correlations revealed differences between treatment types at different taxonomic levels. At the phylum level, starch-containing treatments tended to decrease Bacteroidetes as compared to treatments without starch (Table 4.3, Figure 4.14), with Bacteroidetes negatively corelated to STAR (ρ = -0.52; Table 4.4). The Bacteroidetes phylum is particularly adept at degrading complex carbohydrates like cellulose and hemicellulose (El Kaoutari et al., 2013), suggesting that starch-containing treatments transitioned away from degrading complex plant carbohydrates and towards other energy sources. Muribaculaceae, which belongs to the Bacteroidetes phylum, was additionally detected by ANCOM and Spearman correlations to be decreased in starch-containing treatments compared to treatments without starch and positively correlated to BB (ρ = 0.53). Muribaculaceae degrade complex carbohydrates (Wang et al., 2020) and their abundance in the feces is positively correlated with fecal propionate concentrations in mice (Smith et al., 2019), and the increase in Muribaculaceae may have been associated with the increase in propionate in treatments without starch.

Lactate production was likely also linked to changes in the microbiome due to treatment. Lactic acid producing bacteria are microbes that can rapidly produce lactate from carbohydrates and include the genera *Lactobacillus*, *Lactococcus*, *Streptococcus*, and *Leuconostoc* (Mokoena, 2017; Wang et al., 2021). The Streptococcaceae family, which contains the *Lactococcus* and *Streptococcus* genera, was not detected by ANCOM as displaying changes in abundance based on treatment type but did display a relative abundance average of 77.6% of starch-containing treatments and 60.9% in treatments without starch (Figure 4.14). These numeric differences between treatment types likely contributed to overall lactate concentration differences. The relative abundance of the *Lactobacillus* genus was detected to be changed based on treatment, with SBA and SBB treatments tending to exhibit higher abundance of *Lactobacillus* compared to FECC, BA, and BB. Although only a trend, STAR numerically increased *Lactobacillus* levels compared to all other treatments (2.103% vs. a range of 0 to 1.629%; Table 4.3). *Lactobacillus* is commonly associated with acidosis in the rumen (Sato et al., 2016) due to its rapid lactate-producing abilities (Hernandez et al., 2008), and may have contributed to treatment lactate concentration differences.

The BB treatment accounted for more than half of the total Spearman correlations as compared to other treatments (28 out of the 47 total) and contributed to those taxa that also correlated with another treatment group. Specifically, BB and STAR both correlated to *Rikenellaceae RC9 gut group* (ρ = 0.53 and -0.58, respectively), BB and SBA both correlated to *Bacteroides* (ρ = 0.57 and -0.55, respectively), and BB and SBB both correlated to *Ruminobacter* (ρ = -0.52 and 0.57, respectively). Although not identified by ANCOM as differentially abundant between treatment groups, *Rikenellaceae RC9 gut group* displayed higher relative abundance in treatments without starch (average 0.293%) compared to those with starch (average 0.082%; data not shown). While minor players, *Rikenellaceae RC9 gut group* may degrade structural carbohydrates (Zened et al., 2013), play a vital role in lipid metabolism (Zhou et al., 2018), and are associated with acetate and butyrate concentrations (Wang et al., 2020). Zened et al. (2013) observed decreased *Rikenellaceae RC9 gut group* relative abundances when feeding a diet high in starch, again suggesting that the genus degrades structural carbohydrates. The negative correlation between *Rikenellaceae RC9 gut group* and STAR likely relates to the higher concentration of starch as compared to those treatments without added starch. *Bacteroides* demonstrated increased relative abundance in buffer treatments (average 1.19%) as compared to treatments containing starch (average 0.003%; P = 0.05; data not shown). *Bacteroides*, as part of the Bacteroidetes phylum, contain various cellulose-, hemicellulose-, and oligosaccharide-degrading enzymes (Wirth et al., 2018). Additionally, Chuang et al. (2020) found that *Bacteroides* was enriched in the rumen of cows fed diets high in protein, while Wu et al. (2011) observed increased *Bacteroides* enrichment in humans with diets containing high levels of fat and protein. This suggests that *Bacteroides* may degrade both complex carbohydrates and protein. By 12 h, BA and BB cultures had exhausted the available simple carbohydrates and seemed to begin degrading available protein and any remaining complex carbohydrates as evidenced by increased NH_3-N and continued increases in acetate. Thus, increased *Bacteroides* in BA and BB due to the presence of available complex carbohydrates and protein is in agreement with the literature. Although not identified by ANCOM, *Ruminobacter* displayed numerically higher relative abundance in SBB (0.242%) as compared to BB (0.009%; data not shown). Members of the *Ruminobacter* genus degrade simple carbohydrates like starch to produce acetate as a major end-product and trace amounts of lactate (Stackebrandt and Hespell, 2006). Taken together, starch-containing treatments increased microbes best suited to fermentation of simple carbohydrates. BB seemed to restore functionality to the microbial community compared to other treatments, particularly those microbes that degrade complex carbohydrates and protein. In our previous study, buffer B inclusion with abomasally infused starch produced positive changes to the lymphocyte kinome profile suggesting moderation in metabolic and immune activity as compared to starch infusion alone (Chapter 3), seemingly in agreement with the findings in the current study.

ANCOM testing additionally identified the phylum *Deltaproteobacteria* and order *Desulfovibrionales* to be differentially abundant between treatments, with *Mailhella* (a genus within these classifications) positively correlating to BB ($\rho = 0.68$). Taxa within *Desulfovibrionales* are known for their ability to reduce sulfate to hydrogen sulfide (Gibson et al., 1988) and for consuming available H_2 (Jangid et al., 2022). Utilization of available H_2 may have aided in increasing culture pH as seen in the BB treatment, but H_2S is highly toxic to animals (Shah et al., 2020). In humans, sulfate-reducing bacteria are associated with gastrointestinal diseases such as irritable bowel syndrome (Gobert et al., 2016), acute ulcerative colitis (Rowan et al., 2010), and colorectal cancer (Yachida et al., 2019). Despite positive correlations to a multitude of taxa with varied functions, the restorative actions of BB may also allow for the growth of opportunistic bacteria.

4.6 Conclusions

We sought to evaluate the changes to fermentation and microbial populations when exposed to hindgut buffers in the presence and absence of acidosis-inducing levels of starch. Starch inclusion decreased culture pH and propionate concentrations, and increased gas production, lactate, LPS, and butyrate concentrations as compared to the control. Additionally, starch inclusion changed microbial beta diversity and tended to increase amylolytic bacteria like *Lactobacillus* while tending to decrease fiber-digesting bacteria like *Bacteroidetes*. When compared back to the control, buffer A and B in the absence of starch increased pH, acetate, and total VFA concentrations. They additionally changed beta diversity, while buffer B increased alpha diversity and positively correlated to several microbial taxa, suggesting an improved maintenance of functionality in the microbiome by 24 h. Buffer inclusion, particularly buffer B, to starch-containing cultures increased pH, gas production, acetate, propionate, and butyrate concentrations, but failed to alleviate the negative effects of starch on the microbiome. In cultures with starch, buffer addition seemed to adjust the microbiome's capacity to utilize the starch as an energy source, but with relatively few changes to the microbial makeup. Additional production of VFA without assuaging the deleterious effects of starch-induced acidosis suggests that buffer inclusion at the evaluated dosage may in fact further challenge cows experiencing hindgut acidosis.

TABLES

Table 4.1: Effects of control and buffer treatments on pH, gas production, NH_3-N, volatile fatty acid and lactate, total protein and carbohydrate, and endotoxin concentrations[2].

	Treatment[1]							*P* values		
	FECC	STAR	SBA	SBB	BA	BB	SEM	Treatment	Time	Treatment × Time
pH	6.21[b]	5.24[d]	5.38[c]	5.47[c]	6.28[ab]	6.34[a]	0.03	< 0.01	< 0.01	< 0.01
Cumulative gas production (mL)	15.7[c]	36.2[b]	45.7[a]	45.7[a]	12.9[c]	13.6[c]	1.27	< 0.01	< 0.01	< 0.01
NH_3-N (mg/dL)	10.7[a]	6.92[b]	5.72[c]	5.32[c]	10.3[a]	10.6[a]	0.15	< 0.01	< 0.01	< 0.01
VFA, mM										
Acetate	9.66[c]	9.52[c]	12.7[ab]	13.7[a]	11.9[b]	12.6[ab]	0.20	< 0.01	< 0.01	< 0.01
Propionate	4.39[a]	2.30[c]	2.98[bc]	3.30[b]	4.70[a]	4.78[a]	0.18	< 0.01	< 0.01	< 0.01
Butyrate	1.20[c]	2.07[b]	3.02[a]	3.26[a]	1.42[c]	1.53[c]	0.08	< 0.01	< 0.01	< 0.01
Isobutyrate	0.07[ab]	0.07[ab]	0.07[ab]	0.07[b]	0.07[ab]	0.08[a]	0.003	< 0.01	< 0.01	0.51
Valerate	0.07	0.07	0.07	0.07	0.07	0.07	0.001	0.77	< 0.01	0.14
Isovalerate	0.05[bc]	0.04[d]	0.05[cd]	0.05[cd]	0.05[ab]	0.06[a]	0.001	< 0.01	< 0.01	< 0.01
Total VFA	15.4[c]	14.1[c]	19.1[ab]	20.5[a]	18.2[b]	19.2[ab]	0.36	< 0.01	< 0.01	< 0.01
Lactate, mM	7.95[b]	21.2[a]	19.3[a]	19.0[a]	5.82[b]	5.29[b]	0.46	< 0.01	< 0.01	< 0.01
Total Carbohydrate (µg/ml)	989[b]	1616[a]	1479[a]	1530[a]	985[b]	953[b]	31.3	< 0.01	< 0.01	< 0.01

Table 4.1 continued

Total Protein (mg/ml)	10.1[b]	12.3[a]	11.7[a]	11.6[a]	9.41[b]	9.38[b]	0.18	< 0.01	< 0.01	< 0.01
LPS (EU/mL supernatant, $\log_{10}$)	4.34[b]	4.59[a]	4.56[a]	4.65[a]	4.37[b]	4.37[b]	0.03	< 0.01	< 0.01	< 0.01

[1]Treatments were fecal inoculant alone (FECC), fecal inoculant and 1% starch (STAR), fecal inoculant and 0.05% buffer prototype 1 (BA), fecal inoculant with 1% starch and 0.05% buffer prototype 1 (SBA), fecal inoculant and 0.05% buffer prototype 2 (BB), or fecal inoculant with 1% starch and 0.05% buffer prototype 2 (SBB).
[2]pH, cumulative gas production, NH_3-N, VFA, and lactate concentrations were measured at 0, 3, 6, 12, 18, and 24 h. Total carbohydrate concentrations were measured at 0, 12, and 24 h. Total protein concentrations were measured at 0 and 24 h, while LPS concentrations were measured at 0, 6, and 24 h.
[a-d]Differing letters ($P \leq 0.05$) using Tukey's Honestly Significant Difference test.

Table 4.2: Comparison of treatments under beta diversity measures through pairwise PERMANOVA.

Treatment[1]		*P*-Value[2]		
Group 1	Group 2	Bray-Curtis	Unweighted UniFrac	Weighted UniFrac
	0 h			
BA	BB	0.86	0.92	0.84
BA	FECC	0.86	0.90	0.84
BA	SBA	0.90	0.98	0.84
BA	SBB	0.85	0.89	0.84
BA	STAR	0.85	0.92	0.84
BB	FECC	0.95	0.92	0.84
BB	SBA	0.85	0.90	0.84
BB	SBB	1.00	1.00	0.86
BB	STAR	0.85	0.94	0.84
FECC	SBA	0.85	0.90	0.84
FECC	SBB	0.93	1.00	0.86
FECC	STAR	0.86	0.90	0.84
SBA	SBB	0.85	0.90	0.84
SBA	STAR	0.86	0.90	0.91
SBB	STAR	0.85	0.89	0.84
	6 h			
BA	BB	0.85	0.98	0.84
BA	FECC	0.82	0.89	0.84
BA	SBA	0.82	0.19	0.84
BA	SBB	0.82	0.39	0.84
BA	STAR	0.82	0.19	0.84
BB	FECC	0.82	0.72	0.77
BB	SBA	0.82	0.19	0.84
BB	SBB	0.82	0.22	0.84
BB	STAR	0.82	0.12	0.84
FECC	SBA	0.82	0.72	0.84

Table 4.2 continued

FECC	SBB	0.78	0.66	0.74
FECC	STAR	0.82	0.75	0.91
SBA	SBB	0.85	0.89	0.87
SBA	STAR	0.82	0.89	0.84
SBB	STAR	0.82	0.89	0.85
	24 h			
BA	BB	0.85	0.89	0.84
BA	FECC	0.78	0.19	0.84
BA	SBA	0.52	0.04	0.51
BA	SBB	0.64	0.04	0.71
BA	STAR	0.18	0.04	0.18
BB	FECC	0.58	0.04	0.80
BB	SBA	0.41	0.04	0.43
BB	SBB	0.58	0.04	0.61
BB	STAR	0.12	0.04	0.12
FECC	SBA	0.52	0.04	0.61
FECC	SBB	0.55	0.04	0.64
FECC	STAR	0.29	0.04	0.28
SBA	SBB	0.88	0.90	0.87
SBA	STAR	0.55	0.89	0.59
SBB	STAR	0.37	0.78	0.39

[1]Treatments were as described in footnote 1 of Table 4.1.
[2]Pairwise PERMANOVA calculated using the ‘pairwise.perm.manova’ function in the ‘RVAideMemoire’ R package.

Table 4.3: Mean relative abundances of the ANCOM identified taxa determined to be differentially abundant between treatment groups at 24 hours.

	Treatment[1] Relative Abundance (%)						ANCOM	
	FECC	STAR	SBA	SBB	BA	BB	W[2]	clr[3]
Bacteroidetes[4]	7.395[x]	0.955[y]	1.400[y]	2.223[y]	6.936[x]	7.488[x]	5	10.54
Deltaproteobacteria[5]	0.032[z]	0[z]	0.005[z]	0.005[z]	0.098[y]	0.212[x]	17	15.06
Desulfovibrionales[6]	0.032[z]	0[z]	0.005[z]	0.005[z]	0.098[y]	0.212[x]	22	14.59
Muribaculaceae[7]	0.982[a]	0.022[b]	0.029[b]	0.066[b]	2.132[a]	2.389[a]	43	29.56
Lactobacillaceae[7]	0.036[z]	2.103[wxyz]	1.629[x]	1.415[y]	0[z]	0[z]	42	15.56
Lactobacillus[8]	0.036[z]	2.103[wxyz]	1.629[x]	1.415[y]	0[z]	0[z]	125	16.49

[1]Treatments were as described in footnote 1 of Table 4.1.
[2]The W-statistic is the strength of the ANCOM test for the tested number of species.
[3]The clr F-statistic is a measure of the effect size difference for a particular species between treatment groups. ANCOM determines significance by plotting the F-statistic on the x-axis by the W-statistic on the y-axis.
[4-8]Phylum, class, order, family, and genus taxonomic levels, respectively.
[a-b]Superscripts within the row indicates $P \leq 0.05$ by pairwise Wilcoxon rank sum tests with post hoc testing using the Benjamini-Hochberg false discovery rate adjustment correction.
[w-z]Superscripts within the row indicates $0.05 \leq P \leq 0.10$ by pairwise Wilcoxon rank sum tests with post hoc testing using the Benjamini-Hochberg false discovery rate adjustment correction.

Table 4.4: Spearman correlations of taxa to treatments at 24 h.

	Treatment					
	FECC	STAR	SBA	SBB	BA	BB
Phylum						
Bacteroidetes		-0.52				
Class						
Bacteroidia[1]		-0.52				
Clostridia[2]						0.52
Deltaproteobacteria[3]						0.68
Order						
Betaproteobacteriales[3]		-0.53				
Bacteroidales[1]		-0.52				
Clostridiales[2]						0.52
Enterobacteriales[3]	0.63					
Desulfovibrionales[3]						0.68
Family						
Bacteroidaceae[1]			-0.55			
Burkholderiaceae[3]		-0.53				
Prevotellaceae[1]		-0.52				
Rikenellaceae[1]		-0.52				
Christensenellaceae[2]						0.52
Rikenellaceae[1]						0.53
Muribaculaceae[1]						0.53
Clostridiales vadinBB60 group[2]					0.53	
Bacteroidaceae[1]						0.57
Ruminococcaceae[2]						0.60
Enterobacteriaceae[3]	0.63					
Genera						
Rikenellaceae RC9 gut group[1]		-0.58				0.53
Bacteroides[1]			-0.55			0.57
Prevotella 1[1]		-0.53				
Parasutterella[3]		-0.53				

Table 4.4 continued

Ruminobacter[3]				0.57		-0.52
Sutterella[3]					0.51	
Ruminococcaceae UCG 009[2]						0.51
Uncultured Lachnospiraceae[2]						0.51
Christensenellaceae R7 group[2]						0.52
Uncultured Muribaculaceae bacterium[1]						0.53
Uncultured Clostridiales vadinBB60 group bacterium[2]					0.53	
Alloprevotella[1]						0.55
Lachnospiraceae AC2044 group[2]						0.56
Ruminococcaceae; g_[2]						0.56
Ruminococcaceae UCG 005[2]						0.57
Marvinbryantia[2]						0.57
Lachnospiraceae UCG 004[2]						0.60
Oribacterium[2]	0.60					
Hydrogenoanaerobacterium[2]						0.61
Escherichia Shigella[3]	0.63					
Lachnoclostridium 1[2]	0.63					
Ruminococcus gauvreauii group[2]						0.64
Lachnoclostridium[2]						0.64
Oscillobacter[2]						0.65
Shuttleworthia[2]	0.67					
Mailhella[3]						0.68
Angelakisella[2]						0.86

Pairwise Spearman rank correlations (ρ) were calculated with R statistical software and significance was determined at ($0.5 \leq \rho \leq -0.5$). The ρ is moderate with (|0.5| to |0.7|), strong with (|0.7| to |0.9|), and substantial with (|0.9| to |1.0|). Red boxes indicate negative correlation and green indicates a positive correlation. Yellow rows indicate taxa significantly correlated with two treatment groups.

[1]Belonging to the Bacteroidetes phylum.

[2]Belonging to the Firmicutes phylum.

[3]Belonging to the Proteobacteria phylum.

FIGURES

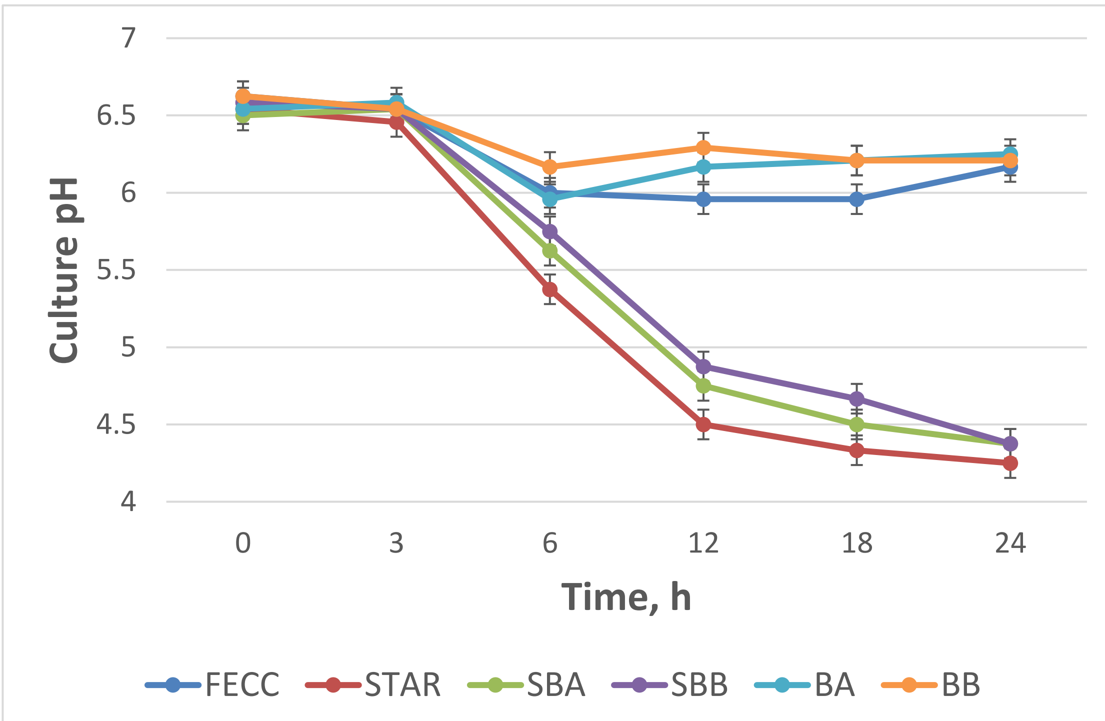

Figure 4.1: Treatment[1] by time plot[2] displaying culture pH. [1]Treatments were as described in footnote 1 of Table 4.1. [2]Error bars are standard error of the mean.

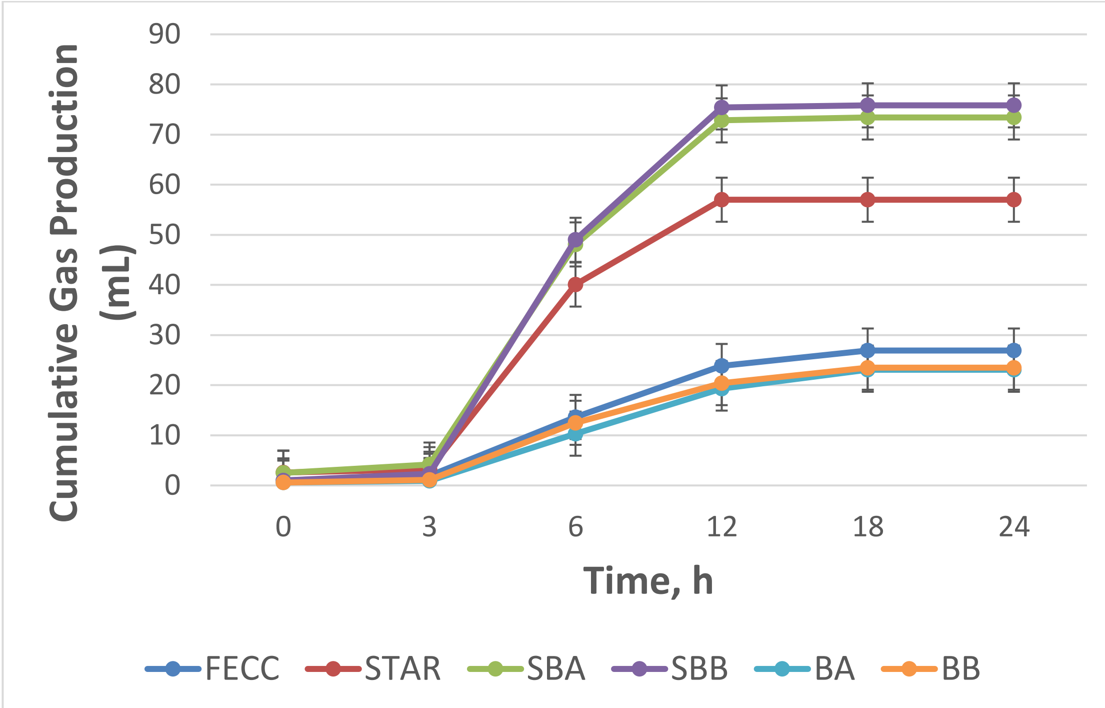

Figure 4.2: Treatment[1] by time plot[2] displaying cumulative gas production.
[1]Treatments were as described in footnote 1 of Table 4.1. [2]Error bars are standard error of the mean.

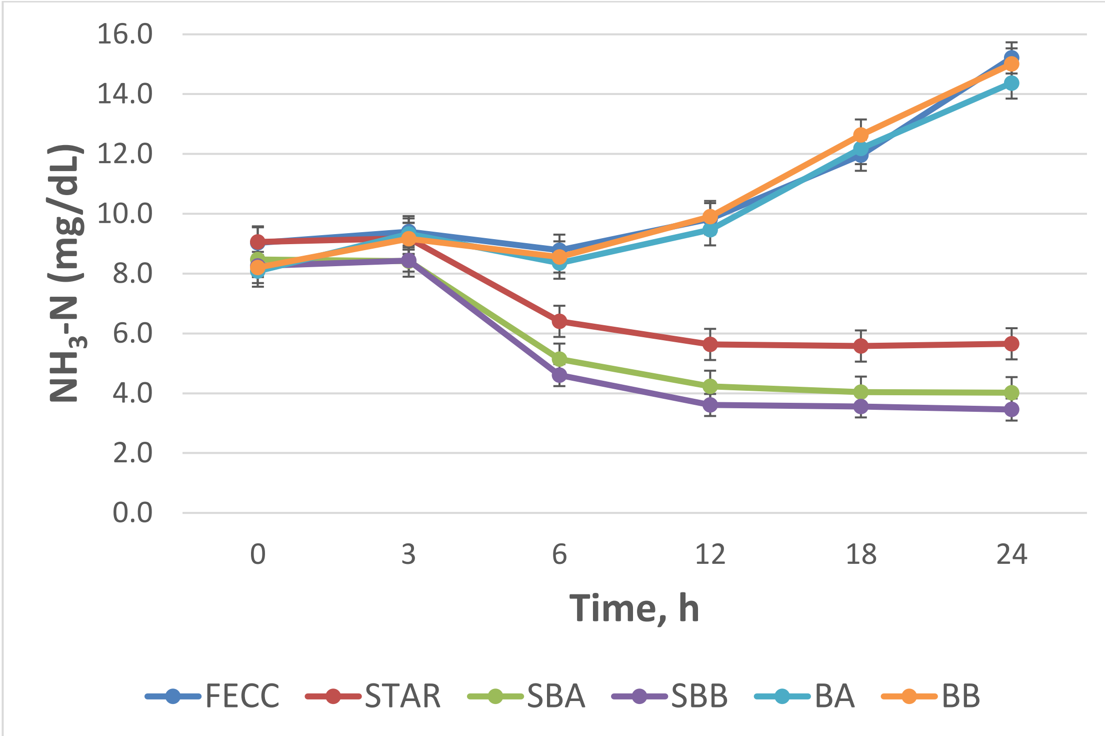

Figure 4.3: Treatment[1] by time plot[2] displaying NH_3-N concentration. [1]Treatments were as described in footnote 1 of Table 4.1. [2]Error bars are standard error of the mean.

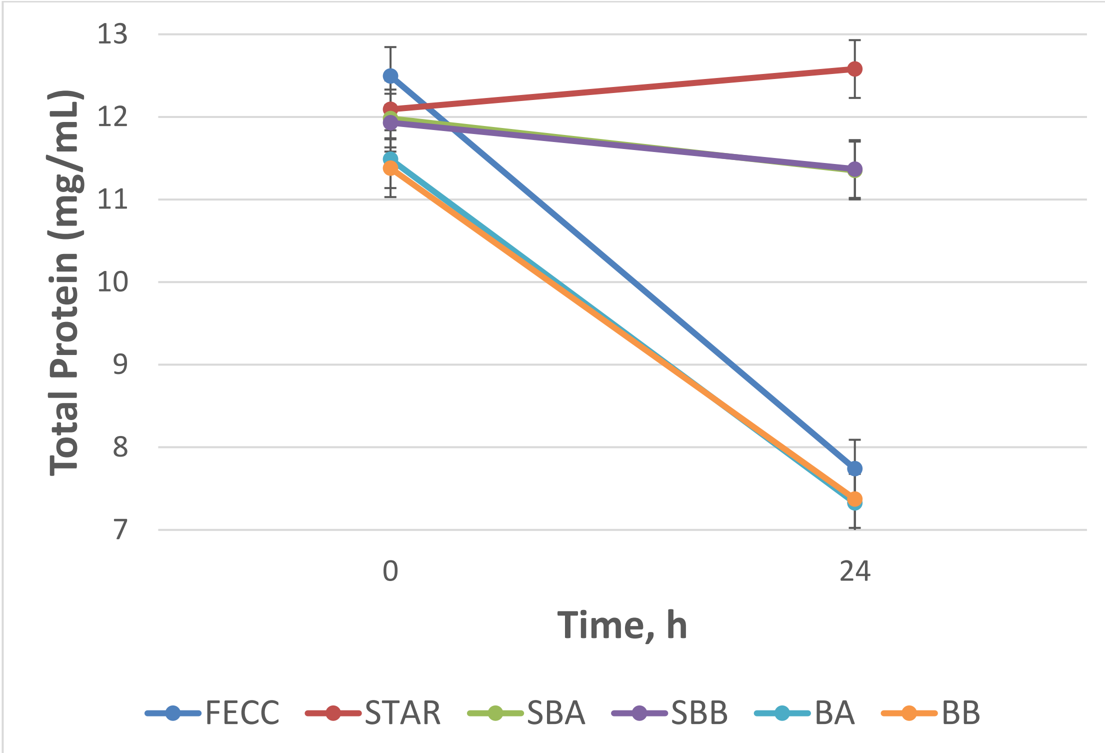

Figure 4.4: Treatment[1] by time plot[2] displaying total protein concentration.
[1]Treatments were as described in footnote 1 of Table 4.1. [2]Error bars are standard error of the mean.

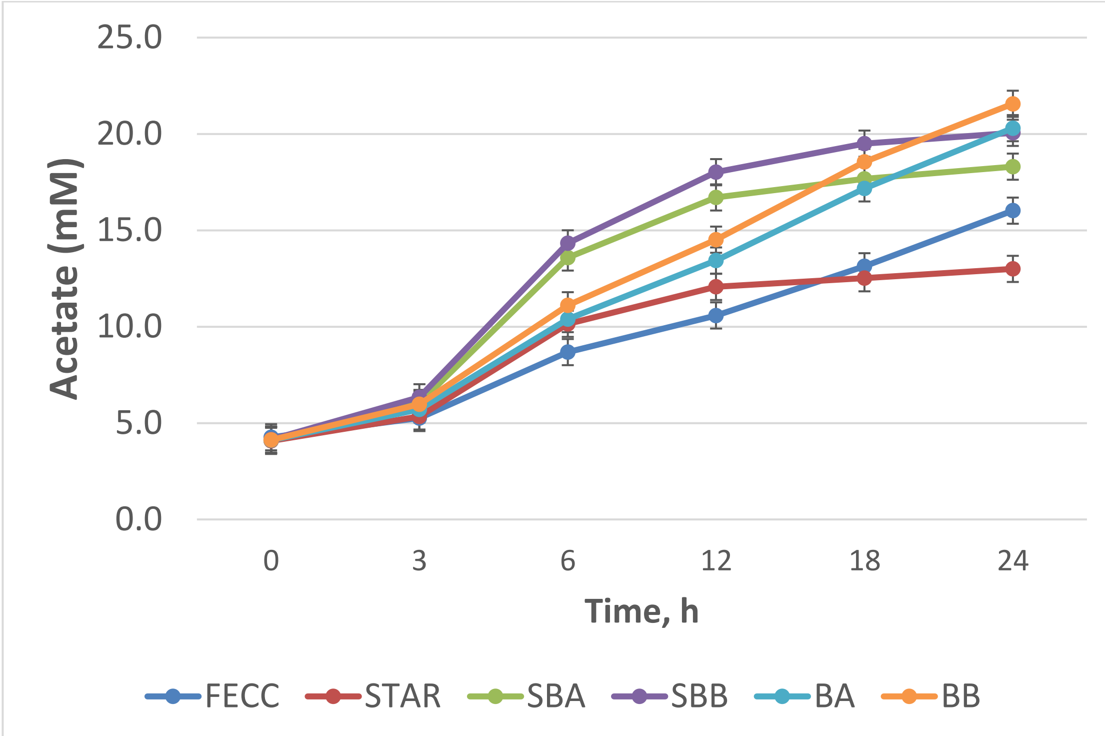

Figure 4.5: Treatment[1] by time plot[2] displaying acetate concentration. [1]Treatments were as described in footnote 1 of Table 4.1. [2]Error bars are standard error of the mean.

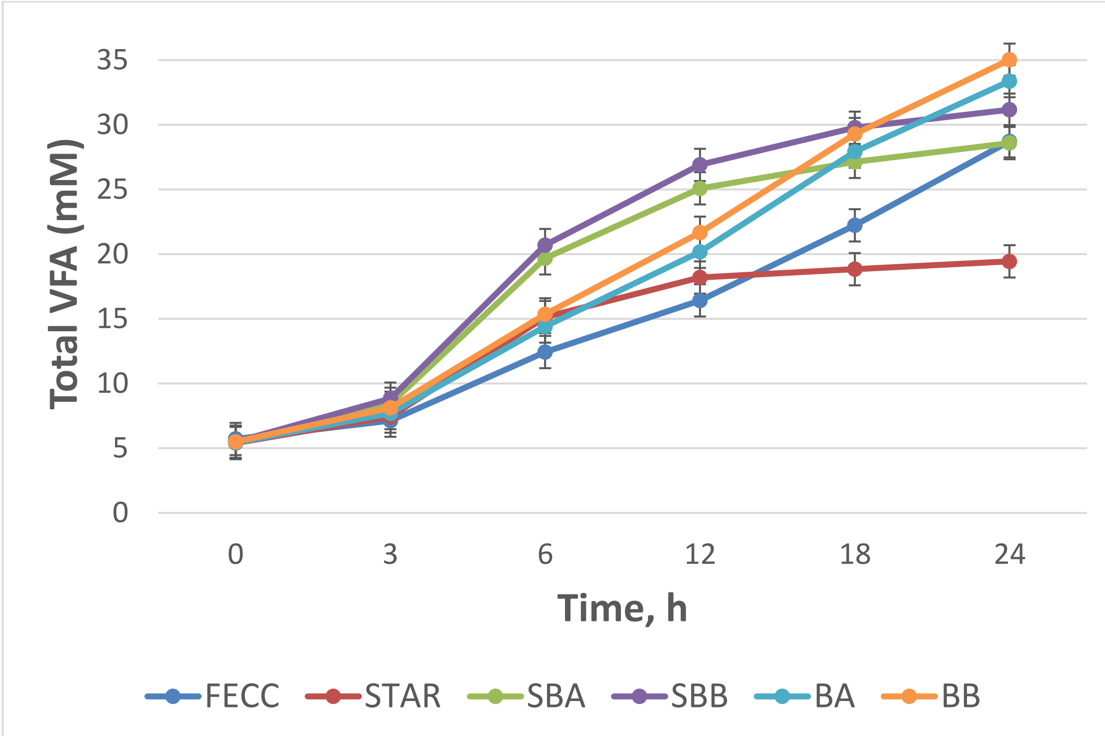

Figure 4.6: Treatment[1] by time plot[2] displaying total VFA concentration. [1]Treatments were as described in footnote 1 of Table 4.1. [2]Error bars are standard error of the mean.

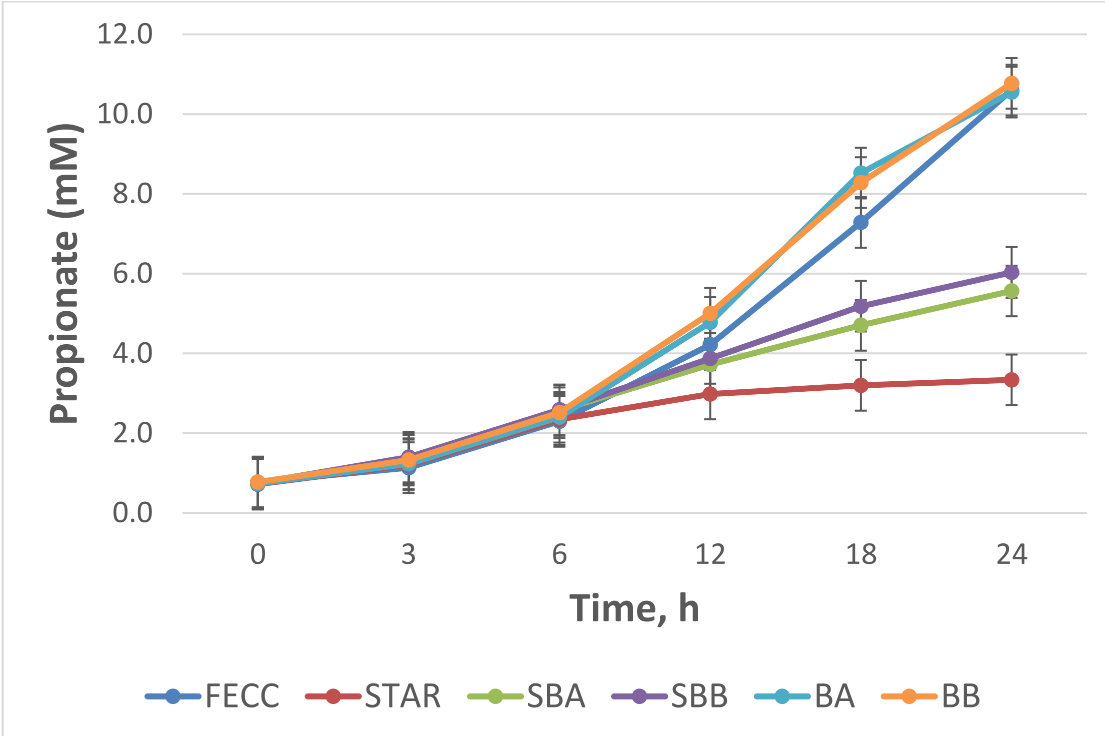

Figure 4.7: Treatment[1] by time plot[2] displaying propionate concentration. [1]Treatments were as described in footnote 1 of Table 4.1. [2]Error bars are standard error of the mean.

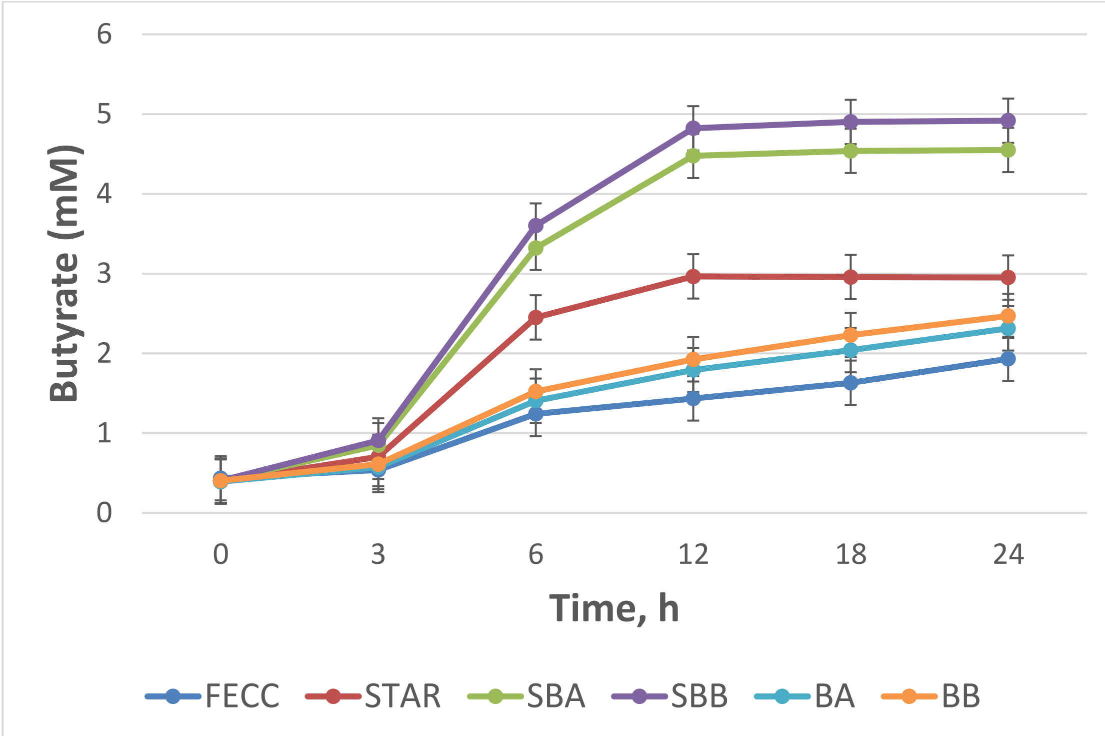

Figure 4.8: Treatment[1] by time plot[2] displaying butyrate concentration. [1]Treatments were as described in footnote 1 of Table 4.1. [2]Error bars are standard error of the mean.

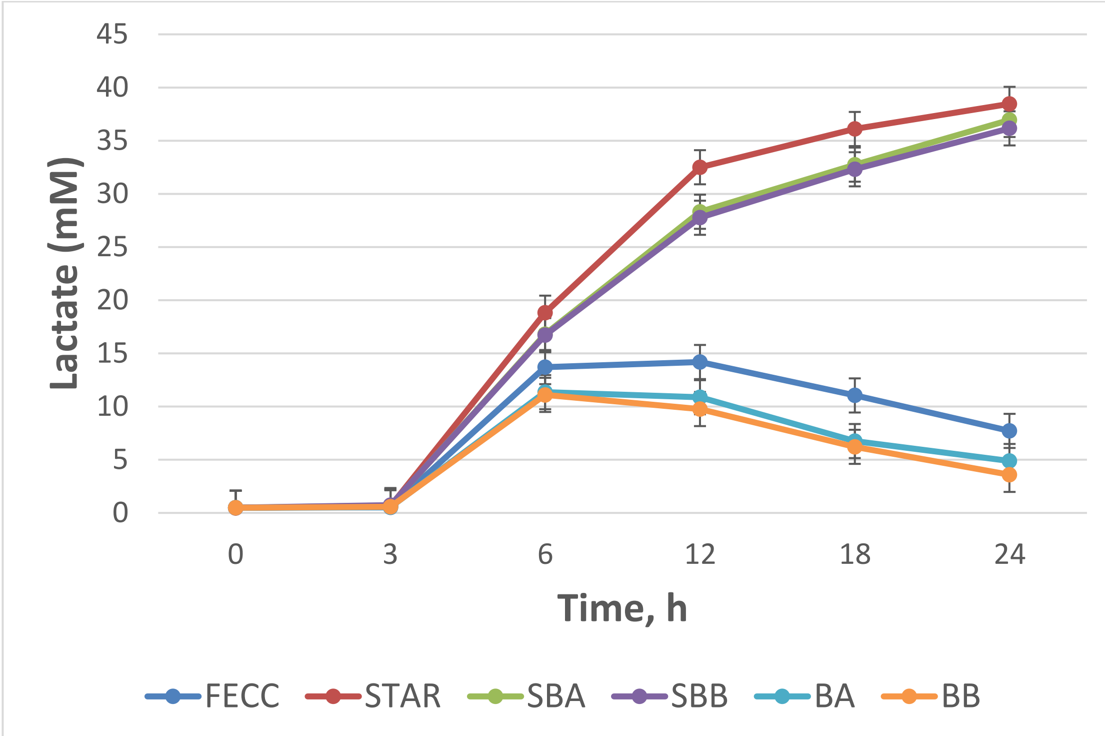

Figure 4.9: Treatment[1] by time plot[2] displaying lactate concentration. [1]Treatments were as described in footnote 1 of Table 4.1. [2]Error bars are standard error of the mean.

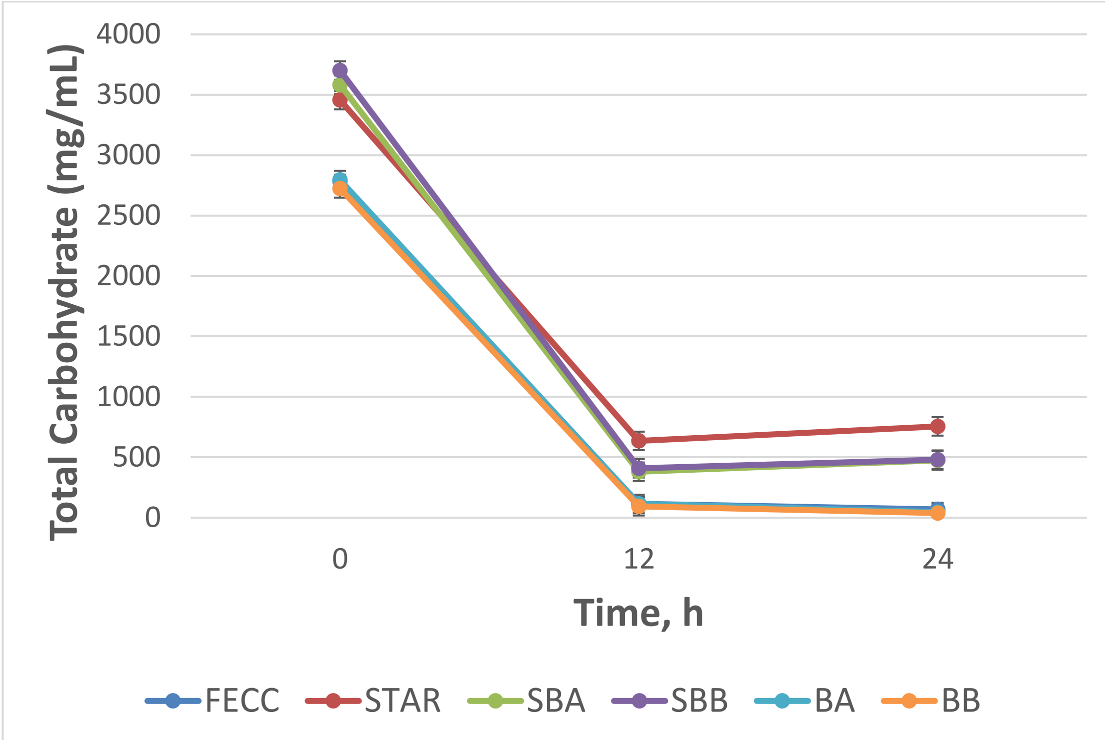

Figure 4.10: Treatment[1] by time plot[2] displaying total carbohydrate concentration. [1]Treatments were as described in footnote 1 of Table 4.1. [2]Error bars are standard error of the mean.

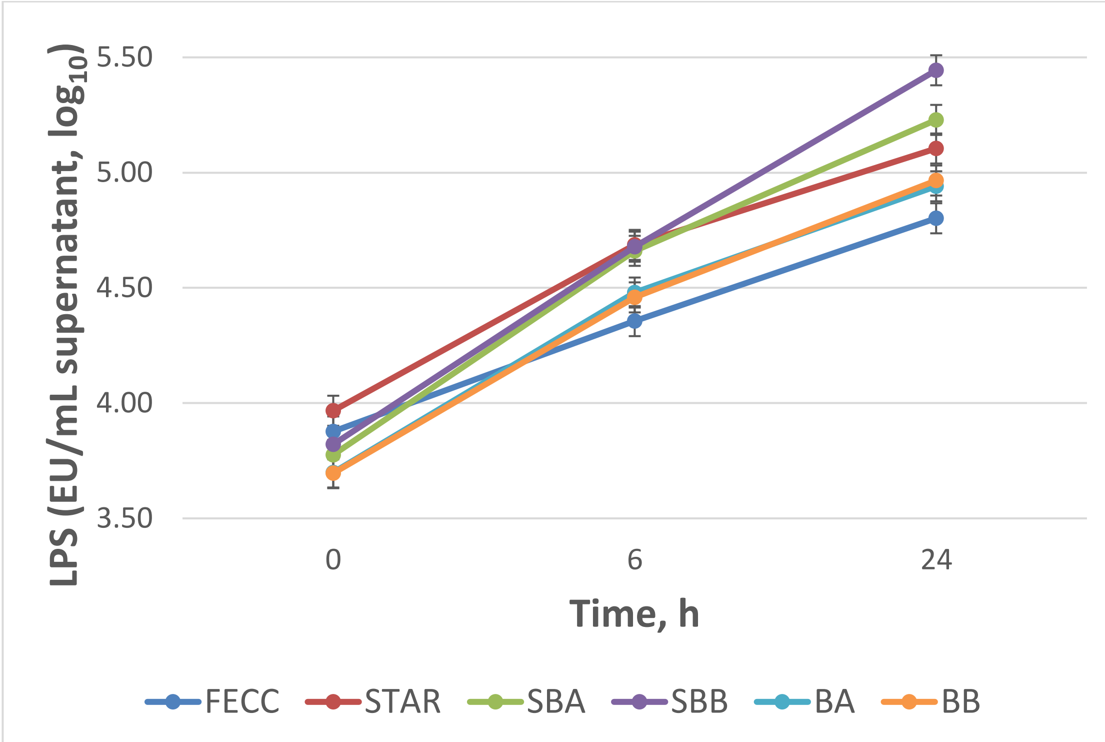

Figure 4.11: Treatment[1] by time plot[2] displaying LPS concentration. [1]Treatments were as described in footnote 1 of Table 4.1. [2]Error bars are standard error of the mean

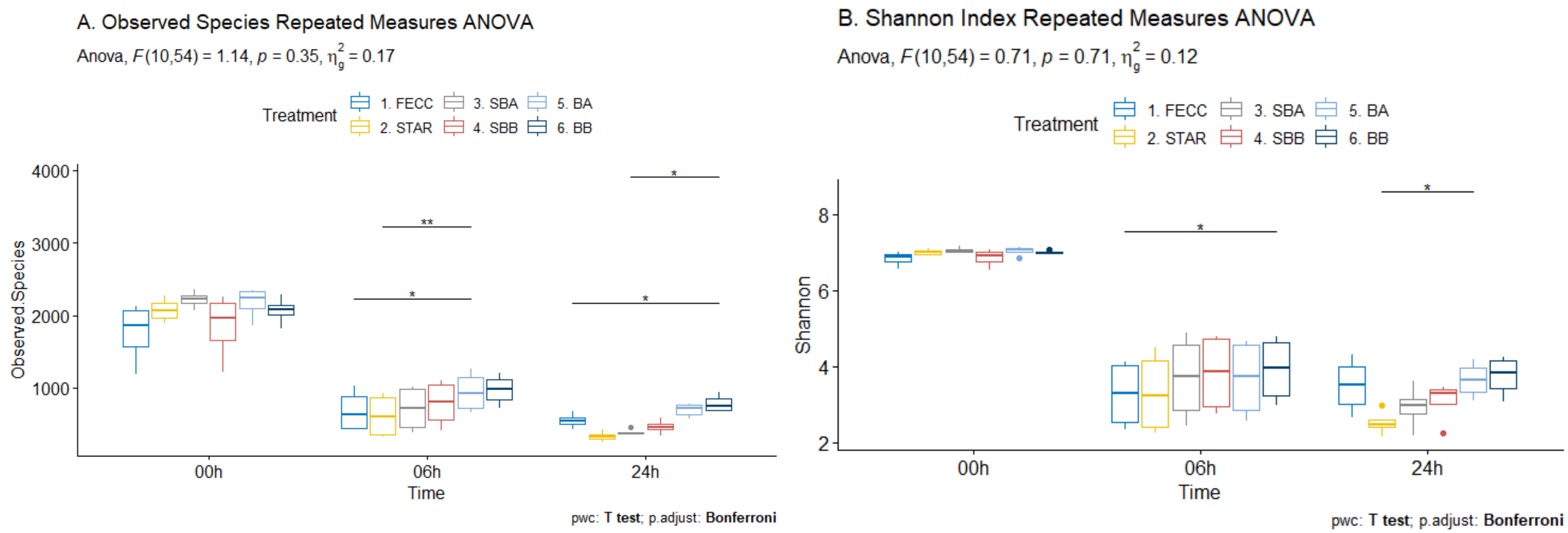

Figure 4.12: Alpha Diversity plots of Observed species and Shannon index comparing treatments[1] within sampling time points. [1]Treatments were as described in footnote 1 of Table 4.1. *$P \le 0.05$ as described in Table 4.3. **$P \le 0.01$ between two treatments.

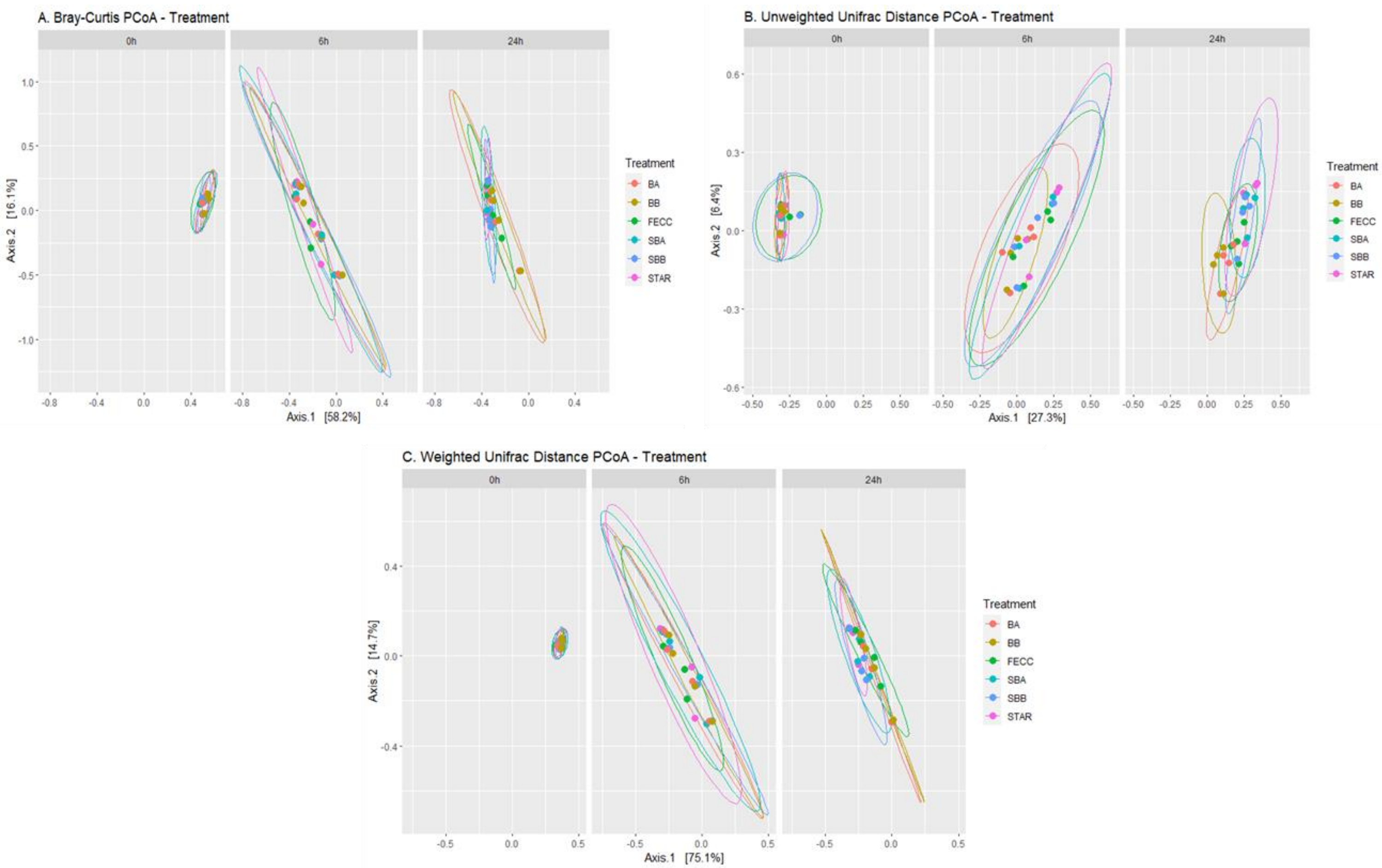

Figure 4.13: Beta diversity principal coordinate analysis (PCoA) plots comparing treatment types using Bray-Curtis Dissimilarity, Weighted UniFrac, and Unweighted UniFrac.

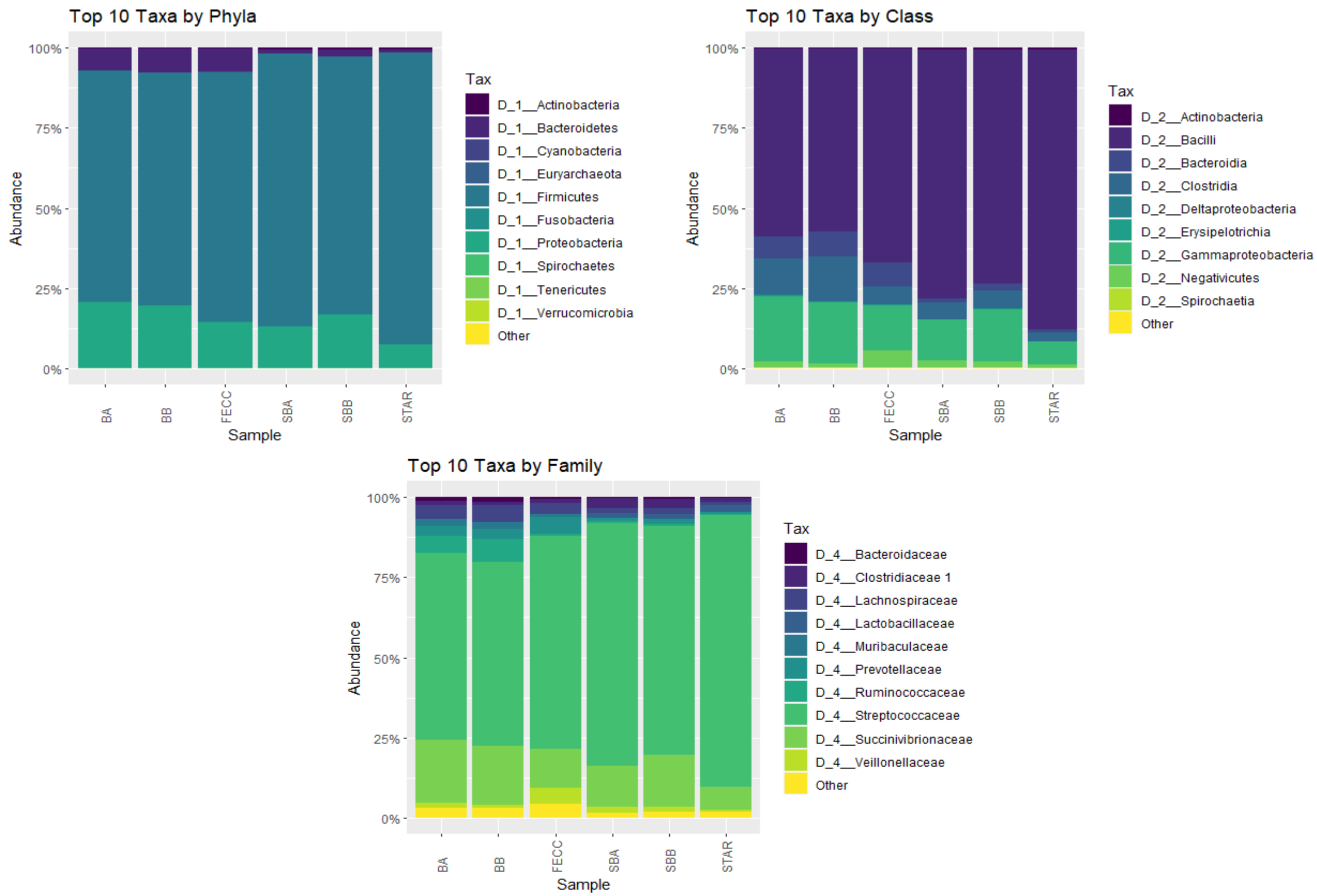

4.14: Relative abundance taxa bar plots of the top 10 or fewer bacteria at the phyla, class, and family levels at 24 hours

REFERENCES

Abeyta, M.A., E.A. Horst, E.J. Mayorga, B.M. Goetz, M. Al-Qaisi, C.S. McCarthy, M.R. O'Neil, B.C. Dooley, P. Piantoni, G.F. Schroeder, and L.H. Baumgard. 2023. Effects of hindgut acidosis on metabolism, inflammation, and production in dairy cows consuming a standard lactation diet. J. Dairy Sci. 106:1429–1440. doi:10.3168/jds.2022-22303.

Ahmed, M.G., A.A. Al-Sagheer, S.Z. El-Zarkouny, and E.A. Elwakeel. 2022. Potential of selected plant extracts to control severe subacute ruminal acidosis in vitro as compared with monensin. BMC Vet. Res. 18:1–11. doi:10.1186/s12917-022-03457-4.

Amanzougarene, Z., and M. Fondevila. 2020. Fitting of the In Vitro Gas Production Technique to the Study of High Concentrate Diets. Anim. an Open Access J. from MDPI 10:1–13. doi:10.3390/ANI10101935.

Arce-Cordero, J.A., T. Liu, A. Ravelo, R.R. Lobo, B.C. Agustinho, H.F. Monteiro, K.C. Jeong, and A.P. Faciola. 2022. Effects of calcium-magnesium carbonate and calcium-magnesium hydroxide as supplemental sources of magnesium on ruminal microbiome. Transl. Anim. Sci. 6:1–10. doi:10.1093/tas/txac092.

Bach, A., I. Guasch, G. Elcoso, J. Duclos, and H. Khelil-Arfa. 2018. Modulation of rumen pH by sodium bicarbonate and a blend of different sources of magnesium oxide in lactating dairy cows submitted to a concentrate challenge. J. Dairy Sci. 101:9777–9788. doi:10.3168/jds.2017-14353.

Bailey, S.R., M.L. Baillon, A.N. Rycroft, P.A. Harris, and J. Elliott. 2003. Identification of equine cecal bacteria producing amines in an in vitro model of carbohydrate overload. Appl. Environ. Microbiol. 69:2087–2093. doi:10.1128/AEM.69.4.2087-2093.2003.

Bedford, A., and J. Gong. 2018. Implications of butyrate and its derivatives for gut health and animal production. Anim. Nutr. 4:151–159. doi:10.1016/j.aninu.2017.08.010.

Biddle, A.S., S.J. Black, and J.L. Blanchard. 2013. An In Vitro Model of the Horse Gut Microbiome Enables Identification of Lactate-Utilizing Bacteria That Differentially Respond to Starch Induction. PLoS One 8:77599. doi:10.1371/journal.pone.0077599.

Bolyen, E., J.R. Rideout, M.R. Dillon, N.A. Bokulich, C.C. Abnet, G.A. Al-Ghalith, H. Alexander, E.J. Alm, M. Arumugam, F. Asnicar, Y. Bai, J.E. Bisanz, K. Bittinger, A. Brejnrod, C.J. Brislawn, C.T. Brown, B.J. Callahan, A.M. Caraballo-Rodríguez, J. Chase, E.K. Cope, R. Da Silva, C. Diener, P.C. Dorrestein, G.M. Douglas, D.M. Durall, C. Duvallet, C.F. Edwardson, M. Ernst, M. Estaki, J. Fouquier, J.M. Gauglitz, S.M. Gibbons, D.L. Gibson, A. Gonzalez, K. Gorlick, J. Guo, B. Hillmann, S. Holmes, H. Holste, C. Huttenhower, G.A. Huttley, S. Janssen, A.K. Jarmusch, L. Jiang, B.D. Kaehler, K. Bin Kang, C.R. Keefe, P. Keim, S.T. Kelley, D. Knights, I. Koester, T. Kosciolek, J. Kreps, M.G.I. Langille, J. Lee, R. Ley, Y.X. Liu, E. Loftfield, C. Lozupone, M. Maher, C. Marotz, B.D. Martin, D. McDonald, L.J. McIver, A. V. Melnik, J.L. Metcalf, S.C. Morgan, J.T. Morton, A.T. Naimey, J.A. Navas-Molina, L.F. Nothias, S.B. Orchanian, T. Pearson, S.L. Peoples, D. Petras, M.L. Preuss, E. Pruesse, L.B. Rasmussen, A. Rivers, M.S. Robeson, P. Rosenthal, N. Segata, M. Shaffer, A. Shiffer, R. Sinha, S.J. Song, J.R. Spear, A.D. Swafford, L.R. Thompson, P.J. Torres, P. Trinh, A. Tripathi, P.J. Turnbaugh, S. Ul-Hasan, J.J.J. van der Hooft, F. Vargas, Y. Vázquez-Baeza, E. Vogtmann, M. von Hippel, W. Walters, Y. Wan, M. Wang, J. Warren, K.C. Weber, C.H.D. Williamson, A.D. Willis, Z.Z. Xu, J.R. Zaneveld, Y. Zhang, Q. Zhu, R. Knight, and J.G. Caporaso. 2019. Reproducible, interactive, scalable and extensible microbiome data science using QIIME 2. Nat. Biotechnol. 37:852–857. doi:10.1038/s41587-019-0209-9.

Bryant, M.P., and L.A. Burkey. 1952. Cultural Methods and Some Characteristics of Some of the More Numerous Groups of Bacteria in the Bovine Rumen. J. Dairy Sci. 36:205–217. doi:10.3168/jds.S0022-0302(53)91482-9.

Callahan, B.J., P.J. McMurdie, M.J. Rosen, A.W. Han, A.J.A. Johnson, and S.P. Holmes. 2016. DADA2: High-resolution sample inference from Illumina amplicon data. Nat. Methods 13:581–583. doi:10.1038/nmeth.3869.

Chen, X., X. Su, J. Li, Y. Yang, P. Wang, F. Yan, J. Yao, and S. Wu. 2021. Real-time monitoring of ruminal microbiota reveals their roles in dairy goats during subacute ruminal acidosis. npj Biofilms Microbiomes 7:1–14. doi:10.1038/s41522-021-00215-6.

Christiansen, M.L., and K.E. Webb. 1990. Intestinal acid flow, dry matter, starch and protein digestibility and amino acid absorption in beef cattle fed a high-concentrate diet with defluorinated rock phosphate, limestone or magnesium oxide.. J. Anim. Sci. 68:2105–2118. doi:10.2527/1990.6872105x.

Chuang, S. Te, S.T. Ho, P.W. Tu, K.Y. Li, Y.L. Kuo, J.S. Shiu, S.Y. Wang, and M.J. Chen. 2020. The rumen specific bacteriome in dry dairy cows and its possible relationship with phenotypes. Animals 10:1–15. doi:10.3390/ani10101791.

Clark, J.H., A.W. Plegge, C.L. Davis, and G.C. McCoy. 1989. Effects of Calcium Carbonate on Ruminal Fermentation, Nutrient Digestibility, and Cow Performance. J. Dairy Sci. 72:493–500. doi:10.3168/jds.S0022-0302(89)79131-1.

Cronin, S.K., A.M. Barnard, S.J. Dietz, M. Lawrence, A.E. Kramer, and T.F. Gressley. 2023. Effect of short-term abomasal corn starch infusions on postruminal fermentation and blood measures. J. Dairy Sci. 106:8658–8669. doi:10.3168/jds.2022-23180.

Dai, X., T.J. Hackmann, R.R. Lobo, and A.P. Faciola. 2020. Lipopolysaccharide stimulates the growth of bacteria that contribute to ruminal acidosis. Appl. Environ. Microbiol. 86:1–17. doi:10.1128/AEM.02193-19.

Darwin, A., A. Barnes, and R. Cord-Ruwisch. 2018. In vitro rumen fermentation of soluble and non-soluble polymeric carbohydrates in relation to ruminal acidosis. Ann. Microbiol. 68:1–8. doi:10.1007/s13213-017-1307-x.

de Carvalho, I.P.C., E. Detmann, H.C. Mantovani, M.F. Paulino, S. de C.V. Filho, V.A.C. Costa, and D.I. Gomes. 2011. Growth and antimicrobial activity of lactic acid bacteria from rumen fluid according to energy or nitrogen source. Rev. Bras. Zootec. 40:1260–1265. doi:10.1590/S1516-35982011000600014.

Dijkstra, J., J.L. Ellis, E. Kebreab, A.B. Strathe, S. López, J. France, and A. Bannink. 2012. Ruminal pH regulation and nutritional consequences of low pH. Anim. Feed Sci. Technol. 172:22–33. doi:10.1016/j.anifeedsci.2011.12.005.

El Kaoutari, A., F. Armougom, J.I. Gordon, D. Raoult, and B. Henrissat. 2013. The abundance and variety of carbohydrate-active enzymes in the human gut microbiota. Nat. Rev. Microbiol. 11:497–504.

Emmanuel, D.G.V., K.L. Madsen, T.A. Churchill, S.M. Dunn, and B.N. Ametaj. 2007. Acidosis and Lipopolysaccharide from Escherichia coli B:055 cause hyperpermeability of rumen and colon tissues. J. Dairy Sci. 90:5552–5557. doi:10.3168/jds.2007-0257.

Erdman, R.A. 1988. Dietary Buffering Requirements of the Lactating Dairy Cow: A Review. J. Dairy Sci. 71:3246–3266. doi:10.3168/jds.S0022-0302(88)79930-0.

Firkins, J.L., Z. Yu, and M. Morrison. 2007. Ruminal nitrogen metabolism: Perspectives for integration of microbiology and nutrition for dairy. J. Dairy Sci. 90:E1–E16. doi:10.3168/jds.2006-518.

Getachew, G., M. Blümmel, H.P.S. Makkar, and K. Becker. 1998. In vitro gas measuring techniques for assessment of nutritional quality of feeds: A review. Anim. Feed Sci. Technol. 72:261–281. doi:10.1016/S0377-8401(97)00189-2.

Gibson, G.R., G.T. Macfarlane, and J.H. Cummings. 1988. Occurrence of sulphate-reducing bacteria in human faeces and the relationship of dissimilatory sulphate reduction to methanogenesis in the large gut. J. Appl. Bacteriol. 65:103–111. doi:10.1111/j.1365-2672.1988.tb01498.x.

Gobert, A.P., G. Sagrestani, E. Delmas, K.T. Wilson, T.G. Verriere, M. Dapoigny, C. Del'Homme, and A. Bernalier-Donadille. 2016. The human intestinal microbiota of constipated-predominant irritable bowel syndrome patients exhibits anti-inflammatory properties. Sci. Rep. 6. doi:10.1038/srep39399.

Goering, H.K., and P.J. Van. 1970. Forage fiber analyses (Apparatus, Reagents, Procedures, and Some Applications). U.S. Dep. Agric. 387–598.

Hall, M.B. 2009. Determination of starch, including maltooligosaccharides, in animal feeds: Comparison of methods and a method recommended for AOAC collaborative study. J. AOAC Int. 92:42–49. doi:10.1093/jaoac/92.1.42.

Hernandez, J.D., P.T. Scott, R.W. Shephard, and R.A.M. Al Jassim. 2008. The characterization of lactic acid producing bacteria from the rumen of dairy cattle grazing on improved pasture supplemented with wheat and barley grain. J. Appl. Microbiol. 104:1754–1763. doi:10.1111/j.1365-2672.2007.03696.x.

Herve, Maxime. 2023. Package "RVAideMemoire."

Jangid, A., S. Fukuda, Y. Suzuki, T.D. Taylor, H. Ohno, and T. Prakash. 2022. Shotgun metagenomic sequencing revealed the prebiotic potential of a grain-based diet in mice. Sci. Rep. 12. doi:10.1038/s41598-022-10762-3.

Johnson, A.C.B. 2023. A COMPARATIVE EVALUATION OF THE MICROBIOME EFFECTS ON EASY AND HARD KEEPER HORSES. UDel Diss.

Kent-Dennis, C., J.R. Aschenbach, P.J. Griebel, and G.B. Penner. 2020. Effects of lipopolysaccharide exposure in primary bovine ruminal epithelial cells. J. Dairy Sci. 103:9587–9603. doi:10.3168/jds.2020-18652.

Khafipour, E., D.O. Krause, and J.C. Plaizier. 2009. A grain-based subacute ruminal acidosis challenge causes translocation of lipopolysaccharide and triggers inflammation. J. Dairy Sci. 92:1060–1070. doi:10.3168/jds.2008-1389.

Klostermann, C.E., M.F. Endika, D. Kouzounis, P.L. Buwalda, P. de Vos, E.G. Zoetendal, J.H. Bitter, and H.A. Schols. 2023. Presence of digestible starch impacts in vitro fermentation of resistant starch. Food Funct. 15:223–235. doi:10.1039/d3fo01763j.

Lahti, L., and S. Shetty. 2017. Tools for Microbiome Analysis in R. Accessed.

Li, S., E. Khafipour, D.O. Krause, A. Kroeker, J.C. Rodriguez-Lecompte, G.N. Gozho, and J.C. Plaizier. 2012. Effects of subacute ruminal acidosis challenges on fermentation and endotoxins in the rumen and hindgut of dairy cows. J. Dairy Sci. 95:294–303. doi:10.3168/jds.2011-4447.

Liu, H., J. Wang, T. He, S. Becker, G. Zhang, D. Li, and X. Ma. 2018. Butyrate: A double-edged sword for health?. Adv. Nutr. 9:21–29. doi:10.1093/advances/nmx009.

Mackie, R.I., F.M.C. Gilchrist, A.M. Robberts, P.E. Hannah, and H.M. Schwartz. 1978. Microbiological and chemical changes in the rumen during the stepwise adaptation of sheep to high concentrate diets. J. Agric. Sci. 90:241–254. doi:10.1017/S0021859600055313.

Mainardi, S.R., B.A. Hengst, S.J. Nebzydoski, L.M. Nemec, and T.F. Gressley. 2011. Effects of abomasal oligofructose on blood and feces of Holstein steers. J. Anim. Sci. 89:2510–2517. doi:10.2527/jas.2010-3348.

Mao, S.Y., R.Y. Zhang, D.S. Wang, and W.Y. Zhu. 2013. Impact of subacute ruminal acidosis (SARA) adaptation on rumen microbiota in dairy cattle using pyrosequencing. Anaerobe 24:12–19. doi:10.1016/J.ANAEROBE.2013.08.003.

Mao, S., W. Huo, J. Liu, R. Zhang, and W. Zhu. 2017. In vitro effects of sodium bicarbonate buffer on rumen fermentation, levels of lipopolysaccharide and biogenic amine, and composition of rumen microbiota. J. Sci. Food Agric. 97:1276–1285. doi:10.1002/jsfa.7861.

McMurdie, P.J., and S. Holmes. 2013. Phyloseq: An R Package for Reproducible Interactive Analysis and Graphics of Microbiome Census Data. PLoS One 8. doi:10.1371/journal.pone.0061217.

Mokoena, M.P. 2017. Lactic acid bacteria and their bacteriocins: Classification, biosynthesis and applications against uropathogens: A mini-review. Molecules 22. doi:10.3390/molecules22081255.

Monteiro, H.F., and A.P. Faciola. 2020. Ruminal acidosis, bacterial changes, and lipopolysaccharides. J. Anim. Sci. 98:1–9. doi:10.1093/jas/skaa248.

Mu, Y., W. Qi, T. Zhang, J. Zhang, and S. Mao. 2022. Multi-omics Analysis Revealed Coordinated Responses of Rumen Microbiome and Epithelium to High-Grain-Induced Subacute Rumen Acidosis in Lactating Dairy Cows. mSystems 7. doi:10.1128/msystems.01490-21.

Muck, R.E., and J.T. Dickerson. 1988. Storage Temperature Effects on Proteolysis in Alfalfa Silage.. Trans. Am. Soc. Agric. Eng. 31:1005–1009. doi:10.13031/2013.30813.

Nagaraja, T.G., and E.C. Titgemeyer. 2007. Ruminal Acidosis in Beef Cattle: The Current Microbiological and Nutritional Outlook,. J. Dairy Sci. 90:E17–E38. doi:10.3168/JDS.2006-478.

Neiderfer, K.P., A.M. Barnard, K.Z. Moyer, A.M. Trench, A.E. Taylor, S.K. Cronin, and T.F. Gressley. 2020. Effects of calcium carbonate, magnesium oxide and encapsulated sodium bicarbonate on measures of post-ruminal fermentation. J. Anim. Physiol. Anim. Nutr. (Berl). 104:802–811. doi:10.1111/jpn.13331.

Neubauer, V., R.M. Petri, E. Humer, I. Kröger, N. Reisinger, W. Baumgartner, M. Wagner, and Q. Zebeli. 2020. Starch-Rich Diet Induced Rumen Acidosis and Hindgut Dysbiosis in Dairy Cows of Different Lactations 10. doi:10.3390/ani10101727.

Oksanen, J., G.L. Simpson, F.G. Blanchet, R. Kindt, P. Legendre, P.R. Minchin, R.B. O'Hara, and P. Solymos. 2022. Package "vegan."

Owens, F.N., D.S. Secrist, W.J. Hill, and D.R. Gill. 1998. Acidosis in Cattle: A Review. J. Anim. Sci. 76:275–286. doi:10.2527/1998.761275x.

Piantoni, P., M.A. Abeyta, G.F. Schroeder, H.A. Tucker, and L.H. Baumgard. 2022. Evaluation of feed restriction and abomasal infusion of resistant starch as models to induce intestinal barrier dysfunction in healthy lactating cows. J. Dairy Sci. 106:1453–1463. doi:10.3168/jds.2022-22376.

Plaizier, J.C., S. Li, A.M. Danscher, H. Derakshani, P.H. Andersen, and E. Khafipour. 2017. Changes in Microbiota in Rumen Digesta and Feces Due to a Grain-Based Subacute Ruminal Acidosis (SARA) Challenge. Microb. Ecol. 74:485–495. doi:10.1007/s00248-017-0940-z.

Plaizier, J.C., S. Li, H.M. Tun, and E. Khafipour. 2017. Nutritional models of experimentally-induced subacute ruminal acidosis (SARA) differ in their impact on rumen and hindgut bacterial communities in dairy cows. Front. Microbiol. 7. doi:10.3389/fmicb.2016.02128.

Plummer, D.T. 1987. Introduction to Practical Biochemistry. Third. McGraw-Hill.

Quast, C., E. Pruesse, P. Yilmaz, J. Gerken, T. Schweer, P. Yarza, J. Peplies, and F.O. Glöckner. 2013. The SILVA ribosomal RNA gene database project: improved data processing and web-based tools. Nucleic Acids Res. 41:D590–D596. doi:10.1093/NAR/GKS1219.

Raab, L., B. Cafantaris, T. Jilg, and K.H. Menke. 1983. Rumen protein degradation and biosynthesis. Br. J. Nutr. 50:569–582. doi:10.1079/bjn19830128.

Ramos, S.C., C.D. Jeong, L.L. Mamuad, S.H. Kim, A.R. Son, M.A. Miguel, M. Islam, Y. Il Cho, and S.S. Lee. 2021. Enhanced RUMINAL fermentation parameters and altered rumen bacterial community composition by formulated rumen buffer agents fed to dairy cows with a high-concentrate diet. Agric. 11:6–8. doi:10.3390/agriculture11060554.

Ramos, S.C., S.H. Kim, C.D. Jeong, L.L. Mamuad, A.R. Son, S.H. Kang, Y. Il Cho, T.G. Kim, J.S. Lee, K.K. Cho, S.S. Lee, and S.S. Lee. 2022. Increasing buffering capacity enhances rumen fermentation characteristics and alters rumen microbiota composition of high-concentrate fed Hanwoo steers. Sci. Rep. 12:1–12. doi:10.1038/s41598-022-24777-3.

Robbers, K., E. Westreicher-Kristen, A. Troescher, and A. Susenbeth. 2019. Effects of abomasally infused amylase and increasing amounts of corn starch on fecal excretion of starch, total and microbial nitrogen, and volatile fatty acids in heifers. J. Anim. Sci. 97:3984–3993. doi:10.1093/jas/skz243.

Rogers, J.A., L.D. Muller, C.L. Davis, W. Chalupa, D.S. Kronfeld, L.F. Karcher, and K.R. Cummings. 1985. Response of Dairy Cows to Sodium Bicarbonate and Limestone in Early Lactation. J. Dairy Sci. 68:646–660. doi:10.3168/jds.S0022-0302(85)80871-7.

Rowan, F., N.G. Docherty, M. Murphy, B. Murphy, J.C. Coffey, and P.R. O'Connell. 2010. Desulfovibrio Bacterial Species Are Increased in Ulcerative Colitis. Dis. Colon Rectum 53:1530–1536. doi:10.1007/DCR.0B013E3181F1E620.

Sato, S. 2016. Pathophysiological evaluation of subacute ruminal acidosis (SARA) by continuous ruminal pH monitoring. Anim. Sci. J. 87:168–177. doi:10.1111/asj.12415.

Schaefer, D.M., L.J. Wheeler, C.H. Noller, R.B. Keyser, and J.L. White. 1982. Neutralization of Acid in the Rumen by Magnesium Oxide and Magnesium Carbonate. J. Dairy Sci. 65:732–739. doi:10.3168/jds.S0022-0302(82)82260-1.

Shah, A.M., J. Ma, Z. Wang, R. Hu, X. Wang, Q. Peng, F.K. Amevor, and N. Goswami. 2020. Production of hydrogen sulfide by fermentation in rumen and its impact on health and production of animals. Processes 8. doi:10.3390/PR8091169.

Sievert, S.J., and R.D. Shaver. 1993. Carbohydrate and Aspergillus oryzae Effects on Intake, Digestion, and Milk Production by Dairy Cows. J. Dairy Sci. 76:245–254. doi:10.3168/jds.S0022-0302(93)77343-9.

Smith, B.J., R.A. Miller, A.C. Ericsson, D.C. Harrison, R. Strong, and T.M. Schmidt. 2019. Changes in the gut microbiome and fermentation products concurrent with enhanced longevity in acarbose-treated mice. BMC Microbiol. 19. doi:10.1186/s12866-019-1494-7.

Stackebrandt, E., and R.B. Hespell. 2006. The Family Succinivibrionaceae. Springer New York.

Steele, M.A., J. Croom, M. Kahler, O. Alzahal, S.E. Hook, K. Plaizier, and B.W. Mcbride. 2011. Bovine rumen epithelium undergoes rapid structural adaptations during grain-induced subacute ruminal acidosis. Am. J. Physiol. - Regul. Integr. Comp. Physiol. 300:1515–1523. doi:10.1152/ajpregu.00120.2010.

Tajima, K., S. Arai, K. Ogata, T. Nagamine, H. Matsui, M. Nakamura, R.I. Aminov, and Y. Benno. 2000. Rumen Bacterial Community Transition During Adaptation to High-grain Diet. Anaerobe 6:273–284. doi:10.1006/ANAE.2000.0353.

van Gastelen, S., J. Dijkstra, S.J.J. Alferink, G. Binnendijk, K. Nichols, T. Zandstra, and A. Bannink. 2021. Abomasal infusion of corn starch and β-hydroxybutyrate in early-lactation Holstein-Friesian dairy cows to induce hindgut and metabolic acidosis. J. Dairy Sci. 104:12520–12539. doi:10.3168/jds.2021-20323.

van Gastelen, S., J. Dijkstra, K. Nichols, and A. Bannink. 2021. Abomasal infusion of ground corn and ammonium chloride in early-lactating Holstein-Friesian dairy cows to induce hindgut and metabolic acidosis. J. Dairy Sci. 104:4174–4191. doi:10.3168/jds.2020-19300.

Van Kessel, J.S., P.C. Nedoluha, A. Williams-Campbell, R.L. Baldwin VI, and K.R. McLeod. 2002. Effects of ruminal and postruminal infusion of starch hydrolysate or glucose on the microbial ecology of the gastrointestinal tract in growing steers. J. Anim. Sci. 80:3027–3034. doi:10.2527/2002.80113027x.

Van Soest, P.J., J.B. Robertson, and B.A. Lewis. 1991. Methods for Dietary Fiber, Neutral Detergent Fiber, and Nonstarch Polysaccharides in Relation to Animal Nutrition. J. Dairy Sci. 74:3583–3597. doi:10.3168/jds.S0022-0302(91)78551-2.

Vogt, J.A., and T.M.S. Wolever. 2003. Fecal acetate is inversely related to acetate absorption from the human rectum and distal colon. J. Nutr. 133:3145–3148. doi:10.1093/jn/133.10.3145.

Wang, B., Q. Kong, X. Li, J. Zhao, H. Zhang, W. Chen, and G. Wang. 2020. A high-fat diet increases gut microbiota biodiversity and energy expenditure due to nutrient difference. Nutrients 12:1–20. doi:10.3390/nu12103197.

Wang, Y., J. Wu, M. Lv, Z. Shao, M. Hungwe, J. Wang, X. Bai, J. Xie, Y. Wang, and W. Geng. 2021. Metabolism Characteristics of Lactic Acid Bacteria and the Expanding Applications in Food Industry. Front. Bioeng. Biotechnol. 9:1–19. doi:10.3389/fbioe.2021.612285.

Wang, Y., L. Xu, J. Liu, W. Zhu, and S. Mao. 2017. A high grain diet dynamically shifted the composition of mucosa-associated microbiota and induced mucosal injuries in the colon of sheep. Front. Microbiol. 8:1–13. doi:10.3389/fmicb.2017.02080.

Westreicher-Kristen, E., K. Robbers, R. Blank, A. Tröscher, U. Dickhoefer, S. Wolffram, and A. Susenbeth. 2018. Postruminal digestion of starch infused into the abomasum of heifers with or without exogenous amylase administration. J. Anim. Sci. 96:1939–1951. doi:10.1093/jas/sky082.

Wirth, R., G. Kádár, B. Kakuk, G. Maróti, Z. Bagi, Á. Szilágyi, G. Rákhely, J. Horváth, and K.L. Kovács. 2018. The planktonic core microbiome and core functions in the cattle rumen by next generation sequencing. Front. Microbiol. 9. doi:10.3389/fmicb.2018.02285.

Wolin, M.J. 1960. A Theoretical Rumen Fermentation Balance. J. Dairy Sci. 43:1452–1459. doi:10.3168/jds.S0022-0302(60)90348-9.

Wu, G.D., J. Chen, C. Hoffmann, K. Bittinger, Y.Y. Chen, S.A. Keilbaugh, M. Bewtra, D. Knights, W.A. Walters, R. Knight, R. Sinha, E. Gilroy, K. Gupta, R. Baldassano, L. Nessel, H. Li, F.D. Bushman, and J.D. Lewis. 2011. Linking long-term dietary patterns with gut microbial enterotypes. Science (80-.). 334:105–108. doi:10.1126/science.1208344.

Xin, Z., W.B. Tucker, and R.W. Hemken. 1989. Effect of Reactivity Rate and Particle Size of Magnesium Oxide on Magnesium Availability, Acid-Base Balance, Mineral Metabolism, and Milking Performance of Dairy Cows. J. Dairy Sci. 72:462–470. doi:10.3168/jds.S0022-0302(89)79128-1.

Yachida, S., S. Mizutani, H. Shiroma, S. Shiba, T. Nakajima, T. Sakamoto, H. Watanabe, K. Masuda, Y. Nishimoto, M. Kubo, F. Hosoda, H. Rokutan, M. Matsumoto, H. Takamaru, M. Yamada, T. Matsuda, M. Iwasaki, T. Yamaji, T. Yachida, T. Soga, K. Kurokawa, A. Toyoda, Y. Ogura, T. Hayashi, M. Hatakeyama, H. Nakagama, Y. Saito, S. Fukuda, T. Shibata, and T. Yamada. 2019. Metagenomic and metabolomic analyses reveal distinct stage-specific phenotypes of the gut microbiota in colorectal cancer. Nat. Med. 25:968–976. doi:10.1038/s41591-019-0458-7.

Zarling, E.J., and M.A. Ruchim. 1987. Protein origin of the volatile fatty acids isobutyrate and isovalerate in human stool. J. Lab. Clin. Med. 109:566–570.

Zened, A., S. Combes, L. Cauquil, J. Mariette, C. Klopp, O. Bouchez, A. Troegeler-Meynadier, and F. Enjalbert. 2013. Microbial ecology of the rumen evaluated by 454 GS FLX pyrosequencing is affected by starch and oil supplementation of diets. FEMS Microbiol. Ecol. 83:504–514. doi:10.1111/1574-6941.12011.

Zhou, L., X. Xiao, Q. Zhang, J. Zheng, M. Li, M. Yu, X. Wang, M. Deng, X. Zhai, and R. Li. 2018. Improved glucose and lipid metabolism in the early life of female offspring by maternal dietary genistein is associated with alterations in the gut microbiota. Front. Endocrinol. (Lausanne). 9. doi:10.3389/fendo.2018.00516.

Appendix A

IACUC PERMISSION

University of Delaware
Institutional Animal Care and Use Committee
Application to Use Animals in Research
(New and 3-Yr submission)

Title of Protocol: Evaluation of hindgut buffers	
AUP Number: 115R-2020-0	**← (4 digits only — if new, leave blank)**
Principal Investigator: Tanya Gressley	
Common Name (Strain/Breed if Appropriate): Holstein cows **Genus Species:** Bos taurus	
Date of Submission: 3/20/20	

Official Use Only

IACUC Approval Signature: Gen Talln, DVM

Date of Approval: 4/24/2020

Revised: 3/05/2019

Appendix B

SUPPLEMENTARY FILES TO CHAPTER 3

Table B.1: Ingredient and nutrient composition of the total mixed ration, percent of DM unless otherwise specified.

Ingredient	Period 1	Periods 2-5
Corn silage	34.40	38.00
Triticale silage	17.35	17.31
Corn grain top dress, 1 kg/d[1]	3.49	3.69
Grain mix		
Ground corn grain	22.90	20.95
Protected soybean meal[2]	4.28	3.92
Solvent extracted soybean meal	3.90	3.57
Solvent extracted canola meal	3.24	2.97
Soybean hulls ground	2.74	2.51
Rumen bypass fat[3]	1.46	1.34
Blood meal ring dried	0.92	0.84
Corn gluten meal	0.76	0.70
Sodium bicarbonate	0.67	0.61
Corn distiller's grain	0.61	0.56
Sugar	0.41	0.38
Trace mineral and vitamin mix[4]	0.41	0.38
Potassium carbonate[5]	0.39	0.36
Sodium chloride	0.38	0.35
Urea	0.35	0.32
Calcium carbonate	0.32	0.29
Rumen protected lysine[6]	0.28	0.26
Monocalcium phosphate[7]	0.22	0.20
Mold inhibitor[8]	0.17	0.16
Potassium and magnesium sulfate[9]	0.15	0.14
Methionine precursor[10]	0.09	0.08
Magnesium oxide	0.06	0.05
Rumen protected methionine[11]	0.04	0.04
B vitamins[12]	0.01	0.01

Table B.1 continued

Monensin[13]	0.01	0.01
Chelated zinc[14]	0.01	0.01
Nutrient		
Crude protein	15.8	15.1 ± 0.3
NDF	30.2	31.2 ± 1.0
ADF	19.8	19.5 ± 0.5
Starch	30.9	30.9 ± 0.6
Ash	8.3	7.2 ± 0.3
NE_L, Mcal/kg	1.68	1.68 ± 0.01

[1]Mixed in the ration during adaptation and washout periods. Applied by hand with the treatments during the treatment periods.
[2]Extruded and expelled soybean meal (J. L. Moyer & Sons, Inc., Turbotville, PA).
[3]EnerG-3 (Virtus Nutrition, Corcoran, CA).
[4]Contained 5.13% calcium, 34% magnesium, 7.13% sulfur, 4.53% potassium, 660 mg/kg Fe, 4,213 mg/kg Zn, 818 mg/kg Cu, 4,099 mg/kg Mn, 65 mg/kg Se, 141 mg/kg Co, 191 mg/kg I, 400 KIU/kg Vitamin A, 100 KIU/kg Vitamin D, and 2,400 IU/kg Vitamin E. (1965 Mill Mix 4 MTX, Renaissance Nutrition, Roaring Spring, PA).
[5]DCAD Plus (Church & Dwight Co., Inc, Princeton, NJ).
[6]AjiPro-L (Ajinomoto Co., Inc., Tokyo, Japan).
[7]Biofos (Mosaic Crop Nutrition, LLC., Lithia, FL).
[8]Myco CURB (Kemin Industries, Inc., Des Moines, IA).
[9]Dynamate (18% K, 11% Mg, 22% S; The Mosaic Company, Plymouth, MN).
[10]HMTBa (MHA, Novus International, Inc., St. Charles, MO).
[11]Smartamine M (Adisseo, Antony, France).
[12]Lactation BV (Jefo, Saint-Hyacinthe, Quebec).
[13]Custom premix produced by Renaissance Nutrition (Roaring Spring, PA) containing 0.485% Rumensin 90.7 (Elanco, Greenfield, IN).
[14]MINTREX Zn (Novus International, Inc., St. Charles, MO).

Table B.2: Sequencing statistics. Read counts and percentages of sequencing data following the dada2 amplicon merging, chimera, and quality filtering steps.

Sample ID	Input	Filtered	% of input passed filter	Denoised	Merged	% of input merged	Non-chimeric	% of input non-chimeric
001	40696	32668	80.27	29465	9680	23.79	4646	11.42
002	49669	40159	80.85	37850	17482	35.2	6936	13.96
003	57560	46481	80.75	43589	19184	33.33	7874	13.68
004	59340	48678	82.03	45662	20343	34.28	8737	14.72
005	42504	33764	79.44	30657	12299	28.94	6125	14.41
006	60853	48231	79.26	44658	18004	29.59	6883	11.31
007	44694	36602	81.89	33877	15142	33.88	8093	18.11
008	46765	37292	79.74	34207	13660	29.21	6740	14.41
009	45946	37335	81.26	35166	18335	39.91	8903	19.38
010	48204	39051	81.01	36795	18749	38.9	8885	18.43
011	46943	38320	81.63	36386	17764	37.84	7741	16.49
012	59067	48784	82.59	46331	23531	39.84	10525	17.82
013	40046	31983	79.87	30836	16494	41.19	6373	15.91
014	52312	42134	80.54	39652	21401	40.91	10221	19.54
015	35547	29396	82.7	26238	9130	25.68	5037	14.17
016	34827	27989	80.37	26376	13312	38.22	6989	20.07
017	61293	48536	79.19	45050	19084	31.14	9185	14.99
018	73371	57631	78.55	54283	22463	30.62	8837	12.04
019	68020	53240	78.27	50243	23790	34.98	9842	14.47
020	77140	62185	80.61	59134	28133	36.47	12634	16.38
021	66061	51540	78.02	49120	21935	33.2	9177	13.89
022	68804	53743	78.11	50702	22229	32.31	9447	13.73
023	55254	44559	80.64	41273	16638	30.11	8792	15.91
024	52976	41695	78.71	39252	19956	37.67	8992	16.97
025	50783	41105	80.94	38275	18101	35.64	9571	18.85
026	54659	44087	80.66	40962	17818	32.6	8637	15.8
027	55084	44863	81.44	42398	20505	37.22	9057	16.44
028	57042	47236	82.81	43991	17834	31.26	8333	14.61
029	39686	31890	80.36	29259	9681	24.39	4066	10.25
030	55965	45185	80.74	42571	21870	39.08	9660	17.26

Table B.2 continued

031	47243	39130	82.83	36644	15871	33.59	7856	16.63
032	53824	43380	80.6	39884	17840	33.15	9582	17.8
033	50331	41249	81.96	38659	18100	35.96	8141	16.17
034	65129	52008	79.85	49695	23133	35.52	8524	13.09
035	60758	49404	81.31	47457	23992	39.49	8776	14.44
036	71583	59743	83.46	56876	27451	38.35	10399	14.53
037	57473	46357	80.66	43200	16982	29.55	7921	13.78
038	64288	51768	80.53	48026	20782	32.33	9518	14.81
039	54317	44397	81.74	42028	18790	34.59	8008	14.74
040	52499	42799	81.52	40841	20593	39.23	8177	15.58
041	58967	46944	79.61	44927	21283	36.09	9077	15.39
042	61303	47972	78.25	45476	22310	36.39	9062	14.78
043	58785	47273	80.42	44502	22020	37.46	10287	17.5
044	66929	53835	80.44	51191	25931	38.74	11377	17
045	62238	49160	78.99	46410	21453	34.47	9149	14.7

Table B.3: Comparison of period and cow under beta diversity measures through pairwise PERMANOVA.

Treatment		*P* Value			
Group 1	Group 2	Observed	Chao1	Shannon	Simpson
Period					
Period 1	Period 2	0.75	0.78	1.00	0.88
Period 1	Period 3	0.04	0.04	0.16	0.20
Period 1	Period 4	0.51	0.54	0.95	0.83
Period 1	Period 5	0.11	0.12	0.28	0.20
Period 2	Period 3	0.40	0.37	0.30	0.59
Period 2	Period 4	1.00	0.99	1.00	1.00
Period 2	Period 5	0.70	0.69	0.47	0.64
Period 3	Period 4	0.64	0.60	0.49	0.59
Period 3	Period 5	0.99	0.98	1.00	0.83
Period 4	Period 5	0.89	0.89	0.69	0.59
Cow					
Cow 1	Cow 2	1.00	1.00	0.96	0.86
Cow 1	Cow 3	0.95	0.95	0.96	0.86
Cow 1	Cow 4	1.00	1.00	1.00	0.95
Cow 1	Cow 5	0.98	0.98	0.96	1.00
Cow 1	Cow 6	0.99	0.99	0.96	0.86
Cow 1	Cow 7	1.00	1.00	1.00	0.86
Cow 1	Cow 8	1.00	1.00	0.96	0.86
Cow 1	Cow 9	1.00	1.00	1.00	0.92
Cow 2	Cow 3	0.99	0.99	0.96	0.95
Cow 2	Cow 4	1.00	1.00	0.96	0.86
Cow 2	Cow 5	1.00	1.00	1.00	0.92
Cow 2	Cow 6	0.95	0.93	0.96	0.86
Cow 2	Cow 7	1.00	1.00	1.00	1.00
Cow 2	Cow 8	1.00	1.00	1.00	0.95
Cow 2	Cow 9	1.00	1.00	0.96	0.86
Cow 3	Cow 4	0.87	0.87	0.96	0.86
Cow 3	Cow 5	1.00	1.00	0.96	0.86
Cow 3	Cow 6	0.46	0.46	0.29	0.29

Table B.3 continued

Cow 3	Cow 7	1.00	1.00	0.96	0.86
Cow 3	Cow 8	0.99	0.99	0.96	0.86
Cow 3	Cow 9	1.00	1.00	0.96	0.86
Cow 4	Cow 5	0.94	0.94	1.00	0.92
Cow 4	Cow 6	1.00	1.00	0.96	0.86
Cow 4	Cow 7	0.99	1.00	0.96	0.86
Cow 4	Cow 8	1.00	1.00	0.96	0.86
Cow 4	Cow 9	1.00	1.00	1.00	0.95
Cow 5	Cow 6	0.59	0.60	0.96	0.86
Cow 5	Cow 7	1.00	1.00	1.00	0.95
Cow 5	Cow 8	1.00	1.00	1.00	1.00
Cow 5	Cow 9	1.00	1.00	0.96	0.92
Cow 6	Cow 7	0.83	0.84	0.96	0.86
Cow 6	Cow 8	0.93	0.94	0.96	0.86
Cow 6	Cow 9	0.84	0.86	0.96	0.86
Cow 7	Cow 8	1.00	1.00	0.96	1.00
Cow 7	Cow 9	1.00	1.00	0.96	0.86
Cow 8	Cow 9	1.00	1.00	0.96	0.86

Table B.4: Comparison of period and cow under beta diversity measures through pairwise PERMANOVA.

Treatment		*P* Value		
Group 1	Group 2	Bray-Curtis	Unweighted UniFrac	Weighted UniFrac
Period				
Period 1	Period 2	0.72	0.78	0.86
Period 1	Period 3	0.37	0.14	0.47
Period 1	Period 4	0.27	0.40	0.58
Period 1	Period 5	0.09	0.03	0.35
Period 2	Period 3	0.79	0.76	0.86
Period 2	Period 4	0.81	0.78	0.94
Period 2	Period 5	0.29	0.40	0.47
Period 3	Period 4	0.79	0.76	0.94
Period 3	Period 5	0.27	0.39	0.47
Period 4	Period 5	0.79	0.87	0.86
Cow				
Cow 1	Cow 2	0.17	0.06	0.36
Cow 1	Cow 3	0.14	0.04	0.38
Cow 1	Cow 4	0.04	0.03	0.15
Cow 1	Cow 5	0.16	0.18	0.42
Cow 1	Cow 6	0.50	0.13	0.38
Cow 1	Cow 7	0.61	0.64	0.38
Cow 1	Cow 8	0.50	0.41	0.45
Cow 1	Cow 9	0.19	0.10	0.38
Cow 2	Cow 3	0.16	0.06	0.42
Cow 2	Cow 4	0.06	0.17	0.22
Cow 2	Cow 5	0.05	0.05	0.38
Cow 2	Cow 6	0.16	0.04	0.35
Cow 2	Cow 7	0.06	0.03	0.19
Cow 2	Cow 8	0.17	0.05	0.32
Cow 2	Cow 9	0.06	0.06	0.30
Cow 3	Cow 4	0.05	0.07	0.22
Cow 3	Cow 5	0.04	0.04	0.16
Cow 3	Cow 6	0.04	0.03	0.15

Table B.4 continued

Cow 3	Cow 7	0.04	0.03	0.16
Cow 3	Cow 8	0.05	0.04	0.20
Cow 3	Cow 9	0.04	0.03	0.22
Cow 4	Cow 5	0.04	0.03	0.16
Cow 4	Cow 6	0.05	0.03	0.15
Cow 4	Cow 7	0.04	0.05	0.15
Cow 4	Cow 8	0.09	0.09	0.20
Cow 4	Cow 9	0.17	0.10	0.38
Cow 5	Cow 6	0.10	0.05	0.38
Cow 5	Cow 7	0.16	0.18	0.30
Cow 5	Cow 8	0.76	0.71	0.80
Cow 5	Cow 9	0.16	0.09	0.38
Cow 6	Cow 7	0.38	0.10	0.43
Cow 6	Cow 8	0.58	0.40	0.84
Cow 6	Cow 9	0.16	0.03	0.42
Cow 7	Cow 8	0.76	0.67	0.67
Cow 7	Cow 9	0.04	0.03	0.18
Cow 8	Cow 9	0.26	0.10	0.38

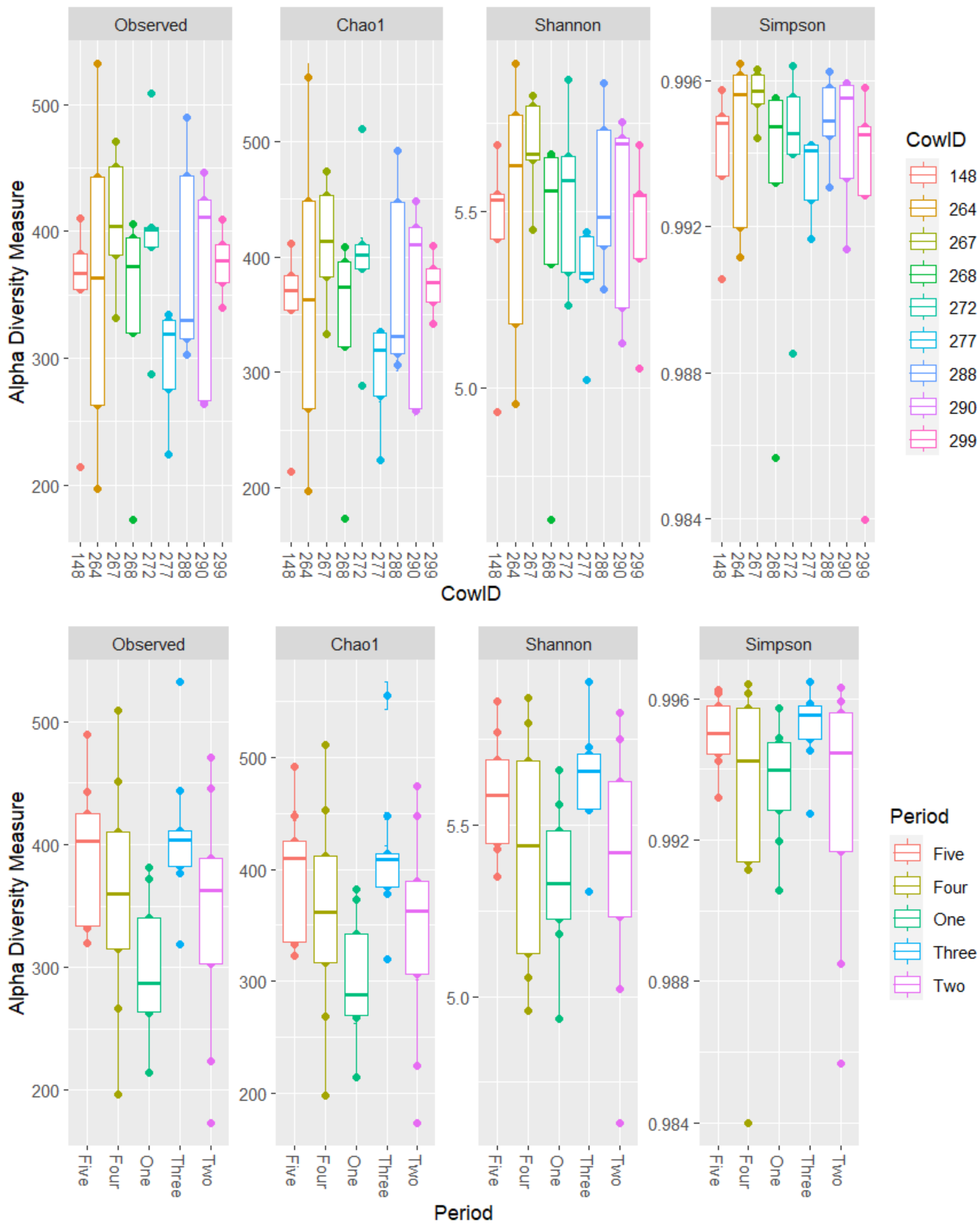

Figure B.1: Alpha diversity box-and-whisker plots comparing periods and cows using observed species, Chao1, Shannon, and Simpson indices.

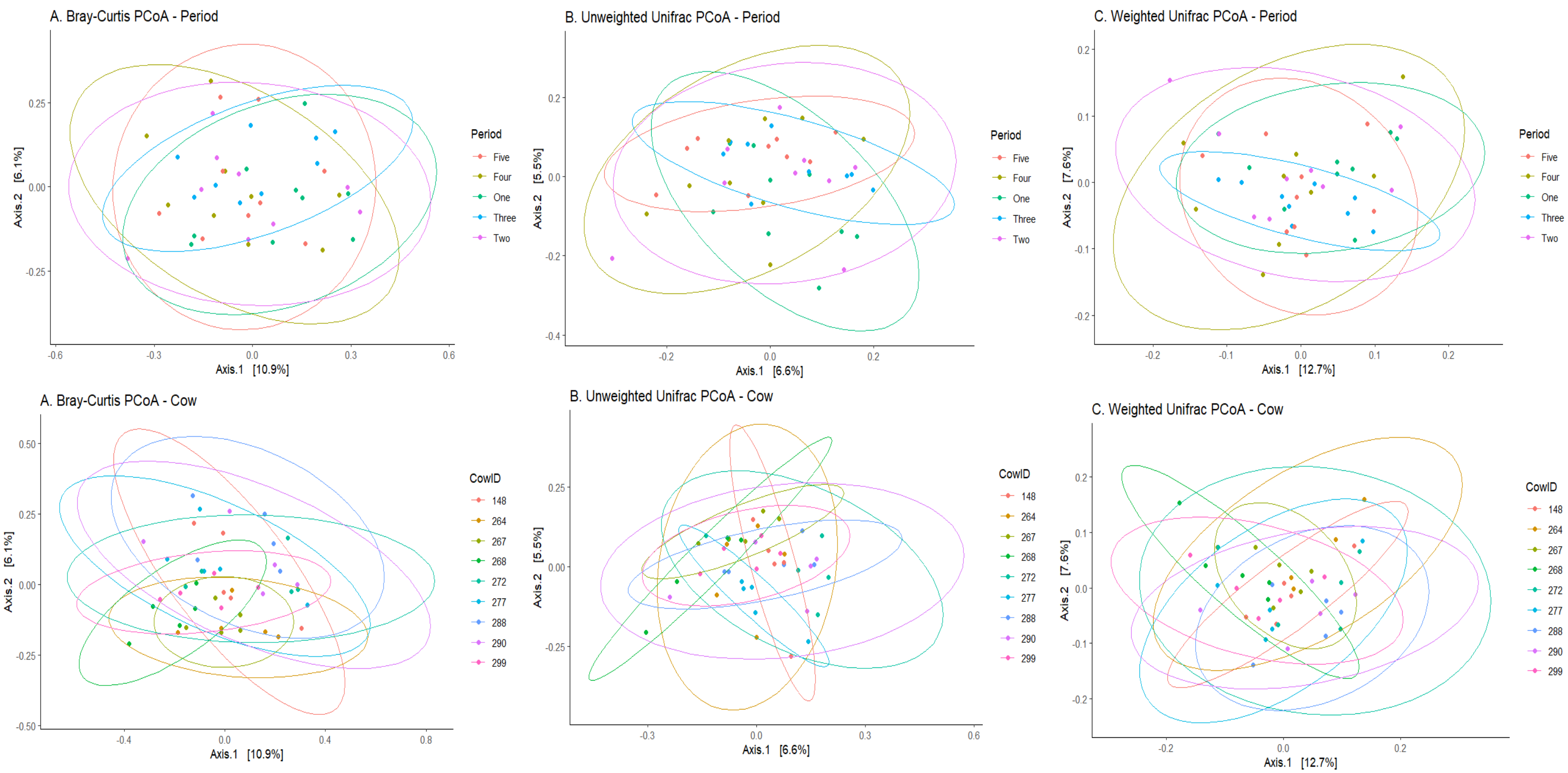

Figure B.2: Beta diversity principal coordinate analysis (PCoA) plots comparing period and cow using Bray-Curtis Dissimilarity, Weighted UniFrac, and Unweighted UniFrac.

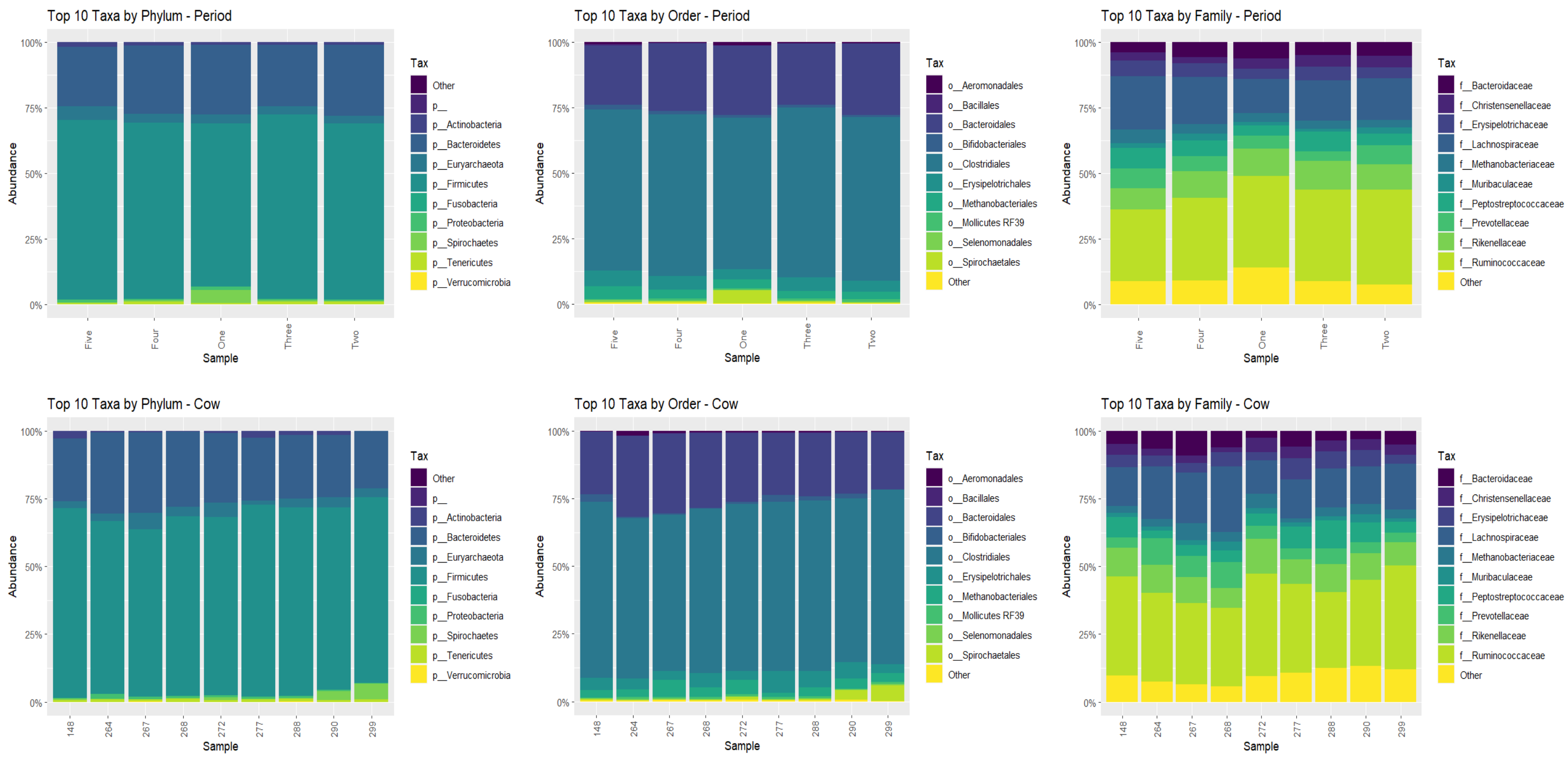

Figure B.3: Relative abundance taxa bar plots of the top 10 taxa at the phylum, order, and family levels organized by period and cow.

Appendix C

SUPPLEMENTARY FILES TO CHAPTER 4

Table C.1: Effects of control and buffer treatments on volatile fatty acid molar proportions.

	Treatment[1]							*P* values		
	FECC	STAR	SBA	SBB	BA	BB	SEM	Treatment	Time	Treatment × Time
VFA, mol %										
Acetate	66.5^{b}	69.2^{a}	69.1^{a}	69.2^{a}	68.5^{ab}	68.8^{a}	0.35	< 0.01	< 0.01	< 0.01
Propionate	23.7^{a}	16.1^{b}	15.6^{b}	15.5^{b}	22.1^{b}	21.6^{a}	0.40	< 0.01	< 0.01	< 0.01
Butyrate	7.89^{b}	12.9^{a}	13.8^{a}	13.8^{a}	7.78^{b}	7.91^{b}	0.20	< 0.01	< 0.01	< 0.01
Isobutyrate	0.74^{a}	0.70^{ab}	0.58^{bc}	0.56^{c}	0.63^{abc}	0.68^{abc}	0.03	< 0.01	< 0.01	0.59
Valerate	0.68^{a}	0.68^{a}	0.57^{b}	0.54^{b}	0.61^{ab}	0.58^{b}	0.02	< 0.01	< 0.01	< 0.01
Isovalerate	0.44^{a}	0.40^{b}	0.35^{c}	0.34^{c}	0.42^{ab}	0.42^{ab}	0.009	< 0.01	< 0.01	0.18

[1]Treatments were fecal inoculant alone (FECC), fecal inoculant and 1% starch (STAR), fecal inoculant and 0.05% buffer prototype 1 (BA), fecal inoculant with 1% starch and 0.05% buffer prototype 1 (SBA), fecal inoculant and 0.05% buffer prototype 2 (BB), or fecal inoculant with 1% starch and 0.05% buffer prototype 2 (SBB).

[2]VFA concentrations were measured at 0, 3, 6, 12, 18, and 24 h.

[a-d]Differing letters ($P \leq 0.05$) using Tukey's Honestly Significant Difference test.

Table C.2: Effect of blank treatments on pH, gas production, NH_3-N, volatile fatty acid and lactate, total protein and carbohydrate, and endotoxin concentrations.

	Treatment[1,2]							*P* values		
	BCON	BSTA	BSBA	BSBB	BBA	BBB	SEM	Treatment	Time	Treatment* Time
pH	6.44	6.38	6.50	6.50	6.50	6.56	0.08	0.61	0.50	0.97
Cumulative gas production (mL)	11.5[a]	9.38[ab]	2.38[c]	2.75[bc]	1.13[c]	1.25[c]	1.63	< 0.01	< 0.01	0.02
NH_3-N (mg/dL)	10.1	10.1	9.59	9.58	9.79	9.78	0.28	0.43	< 0.01	0.76
VFA, mM										
Acetate	4.02	4.08	4.11	4.15	4.06	4.17	0.04	0.12	0.23	1.00
Propionate	0.75	0.75	0.77	0.74	0.73	0.77	0.02	0.78	0.93	0.96
Butyrate	0.38	0.38	0.37	0.37	0.36	0.39	0.01	0.39	0.25	0.90
Isobutyrate	0.13	0.11	0.12	0.11	0.10	0.14	0.01	0.06	0.10	0.73
Valerate	0.07	0.08	0.08	0.08	0.07	0.07	0.005	0.73	0.12	0.67
Isovalerate	0.07	0.07	0.08	0.08	0.07	0.08	0.003	0.77	0.68	0.58
Total VFA	5.42	5.48	5.53	5.51	5.40	5.62	0.06	0.21	0.22	1.00
Lactate, mM	0.38	0.37	0.36	0.38	0.39	0.42	0.03	0.50	0.02	0.98
VFA, mol %										
Acetate	74.0	74.3	74.2	75.0	75.1	74.1	0.44	0.34	0.49	0.93
Propionate	13.9	13.8	13.9	13.6	13.6	13.8	0.28	0.93	0.55	0.92
Butyrate	6.99	6.95	6.79	6.73	6.80	6.95	0.09	0.27	0.38	0.52
Isobutyrate	2.34	2.07	2.16	1.93	1.82	2.50	0.16	0.06	0.09	0.56
Valerate	1.33	1.44	1.46	1.48	1.34	1.31	0.10	0.75	0.16	0.65
Isovalerate	1.39	1.36	1.41	1.37	1.37	1.42	0.05	0.96	0.43	0.41
Total Carbohydrate (µg/ml)	4227[b]	5243[ab]	4903[ab]	5685[a]	4253[b]	4363[b]	229	< 0.01	0.94	1.00
Total Protein (mg/ml)	4.97	5.23	4.76	4.95	5.00	5.25	0.25	0.74	0.71	0.99
LPS (EU/mL supernatant, $\log_{10}$)	3.30	3.40	3.23	3.48	3.35	3.51	0.16	0.82	0.03	0.98

[1]Treatments were sterile culture media alone (BCON), culture media with 1% starch (BSTA), culture media with 1% starch and 0.05% buffer prototype 1 (BSBA), culture media with 1% starch and 0.05% buffer prototype 2 (BSBB), culture media with 0.05% buffer prototype 1 (BBA), or culture media with 0.05% buffer prototype 2 (BBB).
[2]All variables were measured at 0 and 24 h.
[a-c]Superscripts within the row indicates $P \leq 0.05$ by Tukey's Honestly Significant Difference test.

Table C.3: Sequencing statistics. Read counts and percentages of sequencing data following the dada2 amplicon merging, chimera, and quality filtering steps. Samples 1-75 received fecal inoculant, while samples 76-83 contained media and treatment but no feces (blanks).

Sample ID	Input	Filtered	% of input passed filter	Denoised	Merged	% of input merged	Non-chimeric	% of input non-chimeric
1	57050	38425	67.35	36717	20001	35.06	10158	17.81
2	78531	59092	75.25	56853	34325	43.71	18530	23.6
3	73225	54924	75.01	52914	31857	43.51	16916	23.1
4	76188	56848	74.62	54882	33089	43.43	17604	23.11
5	74458	55645	74.73	53607	33179	44.56	18118	24.33
6	44734	33684	75.3	32367	19252	43.04	10822	24.19
7	68720	51793	75.37	51176	45248	65.84	17247	25.1
8	64592	47367	73.33	46809	39915	61.8	15275	23.65
9	70100	48010	68.49	47300	38393	54.77	14806	21.12
10	69518	53048	76.31	52333	43088	61.98	16413	23.61
11	76804	58174	75.74	57355	48744	63.47	18772	24.44
12	56207	42151	74.99	41616	35215	62.65	13611	24.22
13	70390	52336	74.35	51695	45010	63.94	16524	23.47
14	46755	35634	76.21	35410	32595	69.71	11487	24.57
15	65186	50338	77.22	50082	45755	70.19	16306	25.01
16	59425	44259	74.48	43979	39728	66.85	14230	23.95
17	59911	40737	68	40153	34788	58.07	12910	21.55
18	71409	54516	76.34	53781	46048	64.48	17787	24.91
19	26755	20372	76.14	19135	9882	36.94	5332	19.93
20	61513	46840	76.15	45065	28417	46.2	16653	27.07
21	71551	54297	75.89	52652	34947	48.84	20702	28.93
22	51793	37703	72.8	34757	14449	27.9	6171	11.91
23	68285	50759	74.33	48932	29747	43.56	17163	25.13
24	70647	50753	71.84	48839	30013	42.48	16724	23.67
25	78470	51761	65.96	51417	48225	61.46	18679	23.8

Table C.3 continued

26	81449	61089	75	60807	58261	71.53	22350	27.44
27	74502	55470	74.45	55107	50711	68.07	18261	24.51
28	70981	42402	59.74	42157	39080	55.06	14818	20.88
29	87874	64467	73.36	63949	58620	66.71	22663	25.79
30	70600	51671	73.19	51389	48137	68.18	19796	28.04
31	77572	58042	74.82	57490	52518	67.7	20493	26.42
32	82841	60684	73.25	60383	55047	66.45	18154	21.91
33	72514	47596	65.64	47152	40052	55.23	12922	17.82
34	86733	64572	74.45	64157	57498	66.29	19600	22.6
35	79266	59806	75.45	59213	51511	64.98	19969	25.19
36	83489	62112	74.4	61331	52867	63.32	20986	25.14
37	68494	48620	70.98	46068	26962	39.36	15998	23.36
38	51845	37842	72.99	35900	21404	41.28	12615	24.33
39	58673	43763	74.59	42124	27029	46.07	16518	28.15
40	56584	37470	66.22	35371	19992	35.33	11630	20.55
41	53003	39600	74.71	37267	21473	40.51	12639	23.85
42	66902	49635	74.19	47062	27875	41.67	16320	24.39
43	72123	53461	74.12	53109	50728	70.34	20477	28.39
44	68820	50822	73.85	50551	48416	70.35	19421	28.22
45	60128	44785	74.48	44475	41879	69.65	16502	27.44
46	74848	56029	74.86	55636	52310	69.89	20621	27.55
47	82241	59875	72.8	59346	55619	67.63	22484	27.34
48	76433	51228	67.02	50683	46489	60.82	19085	24.97
49	81954	61967	75.61	61445	57506	70.17	22835	27.86
50	86902	66005	75.95	65745	63969	73.61	26222	30.17
51	77976	58941	75.59	58688	56530	72.5	22743	29.17
52	84256	51526	61.15	51274	49274	58.48	19959	23.69
53	65551	48514	74.01	48159	44661	68.13	18649	28.45
54	70625	53660	75.98	53240	48970	69.34	20282	28.72
55	65371	46975	71.86	45137	27532	42.12	14680	22.46
56	62213	41517	66.73	39960	24014	38.6	13235	21.27
57	71140	53106	74.65	51006	30448	42.8	16335	22.96
58	55206	41171	74.58	39997	26400	47.82	15139	27.42
59	69989	51855	74.09	50096	31451	44.94	17629	25.19

Table C.3 continued

60	69796	51423	73.68	49552	30086	43.11	16048	22.99
61	59602	43445	72.89	42942	37552	63	13715	23.01
62	70225	52131	74.23	51546	44715	63.67	16093	22.92
63	67857	48102	70.89	47235	37865	55.8	13510	19.91
64	68473	44785	65.41	44006	34117	49.83	12532	18.3
65	73185	53643	73.3	52761	42199	57.66	16181	22.11
66	71928	53010	73.7	52271	42831	59.55	16806	23.37
67	72996	54671	74.9	54238	48857	66.93	18714	25.64
68	77264	57730	74.72	57334	51674	66.88	17136	22.18
69	49683	37012	74.5	36716	32421	65.26	11074	22.29
70	83751	63824	76.21	63363	55790	66.61	18713	22.34
71	75437	54256	71.92	53200	42149	55.87	15406	20.42
72	63898	42435	66.41	41752	33285	52.09	12585	19.7
73	12121	8804	72.63	8798	8733	72.05	3604	29.73
74	15689	11672	74.4	11633	11243	71.66	4978	31.73
75	11277	8510	75.46	8506	8442	74.86	3388	30.04
76	2815	2051	72.86	2030	1767	62.77	906	32.18
77	5118	3768	73.62	3755	3733	72.94	1692	33.06
78	12851	9936	77.32	9907	9423	73.33	3421	26.62
79	3115	2268	72.81	2260	2238	71.85	933	29.95
80	5143	3560	69.22	3553	3516	68.36	1801	35.02
81	5913	4466	75.53	4460	4404	74.48	2079	35.16
82	3538	2679	75.72	2673	2636	74.51	1358	38.38
83	1859	1418	76.28	1412	1358	73.05	721	38.78

Table C.4: Mean relative abundances of the ANCOM identified taxa determined to be differentially abundant between cows at 24 hours.

	Treatment Relative Abundance (%)				ANCOM	
	Cow 1	Cow 2	Cow 3	Cow 4	W[1]	clr[2]
Actinobacteria[3]	0.699[a]	0.006[c]	0.344[a]	0.062[b]	11	15.37
Spirochaetes[3]	0.248[a]	0.065[b]	0.359[a]	0.038[b]	10	9.33
Tenericutes[3]	0.070[a]	0[b]	0.008[b]	0.038[ab]	10	9.67
Actinobacteria[4]	0.699[a]	0.006[c]	0.344[a]	0.056[b]	18	12.97
Spirochaetia[4]	0.248[a]	0.065[b]	0.359[a]	0.038[b]	16	8.82
Mollicutes[4]	0.070[a]	0[b]	0.008[b]	0.038[ab]	15	9.60
Bifidobacteriales[5]	0.699[a]	0.006[c]	0.344[a]	0.056[b]	23	12.89
Mollicutes RF39[5]	0.070[a]	0[b]	0.005[b]	0.037[ab]	19	10.63
Spirochaetales[5]	0.248[a]	0.065[b]	0.359[a]	0.038[b]	18	8.46
Bifidobacteriaceae[6]	0.699[a]	0.006[c]	0.344[a]	0.056[b]	37	13.77
Lachnospiraciae ND3007 group[7]	0[b]	0[b]	0[b]	0.429[a]	124	208.3
Roseburia[7]	0.082[b]	0.006[c]	0.020[bc]	0.774[a]	124	35.23

[1]The W-statistic is the strength of the ANCOM test for the tested number of species.
[2]The clr F-statistic is a measure of the effect size difference for a particular species between treatment groups. ANCOM determines significance by plotting the F-statistic on the x-axis by the W-statistic on the y-axis.
[3-7]Phylum, class, order, family, and genus taxonomic levels, respectively.
[a-b]Superscripts within the row indicates $P \leq 0.05$ by pairwise Wilcoxon rank sum tests with post hoc testing using the Benjamini-Hochberg false discovery rate adjustment correction.

[w-z]Superscripts within the row indicates $0.05 \leq P \leq 0.10$ by pairwise Wilcoxon rank sum tests with post hoc testing using the Benjamini-Hochberg false discovery rate adjustment correction.

Table C.5: Spearman correlations of taxa to cows at 24 h.

	Cow			
	Cow 1	Cow 2	Cow 3	Cow 4
Phylum				
Actinobacteria	0.52	-0.73		
Firmicutes			0.64	
Fusobacteria			0.65	
Proteobacteria			-0.73	
Spirochaetes			0.53	-0.62
Tenericutes	0.63	-0.57		
Class				
Actinobacteria[1]	0.52	-0.73		
Bacilli[2]			0.64	
Clostridia[2]			-0.54	
Fusobacteriia[3]			0.65	
Gammaproteobacteria[4]			-0.70	
Spirochaetia[5]			0.51	-0.61
Mollicutes[6]	0.63	-0.57		
Order				
Bifidobacteriales[1]	0.52	-0.71		
Flavobacteriales[7]			0.65	
Lactobacillales[2]			0.64	
Clostridiales[2]			-0.54	
Fusobacteriales[3]			0.64	
Aeromonadales[4]			-0.72	0.50
Spirochaetales[5]			0.51	-0.61
Mollicutes RF39[6]	0.67	-0.53		
Family				
Bifidobacteriaceae[1]	0.52	-0.71		
p 251 o5[4]	-0.53			
Flavobacteriaceae[7]			0.65	
Enterococcaceae[2]			-0.50	

Table C.5 continued

Streptococcaceae[2]			0.67	
Unclassified Clostridiales[2]				0.65
Clostridiaceae 1[2]			-0.67	
Lachnospiraceae[2]			-0.57	
Peptostreptococcaceae[2]		-0.72		
Fusobacteriaceae[3]			0.65	
Succinivibrionaceae[4]			-0.72	0.50
Spirochaetaceae[5]			0.51	-0.61
Mollicutes RF39[6]	0.67	-0.52		
Genera				
Bifidobacterium[1]	0.52	-0.71		
Uncultured Parabacteroides sp.[7]				-0.53
Uncultured Bacteroidales bacterium[7]	-0.53			
Unclassified Prevotellaceae genus[7]				0.56
Prevotellaceae UCG 001[7]	-0.61			0.65
Prevotellaceae UCG 003[7]		0.56	-0.58	
dgA 11 gut group[7]			0.64	
Uncultured Flavobacteriaceae[7]			0.65	
Enterococcus[2]			-0.50	
Streptococcus[2]			0.67	
Unclassified Clostridiales genus[2]				0.65
Clostridium sensu stricto 1[2]			-0.67	
Unclassified Lachnospiraceae genus[2]	0.54		-0.54	
Agathobacter[2]	0.53	-0.61		
Anaerosporobacter[2]		-0.50		
Blautia[2]			-0.53	0.60
Butyrivibrio[2]			0.58	
Coprococcus 3[2]				0.59
Lachnospiraceae ND3007 group[2]				0.99
Lachnospiraceae NK3A20 group[2]	0.57	-0.58		
Roseburia[2]		-0.54		0.76
Unclassified Peptostreptococcaceae genus[2]		-0.67		

Table C.5 continued

Paeniclostridium[2]		-0.53		
Romboutsia[2]		-0.56		
Fournierella[2]	0.54			
Ruminiclostridium 5[2]	0.52			
Ruminococcaceae UCG 004[2]			0.52	
Ruminococcaceae UCG 014[2]		-0.71		
Rumminococcus 2[2]			-0.50	0.61
Uncultured Ruminococcaceae[2]				0.58
Candidatus Stoquefichus[2]	-0.50			
Erysipelotrichaceae UCG 004[2]		-0.61		
Quinella[2]			0.52	
Schwartzia[2]	0.50			
Selenomonas 1[2]	0.53			
Fusobacterium[3]			0.65	
Succinivibrio[4]			-0.72	0.50
Treponema 2[5]			0.50	-0.61
Unclassified Mollicutes RF39 genus[7]	0.67	-0.53		

Pairwise Spearman rank correlations (ρ) were calculated with R statistical software and significance was determined at ($0.5 \leq \rho \leq -0.5$). The ρ is moderate with (|0.5| to |0.7|), strong with (|0.7| to |0.9|), and substantial with (|0.9| to |1.0|). Red boxes indicate negative correlation and green indicates a positive correlation. Yellow rows indicate taxa significantly correlated with two treatment groups.

[1]Belonging to the Actinobacteria phylum.
[2]Belonging to the Firmicutes phylum.
[3]Belonging to the Fusobacteria phylum.
[4]Belonging to the Proteobacteria phylum.
[5]Belonging to the Spirochaetes phylum.
[6]Belonging to the Tenericutes phylum.
[7]Belonging to the Bacteroidetes phylum.

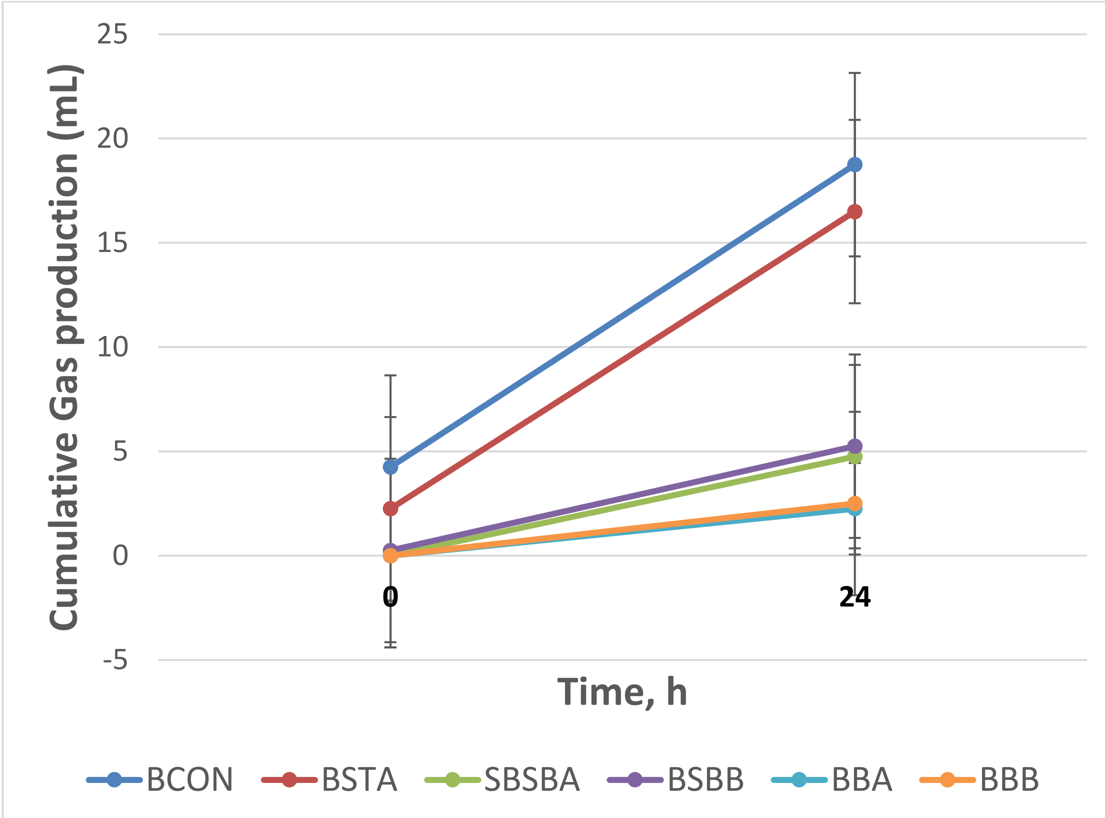

Figure C.1: Treatment[1] by time interaction plot[2] displaying cumulative gas production in blank treatments.[1]Treatments were as described in footnote 1 of Table C.2.

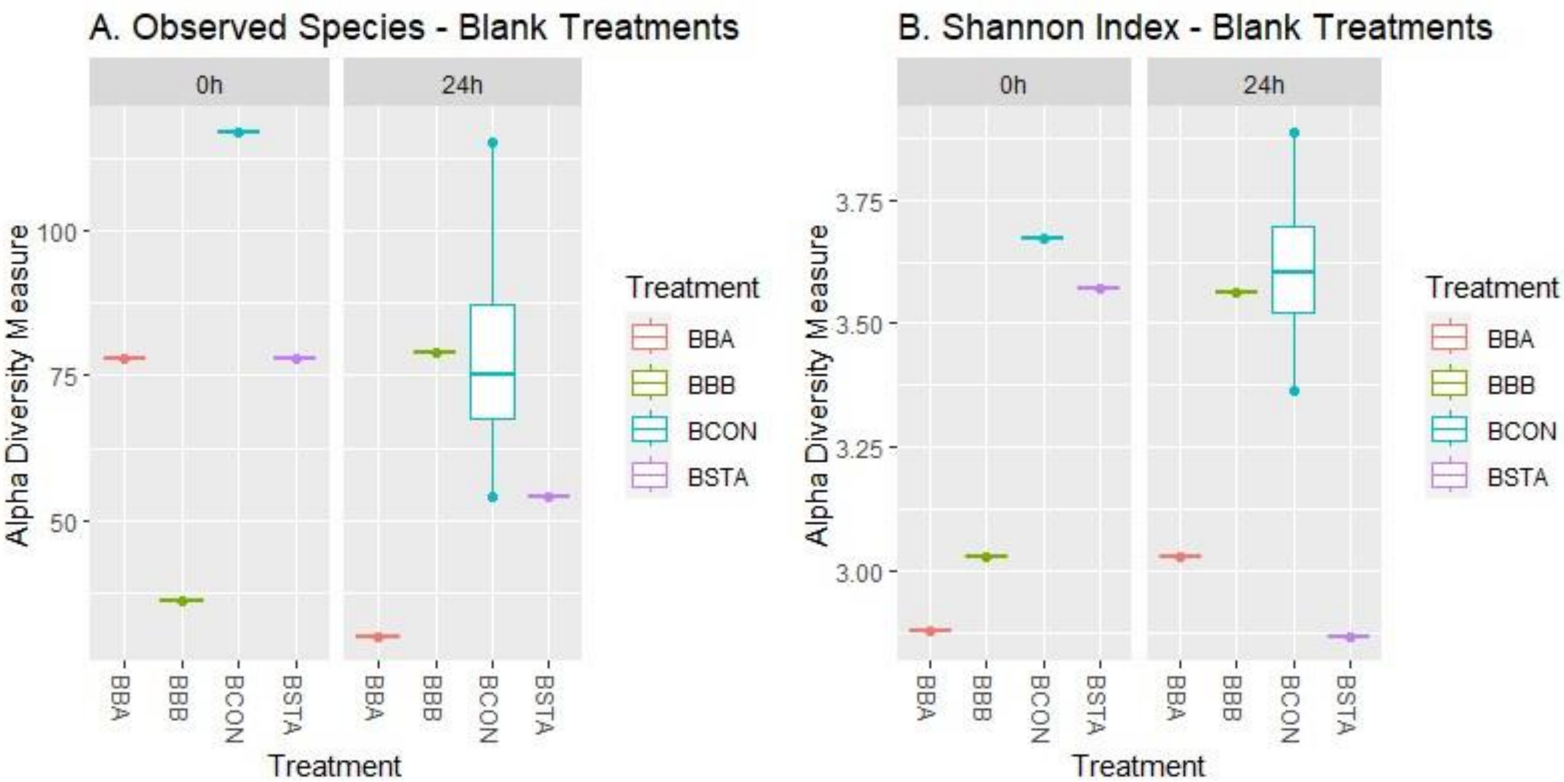

Figure C.2: Alpha Diversity plots of blank treatments[1] using Observed species and Shannon index to compare treatments within sampling time points. [1]Treatments were as described in Footnote 1 of Table C.1.

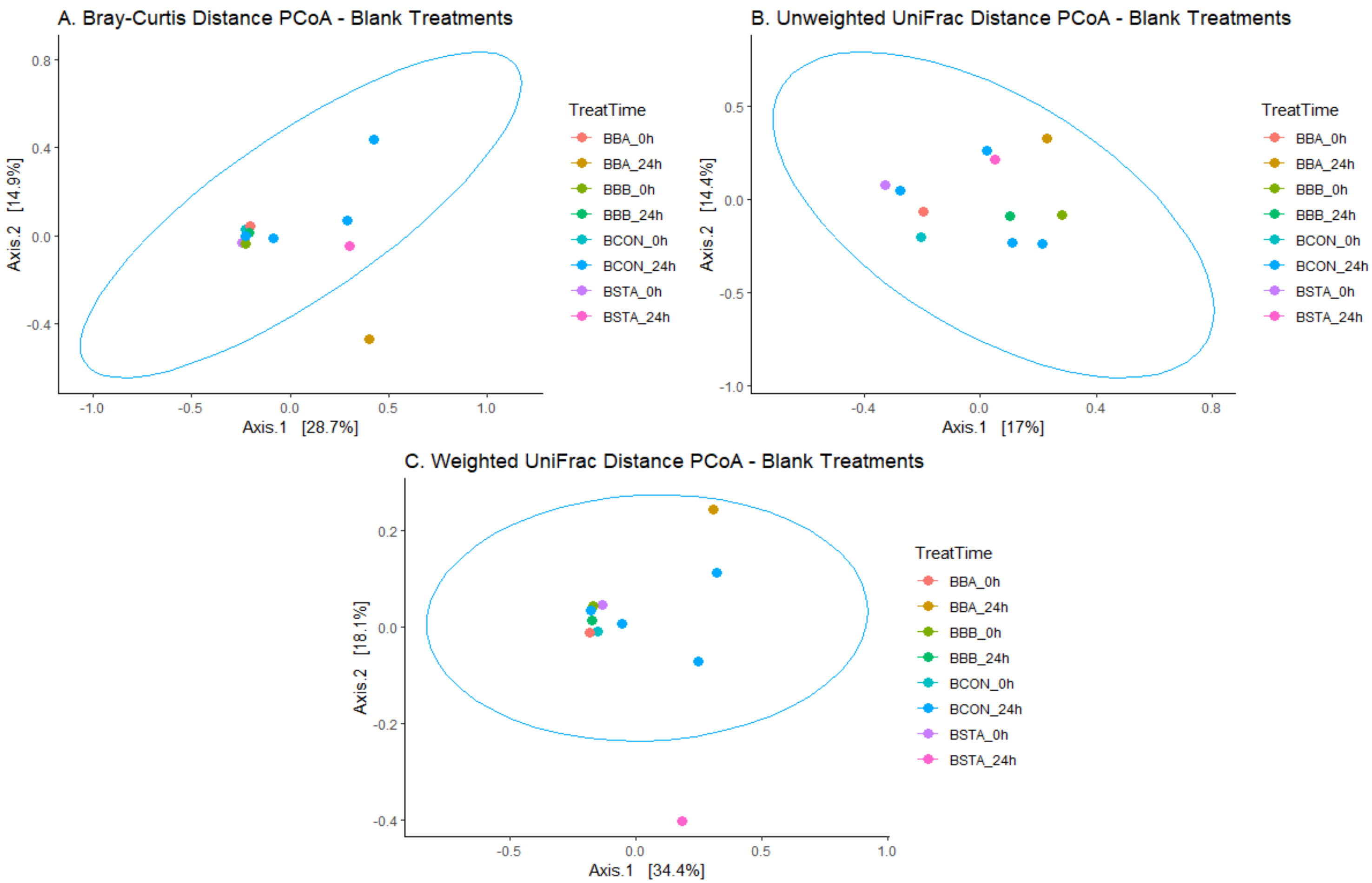

Figure C.3: Beta diversity principal coordinate analysis (PCoA) plots comparing blank treatment types using Bray-Curtis Dissimilarity, Weighted UniFrac, and Unweighted UniFrac.